AR-009-211

DSTO-RR-0027

Transverse Resonance Analysis
Technique for Microwave
and Millimetre-Wave Circuits

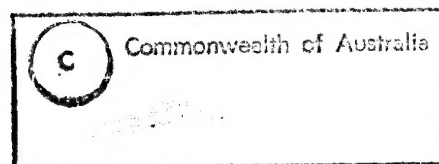Bevan D. Bates and
Geoffrey W. Staines

DTIC
SELECTED
ect 0 5 1995
B

APPROVED

FOR PUBLIC RELEASE

c Commonwealth of Australia

DTIC QUALITY INSPECTED 5

DEPARTMENT ◆ OF DEFENCE
DEFENCE SCIENCE AND TECHNOLOGY ORGANISATION

Transverse Resonance Analysis Technique for Microwave and Millimetre-Wave Circuits

Bevan D. Bates and Geoffrey W. Staines

Electronic Warfare Division
Electronics and Surveillance Research Laboratory

DSTO-RR-0027

ABSTRACT

A transverse resonance mode matching technique has been developed to analyse passive microwave and millimetre-wave waveguides and components. This technique possesses superior computational efficiency when compared to more general approaches such as the finite element method. This advantage is particularly useful for analysing broadband components used in electronic warfare systems. In this report, the theory behind this transverse resonance analysis is presented in detail. Theoretical results for several waveguiding structures are presented and compared with experimental or published data to verify the analysis.

Accession For

NTIS GRA&I ☑
DTIC TAB ☐
Unannounced ☐
Justification

By
Distribution/
Availability Codes

Dist | Avail and/or Special

A-1

RELEASE LIMITATION

Approved for Public Release

DEPARTMENT OF DEFENCE

◆

DEFENCE SCIENCE AND TECHNOLOGY ORGANISATION

Transverse Resonance Analysis Technique for Microwave and Millimetre-Wave Circuits

EXECUTIVE SUMMARY

An efficient and accurate method for analysis of broad bandwidth microwave and millimetre-wave devices has been developed. This report describes the method in detail and the results obtained by applying the method to typical microwave structures are compared with experimental or published data to verify the accuracy of the method.

THIS PAGE INTENTIONALLY BLANK

Authors

Bevan D. Bates
Electronic Warfare Division

Bevan Bates received the B.E., M.Eng.Sc., and Ph.D. degrees in electrical engineering from the University of Queensland, Brisbane, Australia in 1976, 1979 and 1982, respectively. From 1982 to 1983 he was a National Research Council resident Research Associate at the Jet Propulsion Laboratory, California Institute of Technology, Pasadena Ca. From 1984 to 1989 he was a Lecturer and then Senior Lecturer at the University of Melbourne in the Department of Electrical and Electronic Engineering. During 1987 he was a visitor at the National Radio Astronomy Observatory, Charlottesville, VA, engaged in characterising low-noise devices. He is now a Senior Research Scientist with Advanced Concepts Group, Electronic Warfare Division where he is responsible for developing broadband millimetre-wave receivers to meet emerging defence requirements.

Geoffrey W. Staines
Electronic Warfare Division

Geoff Staines received the BSc (Physics) degree from the University of Queensland in 1987, the BSc(Hons) from Flinders University in 1988, and a PhD in plasma physics from Flinders University in 1991. Since 1992, he has been a research scientist in Advanced Concepts Group, Electronic Warfare Division, DSTO Salisbury.

THIS PAGE INTENTIONALLY BLANK

CONTENTS

TABLES

FIGURES

APPENDICES

THIS PAGE INTENTIONALLY BLANK

1 INTRODUCTION

1.1 Purpose of this study

Computer-aided design software for microwave circuits is now readily available, at considerable cost, from companies such as Hewlett Packard, Compact Software, and many others. However, these software packages mostly are directed towards analysing planar integrated circuits using microstrip, and variants such as coplanar waveguide but do not adequately analyse other structures in use especially at mm-wave frequencies. Structures such as rectangular or circular waveguide, finline, dielectric waveguides are only analysed in an approximate manner (many programs are dominant-mode only) if at all. More specifically, some of the limitations have been identified to include: [1]

1. the inability to predict the onset of, and the consequences of, higher order propagating modes.

2. the lack of design information for popularly emerging 'new' transmission media, e.g. finlines.

3. the lack of design information concerning active devices at millimetre wavelengths. (Low frequency design models cannot be successfully extrapolated because of the increasing importance of parasitic elements and the distributed nature of the problem.)

4. the lack of design information relating to discontinuities in transmission media at millimetre wavelengths, and

5. the inability to predict the interaction of circuit elements which are in close proximity to one another.

The main areas of weakness of existing commercial software are thus in the areas of conventional waveguides, finline, dielectric waveguides, transitions between various structures, and the capability to explore new waveguiding structures. These problems are slowly being overcome through the use of field-theory based simulators [2] as a replacement for, or in conjunction with, circuit-theory based simulators. However, even these simulators are mostly oriented toward planar circuits because this is where the greatest commercial demand lies. The exception is some software (mostly based on the finite-element method) such the High-Frequency Structure Simulator from Hewlett Packard. While this is sufficiently general to analyse many circuits, it requires a powerful computer to analyse even relatively simple circuits. There is always a trade off between methods that are relatively simple to implement but require a lot of computation power and methods that are highly efficient but either lack generality or are complex to implement.

This report describes an approach which, while more efficient than general field-theory based methods such as the finite element method, still enables a wide variety of circuits to be analysed. The philosophy has been to pursue the middle ground - that is, a method which is general enough to solve a variety of practical problems that occur particularly in millimetre-wave circuit design, but at the same time is efficient enough to be used for routine design.

The prime motivation for this work has been that many electronic warfare applications require extremely broadband components (multi-octave) and the constraints in the design of these components are much more severe than for narrow band components. For example, in the design of a broadband amplifier or mixer, there is a direct trade off between gain (or conversion loss) and bandwidth. Moreover, high performance for e.g. direction-finding may require a high degree of gain flatness and matching between individual components. This combination of broad bandwidths and high precision can only be economically achieved with accurate computer analysis techniques which are specifically designed for these tasks.

1.2 Review

A wide variety of numerical techniques for the analysis of microwave and millimetre-wave structures have been developed over the years and, aided by the rapid advances in computing technology, many are beginning to now reach a level of maturity. However, no single technique is suited to all problems and this situation is unlikely to change. At present, one must choose a technique (or software package) that is appropriate to the problem being solved, just as a tradesperson chooses the suitable tool based on training and experience. What will happen in the future is that design software will have a range of techniques built into the one package and the user will be largely unaware of which technique is being used because it will be the software rather than the user that will choose the most appropriate technique.

1.2.1 Analysis techniques

Analysis techniques have been described in detail in recent books edited by Itoh [3], Sorrentino [4], and Yamashita [5]. These methods are summarised in Table 1.1 according to the chapter headings in the books and grouped to show where the methods are common to more than one book. There is also a certain amount of overlap between many techniques e.g. the transverse resonance technique uses mode-matching which in turn is fundamentally a moment method. Methods other than transverse resonance and mode matching will not be discussed further in this report.

Table 1.1   Summary of analysis techniques.

Itoh [3]	Sorrentino [4]	Yamashita [5]
The Finite Element Method	Finite-Element Method Finite-Difference Method	The Finite-Element Method
	Boundary-Element Method	The Boundary-Element Method
The Transmission Line Matrix (TLM) Method	Transmission-Line Matrix Method	
Planar Circuit Analysis	Planar-Circuit Approach	
Spectral Domain Approach	Spectral-Domain Approach	The Spectral Domain Method
The Method of Lines	Method of Lines	
Integral Equation Technique	Method of Moments	
The Mode-Matching Method	Mode-Matching and Field-Matching Techniques	The Mode-Matching Method The Point-Matching Method
Transverse Resonance Technique	Transverse Resonance Techniques	
The Waveguide Model for the Analysis of Microstrip Discontinuities		
Generalised Scattering Matrix Technique		
		The Wiener-Hopf and Modified Residue Calculus Techniques
		The Geometrical Theory of Diffraction
		The Equivalent Source Method
		Asymptotic Expansion Methods
		The Beam Propagation Method

1.2.2 Origins and background of current method

A brief summary of work that has influenced the current development follows. This is not an exhaustive review but summarises key developments. The beginnings of the method can be found in the early work on microwave network theory of Montgomery, Dicke and Purcell [6], and Marcuvitz [7] in the well known MIT Radiation Laboratory Series and also a little later in Altschuler and Goldstone [8] who developed network representations of waveguide obstacles. Clarricoats and Oliner [9] derived a transverse-network representation for hybrid modes in inhomogeneously filled waveguides using a method employed previously in the representation of slotted waveguides. Felsen and Marcuvitz [10] described a generalised derivation of the transverse field equations and modal representations of the electromagnetic field in transversely inhomogeneous regions. Kerns [11] discussed concepts and conditions underlying the establishment and use of immittance- and scattering-matrix descriptions of waveguide n-ports. Peng and Oliner [12] discussed a class of open dielectric waveguides which is of direct importance to the areas of integrated optics and millimetre-wave integrated circuits and presented a mathematical formulation based on a rigorous mode-matching procedure. Bornemann and Arndt [13] used transverse resonance to calculate the characteristic impedance of finlines with up to three slots by a rigorous hybrid-mode analysis. Masterman and Clarricoats [14] described a computational method for solving a wide range of transverse waveguide discontinuity problems and showed that in some cases, the solution is found to be sensitive to the way in which infinite series of field functions is truncated. They further showed how the optimum form of truncation can be determined for many configurations of practical importance. Ping and Jingfeng [15] investigated the filter characteristic of NRD waveguide by combining a network approach with mode matching theory in an application of the method of Peng and Oliner. Bates and Ko [16] used multi-modal admittance matrices to represent the coupled radial regions in a waveguide diode mounting structure.

1.3 Scope of this study

The analysis described in this report is a full three-dimensional mode matching analysis using generalised transverse resonance to analyse the constituent two-dimensional cross-sections in passive waveguide structures. The structure is assumed to be lossless and consisting of homogeneous and isotropic cuboidal sub-sections which may be dielectric filled.

1.4 Overview of contents

Chapter 2 describes the technique in detail, while chapter 3 gives results, including dispersion plots for a range of two-dimensional structures and S-parameter results for selected 3-dimensional structures. The results are intended to verify the applicability and accuracy of the analysis and are not a detailed study of any particular structure.

2 TECHNIQUE DEVELOPMENT

2.1 General Procedure

Consider a waveguide circuit element made up of a number of cascaded sections as shown in Figure 2.1. Each section is uniform in the direction of propagation (chosen to be the z-direction), and consists of a number of connected rectangular regions. Each region may contain an arbitrary number of dielectric layers. A brief outline of a transverse resonance mode matching technique to determine the scattering parameters of the circuit element follows:

(i)   **Subdivision of waveguide element**

Each *section* (uniform in the direction of propagation) in the *element* is sub-divided into *layers* and *regions* comprising homogeneous and isotropic segments of rectangular cross-section. Layers aligned vertically and not separated by conducting surfaces are combined vertically to form *subregions*. Vertically aligned subregions are in turn combined to form *regions*. Regions are stacked horizontally to construct sections. For much of the discussion of this chapter, only simple regions such as those shown in Figure 2.1 which consist of a single subregion need be considered. (An example of a subregion is shown in Figure 2.5.) Once the waveguide element is subdivided, the analysis proceeds by first analysing all of the subregions of a section.
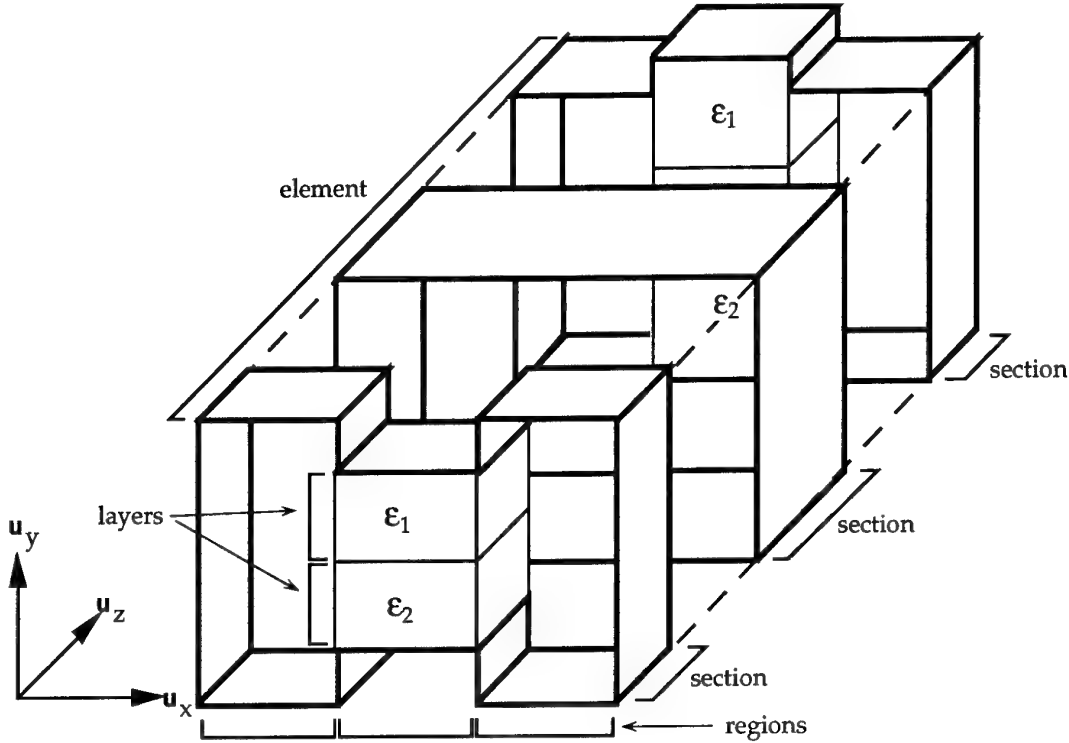
Figure 2.1   Structure geometry

(ii)   **Analysis of section subregions**

The transverse resonance technique is first applied in the y-direction to obtain mode eigenvalues and eigenfunctions for each subregion in each section. The subregion eigenmodes propagate in the u-direction, which lies in the x-z plane. This concept is described further in [12]. These eigenmodes are therefore referred to as u-modes. For a given free-space wavenumber k_0, the propagation constant k_u, or the u-mode eigenvalue, is given by:

$$k_u = \sqrt{k_x^2 + k_z^2}$$
$$= \sqrt{k_0^2 \varepsilon_r - k_y^2}$$

Note that while k_y is dependent on each layer's dielectric constant ε_r and the layer's thickness, k_x (and hence k_u) is constant across a subregion because of field continuity at layer interfaces. Field continuity at subregion interfaces requires k_z to be the uniform across the entire section.

Therefore, by determining the subregion eigenmodes and eigenfunctions, the effect of individual layers is determined, and the analysis proceeds by combining subregions.

(iii) Analysis of individual sections

To obtain the required z-mode eigenvalues and eigenfunctions for each section, the transverse resonance technique is applied in the x-direction. This stage of the calculation is generally the most computationally demanding, since there are a number of steps involved in this process which must be repeated many times. These steps are:

(a)   Assume an initial value of k_z for a particular z-mode in the section.

(b)   From the subregion u-mode data, calculate the corresponding x-mode eigenvalues, or propagation constants k_x, and eigenfunctions for each region. The propagation constants are given by

$$k_x = \sqrt{k_u^2 - k_z^2}$$

(c)   Apply the transverse resonance technique in the x-direction, including x-mode coupling at region interfaces. The assumed value of k_z is varied iteratively and steps (b) and (c) repeated until the transverse resonance condition is satisfied. Such values of k_z correspond to z-mode eigenvalues for the section. The z-mode eigenfunctions are calculated from x-mode data.

(iv) Analysis of complete element

Having obtained the field expansion in the individual sections expressed by the z-mode eigenvalues and eigenfunctions, the scattering parameters of both the sections themselves and the discontinuities arising at section interfaces can be determined. By cascading these scattering matrices, the scattering matrix for the entire waveguide element is readily determined. This constitutes the desired output from the analysis.

2.2   Definitions and conventions

The rectangular coordinate system from [17] shown in Figure 2.1 was adopted, with unit vectors denoted by $(\mathbf{u}_x, \mathbf{u}_y, \mathbf{u}_z)$. The dependence on time t is assumed throughout to be $e^{j\omega t}$ where $j = \sqrt{-1}$ and $\omega = 2\pi f$ and f is the operating frequency.

Let the total electric and magnetic field in the waveguide in the transverse cross-section of the ith section be given by vectors $\mathbf{E}_i$ and $\mathbf{H}_i$ respectively. The total field in the ith two-dimensional section is uniquely described by the tangential fields alone so we may let

$$\mathbf{E}_i = \mathbf{E}_{x_i} + \mathbf{E}_{y_i} + \mathbf{E}_{z_i}$$

$$= \mathbf{E}_{t_i} + \mathbf{E}_{z_i}$$

where $\mathbf{E}_{t_i}$ is the tangential electric field and similarly for the magnetic field. If the field is represented by a sum of normal modes in each subregion of the ith cross-section, then the total tangential fields may be expressed by a weighted sum over all possible modes

$$E_{t_i} = \sum_{m=0}^{\infty} v_i^m e_i^m$$

$$H_{t_i} = \sum_{m=0}^{\infty} i_i^m h_i^m$$

i.e. for each mode

$$\mathbf{E}_{t_i}^m = v_i^m \mathbf{e}_i^m$$

$$\mathbf{H}_{t_i}^m = i_i^m \mathbf{h}_i^m$$

where v_i^m and i_i^m are equivalent voltages and currents which are functions of the propagation coordinate variable only and $\mathbf{e}_i^m$ and $\mathbf{h}_i^m$ are mode functions which depend on the transverse variables (and physical geometry) only. These equivalent voltages and currents can be used in a circuit model of the waveguide e.g. the modal transfer admittance between mode m at port i and mode p at port j is given by

$$y_{ij}^{mp} = \frac{i_i^m}{v_j^p}$$

2.3   Method

Following the general procedure outlined in Section 2.1, the method is developed in greater detail. The transverse resonance technique is applied first in the y-direction in the subregion analysis and then again in the x-direction in the section analysis. Once the required number of section modes have been calculated for each section using the transverse resonance approach, a mode matching technique is used to calculate the scattering parameters of the complete element formed by cascading its constituent sections.

2.3.1   Multilayer parallel plate analysis (subregions)

The first step is to apply the transverse resonance technique in the y-direction to determine the subregion u-mode eigenvalues and eigenfunctions. This mode data will implicitly contain the effects associated with individual layers in a given subregion, reducing the required analysis to the subregion level for each two-dimensional section.

Consider propagation in a multi-dielectric-layer parallel-plate transmission-line structure shown in Figure 2.2 [cf [12], p. 847]. This is a classical Sturm-Liouville eigenvalue problem [18]. To find the eigenvalues (propagation constants) and eigenfunctions (mode functions) for propagation perpendicular to the plates (y-direction), we apply the transverse resonance technique in this direction. Each layer can be then considered as a portion of a lossless transmission line with modes propagating in the y direction, as shown in Figure 2.2. These modes are referred to as y-modes because of their direction of propagation. The voltages and currents on the transmission lines are directly related to the mode functions, and hence the y-mode electromagnetic fields.

Normally, the choice of modes would be transverse electric (TE) and transverse magnetic (TM) to the direction of propagation (y in this case). However, alternative representations using modes that are either TE-to-x and TM-to-x or TE-to-z and TM-to-z may lead to simpler (and computationally more efficient) representations under particular conditions such as subregions or sections with uniform dielectric constants. The choice of representation is discussed further in Section 2.3.2.
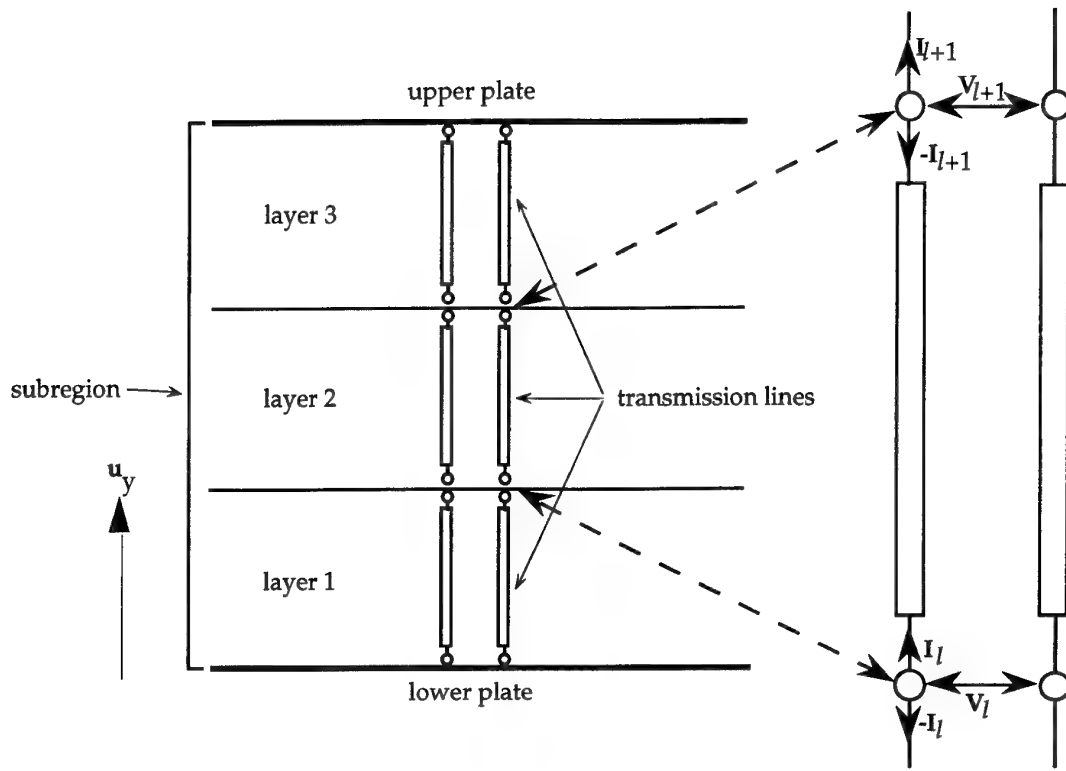
Figure 2.2   Equivalent transmission line network for y-mode analysis

TE and TM-to-y modes are used in multilayered dielectric subregions since there is no coupling between TE and TM modes at dielectric discontinuities, resulting in a more straightforward analysis. For this choice of eigenmode, the characteristic admittance of layer l with relative dielectric constant ε_l is given by

$$Y_l' = \frac{k_{y_l}'}{\omega\mu_0} \qquad \text{for TE} - \text{to} - y \text{ modes}$$

$$Y_l'' = \frac{\omega\varepsilon_0\varepsilon_l}{k_{y_l}''} \qquad \text{for TM} - \text{to} - y \text{ modes}$$

where $\omega = 2\pi f$ where f is the frequency, μ_0 and ε_0 are the permittivity and permeability respectively of a vacuum.

By contrast, TE and TM-to-x and z modes are used only in uniform subregions, which consist of a single dielectric layer, since TE-TM mode coupling would otherwise occur at dielectric discontinuities between layers. For uniform subregions, similar admittances can be defined for TE, TM-to-x and TE, TM-to-z modes as follows

$$Y_l'' = \frac{\omega\varepsilon_0}{k_{y_l}''} \qquad \text{for TE} - \text{to} - \text{x}, \text{TE} - \text{to} - z \text{ modes},$$

$$Y_l' = \frac{k_{y_l}'}{\omega\mu_0} \qquad \text{for TM} - \text{to} - \text{x}, \text{TM} - \text{to} - z \text{ modes}$$

The restriction that these modes can only be used for uniform subregions is reflected by the fact that the dielectric constants for individual layers are no longer contained in the modal admittances.

As stated previously, the propagation constant in the y-direction for the lth layer, k_{y_l}, is related to the propagation constant k_u by

$$k_{y_l}^2 = k_0^2 \varepsilon_l - k_u^2.$$

The subregion analysis proceeds by first assuming the maximum possible value of k_u. The admittances of the transmission lines shown in Figure 2.2 are evaluated for each y-mode. Using these admittance values, the modal voltages and currents used to construct the mode eigenfunctions are calculated at the interfaces of each layer. Depending on the boundary condition (electric or magnetic wall), either the y-mode voltage or the current is set to zero at the lower plate. If the value of k_u is such that the voltage and current at the top plate satisfy the required boundary condition, then k_u is a valid wavenumber, otherwise the value of k_u is iteratively adjusted until the boundary condition is satisfied. Note that this method is preferable to using the usual method of finding a resonance [4] in the total admittance found by summing the transmission line admittances in two directions at an arbitrary plane, because the voltage and current remain finite whereas the admittance may approach $\pm\infty$. The search for valid mode solutions is considerably more difficult with the presence of poles.

The y-mode voltage and current at the end of the line representing the lth layer are obtained from the voltage and current at the start of the line by

$$V_{l+1} = \cos k_{yl}d \ V_l - \frac{j}{Y_l} \sin k_{yl}d \ I_l$$

$$I_{l+1} = \cos k_{yl}d \ I_l - jY_l \sin k_{yl}d \ V_l.$$

with the signs consistent with the convention shown in Figure 2.2.

For a given y-mode, the admittance matrix for a length, d, of transmission line representing layer l is

$$\mathbf{Y} = \begin{bmatrix} -Y_l\left(\coth \alpha_{yl}d + j \cot \beta_{yl}d\right) & Y_l\left(\operatorname{cosech} \alpha_{yl}d + j \cosec \beta_{yl}d\right) \\ Y_l\left(\operatorname{cosech} \alpha_{yl}d + j \cosec \beta_{yl}d\right) - Y_l\left(\coth \alpha_{yl}d + j \cot \beta_{yl}d\right) \end{bmatrix}$$

where Y_l is the modal admittance of the lth layer for $k_{yl} = \beta_{yl} + j\alpha_{yl}$.

Using the appropriate admittance, the transmission line parameters $V_y'(y)$ and $I_y'(y)$ are used to construct mode functions which represent the electric and magnetic fields of TE-to-y, TM-to-x, and TM-to-z modes. Similarly, the parameters $V_y''(y)$ and $I_y''(y)$ are used to construct mode functions which represent the electric and magnetic fields of the TM-to-y, TE-to-x, and TE-to-z modes. Because these parameters are used to represent propagation in the y-direction, they are termed the y-mode voltages and currents.

The amplitudes of the transmission line voltages and currents used to define the y-mode mode functions are normalised to yield the following orthonormality relations:

$$\int_{y_l}^{y_{l+1}} V_y^{'i}(y)V_y^{'j}(y)^* dy = \delta_{ij}$$

for TE-to-y, TM-to-x, and TM-to-z modes,

$$\int_{y_l}^{y_{l+1}} \frac{I_y^{"i}(y)I_y^{"j}(y)*}{\varepsilon(y)}dy = \delta_{ij}$$

for TM-to-y modes and

$$\int_{y_l}^{y_{l+1}} I_y^{"i}(y)I_y^{"j}(y)* \, dy = \delta_{ij}$$

for TE-to-x and TE-to-z modes. In the above expressions, δ_{ij} is the Kronecker delta, $*$ denotes the complex conjugate, and y_l and y_{l+1} are the lower and upper edges of the layer. The phase ambiguity in the normalisation's allows the choice of $V_y(y)$ to be always real, and $I_y(y)$ to be always imaginary.

The orthonormality of $V_y'(y)$ and $I_y''(y)$ are used in Section 2.3.2.2 to calculate the mode coupling between adjacent regions in order to represent the entire two-dimensional cross section.

2.3.2 Two Dimensional (Section) Analysis

Section 2.3.1 has described the subregion analysis which is used to reduce the problem of analysing the various x-y cross-sections of the structure to the subregion level. The effects of individual layers are implictly included in the y-mode and u-mode propagation constants and mode functions. The remainder of the two-dimensional section analysis is concerned with combining subregions into sections.

The two-dimensional analysis described in this section can be applied to a wide variety of waveguiding structures including dielectric guides, finline, microstrip, and coplanar waveguide. The results of the analysis of a range of waveguides are presented in Section 3.1. The z-mode propagation constants, k_z, can be determined, along with the modal fields. These fields can be used to calculate user-defined z-mode impedances, and to calculate the z-mode coupling between connected sections. This coupling is used to cascade the sections to construct the entire waveguide element.

To fully describe the fields for modes propagating in the z-direction in a given section (z-modes), the transverse resonance technique is applied to an equivalent transmission line network representing propagation in the x direction. The modes represented by this network are referred to as x-modes because of their propagation direction. The previously determined y-mode fields which were determined using transverse resonance in the y-direction are combined as weighted sums to generate the fields of each z-mode in the section. The propagation constants of the z-modes are k_z^m ($m = 0, 1, ..., N_z$), where N_z is the total number of z-modes to be considered. Ideally, an infinite number of modes exist, but this number must be truncated for practical purposes.

The x-mode voltages and currents in the x-mode network defining the contribution of the nth y-mode fields to the total fields of the mth z-mode are V_x^{mn} and I_x^{mn}. Figure 2.3 shows the x-mode transmission line network for a simple ridged waveguide cross-section. Note that in general, the transmission lines representing individual x-modes in each region are now coupled at region interfaces. The boundary conditions at the sides of the cross-section determine how the x-mode transmission lines are terminated. The terminations are short circuits for an electric wall, open circuits for a magnetic wall, and the characteristic modal admittances (match) for an open boundary such as in a parallel-plate transmission line.
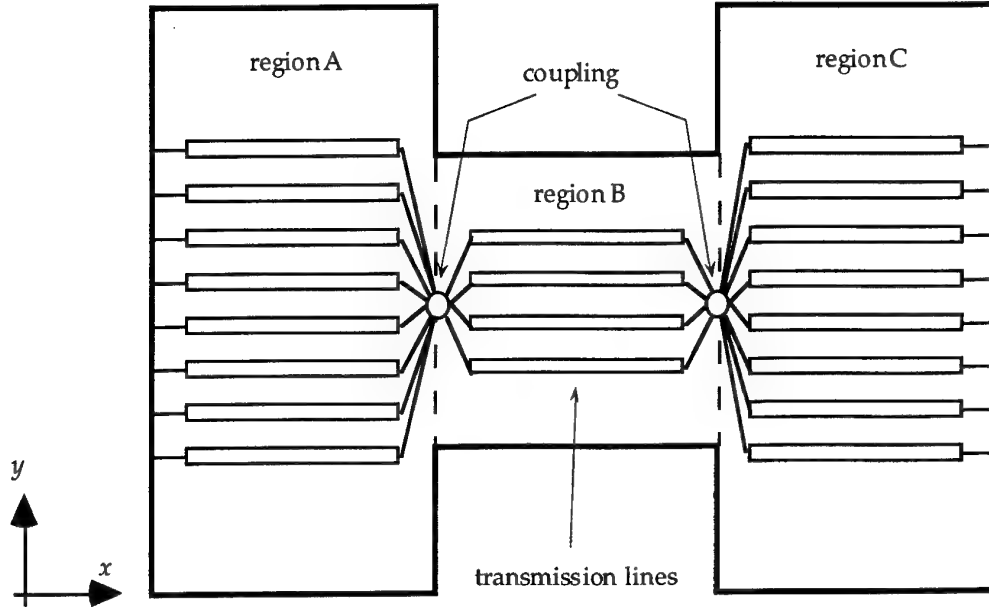
Figure 2.3   Ridged waveguide cross-section showing x-mode transmission line network

The x- mode and y-mode voltages and currents are combined as follows to represent the components of the fields transverse to the x-direction

$$\underline{E} = E_x \mathbf{u}_x + E_y \mathbf{u}_y + E_z \mathbf{u}_z$$
$$= E_x \mathbf{u}_x + E_T \mathbf{u}_T$$

where

$$E_T = \sum_m^{N_z} \sum_n^{N_y} V_x^{mn}(x) \mathbf{e}_T^n(y,z)$$

and

$$\mathbf{H} = H_x \mathbf{u}_x + H_y \mathbf{u}_y + H_z \mathbf{u}_z$$
$$= H_x \mathbf{u}_x + H_T \mathbf{u}_T.$$

where

$$H_T = \sum_m^{N_z} \sum_n^{N_y} I_x^{mn}(x) \mathbf{h}_T^n(y,z)$$

N_y and N_z are the number of transverse eigenmodes and the number of z-modes respectively. The modal fields $\mathbf{e}_T^n$ and $\mathbf{h}_T^n$ can be derived in terms of the y-mode voltages and currents using the expressions derived in Appendix I. The three choices of eigenmodes discussed in Section 2.3.1, ie, TE and TM to either x, y, or z, have features relevant to a discussion of the section analysis. The facility to choose from among the three possible types of mode functions is useful to characterise the z-modes in the structure, to allow various types of excitation to be applied in a straightforward fashion, and to improve

efficiency. In particular, each choice of eigenmode type has specific advantages in special circumstances. These advantages include:

(i)   For regions with layers of different dielectric constants (i.e. dielectric interfaces in the horizontal or x-z *plane*), TE-to-*y* and TM-to-*y* modes must be used. Of the three choices, only these modes have the property that no coupling occurs between different modes at dielectric interfaces, simplifying the subregion analysis of Section 2.3.1 for multilayered subregions. The lack of coupling arises from the orthogonality condition in the definition of the modes.

(ii)   To simplify the analysis of sections containing dielectric slabs with interfaces in the vertical or y-z plane, TE-to-*x* and TM-to-*x* modes can be used, since no coupling occurs between the TE and TM modes at dielectric interfaces that are normal to the reference direction for the modes. As discussed in Section 2.3.1, the subregions in the section must uniform, otherwise there will be coupling between TE and TM-to-*x* *y*-modes at *layer* interfaces. Coupling between mode functions in different subregions results only from discontinuities in the conducting boundary of the section rather than from changes in dielectric constants, making these modes an ideal choice for selected dielectric waveguides.

(iii)   For sections filled with a medium of uniform dielectric constant, TE and TM-to-z modes are uncoupled. Therefore, this choice of modes can lead to considerable savings in computational overhead arising from simplified mode coupling between subregions. In addition, the z-modes subsequently calculated using the *x* and *y*-modes in each sections can be readily identified as TE or TM-to-z, which can simplify the physical interpretation of the results.

A number of two-dimensional transverse resonance analyses have been developed including those described in [12], [13], and [19]-[25]. Although varying significantly in detail, the general procedure is similar in all cases.

2.3.2.1   Mode Function Derivation

In this section, the components of *x*-mode fields transverse to the *x*-direction are related to the voltages and currents on the *y*-mode transmission lines. This step is essential for combining subregions into a complete two-dimensional section using the transmission line network discussed in Section 2.3.2.

The general technique used to generate the mode functions follows Felsen and Marcuvitz [10], and is derived in Appendix I. The derivation of TE and TM-to-*y* mode functions is presented in this section, with the corresponding derivations for TE, TM-to-*x* and TE, TM-to-z modes included in Appendix II for completeness.

TE-to-*y* modes

Since $e_y = 0$, the modal fields transverse to x are

$$\mathbf{e}_T(y,z) = e_z^{'}(y)e^{-jk_z z}\mathbf{u}_z$$

$$\mathbf{h}_T(y,z) = h_y^{'}(y)e^{-jk_z z}\mathbf{u}_y + h_z^{'}(y)e^{-jk_z z}\mathbf{u}_z$$

where $e_z^{'}(y)$, $h_y^{'}(y)$ and $h_z^{'}(y)$ are field coefficients which depend on y only and the prime indicates a TE mode. Following the derivation in Appendix I, the transverse components of the modal electric and magnetic fields are related by

$$k_x Y_x^{'} \mathbf{h}_T(y,z) = \omega\varepsilon\left[\mathbf{1}_t + \frac{\nabla_t\nabla_t}{k^2}\right]\bullet\mathbf{u_x}\times\mathbf{e}_T(y,z)$$

Writing the field components explicitly and cancelling the $e^{-jk_z z}$ factor yields

$$k_x Y'_x (h'_y \mathbf{u_y} + h'_z \mathbf{u_z}) = -\frac{\omega\varepsilon}{k^2}\left(\left(\frac{\partial^2}{\partial y^2} + k^2\right)e'_z \mathbf{u_y} - jk_z\frac{\partial e'_z}{\partial y}\mathbf{u_z}\right)$$

Using

$$\left(\frac{\partial^2}{\partial y^2} + k^2\right)e'_z = \left(\frac{\partial^2}{\partial y^2} + k_y^2\right)e'_z + (k^2 - k_y^2)e'_z$$

$$= k_u^2 e'_z$$

and choosing the arbitrary admittance factor to be

$$Y'_x = \frac{k_u^2}{k_x \omega\mu}$$

then the following relationships between the electric and magnetic field components transverse to x emerge

$$h'_y = -e'_z$$

and

$$h'_z = \frac{jk_z}{k_u^2}\frac{\partial e'_z}{\partial y}$$

The field quantities can be related to the voltages and currents on an equivalent transmission line network as shown in Figure 2.2 by setting

$$e'_z = V'_y(y)$$

This allows the magnetic field components to be specified as

$$h'_y = -V'_y(y)$$

and

$$h'_z = \frac{jk_z}{k_u^2}\frac{d}{dy}V'_y(y)$$

$$= \frac{k_z k_0}{k_u^2}\frac{1}{Y_0}I'_y(y)$$

since, according to transmission line theory,

$$\frac{d}{dy}V'_y(y) = -jk_y\frac{1}{Y'}I'_y(y) = -jk_0\frac{1}{Y_0}I'_y(y)$$

TM-to-y

Proceeding in a manner identical to the TE-to-y mode treatment and using $h_y = 0$, the modal fields transverse to x are

$$\mathbf{h}_T(y,z) = h_z''(y)e^{-jk_z z}\mathbf{u_z}$$

$$\mathbf{e}_T(y,z) = e_y''(y)e^{-jk_z z}\mathbf{u_y} + e_z''(y)e^{-jk_z z}\mathbf{u_z}$$

where $h_z''(y)$, $e_y''(y)$ and $e_z''(y)$ are field coefficients which depend on y only and the double prime indicates a TM mode. Following the derivation in Appendix I, the transverse components of the modal electric and magnetic fields are related by

$$k_x Z_x'' \mathbf{e}_T(y,z) = \omega\left[\mu\mathbf{1}_t + \frac{1}{\omega^2}\ \nabla_t \frac{1}{\varepsilon(y)}\ \nabla_t\right]\bullet\mathbf{h}_T(y,z)\times\mathbf{u_x}$$

Writing the field components explicitly and cancelling the $e^{-jk_z z}$ factor

$$k_x Z_x''(e_y''\mathbf{u_y} + e_z''\mathbf{u_z}) = \frac{\omega\mu}{k_0^2}\left(\left(\frac{\partial}{\partial y}\frac{1}{\varepsilon_l(y)}\frac{\partial}{\partial y} + k_0^2\right)h_z''\mathbf{u_y} - jk_z\frac{1}{\varepsilon_l(y)\partial y}\frac{\partial h_z''}{\partial y}\mathbf{u_z}\right)$$

A simplification can be made using

$$\left(\frac{\partial}{\partial y}\frac{1}{\varepsilon_l(y)}\frac{\partial}{\partial y} + k_0^2\right) = \frac{\partial}{\partial y}\frac{1}{\varepsilon_l(y)}\frac{\partial h_z''}{\partial y} + k_{yl}^2\frac{h_z''}{\varepsilon_l(y)} + \left(k_0^2\varepsilon_l(y) - k_{yl}^2\right)\frac{h_z''}{\varepsilon_l(y)}$$

$$= k_u^2\frac{h_z''}{\varepsilon_l}$$

since $\varepsilon_l(y)$ is constant within each layer. By choosing the arbitrary impedance factor to be

$$Z_x'' = \frac{k_u^2}{k_x\omega\varepsilon_0}$$

then the following relationships between the transverse electric and magnetic field components emerge

$$e_y'' = \frac{h_z''}{\varepsilon_l}$$

and

$$e_z'' = \frac{-jk_z}{k_u^2}\frac{1}{\varepsilon_l}\frac{\partial h_z''}{\partial y}$$

The field quantities can be related to the voltages and currents on the equivalent transmission line network by setting

$$h_z'' = I_y''(y)$$

This allows the electric field components to be specified as

$$e_y^{''} = \frac{I_y^{''}(y)}{\varepsilon_l}$$

and

$$e_z^{''} = \frac{-jk_z}{k_u^2} \frac{1}{\varepsilon_l} \frac{d}{dy} I_y^{''}(y)$$

$$= -\frac{k_z k_0}{k_u^2} Y_0 V_y^{''}(y)$$

2.3.2.2 Mode Coupling

The x-mode fields inside each subregion can now be expressed in terms of y-mode transmission-line voltages and currents. To complete the analysis of a complete section, subregions are stacked together horizontally and the coupling between x-modes in adjacent subregions is evaluated. This coupling satisfies the field continuity across the subregion interface shown in Figure 2.4. The evaluation of this x-mode coupling at subregion interfaces is discussed in this section.

Mode functions in adjacent subregions will be coupled at discontinuities in the conducting region boundaries or dielectric constants between the two subregions. This coupling can be evaluated from continuity of the transverse electric and magnetic field components in the y-z plane of the discontinuity, and from the boundary conditions. Consider an interface between simple regions each consisting of a single subregion, where a change in the region heights or dielectric constants occurs as shown in Figure 2.4.
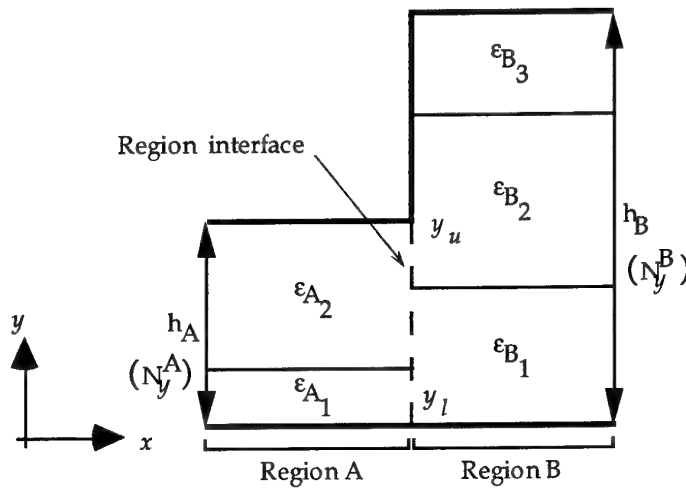
Figure 2.4   Simple region (or subregion) discontinuity

From the definitions of the x-mode voltages and currents stated previously in the introduction to Section 2.3.2, the field components in region A tangential to the discontinuity are given by

$$\mathbf{E}_{T_A} = \sum_m^{N_z} \sum_n^{N_y^A} V_{A_x}^{mn}(x) \mathbf{e}_{T_A}^n(y,z)$$

$$\mathbf{H}_{T_A} = \sum_m^{N_z} \sum_n^{N_y^A} I_{A_x}^{mn}(x) \mathbf{h}_{T_A}^n(y,z)$$

and similarly for region B

$$\mathbf{E}_{T_B} = \sum_m^{N_z} \sum_n^{N_y^B} V_{B_x}^{mn}(x) \mathbf{e}_{T_B}^n(y,z)$$

$$\mathbf{H}_{T_B} = \sum_m^{N_z} \sum_n^{N_y^B} I_{B_x}^{mn}(x) \mathbf{h}_{T_B}^n(y,z)$$

where the summation is over both TE and TM eigenmodes. The ratio between the number of y-modes in regions A and B is determined by the relative convergence criterion

$$\frac{N_y^A}{N_y^B} = \frac{h_A}{h_B}$$

Relative convergence and its explicit role in the solution of characteristic equations encountered in general mode matching analyses is discussed in detail by Leroy [26].

The field matching at the discontinuity requires that

$$\mathbf{E}_{T_B} = \begin{cases} \mathbf{E}_{T_A}, & \text{over aperture} \\ 0, & \text{otherwise} \end{cases}$$

and

$$\mathbf{H}_{T_A} = \mathbf{H}_{T_B} \quad \text{over aperture.}$$

By equating the modal expansions for the fields in regions A and B in the aperture, the coupling relations between the x-mode voltages $V_{A_x}^{mn}(x)$ and $V_{B_x}^{mn}(x)$, and between the x-mode currents $I_{A_x}^{mn}(x)$ and $I_{B_x}^{mn}(x)$ can be evaluated for the mth z mode for all m. This procedure was followed to determine the coupling relations for each of the three types of basis modes, ie., TE, TM to x, y, and z. The coupling expressions were adjusted into a form that guaranteed conservation of complex power across the discontinuity for a finite number of mode functions in each region, while still maintaining the field matching for the ideal case where an infinite number of mode functions are used. In the following section, the TE and TM-to-y mode function coupling expressions are derived. The procedure is to first match the two transverse components of the electric field (the y-component and the z-component), using the appropriate orthonormality relations to simplify the expressions and then repeat the procedure for the two transverse components of the magnetic field. The corresponding derivation for TE, TM-to-x and TE, TM-to-z-modes is given in Appendix III.

Electric Field Matching

y-component

$$\sum_{n}^{N_B^{TM}} V_{B_x}^{''mn} \frac{I_{B_y}^{''n}(y)}{\varepsilon_B(y)} = \sum_{p}^{N_A^{TM}} V_{A_x}^{''mp} \frac{I_{A_y}^{''p}(y)}{\varepsilon_A(y)}$$

After multiplying both sides by $I_{B_y}^{''n}(y)^*$ and integrating along the region interface extending from y_l to $y_u = y_l + h_A$ as shown in Figure 2.4, the orthonormality relation

$$\int_{y_l}^{y_u} I_{B_y}^{''i}(y) \frac{1}{\varepsilon_B(y)} I_{B_y}^{''j}(y)^* dy = \delta_{ij}$$

allows the coupling between the x-mode TM voltages to be determined

$$V_{B_x}^{''mn} = \sum_{p}^{N_A^{TM}} V_{A_x}^{''mp} \int_{y_l}^{y_u} \frac{I_{B_y}^{''n}(y)^* I_{A_y}^{''p}(y)}{\varepsilon_A(y)} dy$$

$$= \sum_{p}^{N_A^{TM}} \mathbf{A}_{np} V_{A_x}^{''mp}$$

where $\mathbf{A}_{np} = \int_{y_l}^{y_u} \frac{I_{B_y}^{''n}(y)^* I_{A_y}^{''p}(y)}{\varepsilon_A(y)} dy$.

z-component

$$\sum_{n}^{N_B^{TE}} V_{B_x}^{'mn} V_{B_y}^{'n}(y) - \sum_{p}^{N_B^{TM}} \frac{k_z^m \omega \varepsilon_0}{k_{u_{p_B}}^{''2}} V_{B_x}^{''mp} V_{B_y}^{''p}(y)$$

$$= \sum_{i}^{N_A^{TE}} V_{A_x}^{'mi} V_{A_y}^{'i}(y) - \sum_{j}^{N_A^{TM}} \frac{k_z^m \omega \varepsilon_0}{k_{u_{j_A}}^{''2}} V_{A_x}^{''mj} V_{A_y}^{''j}(y)$$

After multiplying both sides by $V_{B_y}^{'n}(y)^*$ and integrating along the region interface, the orthonormality relation

$$\int_0^h V_{B_y}^{'i}(y) V_{B_y}^{'j}(y)^* dy = \delta_{ij}$$

allows the coupling between the x-mode TE and TM voltages to be determined

$$V_{B_x}^{'mn} - \sum_{p}^{N_B^{TM}} \frac{k_z^m \omega \varepsilon_0}{k_{u_{p_B}}^{''2}} V_{B_x}^{''mp} \int_{y_l}^{y_u} V_{B_y}^{'n}(y)^* V_{B_y}^{''p}(y) dy$$

$$= \sum_{i}^{N_A^{TE}} V_{A_x}^{'mi} \int_{y_l}^{y_u} V_{B_y}^{'n}(y)^* V_{A_y}^{'i}(y) dy - \sum_{j}^{N_A^{TM}} \frac{k_z^m \omega \varepsilon_0}{k_{u_{j_A}}^{''2}} V_{A_x}^{''mj} \int_{y_l}^{y_u} V_{B_y}^{'n}(y)^* V_{A_y}^{''j} y dy$$

which can be written using suitably defined matrices $\mathbf{F}$, $\mathbf{C}$, and $\mathbf{D}$ as

$$V_{B_x}^{'mn} - \sum_p^{N_B^{TM}} \mathbf{F}_{np} V_{B_x}^{"mp} = \sum_i^{N_A^{TE}} \mathbf{C}_{ni} V_{A_x}^{'mi} - \sum_j^{N_A^{TM}} \mathbf{D}_{nj} V_{A_x}^{"mj}$$

where

$$\mathbf{F}_{np} = \frac{k_z^m \omega \varepsilon_0}{k_{u_{p_B}}^{"2}} \int_{y_l}^{y_u} V_{B_y}^{'n}(y)^* V_{B_y}^{"p}(y) dy$$

$$\mathbf{C}_{ni} = \int_{y_l}^{y_u} V_{B_y}^{'n}(y)^* V_{A_y}^{'i}(y) dy$$

$$\mathbf{D}_{nj} = \frac{k_z^m \omega \varepsilon_0}{k_{u_{j_A}}^{"2}} \int_{y_l}^{y_u} V_{B_y}^{'n}(y)^* V_{A_y}^{"j} y dy$$

In anticipation of later modifications to ensure complex power conservation across the region interface, a matrix $\mathbf{\Phi}$ is defined by

$$\mathbf{\Phi}_{np} = \frac{k_z^m \omega \varepsilon_0}{k_{u_{p_A}}^{"2}} \int_{y_l}^{y_u} V_{A_y}^{'n}(y)^* V_{A_y}^{"p}(y) dy$$

Magnetic Field Matching

y-component

$$\sum_n^{N_A^{TE}} I_{A_x}^{'mn} V_{A_y}^{'n}(y) = \sum_p^{N_B^{TE}} I_{B_x}^{'mp} V_{B_y}^{'p}(y)$$

After multiplying both sides by $V_{A_y}^{'n}(y)^*$ and integrating along the region interface, the orthonormality relation

$$\int_{y_l}^{y_u} V_{A_y}^{'i}(y) V_{A_y}^{'j}(y) dy = \delta_{ij}$$

allows the coupling between the x-mode TE currents to be determined

$$I_{A_x}^{'mn} = \sum_p^{N_B^{TE}} I_{B_x}^{'mp} \int_{y_l}^{y_u} V_{A_y}^{'n}(y)^* V_{B_y}^{'p}(y) dy$$

$$= \sum_p^{N_B^{TE}} \mathbf{C}_{pn}^* I_{B_x}^{'mp}$$

where

$$\mathbf{C}_{pn} = \int_{y_l}^{y_u} V_{A_y}^{'n}(y) V_{B_y}^{'p}(y) dy$$

z-component

$$\sum_{n}^{N_A^{TM}} I_{A_x}^{''mn}(x)I_{A_y}^{''n}(y) + \sum_{p}^{N_A^{TE}} \frac{k_z^m \omega \mu_0}{k_{u_{p_A}}^{'2}} I_{A_x}^{'mp}(x)I_{A_y}^{'p}(y)$$

$$= \sum_{i}^{N_B^{TM}} I_{B_x}^{''mi}(x)I_{B_y}^{''i}(y) + \sum_{j}^{N_B^{TE}} \frac{k_z^m \omega \mu_0}{k_{u_{j_B}}^{'2}} I_{B_x}^{'mj}(x)I_{B_y}^{'j}(y)$$

After multiplying both sides by $I_{A_y}^{''n}(y)^*$ and integrating along the region interface, the orthonormality relation

$$\int_0^h I_{A_y}^{''i}(y) \frac{1}{\varepsilon_A(y)} I_{A_y}^{''j}(y)^* dy = \delta_{ij}$$

allows the coupling between the x-mode TE and TM currents to be determined as

$$I_{A_x}^{''mn} + \sum_{p}^{N_A^{TE}} \frac{k_z^m \omega \mu_0}{k_{u_{p_A}}^{'2}} I_{A_x}^{'mp} \int_{y_l}^{y_u} \frac{I_{A_y}^{''n}(y)^* I_{A_y}^{'p}(y)}{\varepsilon_A(y)} dy$$

$$= \sum_{i}^{N_B^{TM}} I_{B_x}^{''mi} \int_{y_l}^{y_u} \frac{I_{A_y}^{''n}(y)^* I_{B_y}^{''i}(y)}{\varepsilon_A(y)} dy + \sum_{j}^{N_B^{TM}} \frac{k_z^m \omega \mu_0}{k_{u_{j_B}}^{'2}} I_{B_x}^{'mj} \int_{y_l}^{y_u} \frac{I_{A_y}^{''n}(y)^* I_{B_y}^{'j}(y)}{\varepsilon_A(y)} dy$$

which can be written using suitably defined matrices Γ, A and β as

$$I_{A_x}^{''mn} + \sum_{p}^{N_A^{TE}} \Gamma_{np} I_{A_x}^{'mp} = \sum_{i}^{N_B^{TM}} A^*{}_{in} I_{B_x}^{''mi} + \sum_{j}^{N_B^{TM}} \beta_{nj} I_{B_x}^{'mj}$$

where

$$\Gamma_{np} = \frac{k_z^m \omega \mu_0}{k_{u_{p_A}}^{'2}} \int_{y_l}^{y_u} \frac{I_{A_y}^{''n}(y)^* I_{A_y}^{'p}(y)}{\varepsilon_A(y)} dy$$

$$A_{in} = \int_{y_l}^{y_u} \frac{I_{A_y}^{''n}(y) I_{B_y}^{''i}(y)}{\varepsilon_A(y)} dy$$

$$\beta_{nj} = \frac{k_z^m \omega \mu_0}{k_{u_{j_B}}^{'2}} \int_{y_l}^{y_u} \frac{I_{A_y}^{''n}(y)^* I_{B_y}^{'j}(y)}{\varepsilon_A(y)} dy$$

In anticipation of later modifications to ensure complex power conservation across the region interface, define a matrix G is defined by

$$G_{np} = \frac{k_z^m \omega \mu_0}{k_{u_{p_B}}^{'2}} \int_{y_l}^{y_u} I_{B_y}^{''n}(y)^* I_{B_y}^{'p}(y) dy$$

2.3.2.3 Complex Power Conservation

The condition that the transverse electric and magnetic fields be exactly matched across region interface discontinuities will only be satisfied in the ideal case where an infinite number of x-modes are used. For practical purposes, the number of x-modes must be truncated to a finite number, so that exact field matching cannot be achieved in general. However, a physical constraint that power flowing through the region interfaces must be conserved can be enforced on the field matching for an arbitrary finite number of x-modes. That is, the power transmitted in the x-direction from region A must equal the power received in region B, and vice versa. Both the real and imaginary components of the power flow are matched at the interfaces to enforce this most fundamental physical constraint on the x-mode coupling at region interfaces. This general procedure has previously been applied to a two-dimensional mode matching analysis by Mansour and MacPhie [27], although only in homogeneous structures. Omar and Schunemann [28] have shown that conservation of complex power can be applied to inhomogeneous structures, and that it follows directly from field matching. This conclusion has been verified by this work.

By constructing column vectors for the x-mode voltages and currents for the mth z-mode (with the TE and TM components separated), and using the matrices defined in Section 2.3.2.2, the coupling expressions from the field matching can be written in matrix form as

$$
\begin{bmatrix} \mathbf{I} & -\mathbf{F} \\ \mathbf{0} & \mathbf{I} \end{bmatrix}
\begin{bmatrix} \mathbf{V'}_{B_x}^m \\ \mathbf{V''}_{B_x}^m \end{bmatrix} =
\begin{bmatrix} \mathbf{C} & -\mathbf{D} \\ \mathbf{0} & \mathbf{A} \end{bmatrix}
\begin{bmatrix} \mathbf{V'}_{A_x}^m \\ \mathbf{V''}_{A_x}^m \end{bmatrix}
$$

$$
\begin{bmatrix} \mathbf{I} & \mathbf{0} \\ \Gamma & \mathbf{I} \end{bmatrix}
\begin{bmatrix} \mathbf{I'}_{A_x}^m \\ \mathbf{I''}_{A_x}^m \end{bmatrix} =
\begin{bmatrix} \mathbf{C}^\dagger & \mathbf{0} \\ \beta & \mathbf{A}^\dagger \end{bmatrix}
\begin{bmatrix} \mathbf{I'}_{B_x}^m \\ \mathbf{I''}_{B_x}^m \end{bmatrix}
$$

The power flow through the region interface on either side of the discontinuity for the mth z-mode is determined from the fields in region A and region B using the x-mode voltages and currents as follows

$$
P_{A_x}^m = \int_{y_l}^{y_u} \mathbf{E}_{T_A}^m \times \mathbf{H}_{T_A}^{m\,*} \bullet \mathbf{u}_x dy
$$

$$
= \sum_n^{N_y^A} \sum_p^{N_y^A} V_{A_x}^{mn} I_{A_x}^{mp\,*} \int_{y_l}^{y_u} \mathbf{e}_{T_A}^n \times \mathbf{h}_{T_A}^{p\,*} \bullet \mathbf{u}_x \, dy
$$

$$
P_{B_x}^m = \int_{y_l}^{y_u} \mathbf{E}_{T_B}^m \times \mathbf{H}_{T_B}^{m\,*} \bullet \mathbf{u}_x dy
$$

$$
= \sum_n^{N_y^A} \sum_p^{N_y^A} V_{B_x}^{mn} I_{B_x}^{mp\,*} \int_{y_l}^{y_u} \mathbf{e}_{T_B}^n \times \mathbf{h}_{T_B}^{p\,*} \bullet \mathbf{u}_x \, dy
$$

For any given region, e_T^n and h_T^{p*} may be split into TE and TM components and the integral evaluated using the previously defined mode functions as follows

$$\int_{y_l}^{y_u} e_T'^n \times h_T'^{p*} \bullet \mathbf{u_x}\, dy = \int_{y_l}^{y_u} e_z'^n \mathbf{u_z} \times (h_y'^{p*} \mathbf{u_y} + h_z'^{p*} \mathbf{u_z})] \bullet \mathbf{u_x}\, dy$$

$$= \int_{y_l}^{y_u} -e_z'^n (y) h_y'^p (y)^* dy$$

$$= \int_{y_l}^{y_u} V_y'^n (y) V_y'^p (y)^* dy$$

$$= \delta_{np}$$

$$\int_{y_l}^{y_u} e_T''^n \times h_T''^{p*} \bullet \mathbf{u_x}\, dy = \int_{y_l}^{y_u} [(e_y''^n \mathbf{u_y} + e_z''^n \mathbf{u_z}) \times h_z''^{p*} \mathbf{u_z}] \bullet \mathbf{u_x}\, dy$$

$$= \int_{y_l}^{y_u} [e_y''^n (y) h_z''^p (y)^*]\, dy$$

$$= \int_{y_l}^{y_u} \frac{I_y''^n (y) I_y''^p (y)^*}{\varepsilon_r(y)}\, dy$$

$$= \delta_{np}$$

$$\int_{y_l}^{y_u} e_T''^n \times h_T'^{p*} \bullet \mathbf{u_x}\, dy = \int_{y_l}^{y_u} [(e_y''^n \mathbf{u_y} + e_z''^n \mathbf{u_z}) \times (h_y'^{p*} \mathbf{u_y} + h_z'^{p*} \mathbf{u_z})] \bullet \mathbf{u_x}\, dy$$

$$= \int_{y_l}^{y_u} [e_y''^n (y) h_z'^p (y)^* - e_z''^n (y) h_y'^p (y)^*]\, dy$$

$$= \frac{k_z \omega \mu_0}{k_{up}'^2} \int_{y_l}^{y_u} \frac{I_y''^n (y) I_y'^p (y)^*}{\varepsilon_r(y)}\, dy - \frac{k_z^* \omega \varepsilon_0}{k_{un}''^2} \int_{y_l}^{y_u} V_y''^n (y) V_y'^p (y)^*\, dy$$

$$\int_{y_l}^{y_u} e_T'^n \times h_T''^{p*} \bullet \mathbf{u_x}\, dy = 0$$

The coupling between the modal fields in regions A and B is required to be such that the power coupled from region A to region B is the same as the power coupled from region B to region A. For region A

$$
P_{A_x}^m = \begin{bmatrix} I_{A_x}^m \\ \hline I_{A_x}''^m \end{bmatrix}^\dagger \begin{bmatrix} I & \Gamma^\dagger\text{-}\Phi \\ \hline 0 & I \end{bmatrix} \begin{bmatrix} V_{A_x}^m \\ \hline V_{A_x}''^m \end{bmatrix}
$$

$$
= \begin{bmatrix} I_{B_x}^m \\ \hline I_{B_x}''^m \end{bmatrix}^\dagger \begin{bmatrix} C & \beta^\dagger \\ \hline 0 & A \end{bmatrix} \begin{bmatrix} I & \Gamma^\dagger \\ \hline 0 & I \end{bmatrix}^{-1} \begin{bmatrix} I & \Gamma^\dagger\text{-}\Phi \\ \hline 0 & I \end{bmatrix} \begin{bmatrix} V_{A_x}^m \\ \hline V_{A_x}''^m \end{bmatrix}
$$

$$
= \begin{bmatrix} I_{B_x}^m \\ \hline I_{B_x}''^m \end{bmatrix}^\dagger \begin{bmatrix} C & \beta^\dagger\text{-}C\Gamma^\dagger \\ \hline 0 & A \end{bmatrix} \begin{bmatrix} I & \Gamma^\dagger\text{-}\Phi \\ \hline 0 & I \end{bmatrix} \begin{bmatrix} V_{A_x}^m \\ \hline V_{A_x}''^m \end{bmatrix}
$$

$$
= \begin{bmatrix} I_{B_x}^m \\ \hline I_{B_x}''^m \end{bmatrix}^\dagger \begin{bmatrix} C & \beta^\dagger\text{-}C\Phi \\ \hline 0 & A \end{bmatrix} \begin{bmatrix} V_{A_x}^m \\ \hline V_{A_x}''^m \end{bmatrix}
$$

and for region B

$$
P_{B_x}^m = \begin{bmatrix} I_{B_x}^m \\ \hline I_{B_x}''^m \end{bmatrix}^\dagger \begin{bmatrix} I & G^\dagger\text{-}F \\ \hline 0 & I \end{bmatrix} \begin{bmatrix} V_{B_x}^m \\ \hline V_{B_x}''^m \end{bmatrix}
$$

$$
= \begin{bmatrix} I_{B_x}^m \\ \hline I_{B_x}''^m \end{bmatrix}^\dagger \begin{bmatrix} I & G^\dagger\text{-}F \\ \hline 0 & I \end{bmatrix} \begin{bmatrix} I & F \\ \hline 0 & I \end{bmatrix}^{-1} \begin{bmatrix} C & \text{-}D \\ \hline 0 & A \end{bmatrix} \begin{bmatrix} V_{A_x}^m \\ \hline V_{A_x}''^m \end{bmatrix}
$$

$$
= \begin{bmatrix} I_{B_x}^m \\ \hline I_{B_x}''^m \end{bmatrix}^\dagger \begin{bmatrix} I & G^\dagger \\ \hline 0 & I \end{bmatrix} \begin{bmatrix} C & \text{-}D \\ \hline 0 & A \end{bmatrix} \begin{bmatrix} V_{A_x}^m \\ \hline V_{A_x}''^m \end{bmatrix}
$$

$$
= \begin{bmatrix} I_{B_x}^m \\ \hline I_{B_x}''^m \end{bmatrix}^\dagger \begin{bmatrix} C & G^\dagger A\text{-}D \\ \hline 0 & A \end{bmatrix} \begin{bmatrix} V_{A_x}^m \\ \hline V_{A_x}''^m \end{bmatrix}
$$

So to ensure conservation of complex power for an arbitrary number of x-modes, the following substitutions must be made

$$\beta \rightarrow G^\dagger A$$

$$D \rightarrow C\Phi$$

For these substitutions to have physical relevance, they must be automatically satisfied for an infinite number of modes, showing that the fields on each side of the discontinuity

will still match if infinite modes are used. This can be shown using the completeness of an infinite set of eigenmodes as follows

$$[GA]_{np} = \sum_q^{N_B^{TM}} \frac{k_z^m \omega \mu_0}{k_{u_{n_B}}^{'2}} \int_{y_l}^{y_u} \frac{I_{B_y}^{"q}(y) I_{B_y}^{'n}(y)^*}{\varepsilon_B(y)} dy \int_{y_l}^{y_u} \frac{I_{A_y}^{"p}(y') I_{B_y}^{"q}(y')}{\varepsilon_A(y')} dy'$$

$$= \frac{k_z^m \omega \mu_0}{k_{u_{n_B}}^{'2}} \int_{y_l}^{y_u} \int_{y_l}^{y_u} \frac{I_{B_y}^{'n}(y)^* I_{A_y}^{"p}(y')}{\varepsilon_A(y')} \sum_q^{N_B^{TM}} \frac{I_{B_y}^{"q}(y) I_{B_y}^{"q}(y')}{\varepsilon_B(y)} dy \, dy'$$

$$= \frac{k_z^m \omega \mu_0}{k_{u_{n_B}}^{'2}} \int_{y_l}^{y_u} \frac{I_{B_y}^{'n}(y)^* I_{A_y}^{"p}(y)}{\varepsilon_A(y')} dy$$

$$= \left[\beta^\dagger\right]_{np} \quad \text{as required.}$$

Similarly

$$[C\Phi]_{np} = \sum_q^{N_A^{TE}} \int_{y_l}^{y_u} V_{B_y}^{'n}(y)^* V_{A_y}^{'q}(y) dy \frac{k_z^m \omega \varepsilon_0}{k_{u_{p_A}}^{'2}} \int_{y_l}^{y_u} V_{A_y}^{'q}(y')^* V_{A_y}^{"p}(y') dy'$$

$$= \frac{k_z^m \omega \varepsilon_0}{k_{u_{p_A}}^{'2}} \int_{y_l}^{y_u} \int_{y_l}^{y_u} V_{B_y}^{'n}(y)^* V_{A_y}^{"p}(y') \sum_q^{N_A^{TE}} V_{A_y}^{'q}(y')^* V_{A_y}^{'q}(y) \, dy \, dy'$$

$$= \frac{k_z^m \omega \varepsilon_0}{k_{u_{p_A}}^{'2}} \int_{y_l}^{y_u} V_{B_y}^{'n}(y)^* V_{A_y}^{"p}(y) \, dy$$

$$= \mathbf{D}_{np} \quad \text{as required.}$$

The final form for the coupling which guarantees conservation of complex power for any number of x-modes in each region is therefore

$$\begin{bmatrix} I & -F \\ 0 & I \end{bmatrix} \begin{bmatrix} V_{B_x}^{'m} \\ V_{B_x}^{"m} \end{bmatrix} = \begin{bmatrix} C & -C\Phi \\ 0 & A \end{bmatrix} \begin{bmatrix} V_{A_x}^{'m} \\ V_{A_x}^{"m} \end{bmatrix}$$

$$\begin{bmatrix} I & 0 \\ \Gamma & I \end{bmatrix} \begin{bmatrix} I_{A_x}^{'m} \\ I_{A_x}^{"m} \end{bmatrix} = \begin{bmatrix} C^\dagger & 0 \\ A^\dagger G & A^\dagger \end{bmatrix} \begin{bmatrix} I_{B_x}^{'m} \\ I_{B_x}^{"m} \end{bmatrix}$$

2.3.2.4 Constructing Admittance Matrices

So far, only simple region interfaces have been considered, i.e. regions that do not contain subregions separated by conducting boundaries. At this point, it is necessary to consider more complex regions consisting of more than one subregion such as shown in Figure 2.5. The procedure is to calculate the two-port x-mode admittance matrices of the subregions in a given region, calculate the coupling matrices for the interfaces between connected subregions, and then combine the admittance matrices and the coupling to produce a new admittance matrix for the region which now includes the coupling to other regions. In this manner, a series of multiport admittance matrices can be constructed to represent each

region in a given section. When cascaded together in the correct manner, these admittances represent the entire section under consideration. Note that the independent subregions in a given region are vertically aligned but separated by conducting metal surfaces, so that no y-mode coupling exists between them.
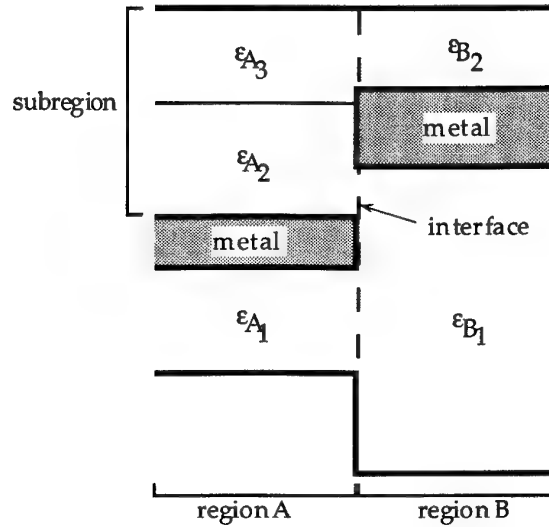
Figure 2.5   Complex region interface with independent layers

The coupling expressions relating the x-mode voltages and currents for the mth z-mode between connected subregions as derived in Section 2.3.2.3 are used in the form

$$
\begin{bmatrix} I_{A_x}^m \\ ---- \\ V_{B_x}^m \end{bmatrix} = \begin{bmatrix} 0 & \vdots & P_I \\ ---------- \\ P_V & \vdots & 0 \end{bmatrix} \begin{bmatrix} V_{A_x}^m \\ ---- \\ I_{B_x}^m \end{bmatrix}
$$

for "step-up" transitions (height of subregion A smaller than height of subregion B), and

$$
\begin{bmatrix} V_{A_x}^m \\ ---- \\ I_{B_x}^m \end{bmatrix} = \begin{bmatrix} 0 & \vdots & P_V \\ ---------- \\ P_I & \vdots & 0 \end{bmatrix} \begin{bmatrix} I_{A_x}^m \\ ---- \\ V_{B_x}^m \end{bmatrix}
$$

for "step-down" transitions (height of subregion A larger than height of subregion B). P_I and P_V are the current and voltage couplings, respectively. These coupling expressions are listed in Appendix IV for the various choices of eigenmode types in subregions A and B.

The coupling expressions above show that currents in the smaller subregion can be expressed in terms of currents in the larger subregion, but not vice versa. This is because of the lack of a suitable constraint on the tangential component of the magnetic field of the larger subregion on the aperture wall. Since magnetic field matching can only be considered over the aperture itself, it is only possible to determine the currents in the smaller subregion from the currents in the larger region. To determine the currents in the larger region from the currents in the smaller region requires the nonexistent magnetic field boundary condition on the aperture wall.

Such a boundary condition does exist for the electric field however, namely that the tangential electric field is required to be zero on the aperture wall. This condition is used to derive the voltage coupling relating the voltages in the larger subregion to the voltages

in the smaller subregion. However, if the tangential electric field must be zero on the aperture wall then an arbitrary electric field is not allowed in the larger subregion. Therefore, it follows that a coupling expression relating the voltage in the smaller subregion to an arbitrary voltage in the larger subregion cannot be defined. These considerations are also discussed in [28]. Note that it is possible to numerically invert the coupling matrices to circumvent this problem if the same number of x-modes are used in each subregion. However, not only does this approach violate relative convergence, it also leads to a very ill-conditioned formulation.

A subregion with a two-port modal admittance matrix Y_S contained in a given region which is coupled to M subregions in a region on the input (left) side and N subregions in another region on the output (right) side is shown schematically in Figure 2.6. The voltage and current couplings at the mth input port are written as $P_{V_i}^m$ and $P_{I_i}^m$ respectively, and the corresponding couplings at the nth output port as $P_{V_o}^n$ and $P_{I_o}^n$ respectively.
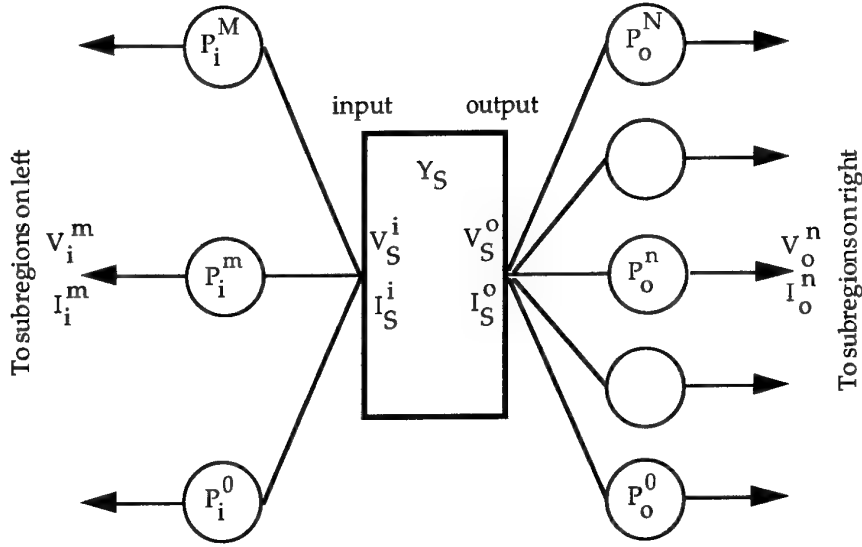
Figure 2.6 **Multiport admittance block constructed from two-port subregion coupled to other subregions**

The voltages at the parallel outputs of the coupling ports sum to yield the total voltage at the subregion admittance ports. Therefore, using the x-mode voltage and current coupling expressions, the voltages and currents at the input and output ports of the subregion were given by

$$V_S^i = \sum_{m}^{M} \mathbf{P}_{V_i}^m V_i^m \qquad \text{for "step – up" transition, undefined otherwise.}$$

$$V_S^o = \sum_{n}^{N} \mathbf{P}_{V_o}^n V_o^n \qquad \text{for "step – down" transition, undefined otherwise.}$$

$$I_i^m = \mathbf{P}_{I_i}^m I_S^i \qquad \text{for "step – down" transition, undefined otherwise.}$$

$$I_o^n = \mathbf{P}_{I_o}^n I_S^o \qquad \text{for "step – up" transition, undefined otherwise.}$$

The restrictions discussed previously relating to the boundary transitions that may be represented by the coupling expressions do not, in practice, restrict the geometry of

structures that can be analysed. Any arbitrary cross-section can be divided such that all the region couplings are included at the input or output ports of the subregion admittances as required. Step-down transitions are assigned to the output of the adjacent subregion to the left, while step-up transitions are assigned to the input of the adjacent subregion to the right.

The current at the input and output ports of the subregion, I_S^i and I_S^o, can be expressed in terms of the input and output voltages, V_S^i and V_S^o using the two-port subregion admittance as

$$I_S^i = \mathbf{Y}_{S_{00}} V_S^i + \mathbf{Y}_{S_{01}} V_S^o$$

$$I_S^o = \mathbf{Y}_{S_{10}} V_S^i + \mathbf{Y}_{S_{11}} V_S^o$$

Therefore, the current at the mth input port can be written as

$$I_i^m = \mathbf{P}_{I_i}^m \mathbf{Y}_{S_{00}} \sum_n^M \mathbf{P}_{V_i}^n V_i^n + \mathbf{P}_{I_i}^m \mathbf{Y}_{S_{01}} \sum_p^N \mathbf{P}_{V_o}^p V_o^p$$

Similarly, the current at the nth output port is given by

$$I_o^n = \mathbf{P}_{I_o}^n \mathbf{Y}_{S_{10}} \sum_n^M \mathbf{P}_{V_i}^m V_i^m + \mathbf{P}_{I_o}^n \mathbf{Y}_{S_{11}} \sum_p^N \mathbf{P}_{V_o}^p V_o^p$$

Therefore, a multiport admittance matrix which represents both the subregion and the coupling to regions on each side containing multiple subregions can be defined

$$\begin{bmatrix} I_i^0 \\ \vdots \\ I_i^M \\ --- \\ I_o^0 \\ \vdots \\ I_o^N \end{bmatrix} = \begin{bmatrix} [\mathbf{Y_{M00}}] & | & [\mathbf{Y_{M01}}] \\ ------ & --- & ------ \\ [\mathbf{Y_{M10}}] & | & [\mathbf{Y_{M11}}] \end{bmatrix} \begin{bmatrix} V_i^0 \\ \vdots \\ V_i^M \\ --- \\ V_o^0 \\ \vdots \\ V_o^N \end{bmatrix}$$

where

$$\mathbf{Y_{M00}}^{np} = \mathbf{P}_{I_i}^n \mathbf{Y}_{S_{00}} \mathbf{P}_{V_i}^p$$

$$\mathbf{Y_{M01}}^{np} = \mathbf{P}_{I_i}^n \mathbf{Y}_{S_{01}} \mathbf{P}_{V_o}^p$$

$$\mathbf{Y_{M10}}^{np} = \mathbf{P}_{I_o}^n \mathbf{Y}_{S_{10}} \mathbf{P}_{V_i}^p$$

$$\mathbf{Y_{M11}}^{np} = \mathbf{P}_{I_o}^n \mathbf{Y}_{S_{11}} \mathbf{P}_{V_o}^p$$

2.3.2.5 Cascading Admittance Matrices

The admittance matrices derived in Section 2.3.2.4 which contain both the subregion modal admittances and the associated couplings are cascaded to represent an entire section. The cascading of two multiple-port admittances $\mathbf{Y_A}$ and $\mathbf{Y_B}$ to form a single multiple-port admittance, $\mathbf{Y_C}$, as shown in Figure 2.7, is similar to simple 2-port admittance cascading.
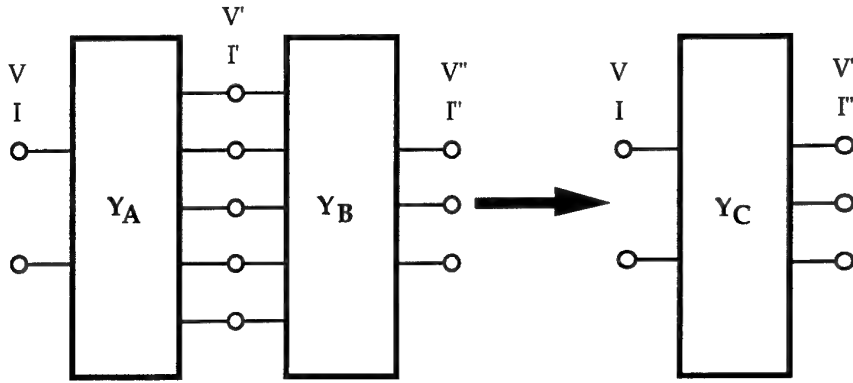
Figure 2.7   Multiport admittance cascade

The currents at the input and output ports for admittance $\mathbf{Y_A}$ are related to the voltages by

$$I_n = \sum_p^N \mathbf{Y_A}_{00}^{np} V_p + \sum_q^{N'} \mathbf{Y_A}_{01}^{nq} V_q'$$

$$I_n' = \sum_p^N \mathbf{Y_A}_{10}^{np} V_p + \sum_q^{N'} \mathbf{Y_A}_{11}^{nq} V_q'$$

and similarly for $\mathbf{Y_B}$

$$-I_n' = \sum_p^{N'} \mathbf{Y_B}_{00}^{np} V_p' + \sum_q^{N''} \mathbf{Y_B}_{01}^{nq} V_q''$$

$$I_n'' = \sum_p^{N'} \mathbf{Y_B}_{10}^{np} V_p' + \sum_q^{N''} \mathbf{Y_B}_{11}^{nq} V_q''$$

In matrix form

$$\mathbf{I} = \mathbf{Y_{A00}} \mathbf{V} + \mathbf{Y_{A01}} \mathbf{V'}$$

$$\mathbf{I'} = \mathbf{Y_{A10}} \mathbf{V} + \mathbf{Y_{A11}} \mathbf{V'} = -\left[\mathbf{Y_{B00}} \mathbf{V'} + \mathbf{Y_{B01}} \mathbf{V''} \right]$$

$$\mathbf{I''} = \mathbf{Y_{B10}} \mathbf{V'} + \mathbf{Y_{B11}} \mathbf{V''}$$

Substituting for $\mathbf{I'}$

$$\left[\mathbf{Y_{A11}} + \mathbf{Y_{B00}} \right] \mathbf{V'} = -\left[\mathbf{Y_{A10}} \mathbf{V} + \mathbf{Y_{B01}} \mathbf{V''} \right]$$

Defining

$$\mathbf{Y_{inv}} = \left[\mathbf{Y_{A11}} + \mathbf{Y_{B00}} \right]^{-1}$$

and substituting for V' allows I, and I" to be determined in terms of V, and V"

$$I = \left[Y_{A00} - Y_{A01} Y_{inv} Y_{A10} \right] V - Y_{A01} Y_{inv} Y_{B01} V''$$

$$I'' = -Y_{B10} Y_{inv} Y_{A10} V + \left[Y_{B11} - Y_{B10} Y_{inv} Y_{B01} \right] V''$$

In matrix form

$$\begin{bmatrix} I \\ \hline I'' \end{bmatrix} = \begin{bmatrix} Y_{C00} & Y_{C01} \\ \hline Y_{C10} & Y_{C11} \end{bmatrix} \begin{bmatrix} V \\ \hline V'' \end{bmatrix}$$

$$= \begin{bmatrix} [Y_{A00} - Y_{A01} Y_{inv} Y_{A10}] & -Y_{A01} Y_{inv} Y_{B01} \\ \hline -Y_{B10} Y_{inv} Y_{A10} & [Y_{B11} - Y_{B10} Y_{inv} Y_{B01}] \end{bmatrix} \begin{bmatrix} V \\ \hline V'' \end{bmatrix}$$

2.3.2.6 Junction Admittance Calculation

By applying the multiport admittance cascading discussed in Section 2.3.2.5 in an appropriate manner, the section to be analysed can be reduced to two multiport admittances Y_L and Y_R representing the structure on the left and right sides of a junction plane. The position of the junction plane can be arbitrary, but is usually set at the left side of the region containing the subregion with the minimum number of y-modes. This subregion is termed the junction subregion. Selecting the subregion with the smallest number of y-modes improves computational efficiency. This situation is shown diagrammatically in Figure 2.8.

A two-port admittance matrix Y_J for the junction was determined in order to apply transverse resonance to the two-dimensional section. This two-port is constructed from the admittances "seen" by looking to the left and right of the junction plane. By definition, the junction subregion is at port n_J of Y_R and port n_J of Y_L. From the definition of Y-parameters, the current at the nth port of Y_L is given by

$$I_L^n = \sum_p^N Y_L^{np} V_L^p$$

and similarly the current at the nth port of Y_R is

$$I_R^n = \sum_p^N Y_R^{np} V_R^p$$

Connecting all the ports of Y_l and Y_R except for the junction port, n_J, leads to

$$I_L^n = -I_R^n \quad \text{and} \quad V_L^n = V_R^n \quad \text{for } n \neq n_J.$$
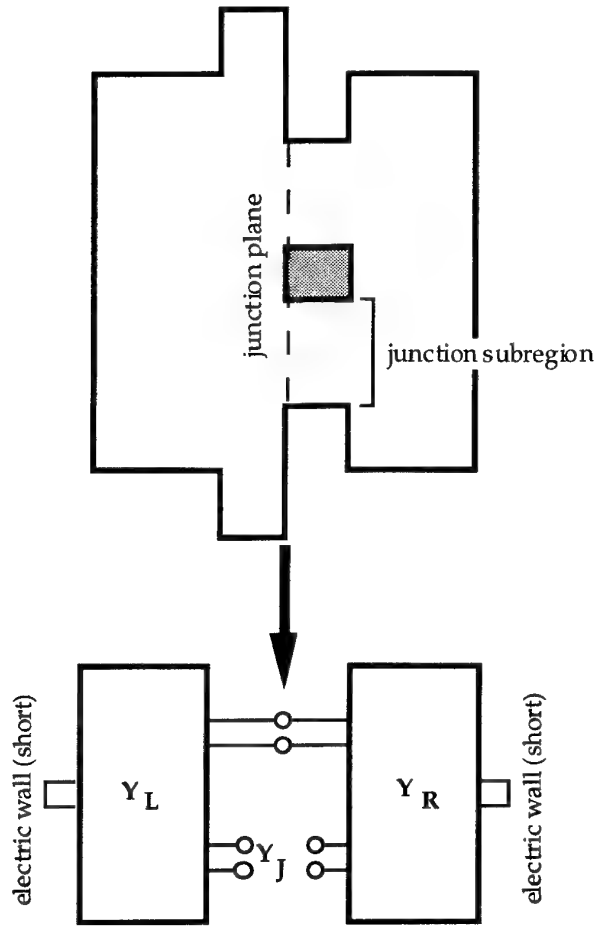
Figure 2.8   Reduction of cross section to 2-port junction admittance

The input and output currents for the junction port, $I_L^{n_J}$ and $I_R^{n_J}$, are given in terms of the voltages at the other ports by

$$I_L^{n_J} = \sum_p^N Y_L^{n_J p} V_L^p$$

$$= Y_L^{n_J n_J} V_L^{n_J} + \sum_{p \neq n_J}^N Y_L^{n_J p} V_L^p$$

$$= Y_L^{n_J n_J} V_L^{n_J} + \sum_{p \neq n_J}^N Y_L^{n_J p} V_R^p$$

and

$$I_R^{n_J} = Y_R^{n_J n_J} V_R^{n_J} + \sum_{p \neq n_J}^N Y_R^{n_J p} V_R^p$$

Now consider the currents at the nth port of Y_1 for $n \neq n_J$

$$I_L^n = Y_L^{nn_J} V_L^{n_J} + \sum_{p \neq n_J}^{N} Y_L^{np} V_R^p$$

and similarly for Y_R

$$I_R^n = Y_R^{nn_J} V_R^{n_J} + \sum_{p \neq n_J}^{N} Y_R^{np} V_R^p$$

Therefore, since $I_L^n = -I_R^n$ for $n \neq n_j$,

$$[Y_L^{nn_J} V_L^{n_J} + Y_R^{nn_J} V_R^{n_J}] = - \sum_{p \neq n_J}^{N} [Y_L^{np} + Y_R^{np}] V_R^p$$

Define

$$\mathbf{Y}_{inv} = \mathbf{A}^{-1}$$

where

$$A_{np} = [Y_L^{np} + Y_R^{np}] \qquad \text{for } n,p \neq n_J.$$

so that for $n \neq n_J$

$$V_R^n = - \sum_{p \neq n_J}^{N} Y_{inv}^{np} [Y_L^{pn_J} V_L^{n_J} + Y_R^{pn_J} V_R^{n_J}]$$

Hence, substituting for V_R^n ($n \neq n_J$)

$$I_L^{n_J} = \left[Y_L^{n_J n_J} - \sum_{p \neq n_J}^{N} \sum_{q \neq n_J}^{N} Y_L^{n_J p} Y_{inv}^{pq} Y_L^{qn_J} \right] V_L^{n_J} - \left[\sum_{p \neq n_J}^{N} \sum_{q \neq n_J}^{N} Y_L^{n_J p} Y_{inv}^{pq} Y_R^{qn_J} \right] V_R^{n_J}$$

$$I_R^{n_J} = - \left[\sum_{p \neq n_J}^{N} \sum_{q \neq n_J}^{N} Y_R^{n_J p} Y_{inv}^{pq} Y_L^{qn_J} \right] V_L^{n_J} + \left[Y_R^{n_J n_J} - \sum_{p \neq n_J}^{N} \sum_{q \neq n_J}^{N} Y_R^{n_J p} Y_{inv}^{pq} Y_R^{qn_J} \right] V_R^{n_J}$$

So the 2-port admittance matrix representing the junction is

$$\begin{bmatrix} I_L^{n_J} \\ --- \\ I_R^{n_J} \end{bmatrix} = \begin{bmatrix} Y_{J00} & | & Y_{J01} \\ ------ & & ------ \\ Y_{J10} & | & Y_{J11} \end{bmatrix} \begin{bmatrix} V_L^{n_J} \\ --- \\ V_R^{n_J} \end{bmatrix}$$

where

$$Y_{J00} = \left[Y_L^{n_J n_J} - \sum_{p \neq n_J}^{N} \sum_{q \neq n_J}^{N} Y_L^{n_J p} Y_{inv}^{pq} Y_L^{q n_J} \right]$$

$$Y_{J01} = - \sum_{p \neq n_J}^{N} \sum_{q \neq n_J}^{N} Y_L^{n_J p} Y_{inv}^{pq} Y_R^{q n_J}$$

$$Y_{J10} = - \sum_{p \neq n_J}^{N} \sum_{q \neq n_J}^{N} Y_R^{n_J p} Y_{inv}^{pq} Y_L^{q n_J}$$

$$Y_{J11} = \left[Y_R^{n_J n_J} - \sum_{p \neq n_J}^{N} \sum_{q \neq n_J}^{N} Y_R^{n_J p} Y_{inv}^{pq} Y_R^{q n_J} \right]$$

If port n_J of Y_L and Y_R are connected together and for there to exist a solution in the absence of an excitation source corresponding to a mode of propagation, then

$$I_L^{n_J} = -I_R^{n_J} \text{ and } V_L^{n_J} = V_R^{n_J}$$

Therefore

$$[Y_{J00} + Y_{J01}]V_R^{n_J} = -[Y_{J10} + Y_{J11}]V_R^{n_J}$$

Hence, a physical value for k_z^m is obtained when the following transverse resonance condition is satisfied

$$[Y_{J00} + Y_{J01} + Y_{J10} + Y_{J11}]V_R^{n_J} = [\mathbf{Y}^{sum}]V_R^{n_J} = 0$$

2.3.2.7 Numerical Techniques for Solving the Transverse Resonance Condition

To complete the section analysis, the propagation constants for the z-directed modes, or z-modes, must be determined. This is achieved by performing an iterative search for k_z values which satisfy the transverse resonance condition derived in Section 2.3.2.6. Two markedly different search methods were used here to determine the k_z values satisfying the transverse resonance condition, depending upon whether the required z-modes were propagating or evanescent (purely real or imaginary k_z), or complex (complex k_z).

Propagating or evanescent modes

To find the propagation constants for purely propagating and evanescent z-modes, an iterative search for both zeroes in the determinant and minima in the minimum singular value of $[\mathbf{Y}^{sum}]$ was conducted by decrementing k_z from some initial value. The minimum singular value of $[\mathbf{Y}^{sum}]$ was found using matrix singular value decomposition [29], a technique first applied to the analysis of two-dimensional microwave and millimetre-wave structures by Labay and Bornemann [30]. Figure 2.9 shows a typical z-mode solution corresponding to a minimum (zero) in the minimum singular value and a zero in the determinant of $[\mathbf{Y}^{sum}]$. Note the determinant pole located close to the zero crossing. This was a common feature of the behaviour of the determinant near z-mode solutions, and prompted the use of the more well-behaved minimum singular value. It must be noted that the minimum singular value was not entirely reliable on its own because of extremely narrow minima sometimes encountered. Such minima cannot be detected unless prohibitively small k_z search step sizes are used. For this reason both the determinant and the minimum singular value of $[\mathbf{Y}^{sum}]$ were used to ensure the reliable identification of

valid k_z solutions. Instances where both the determinant and the minimum singular value were not well-behaved near a given z-mode solution were rare.

The following strategy was adopted for finding propagating and evanescent z-modes:

(i)   Start with a value of k_z no larger than $k_0\sqrt{\varepsilon_{r_{max}}}$, where $\varepsilon_{r_{max}}$ is the maximum dielectric constant in the section. Do a coarse search by stepping in the direction of decreasing k_z with a specified step size. Look for minima in the minimum singular value or a change of sign in the determinant of $[Y^{sum}]$. Closely-spaced zero-pole pairs in the determinant which may not result in a change of sign over a coarse step can also be detected.

(ii)   If a possible solution is detected during the coarse search, a prediction of the location of the solution is made and a fine search initiated over a range of one coarse step either side of the estimated position of the k_z solution. The fine step size is typically set to 1/10 of a coarse step. As for the coarse search, look for minima in the minimum singular value or a change of sign in the determinant of $[Y^{sum}]$.
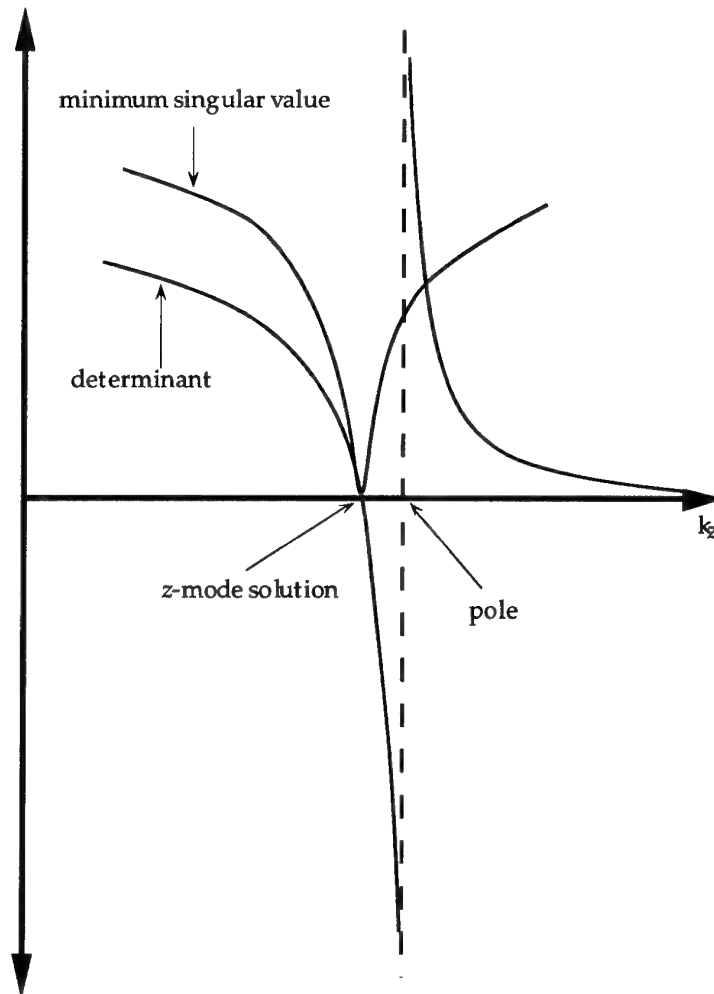
Figure 2.9   Typical z- mode solution

(iii)   If a possible solution is detected during the fine search, an attempt is made to use a quadratic fit to the minimum singular value of $[Y^{sum}]$ to estimate the position of the solution. If this k_z estimate corresponds to a minimum in the minimum singular value then an iterative procedure based on the Brent's method is used to refine the k_z value [31]. Otherwise, a quadratic fit is performed on the determinant to estimate the position of a possible zero crossing. If a determinant zero crossing is detected, then the k_z estimate obtained is refined using a procedure based on the method of false position [32].

(iv)   Before acceptance of the k_z value, a final check is made to ensure that it corresponds to both a zero crossing in the determinant and a minimum in the minimum singular value of $[Y^{sum}]$. If the solution is valid, the next z-mode is sought using the same procedure. If the fine search is not yet at the end of its range (one coarse step beyond the original estimate of the solution) then it is continued to this limit in an attempt to detect other solutions close to the last solution. This situation occurs often in structures with almost degenerate z-modes.

For uniform sections, values of k_0 corresponding to the z-mode cutoff frequencies can be found rather than the z-mode propagation constants at a given frequency as described above for general structures. The search algorithm was identical to the k_z search. For the mth z-mode, the cutoff frequency f_c^m was used to calculate the propagation constant k_z^m at a given frequency using the simple relation

$$k_z^m = \sqrt{k_0^2 \varepsilon_r - k_{T_m}^2}$$

where

$$k_0 = \frac{2\pi f}{c} \quad and \quad k_{T_m} = \frac{2\pi f_c^m}{c}$$

Since the z-mode cutoff frequencies were independent of frequency for uniform sections, determining the cutoff frequencies or k_z values at one frequency was sufficient to analyse a number of frequencies. The k_z values obtained at the first frequency were readily scaled for any number of different frequencies, so that a z-mode search was not required for more than one frequency. This substantially improved computational efficiency when analysing broadband structures.

Complex modes

For finding complex z-modes, ie., z-modes with complex k_z^m values, a contour integration technique based on Cauchy's Theorem is applied in the complex k_z plane to search for zeroes of the determinant of $[Y^{sum}]$. This technique consists of an integration around overlapping circular contours in the complex k_z plane to determine the number of zeroes and their location within the contour. This procedure was initially developed for solving matrix equations by Delves and Lyness [33], and applied to the analysis of microwave structures by Sorrentino and Lampariello [34].

Cauchy's theorem states that

$$S_n = \frac{1}{2\pi j} \int_C z^i \frac{f'(z)}{f(z)} dz$$

$$= \sum_{i=1}^{N_z} z_i^n - \sum_{i=1}^{N_p} p_i^n$$

where N_z and N_p are the number of zeroes and poles of the function $f(z)$ of the complex variable z within the contour. z_i is the position of the ith zero and p_i is the position of the ith pole within the contour. Interpolation using a polynomial of order 4 was used to estimate the derivative $f'(z)$ from values of the function $f(z)$. By setting n=0, $S_0 = N_z - N_p$ is determined. Provided there are not too many zeroes or poles inside the contour, then with a sufficiently high order of n, the various z_i and p_i can be determined analytically. Appendix A.5 describes analytic techniques for extracting the zero and pole locations from the moments S_n for a limited number of poles and zeroes within the contour. Larger numbers of poles and/or zeroes were not considered because of numerical accuracy problems which stemmed from the fact that, in practice, most of the zeroes and poles occurred in closely-spaced zero-pole pairs, so that $z_i^n - p_i^n$ was small for n = 1, 2, 3, ... This was a fundamental limitation on the effectiveness of this technique. However, complex modes were generally few in number and widely-spaced in the k_z plane, allowing this method to be used effectively. If too many zeroes or poles were inside a given contour, smaller contours could be used to cover the same area in the complex k_z plane.

2.3.2.8 Section Voltage and Current Calculation

Once the values of k_z^m are found for each z-mode for m = 0 to N_z, the voltages and currents on the equivalent transmission line network representing propagation in the x direction can be determined. These can then be used to calculate the actual electric and magnetic fields in the cross-section for each z-mode, and hence the z-mode coupling at section interfaces. This in turn allowed sections to be cascaded together to construct the complete waveguide element.

The first step is to use the transverse resonance condition to solve for the modal voltages at the junction

$$\left[Y_{J00} + Y_{J01} + Y_{J10} + Y_{J11} \right] V_R^{n_J} = \left[\mathbf{Y}^{sum} \right] V_R^{n_J} = 0$$

This equation is sufficient to solve for $V_R^{n_J}$ to within an arbitrary factor. This is accounted for by allowing one of the modal voltages to be set to 1. If voltage V_p is set to 1 and removed from the unknown voltage vector, then the pth column of $[\mathbf{Y}^{sum}]$, can be taken to the right-hand side, and the resulting equation solved for the other voltages using a least squares technique. The solution is ideally unique, but the least squares approach ensures robustness to numerical error. In matrix terms, the equation to be solved is

$$\begin{bmatrix} Y_{00}^{sum} & \cdots & Y_{0(p-1)}^{sum} & Y_{0(p+1)}^{sum} & \cdots & Y_{0N}^{sum} \\ \vdots & & \vdots & \vdots & & \vdots \\ \vdots & & \vdots & \vdots & & \vdots \\ \vdots & & \vdots & \vdots & & \vdots \\ \vdots & & \vdots & \vdots & & \vdots \\ \vdots & & \vdots & \vdots & & \vdots \\ Y_{N0}^{sum} & \cdots & Y_{N(p-1)}^{sum} & Y_{N(p+1)}^{sum} & \cdots & Y_{NN}^{sum} \end{bmatrix} \cdot \begin{bmatrix} V_0^{n_J} \\ \vdots \\ \vdots \\ V_{(p-1)}^{n_J} \\ V_{(p+1)}^{n_J} \\ \vdots \\ V_N^{n_J} \end{bmatrix} = \begin{bmatrix} Y_{0p}^{sum} \\ \vdots \\ \vdots \\ Y_{(p-1)p}^{sum} \\ Y_{(p+1)p}^{sum} \\ \vdots \\ Y_{Np}^{sum} \end{bmatrix}$$

If this equation is written as $\mathbf{A.V} = \mathbf{b}$, then the least squares solution would be found by solving $\mathbf{A^\dagger A.V} = \mathbf{A^\dagger.b}$ using standard techniques for linear matrix equations [35].

The modal voltage matrices at the other ports in parallel with the junction, V^n ($n \neq n_J$), are found from the junction voltages using this equation from Section 2.3.2.6

$$V^n = \sum_{p \neq n_J}^{N} Y_{inv}^{np} [Y_L^{pn_J} + Y_R^{pn_J}] V^{n_J}$$

where N is the number of ports in the junction plane and

$$Y_{inv} = [Y_L + Y_R]^{-1}$$

The currents at all of the ports in parallel with the junction were determined using Y_L

$$I_L^n = \sum_{p \neq n_J}^{N} Y_L^{np} V^p = -I_R^n$$

Once the voltages and currents at the ports in parallel with the junction ports were found, the voltages and currents in the remainder of the cross-section could be determined. For a step-down discontinuity to the left of the junction plane, the voltage coupling could be used to determine the voltage on the left side of the discontinuity from the known voltage on the right side. The current to the left of the discontinuity was calculated by evaluating the total admittance of that portion of the structure from the left side boundary up to (but not including) the discontinuity, Y_{left}, so that $I = Y_{left} V$ yielded the required modal currents. For a step-up discontinuity to the left of the junction plane, the current coupling could be used to evaluate the modal currents to the left of the discontinuity from the known modal currents on the right side. As for the step-up case, the admittance of the structure to the left of the discontinuity, Y_{left}, was calculated. The modal voltages on the left side of the discontinuity were subsequently determined using $V = Y_{left}^{-1} I$.

Once the voltage and current at the right edge of a region V_{right} and I_{right} were known, it was a simple matter to calculate the voltage and current at the left edge V_{left} and I_{left} using

$$V_{left} = Y_{10}^{-1} [I_{right} - Y_{11} V_{right}]$$

$$I_{left} = Y_{00} V_{left} + Y_{01} V_{right}$$

where Y is the subregion admittance matrix. Note that Y_{ij} (i,j = 0,1) are diagonal. The next discontinuity (if any) is located at the left edge of the region, so this procedure is repeated until the left boundary of the structure is reached to determine the x-mode voltages and currents for the portion of the structure to the left of the junction plane.

The modal voltages and currents to the right of the junction plane are calculated in a similar fashion, the differences being that the voltage coupling was used to calculate the modal voltages across step-down discontinuities, while the current coupling was used at step-up transitions. The admittance of the portion of the structure to the right of the discontinuity, Y_{right}, was then used to calculate the voltage or current as appropriate. Once the voltage and current at the left edge of a subregion was known, the corresponding voltage and current at the right edge were determined using

$$V_{right} = Y_{01}^{-1} [I_{left} - Y_{00} V_{left}]$$

$$I_{right} = Y_{10} V_{left} + Y_{11} V_{right}$$

This procedure was repeated until the right side boundary of the structure was reached. The x-mode voltages and currents across the entire two-dimensional cross-section were then known.

2.3.2.9 Section Field Calculation

The modal voltages and currents were used to calculate the fields in the cross-section, as well as the total power flowing through it. The y and z components of the fields have been derived previously in order to evaluate the coupling at region interfaces. To complete the field calculations, the x component of the electric and magnetic fields of the mth z-mode were derived. E_x^m was determined from H_y^m and H_z^m, and H_x^m was determined from E_y^m and E_z^m using Maxwell's equations, with the TE and TM field components separated as follows

$$j\omega\varepsilon_0\varepsilon_r E_x^m = \nabla \times \mathbf{H^m} \bullet \mathbf{u}_x$$

$$= \sum_n^{N'}\left[\frac{dh_z^{'n}(y)}{dy} + jk_z h_y^{'n}(y)\right]I_x^{'mn}(x) + \sum_n^{N''}\left[\frac{dh_z^{''n}(y)}{dy} + jk_z h_y^{''n}(y)\right]I_x^{''mn}(x)$$

and similarly for H_x^m

$$j\omega\mu_0 H_x^m = -\nabla \times \mathbf{E^m} \bullet \mathbf{u}_x$$

$$= -\sum_n^{N'}\left[\frac{de_z^{'n}(y)}{dy} + jk_z e_y^{'n}(y)\right]V_x^{'mn}(x) + \sum_n^{N''}\left[\frac{de_z^{''n}(y)}{dy} + jk_z e_y^{''n}(y)\right]V_x^{''mn}(x)$$

The total power P_z^m flowing through the cross-section in the mth z-mode was determined by integrating the z-directed power density over each region and summing over all the regions in the cross-section

$$P_z^m = \int_{x_l}^{x_u}\int_{y_l}^{y_u}(E_x^m H_y^{m*} - E_y^m H_x^{m*})dy\,dx$$

All three field components are listed in Appendix VI for TE and TM-to-x, y, and z modes, together with the z-directed power. For each z-mode, V_x^{mn} and I_x^{mn} were normalised by setting P_z^m to 1 for propagating modes (k_z real), and $j = \sqrt{-1}$ for evanescent modes (k_z imaginary) and complex modes (k_z complex).

2.3.3 Three Dimensional (Element) Analysis

There have been a number of mode matching methods developed to treat three-dimensional discontinuities. Early work concentrated on discontinuities between rectangular waveguide sections [36]-[42], while later efforts have been directed toward more complex structures based on finned waveguides, cross-irises, or T-septa [43]-[50]. Generally, analysis has been restricted to relatively simple, homogeneous structures. The more general derivation presented in this section seeks to extend the capability of the mode matching technique beyond these limitations to allow accurate modelling of microstrip, finline, and dielectric waveguide discontinuities with a single, generic analysis.

The two-dimensional section analysis described in Section 2.3.2 yields the z-mode propagation constants and modal fields for a given number of z-modes in each section of the structure to be analysed. It remains only to cascade these sections together (in the z-direction) to represent the entire waveguide element. To perform this cascading, it is necessary to first calculate the coupling between z-modes in adjacent sections using the modal fields calculated according to the expressions in Section 2.3.2.9. Combining this

coupling with the scattering matrices for each section allows the scattering parameters of the entire element to be determined.

2.3.3.1 Mode Coupling

The z modes in adjacent sections are coupled at the interface between the sections. This interface represents a discontinuity in the section boundaries or dielectric constants. The z-mode coupling can be determined from continuity of the tangential electric and magnetic fields in the $(x\text{-}y)$ plane of the discontinuity and from the boundary conditions. Consider a step change between two sections A and B of an element as shown in Figure 2.10.
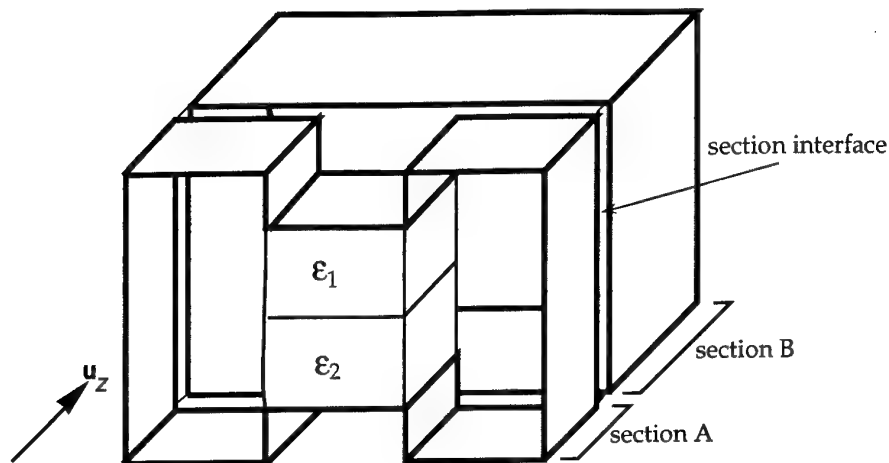
Figure 2.10 Section interface

Using the two-dimensional analysis discussed in Section 2.2, an equivalent z-mode voltage and current can be defined such that the fields tangential to the z-direction in sections A and B are given by

$$\mathbf{E}_{t_A} = \sum_m^{N_z^A} V_{A_z}^m(z) \mathbf{e}_{t_A}^m(x,y)$$

$$\mathbf{H}_{t_A} = \sum_m^{N_z^A} I_{A_z}^m(z) \mathbf{h}_{t_A}^m(x,y)$$

$$\mathbf{E}_{t_B} = \sum_n^{N_z^B} V_{B_z}^n(z) \mathbf{e}_{t_B}^n(x,y)$$

$$\mathbf{H}_{t_B} = \sum_n^{N_z^B} I_{B_z}^n(z) \mathbf{h}_{t_B}^n(x,y)$$

where the summation is over both TE and TM eigenmodes and propagation is assumed to be in th z-direction.

Assuming that the boundary of section B entirely includes the boundary of section A at the interface, the field matching at the discontinuity requires that

$$\mathbf{E}_{t_B} = \begin{cases} \mathbf{E}_{t_A}, & \text{over aperture} \\ 0, & \text{otherwise} \end{cases}$$

and

$$\mathbf{H}_{t_A} = \mathbf{H}_{t_B} \quad \text{over aperture}$$

By equating the modal expansions for the fields in regions A and B in the aperture, the coupling relations between $V_{A_z}^m(z)$ and $V_{B_z}^n(z)$, and between $I_{A_z}^m(z)$ and $I_{B_z}^n(z)$ can be determined. This procedure was followed using each of the three mode types, ie., TE, TM-to-x, y, and z. The coupling expressions were formulated in such a manner as to guarantee conservation of complex power across the discontinuity for a finite number of z-modes in each section. In this section, the z-mode coupling using TE and TM-to-y eigenmodes is derived. The corresponding derivation for TE and TM-to-x and TE and TM to-z modes is given in Appendix A.7.

Electric Field Matching

x-component

$$\sum_m^{N_z^B} V_{B_z}^m \left[\sum_n^{N_B^{TE}} \frac{k_{z_B}^m \omega \mu_0}{k_{u_{n_B}}^{'2}} I_{B_x}^{'mn}(x) V_{B_y}^{'n}(y) + \sum_p^{N_B^{TM}} I_{B_x}^{''mp}(x) V_{B_y}^{''p}(y) \right]$$

$$= \sum_i^{N_z^A} V_{A_z}^i \left[\sum_j^{N_A^{TE}} \frac{k_{z_A}^i \omega \mu_0}{k_{u_{j_A}}^{'2}} I_{A_x}^{'ij}(x) V_{A_y}^{'j}(y) + \sum_k^{N_A^{TM}} I_{A_x}^{''ik}(x) V_{A_y}^{''k}(y) \right] \qquad (2.1)$$

Both sides of Equation 2.1 were multiplied by

$$\sum_s^{N_B^{TE}} I_{B_x}^{'rs}(x)^* V_{B_y}^{''s}(y)^*$$

Integrating over the aperture in the x and y directions and applying orthonormality of the y-modes yields

$$\mathbf{A} \mathbf{V}_{B_z} = \mathbf{B} \mathbf{V}_{A_z}$$

where

$$A_{mn} = \sum_p^{N_B^{TE}} \left[\frac{k_{z_B}^n \omega \mu_0}{k_{u_{p_B}}^{'2}} \int_{x_l}^{x_u} I_{B_x}^{'np}(x) I_{B_x}^{'mp}(x)^* dx \right. \\ \left. + \sum_q^{N_B^{TM}} \int_{x_l}^{x_u} I_{B_x}^{''nq}(x) I_{B_x}^{'mp}(x)^* dx \int_{y_l}^{y_u} V_{B_y}^{''q}(y) V_{B_y}^{'p}(y)^* dy \right]$$

$$B_{mn} = \sum_{p}^{N_B^{TE}} \left[\begin{array}{l} \sum_{q}^{N_A^{TE}} \dfrac{k_{z_A}^n \, \omega\mu_0}{k_{u_{q_A}}^{\prime 2}} \int_{x_l}^{x_u} I_{A_x}^{\prime nq}(x) I_{B_x}^{\prime mp}(x)^* \, dx \int_{y_l}^{y_u} V_{A_y}^{\prime q}(y) V_{B_y}^{\prime p}(y)^* \, dy \\[2em] + \sum_{r}^{N_B^{TM}} \int_{x_l}^{x_u} I_{B_x}^{\prime\prime nr}(x) I_{B_x}^{\prime mp}(x)^* \, dx \int_{y_l}^{y_u} V_{B_y}^{\prime\prime r}(y) V_{B_y}^{\prime p}(y)^* \, dy \end{array} \right]$$

y-component

$$\sum_{m}^{N_z^B} V_{B_z}^m \sum_{n}^{N_B^{TM}} V_{B_x}^{\prime\prime mn}(x) \dfrac{I_{B_y}^{\prime\prime n}(y)}{\varepsilon_B(y)} = \sum_{p}^{N_z^A} V_{A_z}^p \sum_{q}^{N_A^{TM}} V_{A_x}^{\prime\prime pq}(x) \dfrac{I_{A_y}^{\prime\prime q}(y)}{\varepsilon_A(y)} \tag{2.2}$$

Both sides of Equation 2.2 were multiplied by

$$\sum_{s}^{N_B^{TM}} \dfrac{k_{z_B}^r \, {}^* \, \omega\varepsilon_0}{k_{u_{s_B}}^{\prime\prime 2}} V_{B_x}^{\prime\prime rs}(x)^* I_{B_y}^{\prime\prime s}(y)^*$$

Integrating over the aperture in the *x* and *y* directions and applying orthonormality of the *y*-modes yields

$$\mathbf{H V}_{B_z} = \mathbf{J V}_{A_z}$$

where

$$H_{mn} = \sum_{p}^{N_B^{TM}} \dfrac{k_{z_B}^m \, {}^* \, \omega\varepsilon_0}{k_{u_{p_B}}^{\prime\prime 2}} \int_{x_l}^{x_u} V_{B_x}^{\prime\prime np}(x) V_{B_x}^{\prime\prime mp}(x)^* \, dx$$

$$J_{mn} = \sum_{p}^{N_B^{TM}} \sum_{q}^{N_A^{TM}} \dfrac{k_{z_B}^m \, {}^* \, \omega\varepsilon_0}{k_{u_{p_B}}^{\prime\prime 2}} \int_{x_l}^{x_u} V_{A_x}^{\prime\prime nq}(x) V_{B_x}^{\prime\prime mp}(x)^* \, dx \int_{y_l}^{y_u} \dfrac{I_{A_y}^{\prime\prime q}(y) I_{B_y}^{\prime\prime p}(y)^*}{\varepsilon_A(y)} \, dy$$

In addition, multiplying both sides of Equation 2.2 by

$$\sum_{s}^{N_B^{TE}} V_{B_x}^{\prime rs}(x)^* I_{B_y}^{\prime s}(y)^*$$

and integrating over the aperture yields

$$\mathbf{P V}_{B_z} = \mathbf{Q V}_{A_z}$$

where

$$P_{mn} = \sum_p^{N_B^{TE}} \sum_q^{N_B^{TM}} \int_{x_l}^{x_u} V_{B_x}^{'nq}(x) V_{B_x}^{'mp}(x)^* dx \int_{y_l}^{y_u} \frac{I_{B_y}^{''q}(y) I_{B_y}^{'p}(y)^*}{\varepsilon_B(y)} dy$$

$$Q_{mn} = \sum_p^{N_B^{TE}} \sum_q^{N_A^{TM}} \int_{x_l}^{x_u} V_{A_x}^{'nq}(x) V_{B_x}^{'mp}(x)^* dx \int_{y_l}^{y_u} \frac{I_{A_y}^{''q}(y) I_{B_y}^{'p}(y)^*}{\varepsilon_B(y)} dy$$

Magnetic Field Matching

x-component

$$\sum_m^{N_z^A} I_{A_z}^m \left[\sum_n^{N_A^{TE}} V_{A_x}^{'mn}(x) I_{A_y}^{'n}(y) - \sum_p^{N_A^{TM}} \frac{k_{z_A}^m \omega \varepsilon_0}{k_{u_{p_A}}^{''2}} V_{A_x}^{''mp}(x) I_{A_y}^{''p}(y) \right]$$

$$= \sum_i^{N_z^B} I_{B_z}^i \left[\sum_j^{N_B^{TE}} V_{B_x}^{'ij}(x) I_{B_y}^{'n}(y) - \sum_k^{N_B^{TM}} \frac{k_{z_B}^m \omega \varepsilon_0}{k_{u_{k_B}}^{''2}} V_{B_x}^{''mk}(x) I_{B_y}^{''k}(y) \right] \qquad (2.3)$$

Both sides of Equation 2.3 were multiplied by

$$\sum_s^{N_A^{TM}} V_{A_x}^{''rs}(x)^* \frac{I_{B_y}^{''s}(y)^*}{\varepsilon_A(y)}$$

Integrating over the aperture in the x and y directions and applying orthonormality of the y-modes yields

$$\mathbf{K}\mathbf{V}_{B_z} = \mathbf{L}\mathbf{V}_{A_z}$$

where

$$K_{mn} = \sum_p^{N_A^{TM}} \left[\sum_q^{N_A^{TE}} \int_{x_l}^{x_u} V_{A_x}^{'nq}(x) V_{A_x}^{''mp}(x)^* dx \int_{y_l}^{y_u} \frac{I_{A_y}^{'q}(y) I_{A_y}^{''p}(y)^*}{\varepsilon_A(y)} dy \right.$$

$$\left. - \frac{k_{z_A}^n{}^* \omega \varepsilon_0}{k_{u_{p_A}}^{''2}} \int_{x_l}^{x_u} V_{A_x}^{''np}(x) V_{A_x}^{''mp}(x)^* dx \right]$$

$$L_{mn} = \sum_p^{N_A^{TM}} \left[\sum_q^{N_B^{TE}} \int_{x_l}^{x_u} V_{B_x}^{'nq}(x) V_{A_x}^{''mp}(x)^* dx \int_{y_l}^{y_u} \frac{I_{B_y}^{'q}(y) I_{A_y}^{''p}(y)^*}{\varepsilon_A(y)} dy \right.$$

$$\left. - \sum_r^{N_B^{TM}} \frac{k_{z_B}^n \omega \varepsilon_0}{k_{u_{r_A}}^{''2}} \int_{x_l}^{x_u} V_{B_x}^{''nr}(x) V_{A_x}^{''mp}(x)^* dx \int_{y_l}^{y_u} \frac{I_{B_y}^{''r}(y) I_{A_y}^{''p}(y)^*}{\varepsilon_A(y)} dy \right]$$

y-component

$$\sum_m^{N_z^A} I_{A_z}^m \sum_n^{N_A^{TE}} I_{A_x}^{'mn}(x) V_{A_y}^{'n}(y) = \sum_p^{N_z^B} I_{B_z}^p \sum_q^{N_B^{TE}} I_{B_x}^{'pq}(x) I_{B_y}^{'q}(y)$$

(2.4)

Both sides of Equation 2.4 were multiplied by

$$\sum_s^{N_A^{TE}} \frac{k_{z_A}^{r*} \omega\mu_0}{k_{u_{S_A}}^{'2}} I_{A_x}^{'rs}(x)^* V_{A_y}^{'s}(y)^*$$

Integrating over the aperture in the x and y directions and applying orthonormality of the y-modes yields

$$\mathbf{CV}_{B_z} = \mathbf{DV}_{A_z}$$

where

$$C_{mn} = \sum_p^{N_A^{TE}} \frac{k_{z_A}^{m*} \omega\mu_0}{k_{u_{p_A}}^{'2}} \int_{x_l}^{x_u} I_{A_x}^{'np}(x) I_{A_x}^{'mp}(x)^* dx$$

$$D_{mn} = \sum_p^{N_A^{TE}} \sum_q^{N_B^{TE}} \frac{k_{z_A}^{m*} \omega\mu_0}{k_{u_{p_A}}^{'2}} \int_{x_l}^{x_u} I_{B_x}^{'nq}(x) I_{A_x}^{'mp}(x)^* dx \int_{y_l}^{y_u} V_{B_y}^{'q}(y) V_{A_y}^{'p}(y)^* dy$$

In addition, multiplying both sides of Equation 2.4 by

$$\sum_s^{N_A^{TM}} I_{A_x}^{''rs}(x)^* V_{A_y}^{''s}(y)^*$$

and integrating over the aperture yields

$$\mathbf{MV}_{B_z} = \mathbf{NV}_{A_z}$$

where

$$M_{mn} = \sum_p^{N_A^{TM}} \sum_q^{N_A^{TE}} \int_{x_l}^{x_u} I_{A_x}^{'nq}(x) I_{A_x}^{''mp}(x)^* dx \int_{y_l}^{y_u} V_{A_y}^{'q}(y) V_{A_y}^{''p}(y)^* dx$$

$$N_{mn} = \sum_p^{N_A^{TM}} \sum_q^{N_B^{TE}} \int_{x_l}^{x_u} I_{B_x}^{'nq}(x) I_{B_x}^{''mp}(x)^* dx \int_{y_l}^{y_u} V_{B_y}^{'q}(y) V_{B_y}^{''p}(y)^* dy$$

Complex Power Conservation

Several relations now exist between the z-mode voltages and currents at section interfaces. Ultimately, a single coupling expression for the voltages and a single coupling expression for the currents is required. To determine the means by which the previously derived coupling expressions can be combined, a conservation of complex power technique is used.

Conservation of the complex power flowing in the z-direction normal to the section interface is enforced regardless of the number of z-modes used.

The total power carried by the structure is summed over all z-modes as follows

$$P_{A_z}^{tot} = \sum_m^{N_z^A} \sum_n^{N_z^A} V_{A_z}^m I_{A_z}^{n \ *} \int_{x_l}^{x_u} \int_{y_l}^{y_u} \mathbf{e}_{t_A}^m(x,y) \times \mathbf{h}_{t_A}^n(x,y)^* \bullet \mathbf{u}_z \, dy \, dx$$

$$P_{B_z}^{tot} = \sum_m^{N_z^B} \sum_n^{N_z^B} V_{B_z}^m I_{B_z}^{p \ *} \int_{x_l}^{x_u} \int_{y_l}^{y_u} \mathbf{e}_{t_B}^m(x,y) \times \mathbf{h}_{t_B}^n(x,y)^* \bullet \mathbf{u}_z \, dy \, dx$$

Using the field relations in Section 2.3.2.9, the power flow through any given section is

$$P_z^{tot} = \sum_m^{N_z^A} \sum_n^{N_z^A} V_{A_z}^m I_{A_z}^{n \ *} [\sum_p^{N_y^{TE}} \sum_q^{N_y^{TM}} [\int_{x_l}^{x_u} I_x^{''nq}(x) I_x^{'mp}(x)^* \, dx \int_{y_l}^{y_u} V_y^{''q}(y) V_y^{'p}(y)^* \, dy$$

$$- \int_{x_l}^{x_u} V_x^{''nq}(x) V_x^{'mp}(x)^* \, dx \int_{y_l}^{y_u} \frac{I_y^{''q}(y) I_y^{'p}(y)^*}{\varepsilon_r(y)} \, dy]$$

$$+ \sum_p^{N_y^{TE}} \frac{k_z^n \omega \mu_0}{k_{u_p}^{'2}} \int_{x_l}^{x_u} I_x^{'np}(x) I_x^{'mp}(x)^* \, dx$$

$$+ \sum_p^{N_y^{TM}} \frac{k_z^{m \ *} \omega \varepsilon_0}{k_{u_p}^{''2}} \int_{x_l}^{x_u} V_x^{''np}(x) V_x^{''mp}(x)^* \, dx]$$

Therefore P_z^{tot} for section A and section B can be expressed in terms of the previously derived coupling matrices. In addition, the coupling between the modal fields in sections A and B is required to be such that the power coupled from z-modes in section A to z-modes in section B is the same as the power coupled from z-modes in section B to z-modes in section A.

$$P_{A_z}^{tot} = \left[\mathbf{I}_{A_z} \right]^\dagger \left[\mathbf{C}^\dagger + \mathbf{M}^\dagger - \mathbf{K}^\dagger \right] \left[\mathbf{V}_{A_z} \right]$$

$$= \left[\mathbf{I}_{B_z} \right]^\dagger \left[\mathbf{D}^\dagger + \mathbf{N}^\dagger - \mathbf{L}^\dagger \right] \left[\mathbf{V}_{A_z} \right]$$

and

$$P_{B_z}^{tot} = \left[\mathbf{I}_{B_z} \right]^\dagger \left[\mathbf{A} + \mathbf{H} - \mathbf{P} \right] \left[\mathbf{V}_{B_z} \right]$$

$$= \left[\mathbf{I}_{B_z} \right]^\dagger \left[\mathbf{B} + \mathbf{J} - \mathbf{Q} \right] \left[\mathbf{V}_{A_z} \right]$$

So for conservation of complex power, it is required that

$$\mathbf{D}^\dagger + \mathbf{N}^\dagger - \mathbf{L}^\dagger = \mathbf{B} + \mathbf{J} - \mathbf{Q}$$

This relation can be readily verified by inspection of the individual terms in each matrix listed previously. To obtain a single coupling expression for the z-mode current, and a single coupling expression for the z-mode voltage, write

$$\left[\mathbf{I}_{\mathbf{A}_z}\right] = [\mathbf{C_I}]\left[\mathbf{I}_{\mathbf{B}_z}\right], \left[\mathbf{V}_{\mathbf{B}_z}\right] = [\mathbf{C_V}]\left[\mathbf{V}_{\mathbf{A}_z}\right]$$

Therefore, for power conservation

$$[\mathbf{C_I}]^{\dagger}\left[\mathbf{C}^{\dagger} + \mathbf{M}^{\dagger} - \mathbf{K}^{\dagger}\right] = [\mathbf{A} + \mathbf{H} - \mathbf{P}][\mathbf{C_V}]$$

To ensure complex power conservation regardless of the number of z-modes used in each section, the following expressions for the current and voltage coupling will be used

$$[\mathbf{C_I}] = [\mathbf{C} + \mathbf{M} - \mathbf{K}]^{-1}[\mathbf{D} + \mathbf{N} - \mathbf{L}]$$

$$[\mathbf{C_V}] = [\mathbf{A} + \mathbf{H} - \mathbf{P}]^{-1}[\mathbf{B} + \mathbf{J} - \mathbf{Q}]$$

$$= [\mathbf{A} + \mathbf{H} - \mathbf{P}]^{-1}\left[\mathbf{D}^{\dagger} + \mathbf{N}^{\dagger} - \mathbf{L}^{\dagger}\right]$$

The corresponding derivations for TE and TM-to-x and TE and TM-to-z modes are presented in Appendix VII. Appendix VIII contains a summary of the coupling expressions for each of the three mode options.

For sections, with uniform dielectric constants the self-coupling matrices $[\mathbf{A} + \mathbf{H} - \mathbf{P}]$ and $[\mathbf{C} + \mathbf{M} - \mathbf{K}]$ are diagonal. Therefore, calculating these matrices and their inverses requires only a small computational effort for this case.

2.3.3.2 Section Discontinuity Scattering Matrix

Once the z-mode voltage and current coupling matrices are determined for each two-dimensional section discontinuity, the scattering matrix of the discontinuities can be determined. The coupling expressions for the z-mode voltages and currents were used in the form used previously in Section 2.3.2.4

$$\begin{bmatrix} \mathbf{I}_{\mathbf{A}_z} \\ \hline \mathbf{V}_{\mathbf{B}_z} \end{bmatrix} = \begin{bmatrix} \mathbf{0} & \mathbf{P_I} \\ \hline \mathbf{P_V} & \mathbf{0} \end{bmatrix} \begin{bmatrix} \mathbf{V}_{\mathbf{A}_z} \\ \hline \mathbf{I}_{\mathbf{B}_z} \end{bmatrix}$$

for "step-up" transitions (section A cross section enclosed by section B cross section), and

$$\begin{bmatrix} \mathbf{V}_{\mathbf{A}_z} \\ \hline \mathbf{I}_{\mathbf{B}_z} \end{bmatrix} = \begin{bmatrix} \mathbf{0} & \mathbf{P_V} \\ \hline \mathbf{P_I} & \mathbf{0} \end{bmatrix} \begin{bmatrix} \mathbf{I}_{\mathbf{A}_z} \\ \hline \mathbf{V}_{\mathbf{B}_z} \end{bmatrix}$$

for "step-down" transitions (section B cross section enclosed by section A cross section). $\mathbf{P_I}$, and $\mathbf{P_V}$ are the current and voltage couplings, respectively. These coupling expressions are listed in Appendix VIII for the various choices of eigenmodes.

As for the two-dimensional case discussed in Section 2.3.2.4, note that the currents in the smaller section could be expressed in terms of the currents in the larger section, but not vice versa. This is because there was no boundary condition for the magnetic field on the wall of the aperture. Similarly, the voltage in the larger region could be determined from the voltage in the smaller region and the boundary constraint that the component of the electric field tangential to the section interface must disappear on the aperture wall. However, as for the two-dimensional case, this boundary constraint means that a coupling

expression relating the voltage in the smaller region to an arbitrary voltage in the larger region cannot be defined, since an arbitrary electric field cannot be specified in the larger region.

A scattering matrix relating the amplitudes of the incident and reflected waves on each side of the discontinuity is required and this can be derived from the voltage and current coupling relationships. This scattering matrix is written as

$$
\begin{bmatrix} b^I \\ \hline c^{II} \end{bmatrix} = \begin{bmatrix} S_{11} & S_{12} \\ \hline S_{21} & S_{22} \end{bmatrix} \begin{bmatrix} c^I \\ \hline b^{II} \end{bmatrix}
$$
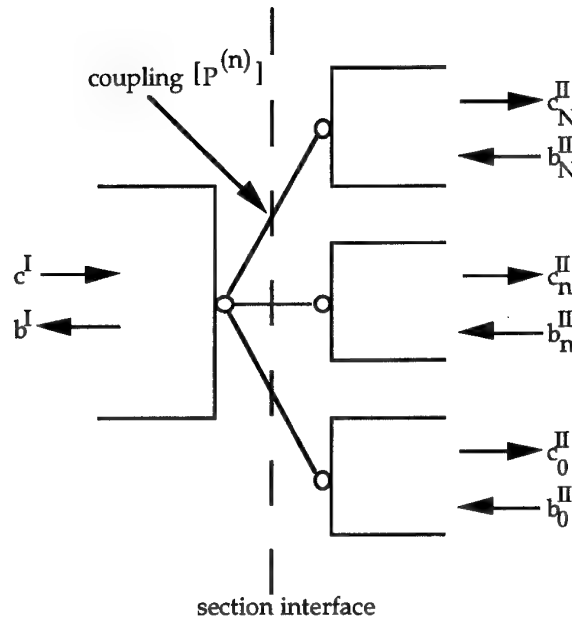
Figure 2.11   Single input section coupled to N output sections

Step-down transitions

Figure 2.11 schematically shows a single input section coupled to N output sections through a step-down discontinuity. The voltage and current coupling between the input section and the nth output section are written as $P_V^{(n)}$ and $P_I^{(n)}$, respectively. Representing the incident and reflected wave amplitudes as shown in Figure 2.11, the following relations can be defined

$$
c^I + b^I = \sum_n^N \mathbf{P}_V^{(n)} \left[c_n^{II} + b_n^{II} \right]
$$

$$
c_n^{II} - b_n^{II} = \mathbf{P}_I^{(n)} \left[c^I - b^I \right]
$$

Therefore

$$b^I = \sum_n^N \mathbf{P}_V^{(n)} \left[\mathbf{P}_I^{(n)} c^I - \mathbf{P}_I^{(n)} b^I + b_n^{II} \right] + \sum_n^N \mathbf{P}_V^{(n)} b_n^{II} - c^I$$

This leads to

$$b^I = - \left[\mathbf{U} + \sum_p^N \mathbf{P}_V^{(p)} \mathbf{P}_I^{(p)} \right]^{-1} \left[\mathbf{U} - \sum_p^N \mathbf{P}_V^{(p)} \mathbf{P}_I^{(p)} \right] c^I$$

$$+ 2 \left[\mathbf{U} + \sum_p^N \mathbf{P}_V^{(p)} \mathbf{P}_I^{(p)} \right]^{-1} \sum_n^N \mathbf{P}_V^{(n)} b_n^{II}$$

and

$$c_n^{II} = \mathbf{P}_I^{(n)} \left(\mathbf{U} + \left[\mathbf{U} + \sum_p^N \mathbf{P}_V^{(p)} \mathbf{P}_I^{(p)} \right]^{-1} \left[\mathbf{U} - \sum_p^N \mathbf{P}_V^{(p)} \mathbf{P}_I^{(p)} \right] \right) c^I$$

$$+ \sum_q^N \left(\mathbf{U} \delta_{nq} - 2 \mathbf{P}_I^{(n)} \left[\mathbf{U} + \sum_p^N \mathbf{P}_V^{(p)} \mathbf{P}_I^{(p)} \right]^{-1} \mathbf{P}_V^{(q)} \right) b_q^{II}$$

In matrix form

$$\begin{bmatrix} b^I \\ --- \\ c_0^{II} \\ \vdots \\ c_N^{II} \end{bmatrix} = \begin{bmatrix} [\, \mathbf{S_{11}} \,] & | & [\quad \mathbf{S_{12}} \quad] \\ ------ & --- & ------------ \\ [\mathbf{S_{21}}] & | & [\quad \mathbf{S_{22}} \quad] \end{bmatrix} \begin{bmatrix} c^I \\ --- \\ b_0^{II} \\ \vdots \\ b_N^{II} \end{bmatrix}$$

where

$$\mathbf{S_{11}} = - \left[\mathbf{U} + \sum_p^N \mathbf{P}_V^{(p)} \mathbf{P}_I^{(p)} \right]^{-1} \left[\mathbf{U} - \sum_p^N \mathbf{P}_V^{(p)} \mathbf{P}_I^{(p)} \right]$$

$$\mathbf{S_{12}}_n = 2 \left[\mathbf{U} + \sum_p^N \mathbf{P}_V^{(p)} \mathbf{P}_I^{(p)} \right]^{-1} \mathbf{P}_V^{(n)}$$

$$\mathbf{S_{21}}_m = \mathbf{P}_I^{(m)} [\mathbf{U} - \mathbf{S_{11}}]$$

$$\mathbf{S_{22}}_{mn} = [\mathbf{U} \delta_{mn} - \mathbf{P}_I^{(m)} \mathbf{S_{12}}_n]$$

Step-up transitions

Figure 2.12 schematically shows N input sections coupled to a single output section through a step-up discontinuity. The voltage and current coupling between the nth input section and the output section are written as $P_V^{(n)}$ and $P_I^{(n)}$, respectively. Representing the incident and reflected wave amplitudes as shown in Figure 2.12, the following relations can be defined

$$c^{II} + b^{II} = \sum_n^N \mathbf{P}_V^{(n)} \left[c_n^I + b_n^I \right]$$

$$c_n^I - b_n^I = \mathbf{P}_I^{(n)} \left[c^{II} - b^{II} \right]$$

Therefore

$$c^{II} = \sum_n^N \mathbf{P}_V^{(n)} \left[-\mathbf{P}_I^{(n)} c^{II} + \mathbf{P}_I^{(n)} b^{II} + c_n^I \right] + \sum_n^N \mathbf{P}_V^{(n)} c_n^I - b^{II}$$

This leads to

$$c^{II} = -2 \left[\mathbf{U} + \sum_p^N \mathbf{P}_V^{(p)} \mathbf{P}_I^{(p)} \right]^{-1} \sum_n^N \mathbf{P}_V^{(n)} c_n^I$$

$$- \left[\mathbf{U} + \sum_p^N \mathbf{P}_V^{(p)} \mathbf{P}_I^{(p)} \right]^{-1} \left[\mathbf{U} - \sum_p^N \mathbf{P}_V^{(p)} \mathbf{P}_I^{(p)} \right] b^{II}$$
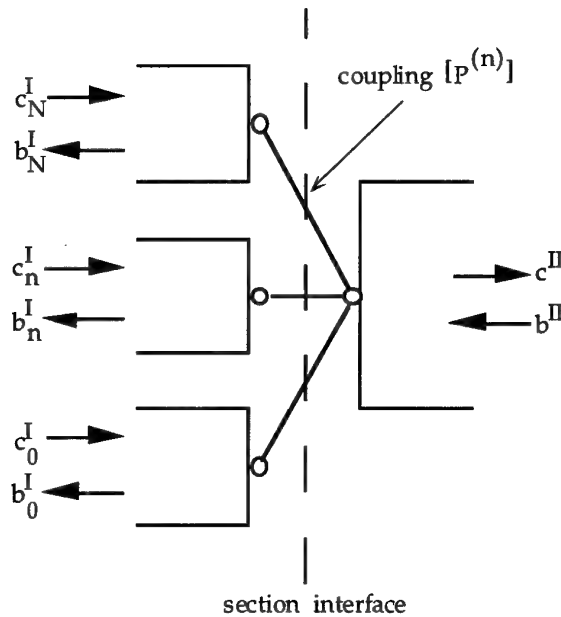
Figure 2.12 N input sections coupled to a single output section

and

$$b_n^1 = \sum_q^N \left(\mathbf{U}\delta_{nq} - 2\mathbf{P}_I^{(n)} \left[\mathbf{U} + \sum_p^N \mathbf{P}_V^{(p)}\mathbf{P}_I^{(p)} \right]^{-1} \mathbf{P}_V^{(q)} \right) c_q^I$$

$$+ \mathbf{P}_I^{(n)} \left(\mathbf{U} + \left[\mathbf{U} + \sum_p^N \mathbf{P}_V^{(p)}\mathbf{P}_I^{(p)} \right]^{-1} \left[\mathbf{U} - \sum_p^N \mathbf{P}_V^{(p)}\mathbf{P}_I^{(p)} \right] \right) b^{II}$$

In matrix form

$$
\begin{bmatrix} b_0^I \\ \vdots \\ b_N^I \\ --- \\ c^{II} \end{bmatrix}
=
\begin{bmatrix} \begin{bmatrix} S_{11} \end{bmatrix} & \vdots & \begin{bmatrix} S_{12} \end{bmatrix} \\ ------------ & & \\ \begin{bmatrix} S_{21} \end{bmatrix} & \vdots & S_{22} \end{bmatrix}
\begin{bmatrix} c_0^I \\ \vdots \\ c_N^I \\ --- \\ b^{II} \end{bmatrix}
$$

where

$$S_{11_{mn}} = [\mathbf{U}\delta_{mn} - \mathbf{P}_I^{(m)} S_{21_n}]$$

$$S_{12_m} = \mathbf{P}_I^{(m)} [\mathbf{U} - S_{22}]$$

$$S_{21_n} = 2 \left[\mathbf{U} + \sum_p^N \mathbf{P}_V^{(p)}\mathbf{P}_I^{(p)} \right]^{-1} \mathbf{P}_V^{(n)}$$

$$S_{22} = -\left[\mathbf{U} + \sum_p^N \mathbf{P}_V^{(p)}\mathbf{P}_I^{(p)} \right]^{-1} \left[\mathbf{U} - \sum_p^N \mathbf{P}_V^{(p)}\mathbf{P}_I^{(p)} \right]$$

2.3.3.3 Scattering Matrix Cascade

The modal scattering matrices for each two-dimensional section discontinuity (in the x-y plane) can be cascaded in the z-direction with the simple 2-port scattering matrices of each section to produce the overall scattering matrix for the entire waveguide element. The general case of two cascaded multiport scattering matrices is shown in Figure 2.13.

The incident and reflected wave amplitudes (c^I,b^I), (c^{II},b^{II}), and (c^{III},b^{III}) are related by

$$
\begin{bmatrix} [\mathbf{b}^I] \\ [\mathbf{c}^{II}] \end{bmatrix}
=
\begin{bmatrix} [S_{11}^I] & [S_{12}^I] \\ [S_{21}^I] & [S_{22}^I] \end{bmatrix}
\begin{bmatrix} [\mathbf{c}^I] \\ [\mathbf{b}^{II}] \end{bmatrix}
$$

and

$$
\begin{bmatrix} [\mathbf{b}^{II}] \\ [\mathbf{c}^{III}] \end{bmatrix}
=
\begin{bmatrix} [S_{11}^{II}] & [S_{12}^{II}] \\ [S_{21}^{II}] & [S_{22}^{II}] \end{bmatrix}
\begin{bmatrix} [\mathbf{c}^{II}] \\ [\mathbf{b}^{III}] \end{bmatrix}
$$
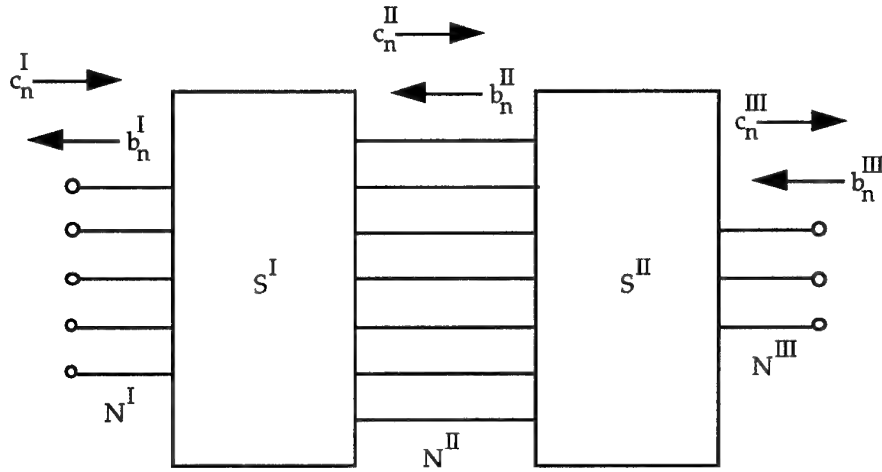
Figure 2.13   Multiport scattering matrix cascade

The required cascaded scattering matrix is given by

$$
\begin{bmatrix} [\mathbf{b}^I] \\ [\mathbf{c}^{III}] \end{bmatrix} = \begin{bmatrix} [\mathbf{S}_{11}^c] & [\mathbf{S}_{12}^c] \\ [\mathbf{S}_{21}^c] & [\mathbf{S}_{22}^c] \end{bmatrix} \begin{bmatrix} [\mathbf{c}^I] \\ [\mathbf{b}^{III}] \end{bmatrix}
$$

The parameters at the cascaded ports are eliminated by first expressing $[\mathbf{b}'']$ as follows

$$
\begin{aligned}
\left[\mathbf{b}''\right] &= \left[\mathbf{S}_{11}''\right]\left[\mathbf{c}''\right] + \left[\mathbf{S}_{12}''\right]\left[\mathbf{b}'''\right] \\
&= \left[\mathbf{S}_{11}''\right]\left[\left[\mathbf{S}_{21}'\right]\left[\mathbf{c}'\right] + \left[\mathbf{S}_{22}'\right]\left[\mathbf{b}''\right]\right] + \left[\mathbf{S}_{12}''\right]\left[\mathbf{b}'''\right]
\end{aligned}
$$

and then by eliminating $[\mathbf{c}'']$ to obtain

$$
\begin{aligned}
\left[\mathbf{b}''\right] &= \left[\left[\mathbf{S}_{11}''\right] + \left[\mathbf{S}_{12}''\right]\left(\mathbf{U} - \left[\mathbf{S}_{11}''\right]\left[\mathbf{S}_{22}'\right]\right)^{-1}\left[\mathbf{S}_{11}''\right]\left[\mathbf{S}_{21}'\right]\right]\left[\mathbf{c}'\right] \\
&\quad + \left[\mathbf{S}_{12}'\right]\left(\mathbf{U} - \left[\mathbf{S}_{11}''\right]\left[\mathbf{S}_{22}'\right]\right)^{-1}\left[\mathbf{S}_{12}''\right]\left[\mathbf{b}'''\right]
\end{aligned}
$$

and finally by writing an expression for $[\mathbf{c}''']$ as

$$
\begin{aligned}
[\mathbf{c}'''] &= [\mathbf{S}_{21}''][\mathbf{c}''] + [\mathbf{S}_{22}''][\mathbf{b}'] \\
&= [\mathbf{S}_{21}'']\left[[\mathbf{S}_{21}'][\mathbf{c}''] + [\mathbf{S}_{22}'][\mathbf{b}'']\right] + [\mathbf{S}_{22}''][\mathbf{b}'] \\
&= [\mathbf{S}_{21}'']\left[\mathbf{U} + [\mathbf{S}_{22}'](\mathbf{U} - [\mathbf{S}_{11}''][\mathbf{S}_{22}'])^{-1}[\mathbf{S}_{11}'']\right][\mathbf{b}'''][\mathbf{S}_{21}'][\mathbf{c}'] \\
&\quad + \left[[\mathbf{S}_{22}''] + [\mathbf{S}_{21}''][\mathbf{S}_{22}'](\mathbf{U} - [\mathbf{S}_{11}''][\mathbf{S}_{22}'])^{-1}[\mathbf{S}_{12}'']\right][\mathbf{b}''']
\end{aligned}
$$

the required parameters can be identified as

$$[S_{11}^c] = \left[[S_{11}^{II}] + [S_{12}^I]\left(U - [S_{11}^{II}][S_{22}^I]\right)^{-1} [S_{11}^{II}][S_{21}^I] \right]$$

$$[S_{12}^c] = [S_{12}^I]\left(U - [S_{11}^{II}][S_{22}^I]\right)^{-1} [S_{12}^{II}]$$

$$[S_{21}^c] = [S_{21}^{II}]\left[U + [S_{22}^I]\left(U - [S_{11}^{II}][S_{22}^I]\right)^{-1} [S_{11}^{II}] \right][S_{21}^I]$$

$$[S_{22}^c] = \left[[S_{22}^{II}] + [S_{21}^{II}][S_{22}^I]\left(U - [S_{11}^{II}][S_{22}^I]\right)^{-1} [S_{12}^{II}] \right]$$

Similar expressions for the case of two-port scattering matrix cascading are presented in [37]. The treatment shown above is superior to that described in [37] in that multiport scattering matrices can be handled, and only a single inverse needs to be evaluated.

The z-mode scattering matrices for uniform sections are diagonal, with elements

$$S_{11}^{mn} = S_{21}^{mn} = 0$$

$$S_{12}^{mn} = S_{21}^{mn} = D_{mn} = \delta_{mn} \exp(-jk_z^m l_s)$$

where l_s is the length of the section and δ_{mn} is the Kronecker delta. Note that this is the only point where the section lengths appear, since all other quantities relating to propagation constants and mode coupling are related to the two-dimensional cross sections of the various sections in the element. This means that only the final scattering matrix cascade needs to be recalculated if section lengths are varied. This leads to considerable savings in computational effort where optimisation of a structure is required with respect to the lengths of individual sections.

To perform the section cascade, the two-port scattering matrices for the uniform sections are first cascaded with the scattering matrix S^D of the discontinuity immediately preceding each section. This yields a multiport scattering matrix S^{II} which includes the discontinuity and the uniform section following it which is given by

$$[S_{11}^{II}] = [S_{11}^D]$$

$$[S_{12}^{II}] = [S_{12}^D][D]$$

$$[S_{21}^{II}] = [D][S_{21}^D]$$

$$[S_{22}^{II}] = [D][S_{22}^D][D]$$

As described in [37], strongly evanescent modes for which $|k_z l_s| < 15$, where l_s is the length of the section, are not considered in the cascade. While such modes play an important role in evaluating the z-mode scattering at individual discontinuities, their fields are extremely weak away from discontinuities. Therefore, once they have been accounted for in the coupling evaluation, their subsequent effect on the overall scattering matrix cascade is negligible.

The section cascade begins at the specified input end of the element, with successive sections represented by S^{II} cascaded to the end of the previous section. The total cascade up to the section to be added is represented by S^I. The general multiport cascade is thus applied repetitively to construct the entire element. The input and output ports for the element are assumed to be terminated with matched impedances. These scattering parameters constitute the output of the three-dimensional analysis.

3 RESULTS

3.1 Two-dimensional Structures

Various two-dimensional waveguiding structures for which theoretical or experimental data are known were analysed using the transverse resonance technique described in Section 2. By comparing the results of the analysis with existing results, both the transverse resonance theory and its implementation in the program TERESA (for $\underline{T}$ransvers$\underline{E}$ $\underline{RES}$onance $\underline{A}$nalysis) could be tested. In each structure, TE and TM-to-y eigenmodes were generally used, although TE and TM-to-z modes are more appropriate for structures with a uniform dielectric constant. Although affecting the required amount of computational effort, the particular choice of TE and TM-to-x, y, or z eigenmodes was found to have no effect on the results.

3.1.1 Double Ridged Waveguide

Montgomery [9] calculated the cutoff frequencies of TE modes in the double ridged waveguide shown in Figure 3.1. A comparison was made these results and results obtained from the transverse resonance analysis. This data is shown in Table 3.1. In the side regions, 9 TE and 8 TM-to-z modes were used, while 3 TE and 2 TM-to-z modes were used in the gap. The number of modes in the side regions was determined from relative convergence given the number of modes in the gap. The number of gap modes was chosen according to convergence of the final results. Note that one more TE-to-z mode was used than TM-to-z modes. This is because the lowest order TE-to-z mode is the TEM-to-u mode for which $k_y = 0$. This mode has no TM-to-z counterpart, so that one extra TE-to-z mode must be used to attain the same k_y value as the highest order TM-to-z mode. This situation also arises when TE and TM-to-x modes are used. If TE and TM-to-y modes are used, one more TM mode than the number of TE modes is used to account for the TEM-to-u mode. This difference arises the different definitions of the various mode types.
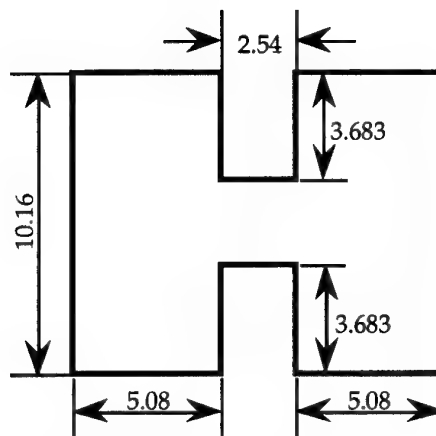
Figure 3.1   Double ridged waveguide cross section [9] (dimensions in mm)

The transverse wavenumbers k_T for various modes are shown in Table 3.1. The modes labelled as "trough" modes are so named because the fields in the gap are only weakly coupled to the fields in the side regions. The agreement in Table 3.1 is generally better than 0.2 %. The simplicity of the ridged waveguide cross section belies its importance in many applications including broadband transitions and filters.

Table 3.1   Comparison of ridged waveguide TE mode cutoff frequencies

Mode	$f_c^{[19]}$ (GHz)	f_c^{TR} (GHz)
TE_{10}	6.857	6.871
TE_{10} (trough)	15.104	15.104
TE_{20}	24.858	24.890
TE_{20} (trough)	29.536	29.541
TE_{30}	32.024	32.026
TE_{11} (trough)	33.271	33.271

3.1.2   Unilateral Finline

Finlines are an important structure extensively used in broadband millimetre-wave applications due to their compactness and the ease of mounting active devices. The theoretical results of Vahldieck [21] for the unilateral finline shown in Figure 3.2 were used to verify the transverse resonance results for this guide. This structure was more complex than the ridged waveguide in that it contained both "step-up" and "step-down" discontinuities on either side of the slot region, as well as a dielectric. Symmetry about the axis shown in Figure 3.2 was invoked to reduce the computational effort required. For convergence, 2 TE and 3 TM-to-y modes were used in the slot region, with 13 TE and 14 TM-to-y modes in the dielectric region and 8 TE and 9 TM-to-y modes in the side regions.
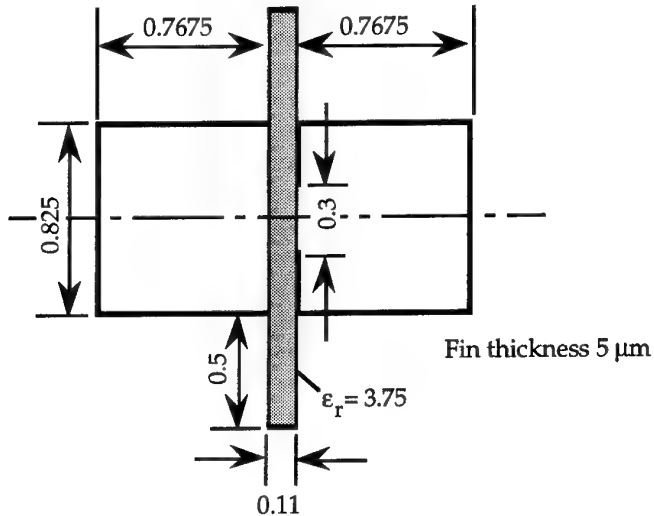
Figure 3.2   Unilateral finline cross section [21] (all dimensions in mm)

A comparison of the normalised wavenumbers k_z/k_0 is shown in Figure 3.3. Note that the agreement is generally better than 3 %. The discrepancies between the two sets of results, particularly for higher order z-modes, may be due to numerical inaccuracy or convergence difficulties in Vahldieck's method as discussed by Mansour and MacPhie [27]. Graph reading errors in obtaining Vahldieck's results could also contribute to the observed discrepancy.
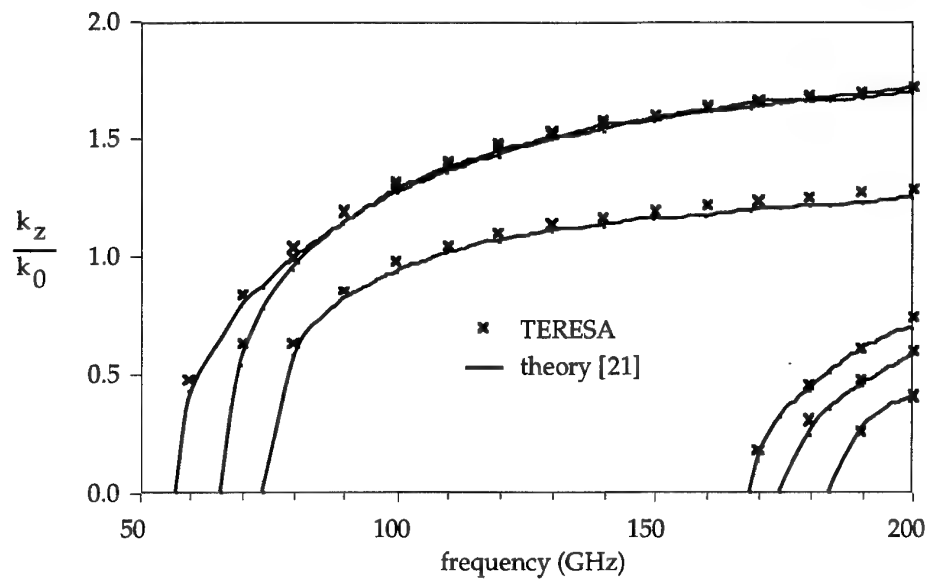
Figure 3.3   Comparison of $\dfrac{k_z}{k_0}$ versus frequency results for unilateral finline

3.1.3   Suspended stripline

The suspended stripline from [27] and [51] shown in Figure 3.4 was analysed using the transverse resonance technique. Symmetry about the axis shown was used to reduce the required computational effort. For convergence, 3 TE and 4 TM-to-y modes were used in the narrow region under the strip, with 4 TE and 5 TM-to-y modes in the other regions.
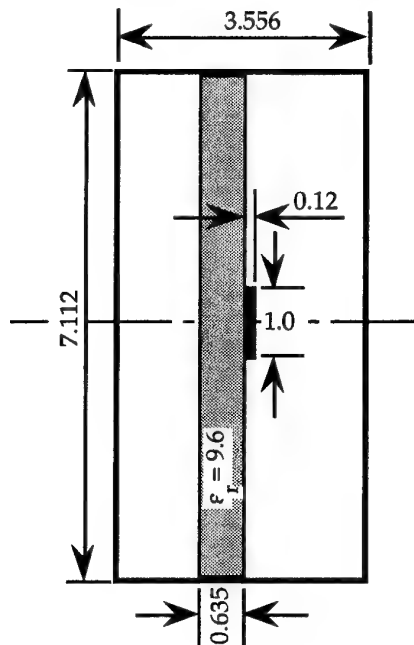
Figure 3.4   Suspended stripline cross section [27]

The results were compared with theoretical results published by Mansour and MacPhie [27], and Bornemann [51] as shown in Figure 3.5. The agreement with [27] is excellent, whereas some discrepancies are again noticed with Bornemann's results, particularly for the higher-order modes. As with the unilateral finline, numerical inaccuracy and convergence difficulties inherent in Bornemann's method are the most probable causes of error.

3.1.4 Coplanar Waveguide

The coplanar waveguide is another structure commonly used for millimetre-wave applications. The coplanar waveguide shown in Figure 3.6 was analysed and the results compared with those of Mansour and MacPhie [27], and Bornemann and Arndt [13]. The calculation of the dominant and first-order odd mode normalised propagation constants k_z/k_0 was performed with the depth, d, of the groove set to 0 and 0.5 mm. Symmetry was used to reduce the size of the calculation, with an electric wall inserted on the axis shown to generate the desired odd symmetry. For convergence, 2 TE and 3 TM-to-y modes were used in the slots, with 8 TE and 9 TM-to-y modes in the side regions. For d = 0, 8 TE and 9 TM-to-y modes were used in the dielectric regions, and 13 TE and 14 TM-to-y modes for the d = 0.5 case, as required by the relative convergence criterion.
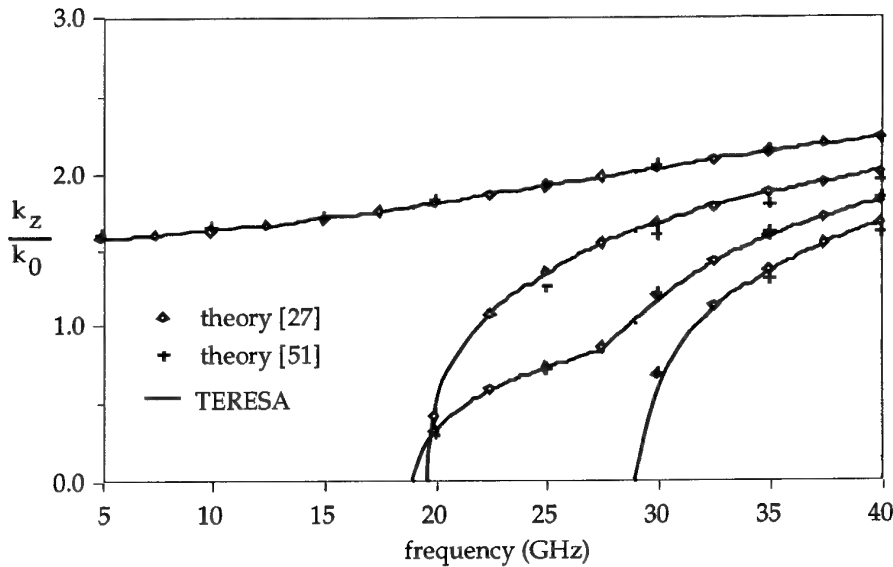
Figure 3.5 Comparison of $\dfrac{k_z}{k_0}$ versus frequency results for suspended stripline

For both groove depths, the agreement with [27] and [13] is close, as shown in Figure 3.7, although the agreement is closer for the d = 0 case. Note that increasing the groove depth decreased the first-order odd mode cutoff frequency, reducing the single-mode bandwidth of the guide [27].

3.1.5 Groove Nonradiative Dielectric Guide

Nonradiative dielectric waveguide is attractive for millimetre-wave applications because of its simplicity, ease of fabrication, and low loss. Tong and Blundell [52] included grooves in the upper and lower plates to fix the dielectric slab in place, as shown in Figure 3.8. The inclusion of a groove, however, renders simple single-mode transverse resonance modelling inaccurate because of mode scattering at the groove discontinuities, so that a generalised, multimode treatment is required.
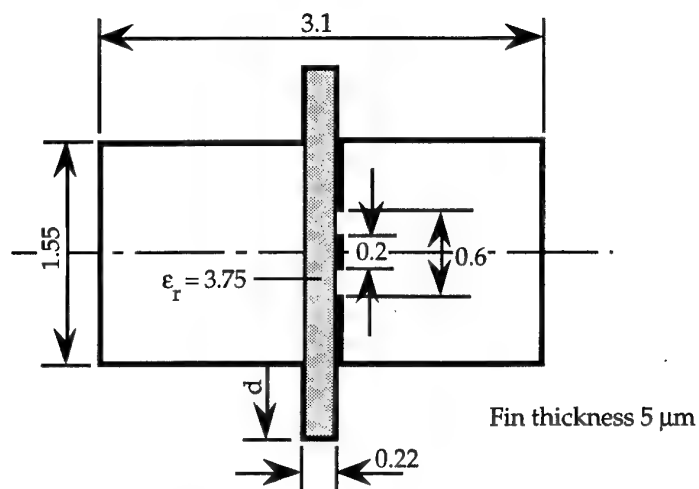
Figure 3.6   Coplanar waveguide cross-section (all dimensions in mm)
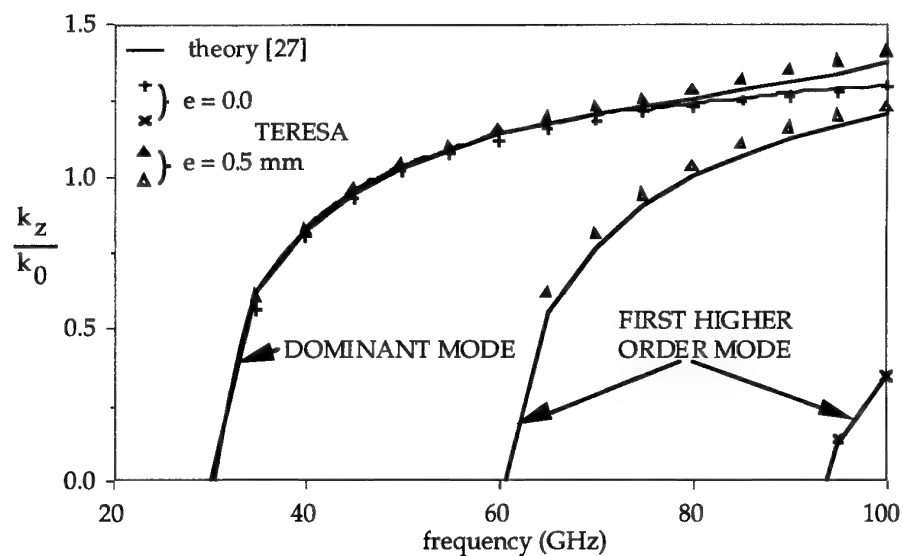
Figure 3.7   Comparison of $\dfrac{k_z}{k_0}$ versus frequency results for coplanar waveguide
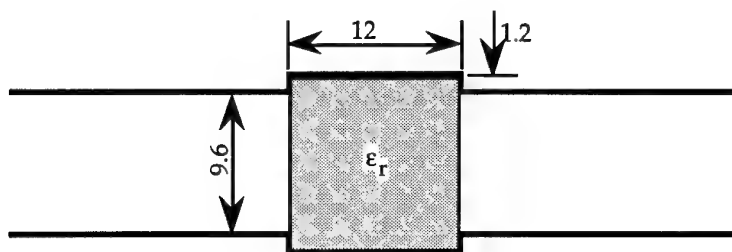
Figure 3.8   Groove nonradiative dielectric (GNRD) waveguide cross section (all dimensions in mm)

Transverse resonance analysis of the groove nonradiative dielectric (GNRD) guide shown in Figure 3.8 yielded values for the normalised wavenumber k_z/k_0 of the LSM_{11} mode which could be compared with experimental data published by Tong and Blundell. GNRD guides with relative dielectric constants, ε_r, of 2.56 and 4.0 were analysed. TE and TM-to-x modes were used in the calculation, with 5 TE and 4 TM modes used in each region to ensure convergence. The agreement with the experimental data shown in Figure 3.11 is generally better than 5 %. This disagreement is also evident in Tong and Blundell's calculations, and so probably originates from experimental errors.
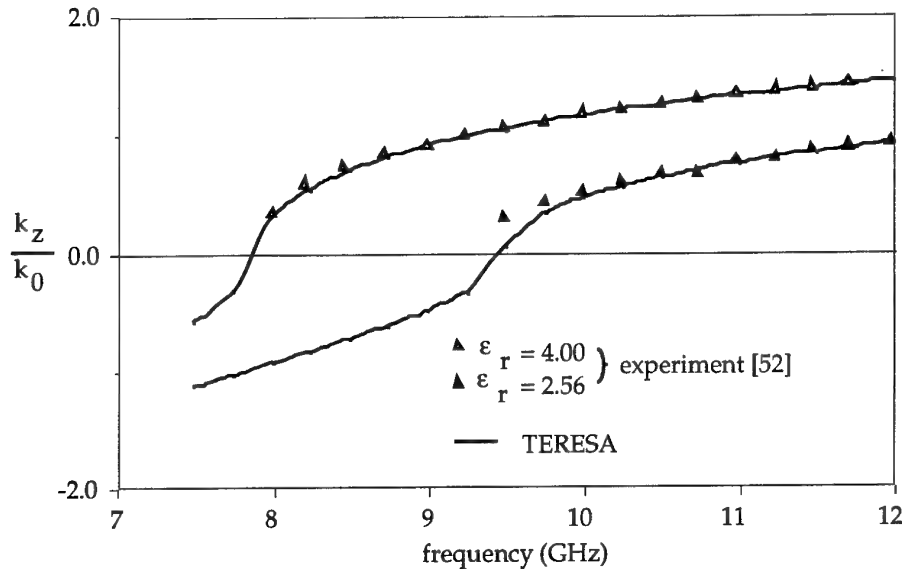
Figure 3.9   Comparison of $\dfrac{k_z}{k_0}$ versus frequency results for GNRD waveguide

3.1.6   Shielded Dielectric Image Guide

A comparison was made between the theoretical results presented by Strube and Arndt [40] and the results from the transverse resonance analysis for the shielded dielectric image guide shown in Figure 3.10. This guide differs from those discussed previously in that it possesses a non-uniform region. For this reason, TE and TM-to-y modes must be used. For convergence, 5 TE and 6 TM-modes were required.
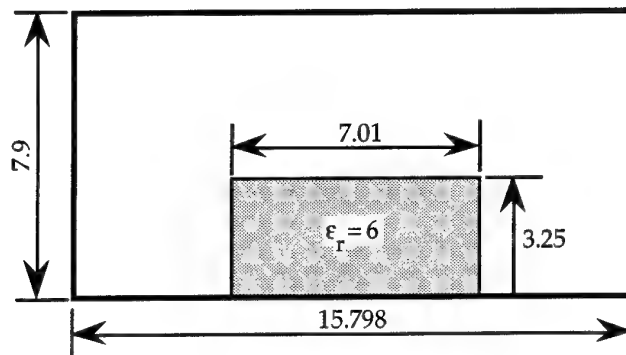
Figure 3.10   Shielded dielectric image guide cross section
(all dimensions in mm)

Unlike the structures previously examined, this guide was found to support a complex mode between 13.8 and 16.3 GHz, as can be seen from Figure 3.11. Complex modes occur as a result of coupling between degenerate z-modes. Although only one mode is shown in Figure 3.11, they must exist in degenerate pairs with propagation constants of opposite sign ($\pm k_z = \pm \beta \pm j \alpha$). While a real power flow exists, the total power transmitted through the cross-section is zero, since equal amounts of power are transmitted in the forward and backward directions. Hence, complex modes do not correspond to power dissipation, and are supported in the lossless waveguide model. The agreement between the two sets of results shown in Figure 3.11 is excellent.
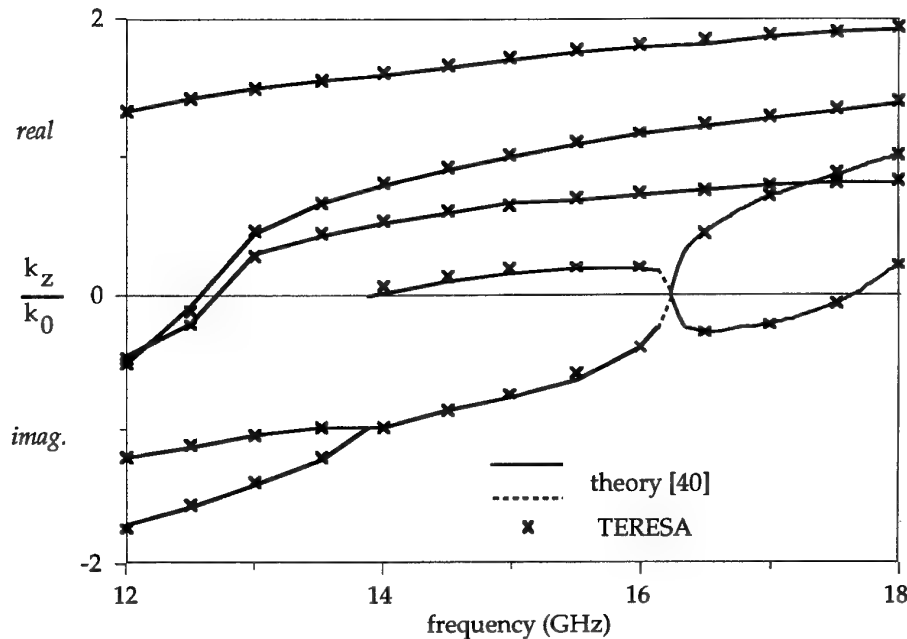
Figure 3.11   Comparison of $\dfrac{k_z}{k_0}$ versus frequency for shielded dielectric image guide

3.2   Three-dimensional Structures

The calculation of the propagation constants, k_z, and the modal fields for the z-modes in two-dimensional sections allowed the scattering parameters for three-dimensional waveguide elements to be calculated. As for Section 3.1, structures for which independent theoretical or experimental results could be found were analysed.

3.2.1   Rectangular Waveguide Transformer

The simplest type of element to analyse comprises cascaded rectangular waveguide elements. A typical example of such a structure is the Ku to X-band transformer shown in Figure 3.12, with dimensions as shown. This structure was analysed by Arndt *et al.* [39]. For analysis by the TERESA program, 6 TE and 5 TM-to-z *y*-modes with 60 z-modes were used in each section. A comparison of the reflection coefficient $|S_{11}|$ given in [39] and by the TERESA program is shown in Figure 3.13. The small error between the two sets of results can be attributed to reading error in obtaining the results from [39] graphically.
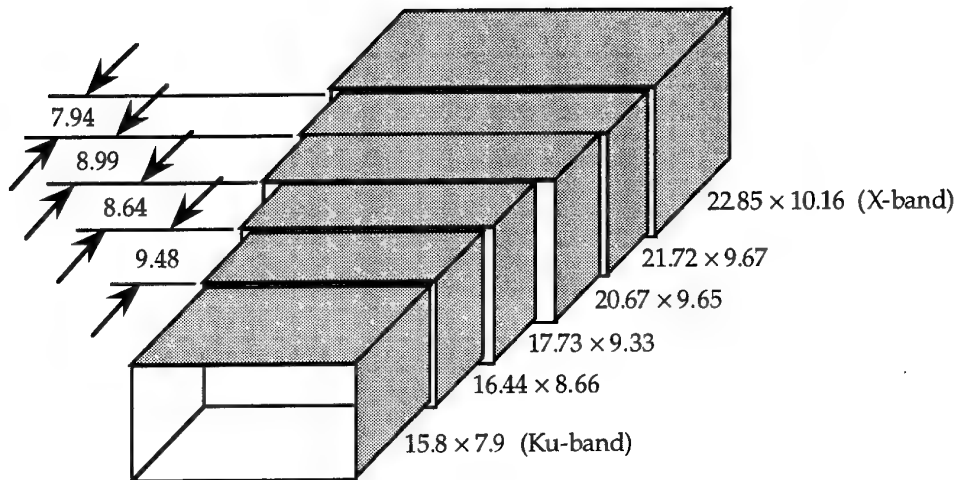
Figure 3.12   Four-section Ku to X-band waveguide transformer   (all dimensions in mm)
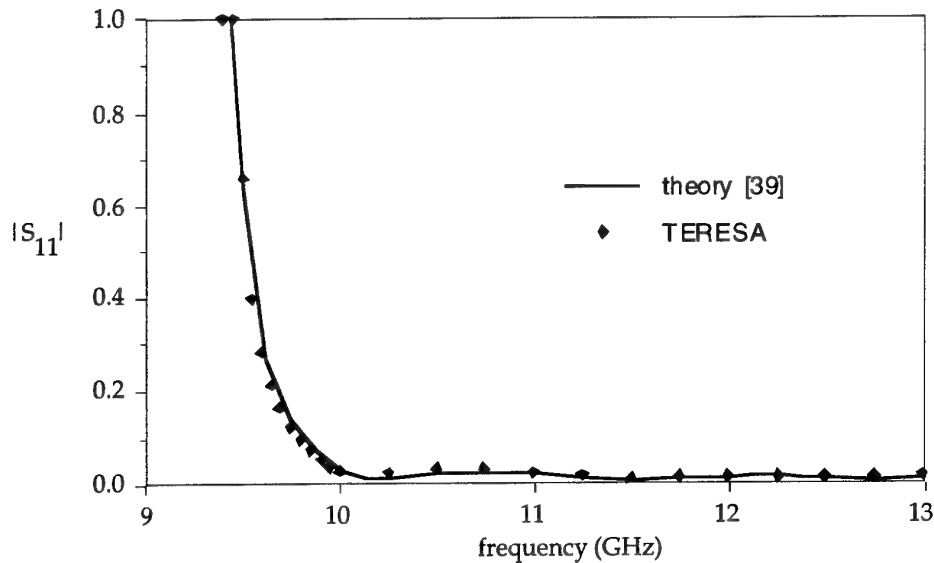
Figure 3.13   Comparison of input reflection coefficient for Ku to X-band transformer

3.2.2   Rectangular Waveguide E-Plane Stubs

A comparison of the magnitudes of S_{11} and S_{12} and the phase of S_{11} with known results was made for the rectangular waveguide with E-plane steps shown in Figure 3.14. This structure was independently analysed by Rozzi and Mongiardo [53]. The results from [53] are compared with the TERESA output in Figure 3.15. The two sets of results agree closely, except at 14.75 GHz where TERESA appears to predict a resonance. Note however that the Rozzi and Mongiardo technique also shows some anomalous behaviour near this frequency. For the TERESA analysis, 4 TE and 3 TM-to-z modes and 35 z-modes were used in the smaller sections, with 6 TE and 5 TM-to-z modes and 55 z-modes used in the larger sections. Symmetry was used to reduce the size of the calculation.

3.2.3   E-Plane Insert Filter

The E-plane metal insert filter shown in Figure 3.16 was analysed, and the results compared to calculations by Vahldieck *et al.* [44], and measurements by Tajima and Sawayama [54]. This comparison is shown in Figure 3.17. The results from the TERESA analysis agree well with those from [44]. A small discrepancy is apparent with the measured results of [54] which can be attributed to graph reading error. For the TERESA analysis, 6 TE and 5 TM-to-z modes and 55 z-modes were used in each section. Symmetry about the y-z plane was invoked to reduce computational effort.
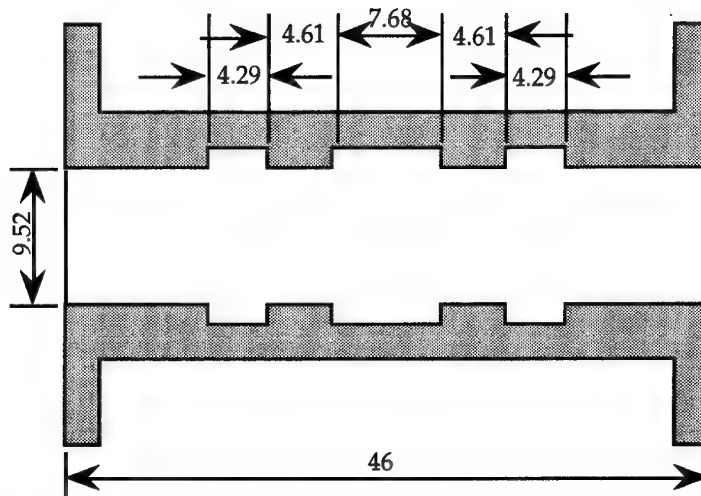
Figure 3.14   WR 75 waveguide with E-plane stubs   (all dimensions in mm)
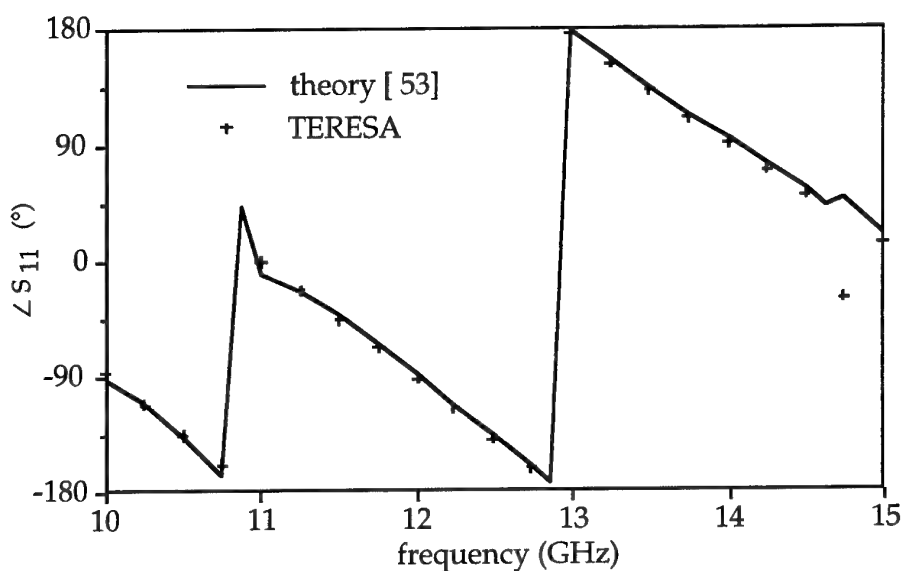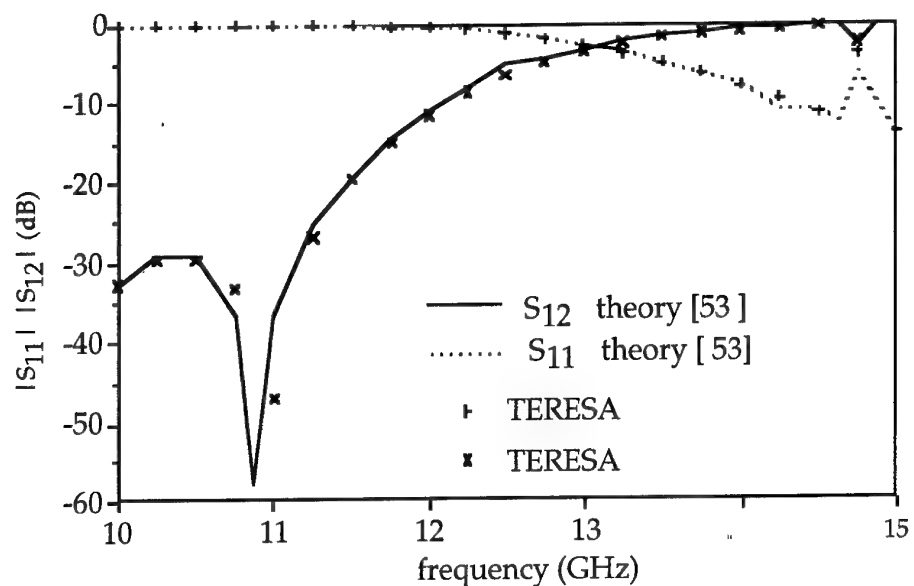
Figure 3.15 Scattering parameter plots for E-plane stubs in rectangular waveguide
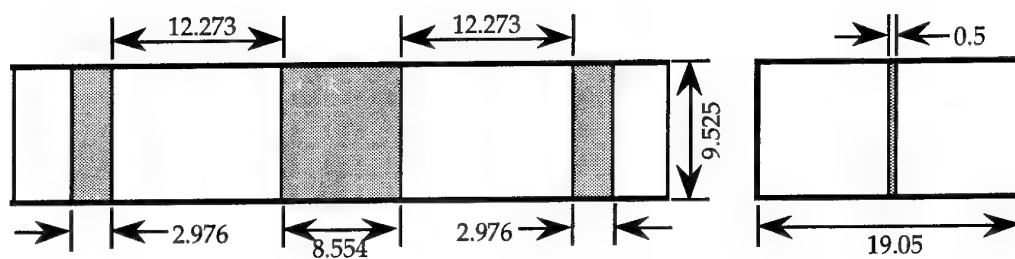
Figure 3.16 Rectangular waveguide E-plane metal insert filter (all dimensions in mm)
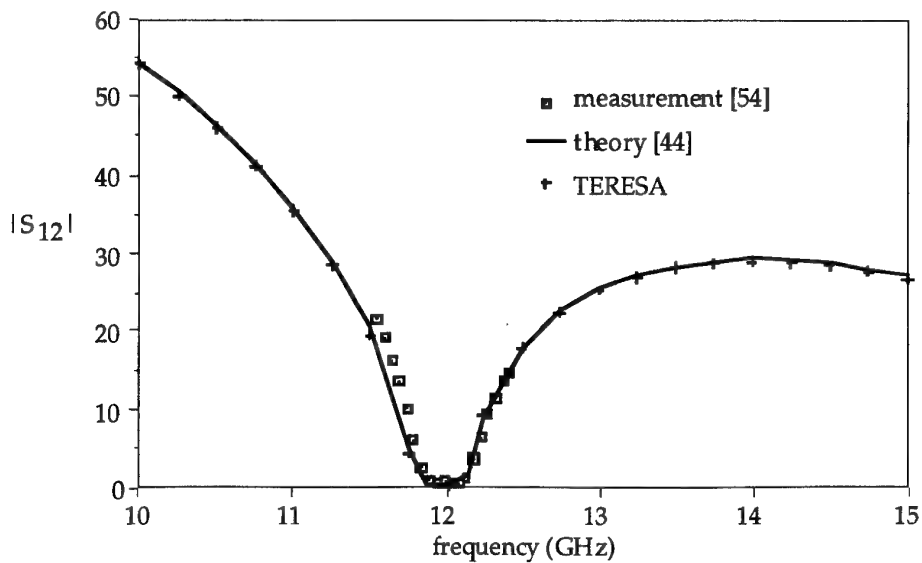
Figure 3.17 Transmission coefficient for E-plane metal insert filter

3.2.4   Square Waveguide Iris Polariser

The square waveguide iris polariser shown in Figure 3.18 was analysed and a comparison made with independent calculated results from [55]. These components are used to excite circularly polarised waves in square aperture antennas by producing a 90 degree differential phase shift between the orthogonal TE_{10} and TE_{01} modes.
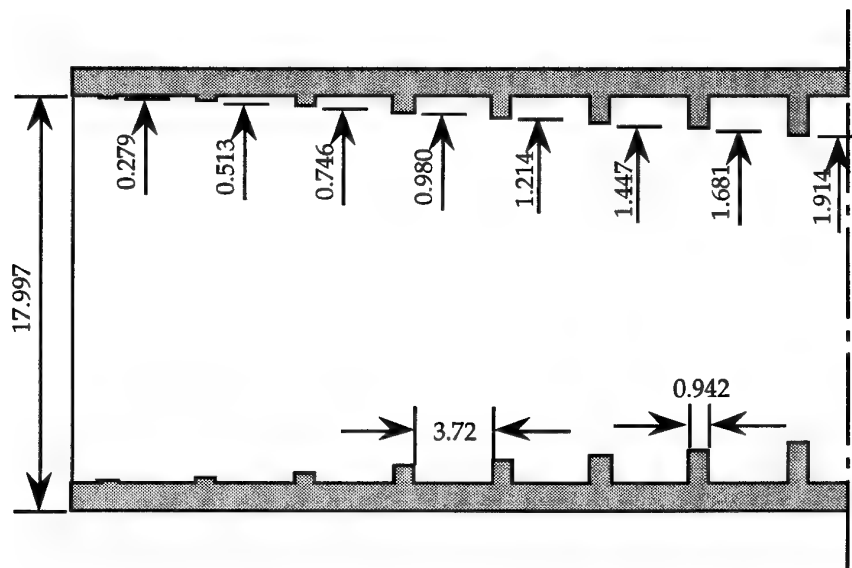
**Figure 3.18 Square waveguide iris polariser
(all dimensions in mm)**

For the TERESA analysis, 20 TE and 21 TM-to-y modes and 60 z-modes were used in each section. Horizontal and vertical symmetry were used to reduce the size of the calculation. For the TE_{10} mode, a horizontal magnetic wall and a vertical electric wall were used, and

a horizontal electric wall and a vertical magnetic wall for the TE_{01} mode. Figure 3.19 shows the good agreement between the TERESA results and the analysis presented in [55].
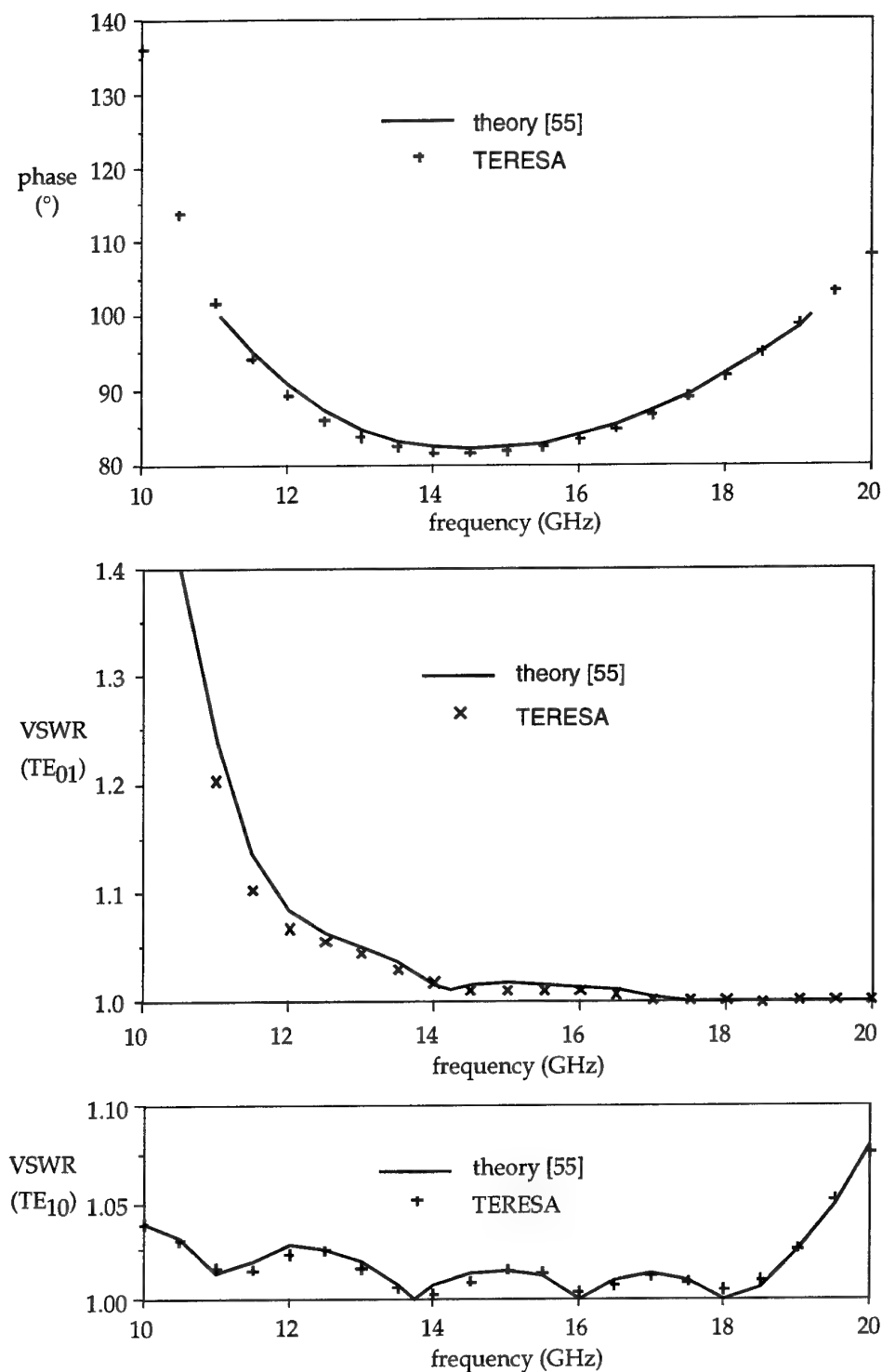
Figure 3.19 VSWR and differential phase shift for square waveguide iris polariser

3.2.5 Ridge Waveguide Notch

The notched ridge waveguide shown in Figure 3.20 was analysed with the results compared to experimental data obtained by the present authors. A resonance was observed at 6.55 GHz. The close agreement between theory and experiment is shown in Figure 3.21. For the TERESA analysis, 60 z-modes were used in each section to ensure convergence.
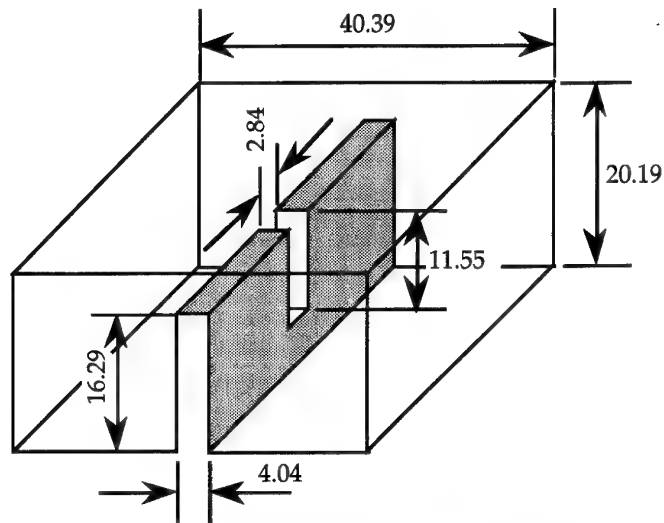
Figure 3.20 Notch in ridge waveguide (all dimensions in mm)
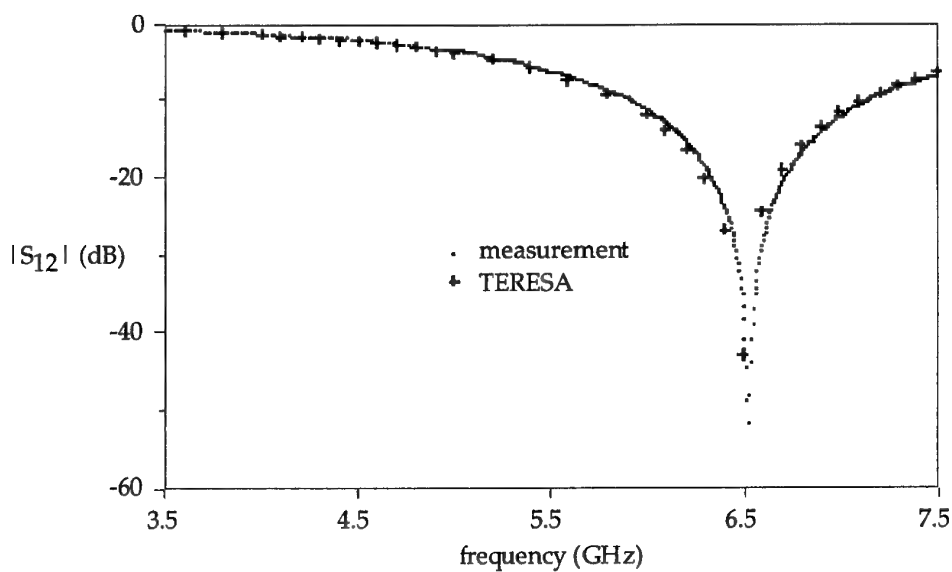
Figure 3.21 Transmission coefficient for notched ridge waveguide

3.2.6   Cross-Iris Filter

The transmission coefficient $|S_{21}|$ was calculated the cross-iris filter shown in Figure 3.22 using the TERESA analysis. In the rectangular section, 8 TE and 9 TM-to-y modes with 60 z-modes were used. For the irises, 3 TE and 4 TM-to-y modes were used in the smaller side regions, and 5 TE and 6 TM-to-y modes in the larger centre region, with a total of 30 z-modes required for convergence. Symmetry about the vertical and horizontal planes was used to reduce the size of the calculation. The results obtained compared well with the calculated and measured results determined by Ihmels and Arndt [50], as shown in Figure 3.23.
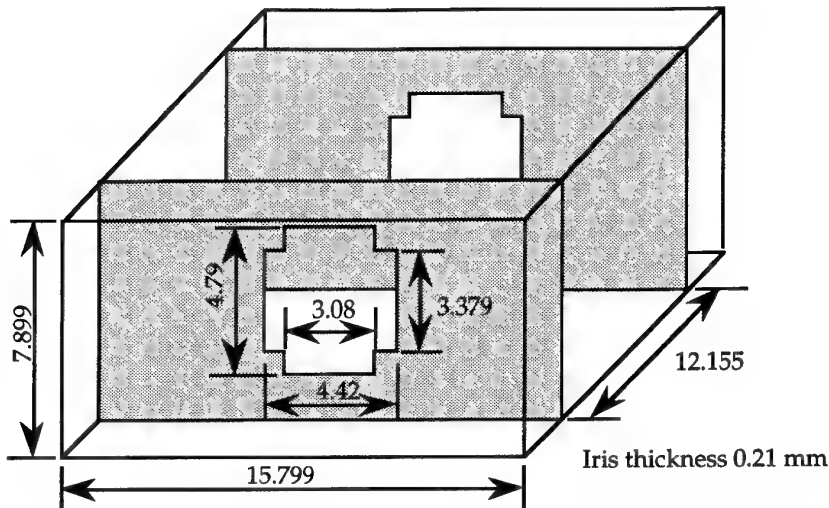
Figure 3.22   Cross iris resonator filter (all dimensions in mm)

4   CONCLUSIONS

A three-dimensional mode matching analysis which uses the generalised transverse resonance technique to analyse the constituent two-dimensional cross-sections in passive waveguide structures has been developed and successfully tested. Comparison with a broad range of waveguide components for which independent experimental or theoretical data could be found revealed close agreement in all cases.

This method potentially offers advantages in speed and efficiency over more generally applicable, but computationally intensive, methods such as the finite element or finite difference methods. It promises to be especially useful for the analysis and optimisation of broadband waveguide components.

Further work will concentrate on the analysis of more complex three-dimensional waveguide components for the design of filters and broadband transitions.
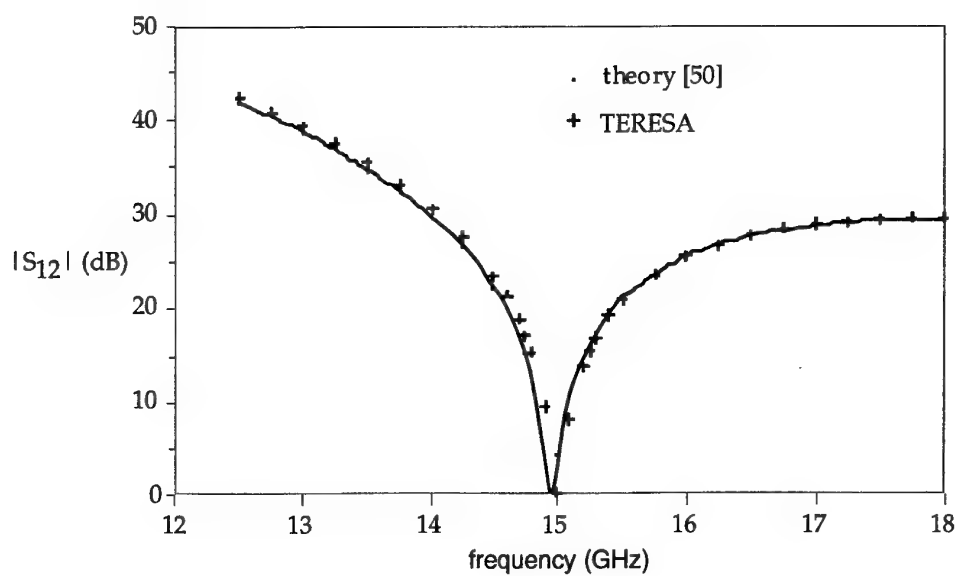
Figure 3.23   Transmission coefficient for cross iris resonator filter

5 REFERENCES

[1]   C. M. D. Rycroft and C. A. Olley, "Modelling of step discontinuities in unilateral finline," *GEC J. Res.*, vol. 5, pp. 226-236, 1987.

[2]   D. G. Swanson Jr., "Simulating EM fields," *IEEE Spectrum*, vol. 28, pp. 34-37, Nov. 1991.

[3]   T. Itoh, Ed., *Numerical Techniques for Microwave and Millimeter-Wave Passive Structures*, New York: John Wiley and Sons, 1989.

[4]   R. Sorrentino, Ed., *Numerical Methods for Passive Microwave and Millimeter Wave Structures*, New York: IEEE Press, 1989.

[5]   E. Yamashita, (Ed.) *Analysis Methods for Electromagnetic Wave Problems*, Norwood, MA: Artech House, 1990.

[6]   C. G. Montgomery, R. H. Dicke, and E. M. Purcell, Eds., *Principles of Microwave Circuits*, New York: McGraw-Hill, 1947.

[7]   N. Marcuvitz, *Waveguide Handbook*, New York: McGraw-Hill, 1951.

[8]   H. M. Altschuler and L. O. Goldstone, "On network representations of certain network obstacles in waveguide regions," *IRE Trans. Microwave Theory Tech.*, vol. MTT-7, pp. 213-221, Apr. 1959.

[9]   P. J. B. Clarricoats and A. A. Oliner, "Transverse-network representation for inhomogeneously filled circular waveguides," *Proc. Inst. Electr. Eng.*, vol. 112, pp. 883-894, May, 1965.

[10] L. B. Felsen and N. Marcuvitz, *Radiation and Scattering of Waves*, Englewood Cliffs, N.J.: Prentice-Hall, 1973.

[11] D. M. Kerns, "Definitions of v, i, Z, Y, a, b, Γ, and S," *Proc. IEEE*, vol. 55, pp. 892-900, June 1967.

[12] S. Peng and A. A. Oliner, "Guidance and leakage properties of a class of open dielectric waveguides: Part I - Mathematical formulations," *IEEE Trans. Microwave Theory Tech.*, vol. MTT-29, pp. 843-854, Sep 1981.

[13] J. Bornemann and F. Arndt, "Calculating the characteristic impedance of finlines by the transverse resonance method," *IEEE Trans. Microwave Theory Tech.*, vol. MTT-34, pp. 85-92, Jan 1986.

[14] P. H. Masterman and P. J. B. Clarricoats, "Computer field-matching solution of waveguide transverse discontinuities," *Proceedings of the IEE*, vol. 118, pp. 51-63, Jan 1971.

[15] M. Jing-Feng and Y. Ping, "The characteristics of NRD waveguide gratings," *Int. J. Infrared Millimeter Waves*, vol. 11, pp. 175-188, Feb. 1990.

[16] B. D. Bates and A. Ko, "Modal analysis of radial-resonator waveguide diode mounts," *IEEE Trans. Microwave Theory Tech.*, vol. 38, pp. 1037-1045, Aug 1990.

[17] R. F. Harrington, *Time-Harmonic Electromagnetic Fields*, New York: McGraw-Hill, 1961.

[18] R. E. Collin, *Field Theory of Guided Waves*, 2nd edition, IEEE Press, p. 421, 1991.

[19] F. Alessandri, U. Goebel, F. Melai and R. Sorrentino, "Theoretical and experimental characterisation of nonsymmetrically shielded coplanar waveguides for millimeter-wave circuits," *IEEE Trans. Microwave Theory Tech.*, vol. 37, Dec 1989, pp. 2020-2026.

[20] J. P. Montgomery, "On the complete eigenvalue solution of ridged waveguide," *IEEE Trans. Microwave Theory Tech.*, vol. MTT-19, pp. 547-555, June 1973.

[21] R. Vahldieck , "Accurate hybrid-mode analysis of various finline configurations including multilayered dielectrics, finite metallisation thickness, and substrate holding grooves," *IEEE Trans. Microwave Theory Tech.*, vol. MTT-32, pp. 1454-1460, Nov 1984.

[22] R. Vahldieck and J. Bornemann, "A modified mode-matching technique and its application to a class of quasi-planar transmission lines," *IEEE Trans. Microwave Theory Tech.*, vol. MTT-33, pp. 916-925, Oct 1987.

[23] J. Tao, "A modified transverse resonance method for the analysis of multilayered, multiconductor quasiplanar structures with finite conductor thickness and mounting grooves," *IEEE Trans. Microwave Theory Tech.*, vol. 40, pp. 1966-1970, Oct 1992.

[24] G. Schiavon, R. Sorrentino and P. Tognolatti, "Characterisation of coupled finlines by generalised transverse resonance method," *International Journal of Numerical Modelling: Electronic Networks, Devices, and Fields*, vol. 1, pp. 45-49, Mar. 1988.

[25] R. Sorrentino and T. Itoh, "Transverse resonance analysis of finline discontinuities," *IEEE Trans. Microwave Theory Tech.*, vol. MTT-32, pp. 1663-1638, Dec 1984.

[26] M. Leroy, "On the convergence of numerical results in modal analysis," *IEEE Transactions on Antennas and Propagation*, vol. AP-31, pp. 655-659, July 1983.

[27] R. R. Mansour and R. H. MacPhie, "A unified hybrid-mode analysis for planar transmission lines with multilayer isotropic/anisotropic substrates," *IEEE Trans. Microwave Theory Tech.*, vol. MTT-35, pp. 1382-1391, Dec. 1987.

[28] A. S. Omar and K. Schunemann, "Transmission matrix representation of finline discontinuities," *IEEE Trans. Microwave Theory Tech.*, vol. MTT-33, pp. 765-770, Sep 1985, .

[29] W. H. Press, B. P. Flannery, S. A. Teukolsky, W. T. Vetterling, *Numerical Recipes*, Cambridge University Press, pp. 52-64, 1986.

[30] V. A. Labay, J. Bornemann, "Matrix singular value decomposition for pole-free solutions of homogeneous matrix equations as applied to numerical modelling methods," *IEEE Microwave and Guided Wave Letters*, vol. 2, pp. 49-51, Feb. 1992.

[31] W. H. Press, B. P. Flannery, S. A. Teukolsky, W. T. Vetterling, *Numerical Recipes*, Cambridge University Press, pp. 283-286, 1986.

[32] *ibid*, pp. 248-251.

[33] L. M. Delves and J. N. Lyness, "A numerical method for locating the zeros of an analytic function," *Math. Comput.*, vol. 21, pp. 543-560, 1967.

[34] P. Lampariello and R. Sorrentino, "The ZEPLS program for solving characteristic equations of electromagnetic structures," *IEEE Trans. Microwave Theory Tech.*, vol. MTT-23, pp. 457-458, May 1975.

[35] W. H. Press, B. P. Flannery, S. A. Teukolsky, W. T. Vetterling, *Numerical Recipes*, Cambridge University Press, pp. 31-38, 1986.

[36] R. Safavi-Naini and R. H. MacPhie, "Scattering at rectangular-to-rectangular waveguide junctions," *IEEE Trans. Microwave Theory Tech.*, vol. 30, pp. 2060-2063, Nov 1982.

[37] H. Patzelt and F. Arndt, "Double-plane steps in rectangular waveguides and their application for transformers, irises, and filters," *IEEE Trans. Microwave Theory Tech.*, vol. MTT-30, pp. 771-776, May 1982.

[38] R. De Smedt and B. Denturck, "Scattering matrix of junctions between rectangular waveguides," *IEE Proceedings*, vol. 130, Pt. H, pp. 183-190, March 1983.

[39] F. Arndt, U. Tucholke, and T. Wriedt, "Computer-optimized multisection transformers between rectangular waveguides of different frequency bands," *IEEE Transactions on Microwave Theory and Techniques*, vol. MTT-32, pp. 1479-1484, Nov 1984.

[40] J. Strube and F. Arndt, "Rigorous hybrid-mode analysis of the transition from rectangular waveguide to shielded dielectric image guide," *IEEE Trans. Microwave Theory Tech.*, vol. MTT-33, pp. 391-400, May 1985.

[41] T. Sieverding and F. Arndt, "Modal analysis of the magic tee," *IEEE Microwave and Guided Wave Letters*, vol. 3, pp. 150-152, May 1993.

[42] T. Sieverding and F. Arndt, "Field theoretic CAD of open or aperture matched T-junction coupled rectangular waveguide structures," *IEEE Trans. Microwave Theory Tech.*, vol. 40, pp. 353-362, Feb 1992.

[43] F. Arndt and G. U. Paul, "The reflection definition of the characteristic impedance of microstrips," *IEEE Trans. Microwave Theory Tech.*, vol. MTT-27, pp. 724-730, Aug 1979.

[44] R. Vahldieck, J. Bornemann, F. Arndt, and D. Grauerholz, "Optimised waveguide E-plane metal insert filters for millimeter-wave applications," *IEEE Trans. Microwave Theory Tech.*, vol. 31, pp. 65-69, Jan. 1983.

[45] J. Bornemann and F. Arndt, "Modal-S-Matrix design of optimum stepped ridged and finned waveguide transformers," *IEEE Trans. Microwave Theory Tech.*, vol. MTT-35, pp. 561-567, June 1987.

[46] J. Bornemann and F. Arndt, "Rigorous design of evanescent-mode E-plane finned waveguide bandpass filters," *1989 IEEE Microwave Theory and Techniques Symposium Digest*, pp. 603-605, 1989.

[47] J. Bornemann and F. Arndt, "Transverse resonance, standing wave, and resonator formulations of the ridge waveguide eigenvalue problem and its application to the design of E-plane finned waveguide filters," *IEEE Trans. Microwave Theory Tech.*, vol. 38, pp. 1104-1113, August 1990.

[48] J. Bornemann and F. Arndt, "Optimum field theory design of stepped E-plane finned waveguide transformers of different inner cross-sections," *1990 IEEE Microwave Theory and Techniques Symposium Digest*, pp. 1071-1074, 1990.

[49] V. A. Labay and J. Bornemann, "A new evanescent-mode filter for densely packaged waveguide applications," *1992 IEEE Microwave Theory and Techniques Symposium Digest*, pp. 901-904, 1992.

[50] R. Ihmels, F. Arndt, "Rigorous modal S-matrix analysis of the cross-iris in rectangular waveguides," *IEEE Microwave and Guided Wave Letters*, vol. 2, pp. 400-402, Oct 1992.

[51] J. Bornemann, "Rigorous field theory analysis of quasiplanar waveguides," *IEE Proceedings*, vol. 132, Pt. H, pp. 1-6, Feb 1985.

[52] C. E. Tong and R. Blundell, "Study of groove nonradiative dielectric waveguide," *Electronics Letters*, vol. 25, pp. 934-936, 6th July 1989.

[53] T. Rozzi, M. Mongiardo, "E-plane steps in rectangular waveguide," *IEEE Transactions on Microwave Theory and Techniques*, Vol. 39, No. 8, pp. 1279-1288, August 1991.

[54] Y. Tajima and Y. Sawayama, "Design and analysis of a waveguide-sandwich microwave filter," *IEEE Trans. Microwave Theory Tech.*, vol. MTT-22, pp. 839-841, Sep 1974.

[55] U. Tucholke, F. Arndt, T. Wriedt, "Field theory design of square waveguide iris polarisers," *IEEE Transactions on Microwave Theory and Techniques*, Vol. MTT-34, No. 1, pp. 156-159, Jan 1986.

THIS PAGE INTENTIONALLY BLANK

APPENDIX I   MODE FUNCTION GENERATOR

The field in each subregion of a given two-dimensional section within the element to be analysed is represented by an expansion in terms of y-modes which are TE and TM to the $x, y,$ or z reference directions. The choice of which direction was most appropriate for a particular type of structure is discussed in Section 2.3.2. The general technique used to generate the fields corresponding to these mode functions follows Felsen and Marcuvitz [10], and is derived in this appendix from Maxwell's equations. These equations are

$$\nabla \times \mathbf{H} = j\omega\varepsilon\mathbf{E} \tag{I.1}$$

$$\nabla \times \mathbf{E} = -j\omega\mu\mathbf{H} \tag{I.2}$$

$$\nabla \bullet \varepsilon\mathbf{E} = 0 \tag{I.3}$$

$$\nabla \bullet \mu\mathbf{H} = 0 \tag{I.4}$$

From Equation I.1

$$\nabla \times \nabla \times \mathbf{H} = \nabla \times (j\omega\varepsilon\mathbf{E})$$

$$(\nabla \times \nabla \times \mathbf{H}) \times \mathbf{u_z} = [\nabla \times (j\omega\varepsilon\mathbf{E})] \times \mathbf{u_z}$$

Using the identity

$$\nabla(\mathbf{A}\bullet\mathbf{B}) = (\mathbf{A}\bullet\nabla)\,\mathbf{B} + (\mathbf{B}\bullet\nabla)\,\mathbf{A} + \mathbf{A} \times (\nabla\times\mathbf{B}) + \mathbf{B}\times(\nabla\times\mathbf{A})$$

then (with $\mathbf{A} = \mathbf{E}$ and $\mathbf{B} = \mathbf{u_z}$)

$$[\nabla \times (j\omega\varepsilon\mathbf{E})] \times \mathbf{u_z} = j\omega\varepsilon\,[\mathbf{E} \times (\nabla \times \mathbf{u_z}) + (\mathbf{E}\bullet\nabla)\,\mathbf{u_z} + (\mathbf{u_z}\bullet\nabla)\,\mathbf{E} - \nabla(\mathbf{E}\bullet\mathbf{u_z})]$$

$$= j\omega\varepsilon\,[0 + 0 + \frac{\partial\mathbf{E_t}}{\partial z} + \frac{\partial\mathbf{E_z}}{\partial z} - \nabla_t\,E_z - \nabla_z\,E_z]$$

$$= j\omega\varepsilon\,[\frac{\partial\mathbf{E_t}}{\partial z} - \nabla_t\,E_z] \tag{I.5}$$

where ∇_t is the transverse gradient operator, and $\mathbf{E_t}$ is the field in the plane transverse to the reference direction to which the modes are to be TE or TM. Note that since the modes are to be recalculated for each subregion layer of differing dielectric constant, ε is regarded as uniform. From Equations I.1 and I.2

$$\nabla \times \nabla \times \mathbf{H} = k^2\mathbf{H} \tag{I.6}$$

where $\qquad\qquad k^2 = \omega^2\mu\varepsilon$

From Equations I.5 and I.6

$$\frac{\partial\mathbf{E}_t}{\partial z} = \frac{1}{j\omega\varepsilon}k^2\mathbf{H}_t \times \mathbf{u_z} + \nabla_t E_z \tag{I.7}$$

Now from Equation I.1

$$\nabla_t \times \mathbf{H_t} = j\omega\varepsilon E_z$$

Thus

$$\nabla_t \times \mathbf{H_t} \bullet \mathbf{u_z} = \nabla_t \bullet \mathbf{H_t} \times \mathbf{u_z} = j\omega\varepsilon E_z$$

$$\nabla_t\nabla_t \bullet \mathbf{H_t} \times \mathbf{u_z} = j\omega\varepsilon\nabla_t E_z \tag{I.8}$$

From Equations I.3 and I.4

$$\frac{\partial \mathbf{E}_t}{\partial z} = \frac{1}{j\omega\varepsilon}\left[k^2\mathbf{H}_t \times \mathbf{u}_z + \nabla_t\nabla_t \bullet \mathbf{H}_t \times \mathbf{u}_z\right]$$

$$= -j\omega\mu\left[\mathbf{1}_t + \frac{\nabla_t\nabla_t}{k^2}\right]\bullet \mathbf{H}_t \times \mathbf{u}_z \qquad (I.9)$$

where $\mathbf{1}_t$ is the transverse unit dyadic $\mathbf{u}_x\mathbf{u}_x + \mathbf{u}_y\mathbf{u}_y$.

Similarly,

$$\frac{\partial \mathbf{H}_t}{\partial z} = -j\omega\varepsilon\left[\mathbf{1}_t + \frac{\nabla_t\nabla_t}{k^2}\right]\bullet \mathbf{u}_z \times \mathbf{E}_t \qquad (I.10)$$

Let

$$\mathbf{E}_t(x, y, z) = \sum_i V_i(z)\mathbf{e}_i(x, y)$$

$$\mathbf{H}_t(x, y, z) = \sum_i I_i(z)\mathbf{h}_i(x, y)$$

Substituting in Equations I.9 and I.10

$$\sum_i \frac{\partial V_i}{\partial z}\mathbf{e}_i(x, y) = -j\omega\mu\left[\mathbf{1}_t + \frac{\nabla_t\nabla_t}{k^2}\right]\bullet \sum_i I_i(z)\mathbf{h}_i(x, y) \times \mathbf{u}_z$$

$$\sum_i \frac{\partial I_i}{\partial z}\mathbf{h}_i(x, y) = -j\omega\varepsilon\left[\mathbf{1}_t + \frac{\nabla_t\nabla_t}{k^2}\right]\bullet \mathbf{u}_z \times \sum_i V_i(z)\mathbf{e}_i(x, y)$$

These equations will be satisfied if

$$\frac{1}{I_i(z)}\frac{\partial V_i}{\partial z}\mathbf{e}_i(x, y) = -j\omega\mu\left[\mathbf{1}_t + \frac{\nabla_t\nabla_t}{k^2}\right]\bullet \mathbf{h}_i(x, y) \times \mathbf{u}_z$$

$$\frac{1}{V_i(z)}\frac{\partial I_i}{\partial z}\mathbf{h}_i(x, y) = -j\omega\varepsilon\left[\mathbf{1}_t + \frac{\nabla_t\nabla_t}{k^2}\right]\bullet \mathbf{u}_z \times \mathbf{e}_i(x, y)$$

Now RHS is independent of z coordinate in both cases and thus we can write

$$\frac{1}{I_i(z)}\frac{\partial V_i}{\partial z}\mathbf{e}_i(x, y) = -j\kappa_i Z_i\mathbf{e}_i(x, y)$$

$$\frac{1}{V_i(z)}\frac{\partial I_i}{\partial z}\mathbf{h}_i(x, y) = -j\kappa_i Y_i\mathbf{h}_i(x, y)$$

ie.

$$\frac{\partial V_i}{\partial z} = -j\kappa_i Z_i I_i(z)$$

$$\frac{\partial I_i}{\partial z} = -j\kappa_i Y_i V_i(z)$$

APPENDIX II MODE FUNCTION DERIVATIONS

Using the mode function generator taken from Felsen and Marcuvitz [10] and derived in Appendix I, the actual y-mode fields can be calculated. These modes are defined as TE or TM to a reference direction x, y, or z, depending on the nature of the section being analysed. TE and TM-to-y mode fields are derived in Section 2.3.2.1, and this appendix contains exactly the same derivation for TE and TM-to-x and TE and TM-to-z modes. For x and z reference directions, note that the single prime denotes TM modes, and the double prime denoted TE modes. This is opposite to the convention adopted for the y reference direction in Section 2.3.2.1. The reason for this was to maintain as many similarities as possible between the derivations in this appendix and the derivation in Section 2.3.2.1. The different convention is also convenient in that it reflects the manner in which the TERESA source code was written to implement the layer mode function calculation for each subregion in a given two-dimensional section. Note that the y-mode normalisations given in Section 2.3.1 are assumed.

TE-to-x ($e_x = 0$)

$$\mathbf{e}_T(y,z) = e_y''(y)e^{-jk_z z}\mathbf{u_y} + e_z''(y)e^{-jk_z z}\mathbf{u_z}$$

$$\mathbf{h}_T(y,z) = h_y''(y)e^{-jk_z z}\mathbf{u_y} + h_z''(y)e^{-jk_z z}\mathbf{u_z}$$

$$k_x Y_x'' \mathbf{h}_T(y,z) = \omega\varepsilon\left[\mathbf{1}_t + \frac{\nabla_T\nabla_T}{k^2}\right]\bullet\mathbf{u_x}\times\mathbf{e}_T(y,z)$$

Thus (after cancelling $e^{-jk_z z}$ factor)

$$k_x Y_x''(h_y''\mathbf{u_y} + h_z''\mathbf{u_z}) = -\frac{1}{\omega\mu_0}\left(\left(\frac{\partial^2}{\partial y^2} + k_0^2\varepsilon_r\right)e_z''\mathbf{u_y} + jk_z\frac{\partial e_y''}{\partial y}\mathbf{u_y} - (k_0^2\varepsilon_r - k_z^2)e_y''\mathbf{u_z} - jk_z\frac{\partial e_z''}{\partial y}\mathbf{u_z}\right)$$

So

$$k_x Y_x'' h_y'' = -\frac{1}{\omega\mu_0}\left(\left(k_0^2\varepsilon_r - k_y^2\right)e_z'' + jk_z\frac{\partial e_y''}{\partial y}\right)$$

Now, since $\nabla.\mathbf{e}'' = 0$, and $e_x'' = 0$

$$\frac{\partial e_y''}{\partial y} = jk_z e_z''$$

Therefore

$$k_x Y_x'' h_y'' = -\frac{k_x^2}{\omega\mu_0}e_z''$$

If Y_x'' is chosen to be

$$Y_x'' = \frac{k_x}{\omega\mu_0}$$

then

$$h_y'' = -e_z''$$

Similarly

$$k_x Y_x'' h_z'' = \frac{1}{\omega\mu_0}\left(\left(k_0^2\varepsilon_r - k_z^2\right)e_y'' + jk_z\frac{\partial e_z''}{\partial y}\right)$$

From $\nabla.\mathbf{e}'' = 0$

$$-k_y^2 e_y'' = jk_z\frac{\partial e_z''}{\partial y}$$

So

$$k_x Y_x'' h_z'' = \frac{k_x^2}{\omega\mu_0}e_y''$$

Hence

$$h_z'' = e_y''$$

As for TM-to-y modes, set

$$h_z'' = e_y'' = I''(y)e^{-jk_z z}$$

Using

$$\frac{dI''}{dy} = -jk_y Y'' V''(y) = -j\omega\varepsilon_0 V''(y)$$

leads to

$$e_z'' = -h_y'' = -\frac{j}{k_z}\frac{\partial e_y''}{\partial y}$$

$$= -\frac{\omega\varepsilon_0}{k_z}V''(y)e^{-jk_z z}$$

TM-to-x ($h_x = 0$)

$$\mathbf{e}_T(y,z) = e_y'(y)e^{-jk_z z}\mathbf{u_y} + e_z'(y)e^{-jk_z z}\mathbf{u_z}$$

$$\mathbf{h}_T(y,z) = h_y'(y)e^{-jk_z z}\mathbf{u_y} + h_z'(y)e^{-jk_z z}\mathbf{u_z}$$

$$k_x Z_x' \mathbf{e}_T(y,z) = \omega\left[\mu\mathbf{1}_t + \frac{1}{\omega^2}\nabla_t\frac{1}{\varepsilon(y)}\nabla_t\right]\bullet\mathbf{h}_T(y,z)\times\mathbf{u_x}$$

Thus, (after cancelling $e^{-jk_z z}$ factor)

$$k_x Z_x' e_y' = \frac{1}{\omega\varepsilon_0\varepsilon_r}\left(\left(k_0^2\varepsilon_0 - k_y^2\right)h_z' + jk_z\frac{\partial h_y'}{\partial y}\right)$$

Now, since $\nabla.\mathbf{h}' = 0$ and $h_x' = 0$

$$\frac{\partial h_y'}{\partial y} = jk_z h_z'$$

So

$$k_x Z_x' e_y' = \frac{k_x^2}{\omega\varepsilon_0\varepsilon_r}h_z'$$

If Z'_x is chosen to be

$$Z'_x = \frac{k_x}{\omega\varepsilon_0\varepsilon_r}$$

then

$$e'_y = h'_z$$

Similarly

$$k_x Z'_x e'_z = -\frac{1}{\omega\varepsilon_0\varepsilon_r}\left(\left(k_0^2\varepsilon_0 - k_z^2\right)h'_y + jk_z\frac{\partial h'_z}{\partial y}\right)$$

From $\nabla.\mathbf{h'} = 0$

$$-k_y^2 h'_y = jk_z\frac{\partial h'_z}{\partial y}$$

So

$$k_x Z'_x e'_z = -\frac{k_x^2}{\omega\varepsilon_0\varepsilon_r}h'_y$$

Hence

$$e'_z = -h'_y$$

As for TE-to-y modes, set

$$e'_z = -h'_y = V'(y)\, e^{-jk_z z}$$

Using

$$\frac{\partial V'}{\partial y} = -jk_y Y' I'(y) = -j\omega\mu_0 I'(y)$$

leads to

$$h'_z = e'_y = -\frac{j}{k_z}\frac{\partial h'_y}{\partial y}e^{-jk_z z}$$
$$= \frac{\omega\mu_0}{k_z}I'(y)\,e^{-jk_z z}$$

TE-to-z $(e_z = 0)$

$$\mathbf{e}_T(y,z) = e''_y(y)\,e^{-jk_z z}\,\mathbf{u}_z$$
$$\mathbf{h}_T(y,z) = h''_y(y)\,e^{-jk_z z}\,\mathbf{u}_y + h''_z(y)\,e^{-jk_z z}\,\mathbf{u}_z$$
$$k_x Y''_x \mathbf{h}_T(y,z) = \omega\varepsilon\left[\mathbf{1}_t + \frac{\nabla_T\nabla_T}{k^2}\right]\bullet \mathbf{u}_x\times\mathbf{e}_T(y,z)$$

Thus (after cancelling $e^{-jk_z z}$ factor)

$$k_x Y''_x(h''_y\mathbf{u}_y + h''_z\mathbf{u}_z) = \frac{1}{\omega\mu_0}\left(\left(k_0^2\varepsilon_r - k_z^2\right)e''_y\mathbf{u}_z - jk_z\frac{\partial e''_y}{\partial y}\mathbf{u}_y\right)$$

If Y''_x is chosen to be

$$Y''_x = \frac{k_T^2}{k_x\omega\mu_0}$$

where

$$k_T^2 = k_x^2 + k_y^2 = k_0^2\varepsilon_r - k_z^2$$

then

$$h''_z = e''_y$$
$$h''_y = -\frac{jk_z}{k_T^2}\frac{\partial e''_y}{\partial y}$$

Let

$$h_z^{''} \quad = \quad e_y^{''} \quad = \quad I^{''}(y)e^{-jk_z z}$$

then

$$h_y^{''} \quad = \quad -\frac{jk_z}{k_T^2}\frac{d}{dy}I^{''}(y)e^{-jk_z z}$$

$$= \quad -\frac{k_z\omega\varepsilon_0}{k_T^2}V^{''}(y)e^{-jk_z z}$$

because

$$\frac{d}{dy}I^{''}(y) = -j\omega\varepsilon_0\,V^{''}(y).$$

TM-to-z ($h_z = 0$)

$$\mathbf{h}_T(y, z) = h_y^{'}(y)\,e^{-jk_z z}\,\mathbf{u}_z$$

$$\mathbf{e}_T(y, z) = e_y^{'}(y)\,e^{-jk_z z}\,\mathbf{u}_y + e_z^{'}(y)\,e^{-jk_z z}\,\mathbf{u}_z$$

$$k_x Z_x^{'}\,\mathbf{e}_T(y, z) = \omega\left[\mu\mathbf{1}_t + \frac{1}{\omega^2}\nabla_T\frac{1}{\varepsilon(y)}\nabla_T\right]\bullet\,\mathbf{h}_T(y, z)\times\,\mathbf{u}_x$$

Thus (after cancelling $e^{-jk_z z}$ factor)

$$k_x Y_x^{'}(e_y^{'}\mathbf{u_y} + e_z^{'}\mathbf{u}_z) = -\frac{1}{\omega\mu_0}\left(\left(k_0^2\varepsilon_r - k_z^2\right)h_y^{'}\mathbf{u}_z - jk_z\frac{\partial h_y^{'}}{\partial y}\mathbf{u}_y\right)$$

If $Z_x^{'}$ is chosen to be

$$Z_x^{'} \quad = \quad \frac{k_T^2}{k_x\omega\varepsilon_0\varepsilon_r}$$

then

$$e_z^{'} \quad = \quad -h_y^{'}$$

$$e_y^{'} \quad = \quad \frac{jk_z}{k_T^2}\frac{\partial h_y^{'}}{\partial y}$$

If

$$e_z^{'} \quad = \quad -h_y^{'} \quad = \quad V^{'}(y)e^{-jk_z z}$$

then

$$e_y^{'} \quad = \quad \frac{-jk_z}{k_T^2}\frac{d}{dy}V^{'}(y)e^{-jk_z z}$$

$$= \quad -\frac{k_z\omega\mu_0}{k_T^2}I^{'}(y)e^{-jk_z z}$$

APPENDIX III   REGION EIGENMODE COUPLING

In this appendix, the coupling between x-modes in adjacent subregions is calculated for TE and TM-to-x and z modes. The derivation is essentially similar to the TE and TM-to-y mode coupling derivation in Section 2.3.2.2, and proceeds using the same approach. The x-mode coupling is evaluated by considering the continuity of their constituent y-mode fields which were derived in Appendix II for TE and TM-to-x and TE and TM-to-z modes and Section 2.3.2.1 for TE and TM-to-y modes. Note that complete listings of each of the coupling matrices is omitted. Appendix IV contains these expressions for the general cases of section subregion coupling between all possible combinations of TE and TM-to-x, y, or z x-modes.

III.1   TE, TM-TO-X COUPLING

III.1.1   Electric Field Matching

To evaluate the x-mode coupling at subregion interfaces, the components of the x-modes' constituent y-mode electric fields tangential to the interface are matched across the interface.

y-component

Matching the y-component of the electric field at the interface between subregions A and B yields the expression

$$\sum_{n}^{N_B^{TE}} V_{B_x}^{''mn} I_{B_y}^{''n}(y) + \frac{\omega\mu_0}{k_z^m} \sum_{p}^{N_B^{TM}} V_{B_x}^{'mp} I_{B_y}^{'p}(y) = \sum_{i}^{N_A^{TE}} V_{A_x}^{''mi} I_{A_y}^{''i}(y) + \frac{\omega\mu_0}{k_z^m} \sum_{j}^{N_A^{TM}} V_{A_x}^{'mj} I_{A_y}^{'j}(y)$$

Using the orthogonality condition for TE-to-x y-modes in subregion B

$$\int_0^h I_{B_y}^{''i}(y) I_{B_y}^{''j}(y)^* \, dy = \delta_{ij}$$

and integrating over the subregion interface yields the coupling equation

$$V_{B_x}^{''mn} + \frac{\omega\mu_0}{k_z^m} \sum_{p}^{N_B^{TM}} V_{B_x}^{'mp} \int_{y_l}^{y_u} I_{B_y}^{''n}(y)^* I_{B_y}^{'p}(y) \, dy = \sum_{i}^{N_A^{TE}} V_{A_x}^{''mi} \int_{y_l}^{y_u} I_{B_y}^{''n}(y)^* I_{A_y}^{''i}(y) \, dy$$

$$+ \frac{\omega\mu_0}{k_z^m} \sum_{j}^{N_A^{TM}} V_{B_x}^{'mj} \int_{y_l}^{y_u} I_{B_y}^{''n}(y)^* I_{A_y}^{'j}(y) \, dy$$

This equation can be expressed in terms of coupling matrices $\mathbf{A}$, $\mathbf{B}$, and $\mathbf{G}$ as

$$V_{B_x}^{''mn} + \sum_{p}^{N_B^{TM}} \mathbf{G}_{np} V_{B_x}^{'mp} = \sum_{i}^{N_A^{TM}} \mathbf{A}_{ni} V_{A_x}^{''mi} + \sum_{j}^{N_A^{TM}} \mathbf{B}_{nj} V_{A_x}^{''mj}$$

Note that $\mathbf{A}$, $\mathbf{B}$, and $\mathbf{G}$ developed for TE and TM-to-x modes are equivalent to matrices derived for TE and TM-to-y mode coupling at subregion interfaces.

z-component

The z-component of the electric field is matched across the interface between subregions A and B in the same fashion as the y-component to yield additional coupling relations. This field matching is expressed as

$$
\sum_n^{N_B^{TM}} V_{B_x}^{'mn} V_{B_y}^{'n} - \frac{\omega \varepsilon_0}{k_z^m} \sum_p^{N_B^{TE}} V_{B_x}^{''mp} V_{B_y}^{''p}(y) = \sum_i^{N_A^{TM}} V_{A_x}^{'mi} V_{A_y}^{'i}(y) - \frac{\omega \varepsilon_0}{k_z^m} \sum_j^{N_A^{TE}} V_{A_x}^{''mj} V_{A_y}^{''j}(y)
$$

Using the orthogonality relationship for TM-to-x y-modes in subregion B

$$
\int_0^h V_{B_y}^{'i}(y) V_{B_y}^{'j}(y) dy = \delta_{ij}
$$

and integrating over the subregion interface yields the coupling equation

$$
V_{B_x}^{'mn} - \frac{\omega \varepsilon_0}{k_z^m} \sum_p^{N_B^{TE}} V_{B_x}^{''mp} \int_{y_l}^{y_u} V_{B_y}^{'n}(y)^* V_{B_y}^{''p}(y)\, dy = \sum_i^{N_A^{TM}} V_{A_x}^{'mi} \int_{y_l}^{y_u} V_{B_y}^{'n}(y)^* V_{A_y}^{'i}(y)\, dy
$$

$$
- \frac{\omega \varepsilon_0}{k_z^m} \sum_j^{N_A^{TE}} V_{A_x}^{''mj} \int_{y_l}^{y_u} V_{B_y}^{'n}(y)^* V_{A_y}^{''j}(y)\, dy
$$

where exactly the same approach is used as for Section 2.3.2.2. This equation can be written in terms of coupling matrices **F**, **C**, and **D** as

$$
V_{B_x}^{'mn} - \sum_p^{N_B^{TE}} \mathbf{F}_{np} V_{B_x}^{''mp} = \sum_i^{N_A^{TM}} \mathbf{C}_{ni} V_{A_x}^{'mi} - \sum_j^{N_A^{TE}} \mathbf{D}_{nj} V_{A_x}^{''mj}
$$

III.1.2 Magnetic Field Matching

To obtain the remainder of the coupling expressions needed to evaluate x-mode coupling at subregion interfaces, the x-modes' constituent y-mode magnetic field components which are tangential to the interface are matched across the interface.

y-component

Matching the y-component of the magnetic field at the interface between subregions A and B yields the expression

$$
\sum_n^{N_A^{TM}} I_{A_x}^{'mn} V_{A_y}^{'n}(y) - \frac{\omega \varepsilon_0}{k_z^m} \sum_p^{N_A^{TE}} I_{A_x}^{''mp} V_{A_y}^{''p}(y) = \sum_i^{N_B^{TM}} I_{B_x}^{'mi} V_{B_y}^{'i}(y) - \frac{\omega \varepsilon_0}{k_z^m} \sum_j^{N_B^{TE}} I_{B}^{''mj} V_{B_y}^{''j}(y)
$$

Using TM-to-x y-mode orthogonality in region A

$$
\int_0^h V_{A_y}^{'i}(y) V_{A_y}^{'j}(y) dy = \delta_{ij}
$$

and integrating over the subregion interface yields the coupling equation

$$
I_{A_x}^{'mn} - \frac{\omega\varepsilon_0}{k_z^m} \sum_p^{N_A^{TE}} I_{A_x}^{''mp} \int_{y_l}^{y_u} V_{A_y}^{'n}(y)^* V_{A_y}^{''p}(y)\, dy = \sum_i^{N_B^{TM}} I_{B_x}^{'mi} \int_{y_l}^{y_u} V_{A_y}^{'n}(y)^* V_{B_y}^{'i}(y)\, dy
$$

$$
- \frac{\omega\varepsilon_0}{k_z^m} \sum_j^{N_B^{TE}} I_{B_x}^{''mj} \int_{y_l}^{y_u} V_{A_y}^{'n}(y)^* V_{B_y}^{''j}(y)\, dy
$$

This equation can be expressed in terms of coupling matrices Φ, C, and Δ as

$$
I_{A_x}^{'mn} - \sum_p^{N_A^{TE}} \Phi_{mp} I_{A_x}^{''mp} = \sum_i^{N_B^{TM}} C_{in}^* I_{B_x}^{'mi} - \sum_j^{N_B^{TE}} \Delta_{nj} I_{B_x}^{''mj}
$$

z-component

Matching the z-component of the magnetic field at the interface between subregions A and B yields the expression

$$
\sum_n^{N_A^{TE}} I_{A_x}^{''mn}(y) I_{A_y}^{''n}(y) + \frac{\omega\mu_0}{k_z^m} \sum_p^{N_A^{TM}} I_{A_x}^{'mp}(y) I_{A_y}^{'p}(y) = \sum_i^{N_B^{TE}} I_{B_x}^{''mi}(y) I_{B_y}^{''i}(y)
$$

$$
+ \frac{\omega\mu_0}{k_z^m} \sum_j^{N_B^{TM}} I_{B_x}^{'mj}(y) I_{B_y}^{'j}(y)
$$

Using the TE-to-x y-mode orthogonality in subregion A

$$
\int_0^h I_{A_y}^{''i}(y) I_{A_y}^{''j}(y)^*\, dy = \delta_{ij}
$$

and integrating over the subregion interface yields the coupling equation

$$
I_{A_x}^{''mn} + \frac{\omega\mu_0}{k_z^m} \sum_p^{N_A^{TM}} I_{A_x}^{'mp} \int_{y_l}^{y_u} I_{A_y}^{''n}(y)^* I_{A_y}^{'p}(y)\, dy = \sum_i^{N_B^{TE}} I_{B_x}^{''mi} \int_{y_l}^{y_u} I_{A_y}^{''n}(y)^* I_{B_y}^{''i}(y)\, dy
$$

$$
+ \frac{\omega\mu_0}{k_z^m} \sum_j^{N_B^{TM}} I_{B_x}^{'mj} \int_{y_l}^{y_u} I_{A_y}^{''n}(y)^* I_{B_y}^{'j}(y)\, dy
$$

This equation can be expressed in terms of the coupling matrices Γ, A, and β as

$$
I_{A_x}^{''mn} + \sum_p^{N_A^{TM}} \Gamma_{np} I_{A_x}^{'mp} = \sum_i^{N_B^{TE}} A_{in}^* I_{B_x}^{''mi} + \sum_j^{N_B^{TM}} \beta_{nj} I_{B_x}^{'mj}
$$

III.1.3 Complex Power Conservation

As for the TE and TM-to-y mode derivation in Section 2.3.2.3, the coupling expressions from the field matching for the TE and TM-to-x modes are written in matrix form as

$$
\begin{bmatrix} \mathbf{I} & | & -\mathbf{F} \\ \hline \mathbf{G} & | & \mathbf{I} \end{bmatrix} \begin{bmatrix} \mathbf{V}_{B_x}^m \\ \mathbf{V}_{B_x}^{'m} \end{bmatrix} = \begin{bmatrix} \mathbf{C} & | & -\mathbf{D} \\ \hline \mathbf{B} & | & \mathbf{A} \end{bmatrix} \begin{bmatrix} \mathbf{V}_{A_x}^m \\ \mathbf{V}_{A_x}^{'m} \end{bmatrix}
$$

$$
\begin{bmatrix} \mathbf{I} & | & -\Phi \\ \hline \Gamma & | & \mathbf{I} \end{bmatrix} \begin{bmatrix} \mathbf{I}_{A_x}^m \\ \mathbf{I}_{A_x}^{'m} \end{bmatrix} = \begin{bmatrix} \mathbf{C}^\dagger & | & -\Delta \\ \hline \beta & | & \mathbf{A}^\dagger \end{bmatrix} \begin{bmatrix} \mathbf{I}_{B_x}^m \\ \mathbf{I}_{B_x}^{'m} \end{bmatrix}
$$

The power flow through the discontinuity for the mth z-mode is determined from the fields in both region A and region B

$$
P_{A_x}^m = \int_{y_l}^{y_u} \mathbf{E}_{T_A}^m \times \mathbf{H}_{T_A}^{m*} dy = \sum_n^{N_y^A} \sum_p^{N_y^A} V_{A_x}^{mn} I_{A_x}^{mp*} \int_{y_l}^{y_u} \mathbf{e}_{T_A}^n \times \mathbf{h}_{T_A}^{p*} dy
$$

$$
P_{B_x}^m = \int_{y_l}^{y_u} \mathbf{E}_{T_B}^m \times \mathbf{H}_{T_B}^{m*} dy = \sum_n^{N_y^B} \sum_p^{N_y^B} V_{B_x}^{mn} I_{B_x}^{mp*} \int_{y_l}^{y_u} \mathbf{e}_{T_B}^n \times \mathbf{h}_{T_B}^{p*} dy
$$

For any given region, $\mathbf{e}_{T_B}^n$ and $\mathbf{h}_{T_B}^{p*}$ may be split into TE and TM components and the power integral evaluated as follows

$$
\int_{y_l}^{y_u} \mathbf{e}_T^{'n} \times \mathbf{h}_T^{'p*} \bullet \mathbf{u_x} dy = \int_{y_l}^{y_u} \left[(e_y^{'n} \mathbf{u_y} + e_z^{'n} \mathbf{u_z}) \times (h_y^{'p*} \mathbf{u_y} + h_z^{'p*} \mathbf{u_z}) \right] \bullet \mathbf{u_x} dy
$$

$$
= \int_{y_l}^{y_u} e_y^{'n}(y) h_z^{'p}(y)^* - e_z^{'n}(y) h_y^{'p}(y)^* dy
$$

$$
= \frac{\omega^2 \mu_0^2}{k_z^m k_z^{m*}} \int_{y_l}^{y_u} I_y^{'n}(y) I_y^{'p}(y)^* dy + \int_{y_l}^{y_u} V_y^{'n}(y) V_y^{'p}(y)^* dy
$$

$$
= \frac{\omega^2 \mu_0^2}{k_z^m k_z^{m*}} \int_{y_l}^{y_u} I_y^{'n}(y) I_y^{'p}(y)^* dy + \delta_{np}
$$

$$\int_{y_l}^{y_u} \mathbf{e}_T^{"n} \times \mathbf{h}_T^{"p*} \bullet \mathbf{u_x} dy = \int_{y_l}^{y_u} \left[(e_y^{"n} \mathbf{u_y} + e_z^{"n} \mathbf{u_z}) \times (h_y^{"p*} \mathbf{u_y} + h_z^{"p*} \mathbf{u_z}) \right] \bullet \mathbf{u_x} dy$$

$$= \int_{y_l}^{y_u} e_y^{"n}(y) h_z^{"p}(y)^* dy - \int_{y_l}^{y_u} e_z^{"n}(y) h_y^{"p}(y)^* dy$$

$$= \int_{y_l}^{y_u} I_y^{"n}(y) I_y^{"p}(y)^* dy + \frac{\omega^2 \varepsilon_0^2}{k_z^m k_z^{m*}} \int_{y_l}^{y_u} V_y^{"n}(y) V_y^{"p}(y)^* dy$$

$$= \delta_{np} + \frac{\omega^2 \varepsilon_0^2}{k_z^m k_z^{m*}} \int_{y_l}^{y_u} V_y^{"n}(y) V_y^{"p}(y)^* dy$$

$$\int_{y_l}^{y_u} \mathbf{e}_T^{"n} \times \mathbf{h}_T^{'p*} \bullet \mathbf{u_x} dy = \int_{y_l}^{y_u} \left[(e_y^{"n} \mathbf{u_y} + e_z^{"n} \mathbf{u_z}) \times (h_y^{'p*} \mathbf{u_y} + h_z^{'p*} \mathbf{u_z}) \right] \bullet \mathbf{u_x} dy$$

$$= \int_{y_l}^{y_u} \left[e_y^{"n}(y) h_z^{'p}(y)^* - e_z^{"n}(y) h_y^{'p}(y)^* \right] dy$$

$$= \frac{\omega \mu_0}{k_z^{m*}} \int_{y_l}^{y_u} I_y^{"n}(y) I_y^{'p}(y)^* dy - \frac{\omega \varepsilon_0}{k_z^m} \int_{y_l}^{y_u} V_y^{"n}(y) V_y^{'p}(y)^* dy$$

$$= \left[\Gamma^\dagger - \Phi \right]_{pn} \text{ in region A and } \left[\mathbf{G}^\dagger - \mathbf{F} \right]_{pn} \text{ in region B}$$

$$\int_{y_l}^{y_u} \mathbf{e}_T^{'n} \times \mathbf{h}_T^{"p*} \bullet \mathbf{u_x} dy = \int_{y_l}^{y_u} \left[(e_y^{'n} \mathbf{u_y} + e_z^{'n} \mathbf{u_z}) \times (h_y^{"p*} \mathbf{u_y} + h_z^{"p*} \mathbf{u_z}) \right] \bullet \mathbf{u_x} dy$$

$$= \int_{y_l}^{y_u} \left[e_y^{'n}(y) h_z^{"p}(y)^* - e_z^{'n}(y) h_y^{"p}(y)^* \right] dy$$

$$= \frac{\omega \mu_0}{k_z^m} \int_{y_l}^{y_u} I_y^{'n}(y) I_y^{"p}(y)^* dy - \frac{\omega \varepsilon_0}{k_z^{m*}} \int_{y_l}^{y_u} V_y^{'n}(y) V_y^{"p}(y)^* dy$$

$$= \left[\Gamma - \Phi^\dagger \right]_{pn} \text{ in region A and } \left[\mathbf{G} - \mathbf{F}^\dagger \right]_{pn} \text{ in region B}$$

Note that † denotes the conjugate transpose of the superscripted matrices. From the completeness relationships shown below, the power crossing the discontinuity can be calculated for the modes in both region A and region B.

$$
\left[G^\dagger G \right]_{np} = \sum_q^{N_B^{TE}} \frac{\omega^2 \mu_0^2}{k_z^m k_z^{m*}} \int_{y_l}^{y_u} I_{B_y}^{"q}(y) I_{B_y}^{'n}(y)^* dy \int_{y_l}^{y_u} I_{B_y}^{'p}(y') I_{B_y}^{"q}(y')^* dy'
$$

$$
= \frac{\omega^2 \mu_0^2}{k_z^m k_z^{m*}} \int_{y_l}^{y_u} I_{B_y}^{'n}(y)^* I_{B_y}^{'p}(y) \, dy
$$

$$
\left[\Gamma^\dagger \Gamma \right]_{np} = \sum_q^{N_A^{TE}} \frac{\omega^2 \mu_0^2}{k_z^m k_z^{m*}} \int_{y_l}^{y_u} I_{A_y}^{"q}(y) I_{A_y}^{'n}(y)^* dy \int_{y_l}^{y_u} I_{A_y}^{'p}(y') I_{A_y}^{"q}(y')^* dy'
$$

$$
= \frac{\omega^2 \mu_0^2}{k_z^m k_z^{m*}} \int_{y_l}^{y_u} I_{A_y}^{'n}(y)^* I_{A_y}^{'p}(y) \, dy
$$

$$
\left[F^\dagger F \right]_{np} = \sum_q^{N_B^{TM}} \frac{\omega^2 \varepsilon_0^2}{k_z^m k_z^{m*}} \int_{y_l}^{y_u} V_{B_y}^{'q}(y) V_{B_y}^{"n}(y)^* dy \int_{y_l}^{y_u} V_{B_y}^{"p}(y') V_{B_y}^{'q}(y')^* dy'
$$

$$
= \frac{\omega^2 \varepsilon_0^2}{k_z^m k_z^{m*}} \int_{y_l}^{y_u} V_{B_y}^{"n}(y)^* V_{B_y}^{"p}(y) \, dy
$$

$$
\left[\Phi^\dagger \Phi \right]_{np} = \sum_q^{N_A^{TE}} \frac{\omega^2 \varepsilon_0^2}{k_z^m k_z^{m*}} \int_{y_l}^{y_u} V_{A_y}^{'q}(y) V_{A_y}^{"n}(y)^* dy \int_{y_l}^{y_u} V_{A_y}^{"p}(y') V_{A_y}^{'q}(y')^* dy'
$$

$$
= \frac{\omega^2 \varepsilon_0^2}{k_z^m k_z^{m*}} \int_{y_l}^{y_u} V_{A_y}^{"n}(y)^* V_{A_y}^{"p}(y) \, dy
$$

So, for region A

$$
P_{A_x}^m =
\begin{bmatrix} I_{A_x}^m \\ \hline I_{A_x}^{"m} \end{bmatrix}^\dagger
\begin{bmatrix} I + \Gamma^\dagger \Gamma & | & \Gamma^\dagger - \Phi \\ \hline \Gamma - \Phi^\dagger & | & I + \Phi^\dagger \Phi \end{bmatrix}
\begin{bmatrix} V_{A_x}^m \\ \hline V_{A_x}^{"m} \end{bmatrix}
$$

$$
=
\begin{bmatrix} I_{B_x}^m \\ \hline I_{B_x}^{"m} \end{bmatrix}^\dagger
\begin{bmatrix} C & | & \beta^\dagger \\ \hline -\Delta^\dagger & | & A \end{bmatrix}
\begin{bmatrix} I & | & \Gamma^\dagger \\ \hline -\Phi^\dagger & | & I \end{bmatrix}^{-1}
\begin{bmatrix} I + \Gamma^\dagger \Gamma & | & \Gamma^\dagger - \Phi \\ \hline \Gamma - \Phi^\dagger & | & I + \Phi^\dagger \Phi \end{bmatrix}
\begin{bmatrix} V_{A_x}^m \\ \hline V_{A_x}^{"m} \end{bmatrix}
$$

From the relationship

$$
\begin{bmatrix} I & -\Phi \\ \Gamma & I \end{bmatrix}^{-1} = \begin{bmatrix} [I+\Phi\Gamma]^{-1} & [I+\Phi\Gamma]^{-1}\Phi \\ -[I+\Gamma\Phi]^{-1}\Gamma & [I+\Gamma\Phi]^{-1} \end{bmatrix}
$$

$$
= \left[\begin{bmatrix} I & \Gamma^\dagger \\ -\Phi^\dagger & I \end{bmatrix}^{-1} \right]^\dagger
$$

$$
= \begin{bmatrix} [I+\Phi\Gamma]^{-1} & \Phi[I+\Gamma\Phi]^{-1} \\ -\Gamma[I+\Phi\Gamma]^{-1} & [I+\Gamma\Phi]^{-1} \end{bmatrix}
$$

it follows that $[I+\Gamma\Phi]^{-1}\Gamma = \Gamma[I+\Phi\Gamma]^{-1}$ and $[I+\Phi\Gamma]^{-1}\Phi = \Phi[I+\Gamma\Phi]^{-1}$. Using these new relations

$$
\begin{bmatrix} I+\Gamma^\dagger\Gamma & \Gamma^\dagger-\Phi \\ \Gamma-\Phi^\dagger & I+\Phi^\dagger\Phi \end{bmatrix} \begin{bmatrix} I & -\Phi \\ \Gamma & I \end{bmatrix}^{-1} = \begin{bmatrix} I & \Gamma^\dagger \\ -\Phi^\dagger & I \end{bmatrix}^{-1}
$$

Hence the power in subregion A is given by

$$
P_{A_x}^m = \begin{bmatrix} I_{B_x}^m \\ I_{B_x}^{"m} \end{bmatrix}^\dagger \begin{bmatrix} C & \beta^\dagger \\ -\Delta^\dagger & A \end{bmatrix} \begin{bmatrix} I & -\Phi \\ \Gamma & I \end{bmatrix} \begin{bmatrix} V_{A_x}^m \\ V_{A_x}^{"m} \end{bmatrix}
$$

$$
= \begin{bmatrix} I_{B_x}^m \\ I_{B_x}^{"m} \end{bmatrix}^\dagger \begin{bmatrix} C+B^\dagger G & \beta^\dagger-C\Phi \\ A\Gamma-\Delta^\dagger & A+\Delta^\dagger\Phi \end{bmatrix} \begin{bmatrix} V_{A_x}^m \\ V_{A_x}^{"m} \end{bmatrix}
$$

Similarly, for region B

$$
P_{B_x}^m = \begin{bmatrix} I_{B_x}^m \\ I_{B_x}^{"m} \end{bmatrix}^\dagger \begin{bmatrix} I+G^\dagger G & G^\dagger-F \\ G-F^\dagger & I+F^\dagger F \end{bmatrix} \begin{bmatrix} V_{B_x}^m \\ V_{B_x}^{"m} \end{bmatrix}
$$

$$
= \begin{bmatrix} I_{B_x}^m \\ I_{B_x}^{"m} \end{bmatrix}^\dagger \begin{bmatrix} I+G^\dagger G & G^\dagger-F \\ G-F^\dagger & I+F^\dagger F \end{bmatrix} \begin{bmatrix} I & -F \\ G & I \end{bmatrix}^{-1} \begin{bmatrix} C & -D \\ B & A \end{bmatrix} \begin{bmatrix} V_{A_x}^m \\ V_{A_x}^{"m} \end{bmatrix}
$$

Using the relationship

$$
\begin{bmatrix} I & -F \\ G & I \end{bmatrix}^{-1} = \begin{bmatrix} [I+FG]^{-1} & [I+FG]^{-1}F \\ -[I+GF]^{-1}G & [I+GF]^{-1} \end{bmatrix}
$$

$$
= \left[\begin{bmatrix} I & G^\dagger \\ -F^\dagger & I \end{bmatrix}^{-1} \right]^\dagger
$$

$$
= \begin{bmatrix} [I+FG]^{-1} & F[I+GF]^{-1} \\ -G[I+FG]^{-1} & [I+GF]^{-1} \end{bmatrix}
$$

it follows that $[I+GF]^{-1}G = G[I+FG]^{-1}$ and $[I+FG]^{-1}F = F[I+GF]^{-1}$. Using these new relations

$$
\begin{bmatrix} I+G^\dagger G & G^\dagger\text{-}F \\ G\text{-}F^\dagger & I+F^\dagger F \end{bmatrix} \begin{bmatrix} I & -F \\ G & I \end{bmatrix}^{-1} = \begin{bmatrix} I & G^\dagger \\ -F^\dagger & I \end{bmatrix}^{-1}
$$

Therefore, the power in subregion B is given by

$$
P_{B_x}^m = \begin{bmatrix} I_{B_x}^m \\ I_{B_x}^{\prime\prime m} \end{bmatrix}^\dagger \begin{bmatrix} I & G^\dagger \\ -F^\dagger & I \end{bmatrix} \begin{bmatrix} C & -D \\ B & A \end{bmatrix} \begin{bmatrix} V_{A_x}^m \\ V_{A_x}^{\prime\prime m} \end{bmatrix}
$$

$$
= \begin{bmatrix} I_{B_x}^m \\ I_{B_x}^{\prime\prime m} \end{bmatrix}^\dagger \begin{bmatrix} C + G^\dagger B & G^\dagger A\text{-}D \\ B\text{-}F^\dagger C & A+F^\dagger D \end{bmatrix} \begin{bmatrix} V_{A_x}^m \\ V_{A_x}^{\prime\prime m} \end{bmatrix}
$$

The following substitutions will ensure that $P_{A_x}^m = P_{B_x}^m$ for any number of x-modes in subregions A and B

$$
D \rightarrow C\Phi
$$

$$
B \rightarrow A\Gamma
$$

$$
\Delta \rightarrow C^\dagger F
$$

$$
\beta \rightarrow A^\dagger G
$$

As in Section 2.3.2.3, these relationships must be satisfied automatically for an infinite number of modes in subregions A and B, since both the field matching and power conservation will in principle be perfect. This can be proven by using completeness relations for the y-mode fields as follows

$$[A\Gamma]_{np} = \sum_q^{N_A^{TE}} \int_{y_l}^{y_u} I_{A_y}^{\prime\prime q}(y') I_{B_y}^{\prime\prime n}(y')^* \, dy' \bullet \frac{\omega\mu_0}{k_z^m} \int_{y_l}^{y_u} I_{A_y}^{\prime\prime q}(y)^* I_{A_y}^{\prime p}(y) \, dy$$

$$= \frac{\omega\mu_0}{k_z^m} \int_{y_l}^{y_u}\int_{y_l}^{y_u} I_{B_y}^{\prime\prime n}(y)^* I_{A_y}^{\prime p}(y') \sum_q^{N_A^{TE}} I_{A_y}^{\prime\prime q}(y)^* I_{A_y}^{\prime\prime q}(y') \, dy \, dy'$$

$$= \frac{\omega\mu_0}{k_z^m} \int_{y_l}^{y_u} I_{B_y}^{\prime\prime n}(y)^* I_{A_y}^{\prime p}(y) \, dy$$

$$= B_{np} \quad \text{as required.}$$

Similarly

$$[C\Phi]_{np} = \sum_q^{N_A^{TM}} \int_{y_l}^{y_u} V_{B_y}^{\prime n}(y)^* V_{A_y}^{\prime q}(y) \, dy \bullet \frac{\omega\varepsilon_0}{k_z^m} \int_{y_l}^{y_u} V_{A_y}^{\prime q}(y')^* V_{A_y}^{\prime\prime p}(y') \, dy'$$

$$= \frac{\omega\varepsilon_0}{k_z^m} \int_{y_l}^{y_u}\int_{y_l}^{y_u} V_{B_y}^{\prime n}(y)^* V_{A_y}^{\prime\prime p}(y') \sum_q^{N_A^{TM}} V_{A_y}^{\prime q}(y')^* V_{A_y}^{\prime q}(y) \, dy \, dy'$$

$$= \frac{\omega\varepsilon_0}{k_z^m} \int_{y_l}^{y_u} V_{B_y}^{\prime n}(y)^* V_{A_y}^{\prime\prime p}(y) \, dy$$

$$= D_{np} \quad \text{as required.}$$

$$\left[A^\dagger G\right]_{np} = \sum_q^{N_B^{TE}} \int_{y_l}^{y_u} I_{B_y}^{\prime\prime q}(y') I_{A_y}^{\prime\prime n}(y')^* \, dy' \cdot \frac{\omega\mu_0}{k_z^m} \int_{y_l}^{y_u} I_{B_y}^{\prime\prime q}(y)^* I_{B_y}^{\prime p}(y) \, dy$$

$$= \frac{\omega\mu_0}{k_z^m} \int_{y_l}^{y_u}\int_{y_l}^{y_u} I_{A_y}^{\prime\prime n}(y)^* I_{B_y}^{\prime p}(y') \sum_q^{N_B^{TE}} I_{B_y}^{\prime\prime q}(y)^* I_{B_y}^{\prime\prime q}(y') \, dy \, dy'$$

$$= \frac{\omega\mu_0}{k_z^m} \int_{y_l}^{y_u} I_{A_y}^{\prime\prime n}(y)^* I_{B_y}^{\prime p}(y) \, dy$$

$$= \beta_{np} \quad \text{as required.}$$

$$\left[C^\dagger F\right]_{np} = \sum_q^{N_B^{TM}} \int_{y_l}^{y_u} V_{A_y}^{\prime m}(y)^* V_{B_y}^{\prime q}(y)dy \frac{\omega\varepsilon_0}{k_z^m} \int_{y_l}^{y_u} V_{B_y}^{\prime q}(y')^* V_{B_y}^{\prime\prime p}(y')\,dy'$$

$$= \frac{\omega\varepsilon_0}{k_z^m} \int_{y_l}^{y_u}\int_{y_l}^{y_u} V_{A_y}^{\prime m}(y)^* V_{B_y}^{\prime\prime p}(y') \sum_q^{N_B^{TM}} V_{B_y}^{\prime q}(y')^* V_{B_y}^{\prime q}(y)\,dy\,dy'$$

$$= \frac{\omega\varepsilon_0}{k_z^m} \int_{y_l}^{y_u} V_{A_y}^{\prime m}(y)^* V_{B_y}^{\prime\prime p}(y)\,dy$$

$$= \Delta_{np} \quad \text{as required.}$$

The final form for the coupling between TE and TM-to-x modes in adjacent subregions A and B which ensures conservation of complex power is therefore

$$\begin{bmatrix} I & -F \\ \hline G & I \end{bmatrix} \begin{bmatrix} V_{B_x}^{\prime m} \\ \hline V_{B_x}^{\prime\prime m} \end{bmatrix} = \begin{bmatrix} C & -C\Phi \\ \hline A\Gamma & A \end{bmatrix} \begin{bmatrix} V_{A_x}^{\prime m} \\ \hline V_{A_x}^{\prime\prime m} \end{bmatrix}$$

$$\begin{bmatrix} I & -\Phi \\ \hline \Gamma & I \end{bmatrix} \begin{bmatrix} I_{A_x}^{\prime m} \\ \hline I_{A_x}^{\prime\prime m} \end{bmatrix} = \begin{bmatrix} C^\dagger & -C^\dagger F \\ \hline A^\dagger G & A^\dagger \end{bmatrix} \begin{bmatrix} I_{B_x}^{\prime m} \\ \hline I_{B_x}^{\prime\prime m} \end{bmatrix}$$

III.2 TE, TM-TO-Z COUPLING

III.2.1 Electric Field Matching

To evaluate the x-mode coupling at subregion interfaces, the components of the x-modes' constituent y-mode electric fields tangential to the interface are matched across the interface.

y-component

Matching the y-component of the electric field at the interface between subregions A and B yields the expression

$$\sum_n^{N_B^{TE}} V_{B_x}^{\prime\prime mn} I_{B_y}^{\prime\prime n}(y) - \frac{k_z^m \omega\mu_0}{k_{T_m}^2} \sum_p^{N_B^{TM}} V_{B_x}^{\prime mp} I_{B_y}^{\prime p}(y) = \sum_i^{N_A^{TE}} V_{A_x}^{\prime\prime mi} I_{A_y}^{\prime\prime i}(y)$$

$$- \frac{k_z^m \omega\mu_0}{k_{T_m}^2} \sum_j^{N_A^{TM}} V_{A_x}^{\prime mj} I_{A_y}^{\prime j}(y)$$

Using the orthogonality of TE-to-z y-modes in region B

$$\int_0^h I_{B_y}^{\prime\prime i}(y) I_{B_y}^{\prime\prime j}(y)^* dy = \delta_{ij}$$

and integrating over the subregion interface yields the coupling equation

$$V_{B_x}^{''mn} - \frac{k_z^m \omega \mu_0}{k_{T_m}^2} \sum_p^{N_B^{TM}} V_{B_x}^{'mp} \int_{y_l}^{y_u} I_{B_y}^{''n}(y)^* I_{B_y}^{'p}(y)\,dy = \sum_i^{N_A^{TE}} V_{A_x}^{''mi} \int_{y_l}^{y_u} I_{B_y}^{''n}(y)^* I_{A_y}^{'i}(y)\,dy$$

$$- \frac{k_z^m \omega \mu_0}{k_{T_m}^2} \sum_j^{N_A^{TM}} V_{A_x}^{'mj} \int_{y_l}^{y_u} I_{B_y}^{''n}(y)^* I_{A_y}^{'j}(y)\,dy$$

This equation can be expressed in terms of the coupling matrices **G**, **A**, and **B** as

$$V_{B_x}^{''mn} - \sum_p^{N_B^{TM}} \mathbf{G}_{np} V_{B_x}^{'mp} = \sum_i^{N_A^{TE}} \mathbf{A}_{ni} V_{A_x}^{''mi} - \sum_j^{N_A^{TM}} \mathbf{B}_{nj} V_{A_x}^{'mj}$$

In anticipation of the further derivation to ensure power conservation, also define

$$\Gamma_{np} = \frac{k_z^m \omega \mu_0}{k_{T_m}^2} \int_{y_l}^{y_u} I_{A_y}^{''n}(y)^* I_{A_y}^{'p}(y)\,dy$$

z-component

Matching the z-component of the electric field at the interface between subregions A and B yields the expression

$$\sum_n^{N_B^{TM}} V_{B_x}^{'mn} V_{B_y}^{'n}(y) = \sum_i^{N_A^{TM}} V_{A_x}^{'mi} V_{A_y}^{'i}(y)$$

Using orthogonality between TM-to-z y-modes in subregion B

$$\int_0^h V_{B_y}^{'i}(y) V_{B_y}^{'j}(y)^*\,dy = \delta_{ij}$$

and integrating over the subregion interface yields the coupling equation

$$V_{B_x}^{'mn} = \sum_i^{N_A^{TM}} V_{A_x}^{'mi} \int_{y_l}^{y_u} V_{B_y}^{'n}(y)^* V_{A_y}^{'i}(y)\,dy$$

This equation can be expressed in terms of the coupling matrix **C** as

$$V_{B_x}^{'mn} = \sum_i^{N_A^{TM}} \mathbf{C}_{ni} V_{A_x}^{'mi}$$

III.2.2 Magnetic Field Matching

To obtain the remainder of the coupling expressions needed to evaluate x-mode coupling at subregion interfaces, the x-modes' constituent y-mode magnetic field components which are tangential to the interface are matched across the interface.

y-component

Matching the y-component of the magnetic field at the interface between subregions A and B yields the expression

$$\sum_n^{N_A^{TM}} I_{A_x}^{'mn} V_{A_y}^{'n}(y) + \frac{k_z^m \omega \varepsilon_0}{k_{T_m}^2} \sum_p^{N_A^{TE}} I_{A_x}^{''mp} V_{A_y}^{''p}(y) = \sum_i^{N_B^{TM}} I_{B_x}^{'mi} V_{B_y}^{'i}(y) + \frac{k_z^m \omega \varepsilon_0}{k_{T_m}^2} \sum_j^{N_B^{TE}} I_{B_x}^{''mj} V_{B_y}^{''j}(y)$$

Using orthogonality of TM-to-z y-modes in subregion A

$$\int_0^h V_{A_y}^{'i}(y) V_{A_y}^{'j}(y)^* \, dy = \delta_{ij}$$

and integrating over the subregion interface yields the coupling equation

$$I_{A_x}^{'mn} + \frac{k_z^m \omega \varepsilon_0}{k_{T_m}^2} \sum_p^{N_A^{TE}} I_{A_x}^{''mp} \int_{y_l}^{y_u} V_{A_y}^{'n}(y)^* V_{A_y}^{''p}(y) \, dy = \sum_i^{N_B^{TM}} I_{B_x}^{'mi} \int_{y_l}^{y_u} V_{A_y}^{'n}(y)^* V_{B_y}^{'i}(y) \, dy$$

$$+ \frac{k_z^m \omega \varepsilon_0}{k_{T_m}^2} \sum_j^{N_B^{TE}} I_{B_x}^{''mj} \int_{y_l}^{y_u} V_{A_y}^{'n}(y)^* V_{B_y}^{''j}(y) \, dy$$

This equation can be expressed in terms of the coupling matrices Φ, C, and Δ as

$$I_{A_x}^{'mn} + \sum_p^{N_A^{TE}} \Phi_{mp} I_{A_x}^{''mp} = \sum_i^{N_B^{TM}} C_{in}^* I_{B_x}^{'mi} + \sum_j^{N_B^{TE}} \Delta_{nj} I_{B_x}^{''mj}$$

In anticipation of the further derivation to ensure power conservation, also define

$$\mathbf{F}_{np} = \frac{k_z^m \omega \varepsilon_0}{k_{T_m}^2} \int_{y_l}^{y_u} V_{B_y}^{'n}(y)^* V_{B_y}^{''p}(y) \, dy$$

z-component

Matching the z-component of the magnetic field at the interface between subregions A and B yields the expression

$$\sum_n^{N_A^{TE}} I_{A_x}^{''mn} I_{A_y}^{''n}(y) = \sum_i^{N_B^{TE}} I_{B_x}^{''mi} I_{B_y}^{''i}(y)$$

Using orthogonality of TE-to-z y-modes in subregion A

$$\int_0^h I_{A_y}^{''i}(y) I_{A_y}^{''j}(y)^* \, dy = \delta_{ij}$$

and integrating over the subregion interface yields the coupling equation

$$I_{A_x}^{''mn} = \sum_i^{N_B^{TE}} I_{B_x}^{''mi} \int_{y_l}^{y_u} I_{A_y}^{''n}(y)^* I_{B_y}^{''i}(y) \, dy$$

This equation can be expressed in terms of the coupling matrix $\mathbf{A}$ as

$$I_{A_x}^{'mn} = \sum_i^{N_B^{TE}} \mathbf{A}_{in}^* I_{B_x}^{''mi}$$

III.2.3   Complex Power Conservation

To ensure power conservation across the subregion interface regardless of the number of x-modes in subregions A or B, the technique described in Section 2.3.2.3 is used. By constructing column vectors for the transverse eigenmode voltages and currents for the mth z-mode, with the TE and TM components separated, the coupling expressions from the field matching can be written in matrix form

$$
\begin{bmatrix} \mathbf{I} & | & \mathbf{0} \\ ---- & | & ---- \\ -\mathbf{G} & | & \mathbf{I} \end{bmatrix}
\begin{bmatrix} V_{B_x}^{'m} \\ ---- \\ V_{B_x}^{''m} \end{bmatrix}
=
\begin{bmatrix} \mathbf{C} & | & \mathbf{0} \\ ---- & | & ---- \\ -\mathbf{B} & | & \mathbf{A} \end{bmatrix}
\begin{bmatrix} V_{A_x}^{'m} \\ ---- \\ V_{A_x}^{''m} \end{bmatrix}
$$

$$
\begin{bmatrix} \mathbf{I} & | & \Phi \\ ---- & | & ---- \\ \mathbf{0} & | & \mathbf{I} \end{bmatrix}
\begin{bmatrix} I_{A_x}^{'m} \\ ---- \\ I_{A_x}^{''m} \end{bmatrix}
=
\begin{bmatrix} \mathbf{C}^\dagger & | & \Delta \\ ---- & | & ---- \\ \mathbf{0} & | & \mathbf{A}^\dagger \end{bmatrix}
\begin{bmatrix} I_{B_x}^{'m} \\ ---- \\ I_{B_x}^{''m} \end{bmatrix}
$$

The power flow through the discontinuity for the mth z mode is determined from the fields in both region A and region B. The coupling between the modal fields in regions A and B must ensure that the power coupled from modes in region A to modes in region B is the same as the power coupled in the opposite direction.

$$P_{A_x}^m = \int_{y_l}^{y_u} \mathbf{E}_{T_A}^m \times \mathbf{H}_{T_A}^{m*} dy = \sum_n^{N_y^A} \sum_p^{N_y^A} V_{A_x}^{mn} I_{A_x}^{mp*} \int_{y_l}^{y_u} \mathbf{e}_{T_A}^n \times \mathbf{h}_{T_A}^{p*} dy$$

$$P_{B_x}^m = \int_{y_l}^{y_u} \mathbf{E}_{T_B}^m \times \mathbf{H}_{T_B}^{m*} dy = \sum_n^{N_y^B} \sum_p^{N_y^B} V_{B_x}^{mn} I_{B_x}^{mp*} \int_{y_l}^{y_u} \mathbf{e}_{T_B}^n \times \mathbf{h}_{T_B}^{p*} dy$$

For any given region, $\mathbf{e}_{T_B}^n$ and $\mathbf{h}_{T_B}^{p*}$ may be split into TE and TM components and the power integral evaluated as follows

$$\int_{y_l}^{y_u} \mathbf{e}_T^{'n} \times \mathbf{h}_T^{'p*} \bullet \mathbf{u_x} dy = \int_{y_l}^{y_u} \left[e_z^{'n} \mathbf{u_z} \times (h_y^{'p*} \mathbf{u_y} + h_z^{'p*} \mathbf{u_z}) \right] \bullet \mathbf{u_x} dy$$

$$= \int_{y_l}^{y_u} -e_z^{'n}(y) h_y^{'p}(y)^* dy$$

$$= \int_{y_l}^{y_u} V_y^{'n}(y) V_y^{'p}(y)^* dy$$

$$= \delta_{np}$$

$$\int_{y_l}^{y_u} \mathbf{e}_T^{"n} \times \mathbf{h}_T^{"p*} \bullet \mathbf{u_x}\, dy = \int_{y_l}^{y_u} \left[(e_y^{"n}\mathbf{u_y} + e_z^{"n}\mathbf{u_z}) \times h_z^{"p*}\mathbf{u_z} \right] \bullet \mathbf{u_x}\, dy$$

$$= \int_{y_l}^{y_u} \left[e_y^{"n}(y) h_z^{"p}(y)^* \right] dy$$

$$= -\int_{y_l}^{y_u} I_y^{"n}(y) I_y^{"p}(y)^* dy$$

$$= \delta_{np}$$

$$\int_{y_l}^{y_u} \mathbf{e}_T^{'n} \times \mathbf{h}_T^{"p*} \bullet \mathbf{u_x}\, dy = \int_{y_l}^{y_u} \left[(e_y^{'n}\mathbf{u_y} + e_y^{'n}\mathbf{u_z}) \times (h_y^{"p*}\mathbf{u_y} + h_z^{"p*}\mathbf{u_z}) \right] \bullet \mathbf{u_x}\, dy$$

$$= \int_{y_l}^{y_u} \left[-e_y^{'n}(y) h_z^{"p}(y)^* - e_z^{'n}(y) h_y^{"p}(y)^* \right] dy$$

$$= -\frac{k_z \omega \mu_0}{k_T^2} \int_{y_l}^{y_u} I_y^{'n}(y) I_y^{"p}(y)^* dy + \frac{k_z^* \omega \varepsilon_0}{k_T^{2*}} \int_{y_l}^{y_u} V_y^{'n}(y) V_y^{"p}(y)^* dy$$

$$\int_{y_l}^{y_u} \mathbf{e}_T^{"n} \times \mathbf{h}_T^{'p*} \bullet \mathbf{u_x}\, dy = 0$$

Using the previously defined TE and TM-to-z x-mode coupling matrices, the power in region A is given by

$$P_{A_x}^m = \begin{bmatrix} I_{A_x}^{'m} \\ \hline I_{A_x}^{"m} \end{bmatrix}^\dagger \begin{bmatrix} I & \vline & 0 \\ \hline \Phi^\dagger\text{-}\Gamma & \vline & I \end{bmatrix} \begin{bmatrix} V_{A_x}^{'m} \\ \hline V_{A_x}^{"m} \end{bmatrix}$$

$$= \begin{bmatrix} I_{B_x}^{'m} \\ \hline I_{B_x}^{"m} \end{bmatrix}^\dagger \begin{bmatrix} C & \vline & 0 \\ \hline \Delta^\dagger & \vline & A \end{bmatrix} \begin{bmatrix} I & \vline & 0 \\ \hline \Phi^\dagger & \vline & I \end{bmatrix}^{-1} \begin{bmatrix} I & \vline & 0 \\ \hline \Phi^\dagger\text{-}\Gamma & \vline & I \end{bmatrix} \begin{bmatrix} V_{A_x}^{'m} \\ \hline V_{A_x}^{"m} \end{bmatrix}$$

$$= \begin{bmatrix} I_{B_x}^{'m} \\ \hline I_{B_x}^{"m} \end{bmatrix}^\dagger \begin{bmatrix} C & \vline & 0 \\ \hline \Delta^\dagger\text{-}A\Phi^\dagger & \vline & A \end{bmatrix} \begin{bmatrix} I & \vline & 0 \\ \hline \Phi^\dagger\text{-}\Gamma & \vline & I \end{bmatrix} \begin{bmatrix} V_{A_x}^{'m} \\ \hline V_{A_x}^{"m} \end{bmatrix}$$

$$= \begin{bmatrix} I_{B_x}^{'m} \\ \hline I_{B_x}^{"m} \end{bmatrix}^\dagger \begin{bmatrix} C & \vline & 0 \\ \hline \Delta^\dagger\text{-}A\Gamma & \vline & A \end{bmatrix} \begin{bmatrix} V_{A_x}^{'m} \\ \hline V_{A_x}^{"m} \end{bmatrix}$$

Similarly, for region B

$$
P_{B_x}^m = \begin{bmatrix} I_{B_x}^m \\ \hline I_{B_x}^{''m} \end{bmatrix}^{\dagger} \begin{bmatrix} I & \vdots & 0 \\ \hline F^{\dagger}\text{-}G & \vdots & I \end{bmatrix} \begin{bmatrix} V_{B_x}^m \\ \hline V_{B_x}^{''m} \end{bmatrix}
$$

$$
= \begin{bmatrix} I_{B_x}^m \\ \hline I_{B_x}^{''m} \end{bmatrix}^{\dagger} \begin{bmatrix} I & \vdots & 0 \\ \hline F^{\dagger}\text{-}G & \vdots & I \end{bmatrix} \begin{bmatrix} I & \vdots & 0 \\ \hline \text{-}G & \vdots & I \end{bmatrix}^{-1} \begin{bmatrix} C & \vdots & 0 \\ \hline \text{-}B & \vdots & A \end{bmatrix} \begin{bmatrix} V_{A_x}^m \\ \hline V_{A_x}^{''m} \end{bmatrix}
$$

$$
= \begin{bmatrix} I_{B_x}^m \\ \hline I_{B_x}^{''m} \end{bmatrix}^{\dagger} \begin{bmatrix} I & \vdots & 0 \\ \hline F^{\dagger} & \vdots & I \end{bmatrix} \begin{bmatrix} C & \vdots & 0 \\ \hline \text{-}B & \vdots & A \end{bmatrix} \begin{bmatrix} V_{A_x}^m \\ \hline V_{A_x}^{''m} \end{bmatrix}
$$

$$
= \begin{bmatrix} I_{B_x}^m \\ \hline I_{B_x}^{''m} \end{bmatrix}^{\dagger} \begin{bmatrix} C & \vdots & 0 \\ \hline F^{\dagger}C\text{-}B & \vdots & A \end{bmatrix} \begin{bmatrix} V_{A_x}^m \\ \hline V_{A_x}^{''m} \end{bmatrix}
$$

Note that $\dagger$ denotes the conjugate transpose of the superscripted matrices. From the completeness relationships shown below, the power crossing the discontinuity can be calculated for the modes in both region A and region B. The following substitutions will ensure that $P_{A_x}^m = P_{B_x}^m$ for any number of x-modes in subregions A and B

$$\Delta \rightarrow C^{\dagger}F$$

$$B \rightarrow A\Gamma$$

As in Section 2.3.2.3, these relationships must be satisfied automatically for an infinite number of modes in subregions A and B, since both the field matching and power conservation will in principle be perfect. This can be proven by using completeness relations for the y-mode fields as follows

$$
\left[C^{\dagger}F \right]_{np} = \sum_q^{N_B^{TM}} \frac{k_z^m \omega \varepsilon_0}{k_{T_m}^2} \int_{y_l}^{y_u} V_{B_y}^{'q}(y) V_{A_y}^{'n}(y)^* \, dy \int_{y_l}^{y_u} V_{B_y}^{''p}(y') V_{B_y}^{'q}(y')^* \, dy'
$$

$$
= \frac{k_z^m \omega \varepsilon_0}{k_{T_m}^2} \int_{y_l}^{y_u} \int_{y_l}^{y_u} V_{A_y}^{'n}(y)^* V_{B_y}^{''p}(y') \sum_q^{N_B^{TM}} V_{B_y}^{'q}(y)^* V_{B_y}^{'q}(y') \, dy \, dy'
$$

$$
= \frac{k_z^m \omega \varepsilon_0}{k_{T_m}^2} \int_{y_l}^{y_u} V_{A_y}^{'n}(y)^* V_{B_y}^{''p}(y) \, dy
$$

$$
= \left[\Delta^{\dagger} \right]_{np} \quad \text{as required.}
$$

Similarly

$$[A\Gamma]_{np} = \sum_q^{N_A^{TE}} \int_{y_l}^{y_u} I_{B_y}^{''n}(y)^* I_{A_y}^{''q}(y)\,dy \frac{k_z^m \omega\mu_0}{k_{T_m}^2} \int_{y_l}^{y_u} I_{A_y}^{'p}(y') I_{A_y}^{''q}(y')^*\,dy'$$

$$= \frac{k_z^m \omega\mu_0}{k_{T_m}^2} \int_{y_l}^{y_u}\int_{y_l}^{y_u} I_{A_y}^{''n}(y)^* I_{A_y}^{'p}(y') \sum_q^{N_A^{TE}} I_{A_y}^{''q}(y')^* I_{A_y}^{''q}(y)\,dy\,dy'$$

$$= \frac{k_z^m \omega\mu_0}{k_{T_m}^2} \int_{y_l}^{y_u} I_{B_y}^{''n}(y)^* I_{A_y}^{'p}(y)\,dy$$

$$= \mathbf{B}_{np} \quad \text{as required.}$$

The final form for the coupling which guarantees conservation of complex power regardless of the number of x-modes in subregions A and B is therefore

$$\begin{bmatrix} I & | & 0 \\ \hline -G & | & I \end{bmatrix} \begin{bmatrix} V_{B_x}^{'m} \\ \hline V_{B_x}^{''m} \end{bmatrix} = \begin{bmatrix} C & | & 0 \\ \hline -A\Gamma & | & A \end{bmatrix} \begin{bmatrix} V_{A_x}^{'m} \\ \hline V_{A_x}^{''m} \end{bmatrix}$$

$$\begin{bmatrix} I & | & 0 \\ \hline \Gamma & | & I \end{bmatrix} \begin{bmatrix} I_{A_x}^{'m} \\ \hline I_{A_x}^{''m} \end{bmatrix} = \begin{bmatrix} C^\dagger & | & C^\dagger F \\ \hline 0 & | & A^\dagger \end{bmatrix} \begin{bmatrix} I_{B_x}^{'m} \\ \hline I_{B_x}^{''m} \end{bmatrix}$$

APPENDIX IV   SUBREGION COUPLING SUMMARY

The coupling between adjacent subregions has been determined using a field matching technique in Section 2.3.2.2 for TE and TM-to-y y-modes and Appendix III for TE and TM-to-x and TE and TM-to-z y-modes. The coupling expressions subsequently obtained ensure that the complex power crossing the subregion interface was conserved, while still satisfying the field matching criteria when an infinite number of modes are included. The coupling expressions for two subregions where the x-mode fields are expressed in terms of mode functions which may be TE and TM-to-x, y, or z are listed in this section. The full derivation is not considered worth repeating, and is almost identical to the approach described in Section 2.3.2.2 and Appendix III. The full coupling expressions for arbitrary y-mode reference directions allows the use of different combinations of TE and TM-to-x, y, and z y-modes in the same two-dimensional cross-section.

IV.1   TE, TM-TO-Y MODES IN A, TE, TM-TO-Y MODES IN B

$$\begin{bmatrix} I & \vline & -F \\ \hline 0 & \vline & I \end{bmatrix} \begin{bmatrix} V_{B_x}^m \\ \hline V_{B_x}''^m \end{bmatrix} = \begin{bmatrix} C & \vline & -C\Phi \\ \hline 0 & \vline & A \end{bmatrix} \begin{bmatrix} V_{A_x}^m \\ \hline V_{A_x}''^m \end{bmatrix}$$

$$\begin{bmatrix} I & \vline & 0 \\ \hline \Gamma & \vline & I \end{bmatrix} \begin{bmatrix} I_{A_x}^m \\ \hline I_{A_x}''^m \end{bmatrix} = \begin{bmatrix} C^\dagger & \vline & 0 \\ \hline A^\dagger G & \vline & A^\dagger \end{bmatrix} \begin{bmatrix} I_{B_x}^m \\ \hline I_{B_x}''^m \end{bmatrix}$$

$$A_{np} = \int_{y_l}^{y_u} \frac{I_{B_y}''^n(y)^* I_{A_y}''^p(y)}{\varepsilon_A(y)} dy$$

$$C_{np} = \int_{y_l}^{y_u} V_{B_y}'^n(y)^* V_{A_y}'^p(y) dy$$

$$F_{np} = \frac{k_z^m \omega \varepsilon_0}{k_{u_{P_B}}''^2} \int_{y_l}^{y_u} V_{B_y}'^n(y)^* V_{B_y}''^p(y) dy$$

$$\Phi_{np} = \frac{k_z^m \omega \varepsilon_0}{k_{u_{P_A}}''^2} \int_{y_l}^{y_u} V_{A_y}'^n(y)^* V_{A_y}''^p(y) dy$$

$$G_{np} = \frac{k_z^m \omega \mu_0}{k_{u_{P_B}}'^2} \int_{y_l}^{y_u} \frac{I_{B_y}''^n(y)^* I_{B_y}'^p(y)}{\varepsilon_B(y)} dy$$

$$\Gamma_{np} = \frac{k_z^m \omega \mu_0}{k_{u_{P_A}}'^2} \int_{y_l}^{y_u} \frac{I_{A_y}''^n(y)^* I_{A_y}'^p(y)}{\varepsilon_A(y)} dy$$

IV.2   TE, TM-TO-X MODES IN A, TE, TM-TO-X MODES IN B

$$
\begin{bmatrix} \mathbf{I} & \vdots & -\mathbf{F} \\ \cdots\cdots\cdots\cdots & & \\ \mathbf{G} & \vdots & \mathbf{I} \end{bmatrix}
\begin{bmatrix} V_{B_x}^{'m} \\ \cdots \\ V_{B_x}^{''m} \end{bmatrix}
=
\begin{bmatrix} \mathbf{C} & \vdots & -\mathbf{C}\Phi \\ \cdots\cdots\cdots\cdots & & \\ \mathbf{A}\Gamma & \vdots & \mathbf{A} \end{bmatrix}
\begin{bmatrix} V_{A_x}^{'m} \\ \cdots \\ V_{A_x}^{''m} \end{bmatrix}
$$

$$
\begin{bmatrix} \mathbf{I} & \vdots & -\Phi \\ \cdots\cdots\cdots\cdots & & \\ \Gamma & \vdots & \mathbf{I} \end{bmatrix}
\begin{bmatrix} I_{A_x}^{'m} \\ \cdots \\ I_{A_x}^{''m} \end{bmatrix}
=
\begin{bmatrix} \mathbf{C}^\dagger & \vdots & -\mathbf{C}^\dagger\mathbf{F} \\ \cdots\cdots\cdots\cdots & & \\ \mathbf{A}^\dagger\mathbf{G} & \vdots & \mathbf{A}^\dagger \end{bmatrix}
\begin{bmatrix} I_{B_x}^{'m} \\ \cdots \\ I_{B_x}^{''m} \end{bmatrix}
$$

$$
\mathbf{A}_{np} = \int_{y_l}^{y_u} I_{B_y}^{''n}(y)^* \, I_{A_y}^{''p}(y)\, dy
$$

$$
\mathbf{C}_{np} = \int_{y_l}^{y_u} V_{B_y}^{'n}(y)^* \, V_{A_y}^{'p}(y)\, dy
$$

$$
\mathbf{F}_{np} = \frac{\omega\varepsilon_0}{k_z^m} \int_{y_l}^{y_u} V_{B_y}^{'n}(y)^* \, V_{B_y}^{''p}(y)\, dy
$$

$$
\Phi_{np} = \frac{\omega\varepsilon_0}{k_z^m} \int_{y_l}^{y_u} V_{A_y}^{'n}(y)^* \, V_{A_y}^{''p}(y)\, dy
$$

$$
\mathbf{G}_{np} = \frac{\omega\mu_0}{k_z^m} \int_{y_l}^{y_u} I_{B_y}^{''n}(y)^* \, I_{B_y}^{'p}(y)\, dy
$$

$$
\Gamma_{np} = \frac{\omega\mu_0}{k_z^m} \int_{y_l}^{y_u} I_{A_y}^{''n}(y)^* \, I_{A_y}^{'p}(y)\, dy
$$

IV.3   TE, TM-TO-Z MODES IN A, TE, TM-TO-Z MODES IN B

$$
\begin{bmatrix} \mathbf{I} & \vdots & \mathbf{0} \\ \text{------} & \vdots & \text{------} \\ \mathbf{-G} & \vdots & \mathbf{I} \end{bmatrix}
\begin{bmatrix} V_{B_x}^m \\ \text{----} \\ V_{B_x}^{"m} \end{bmatrix}
=
\begin{bmatrix} \mathbf{C} & \vdots & \mathbf{0} \\ \text{------} & \vdots & \text{------} \\ \mathbf{-A\Gamma} & \vdots & \mathbf{A} \end{bmatrix}
\begin{bmatrix} V_{A_x}^m \\ \text{----} \\ V_{A_x}^{"m} \end{bmatrix}
$$

$$
\begin{bmatrix} \mathbf{I} & \vdots & \Phi \\ \text{------} & \vdots & \text{------} \\ \mathbf{0} & \vdots & \mathbf{I} \end{bmatrix}
\begin{bmatrix} I_{A_x}^m \\ \text{----} \\ I_{A_x}^{"m} \end{bmatrix}
=
\begin{bmatrix} \mathbf{C}^\dagger & \vdots & \mathbf{C}^\dagger \mathbf{F} \\ \text{------} & \vdots & \text{------} \\ \mathbf{0} & \vdots & \mathbf{A}^\dagger \end{bmatrix}
\begin{bmatrix} I_{B_x}^m \\ \text{----} \\ I_{B_x}^{"m} \end{bmatrix}
$$

$$
\mathbf{A}_{np} = \int_{y_l}^{y_u} I_{B_y}^{"n}(y)^* \, I_{A_y}^{"p}(y) \, dy
$$

$$
\mathbf{C}_{np} = \int_{y_l}^{y_u} V_{B_y}^{'n}(y)^* \, V_{A_y}^{'p}(y) \, dy
$$

$$
\mathbf{F}_{np} = \frac{k_z^m \omega \varepsilon_0}{k_{T_m}^2} \int_{y_l}^{y_u} V_{B_y}^{'n}(y)^* \, V_{B_y}^{"p}(y) \, dy
$$

$$
\Phi_{np} = \frac{k_z^m \omega \varepsilon_0}{k_{T_m}^2} \int_{y_l}^{y_u} V_{A_y}^{'n}(y)^* \, V_{A_y}^{"p}(y) \, dy
$$

$$
\mathbf{G}_{np} = \frac{k_z^m \omega \mu_0}{k_{T_m}^2} \int_{y_l}^{y_u} I_{B_y}^{"n}(y)^* \, I_{B_y}^{'p}(y) \, dy
$$

$$
\Gamma_{np} = \frac{k_z^m \omega \mu_0}{k_{T_m}^2} \int_{y_l}^{y_u} I_{A_y}^{"n}(y)^* \, I_{A_y}^{'p}(y) \, dy
$$

IV.4   TE, TM-TO-Y MODES IN A, TE, TM-TO-X MODES IN B

$$
\begin{bmatrix} I & -F \\ \hline G & I \end{bmatrix}
\begin{bmatrix} V_{B_x}^m \\ \hline V_{B_x}^{'m} \end{bmatrix}
=
\begin{bmatrix} C & -C\Phi \\ \hline 0 & A \end{bmatrix}
\begin{bmatrix} V_{A_x}^m \\ \hline V_{A_x}^{'m} \end{bmatrix}
$$

$$
\begin{bmatrix} I & 0 \\ \hline \Gamma & I \end{bmatrix}
\begin{bmatrix} I_{A_x}^m \\ \hline I_{A_x}^{'m} \end{bmatrix}
=
\begin{bmatrix} C^\dagger & -C^\dagger F \\ \hline A^\dagger G & A^\dagger \end{bmatrix}
\begin{bmatrix} I_{B_x}^m \\ \hline I_{B_x}^{'m} \end{bmatrix}
$$

$$
A_{np} = \int_{y_l}^{y_u} \frac{I_{B_y}^{''n}(y)^* \, I_{A_y}^{''p}(y)}{\varepsilon_A(y)} \, dy
$$

$$
C_{np} = \int_{y_l}^{y_u} V_{B_y}^{'n}(y)^* \, V_{A_y}^{'p}(y) \, dy
$$

$$
F_{np} = \frac{\omega \varepsilon_0}{k_z^m} \int_{y_l}^{y_u} V_{B_y}^{'n}(y)^* \, V_{B_y}^{''p}(y) \, dy
$$

$$
\Phi_{np} = \frac{k_z^m \omega \varepsilon_0}{k_{u\,p_A}^{''2}} \int_{y_l}^{y_u} V_{A_y}^{'n}(y)^* \, V_{A_y}^{''p}(y) \, dy
$$

$$
G_{np} = \frac{\omega \mu_0}{k_z^m} \int_{y_l}^{y_u} I_{B_y}^{''n}(y)^* \, I_{B_y}^{'p}(y) \, dy
$$

$$
\Gamma_{np} = \frac{k_z^m \omega \mu_0}{k_{u\,p_A}^{'2}} \int_{y_l}^{y_u} \frac{I_{A_y}^{''n}(y)^* \, I_{A_y}^{'p}(y)}{\varepsilon_A(y)} \, dy
$$

IV.5. TE, TM-TO-X MODES IN A, TE, TM-TO-Y MODES IN B

$$
\begin{bmatrix} I & \vdots & -F \\ \cdots\cdots\cdots & \\ 0 & \vdots & I \end{bmatrix}
\begin{bmatrix} V_{B_x}'^m \\ \cdots \\ V_{B_x}''^m \end{bmatrix}
=
\begin{bmatrix} C & \vdots & -C\Phi \\ \cdots\cdots\cdots & \\ A\Gamma & \vdots & A \end{bmatrix}
\begin{bmatrix} V_{A_x}'^m \\ \cdots \\ V_{A_x}''^m \end{bmatrix}
$$

$$
\begin{bmatrix} I & \vdots & -\Phi \\ \cdots\cdots\cdots & \\ \Gamma & \vdots & I \end{bmatrix}
\begin{bmatrix} I_{A_x}^m \\ \cdots \\ I_{A_x}''^m \end{bmatrix}
=
\begin{bmatrix} C^\dagger & \vdots & 0 \\ \cdots\cdots\cdots & \\ A^\dagger G & \vdots & A^\dagger \end{bmatrix}
\begin{bmatrix} I_{B_x}^m \\ \cdots \\ I_{B_x}''^m \end{bmatrix}
$$

$$
\mathbf{A}_{np} = \int_{y_l}^{y_u} I_{B_y}''^n (y)^* I_{A_y}''^p (y)\, dy
$$

$$
\mathbf{C}_{np} = \int_{y_l}^{y_u} V_{B_y}'^n (y)^* V_{A_y}'^p (y)\, dy
$$

$$
\mathbf{F}_{np} = \frac{k_z^m \omega \varepsilon_0}{k_{u_{p_B}}''^2} \int_{y_l}^{y_u} V_{B_y}'^n (y)^* V_{B_y}''^p (y)\, dy
$$

$$
\Phi_{np} = \frac{\omega \varepsilon_0}{k_z^m} \int_{y_l}^{y_u} V_{A_y}'^n (y)^* V_{A_y}''^p (y)\, dy
$$

$$
\mathbf{G}_{np} = \frac{k_z^m \omega \mu_0}{k_{u_{p_B}}'^2} \int_{y_l}^{y_u} \frac{I_{B_y}''^n (y)^* I_{B_y}'^p (y)}{\varepsilon_B(y)}\, dy
$$

$$
\Gamma_{np} = \frac{\omega \mu_0}{k_z^m} \int_{y_l}^{y_u} I_{A_y}''^n (y)^* I_{A_y}'^p (y)\, dy
$$

IV.6 TE, TM-TO-X MODES IN A, TE, TM-TO-Z MODES IN B

$$
\begin{bmatrix} I & \vdots & 0 \\ \text{-----} & \vdots & \text{-----} \\ \text{-}G & \vdots & I \end{bmatrix}
\begin{bmatrix} V_{B_x}^{'m} \\ \text{----} \\ V_{B_x}^{''m} \end{bmatrix}
=
\begin{bmatrix} C & \vdots & \text{-}C\Phi \\ \text{-----} & \vdots & \text{-----} \\ A\Gamma & \vdots & A \end{bmatrix}
\begin{bmatrix} V_{A_x}^{'m} \\ \text{----} \\ V_{A_x}^{''m} \end{bmatrix}
$$

$$
\begin{bmatrix} I & \vdots & \text{-}\Phi \\ \text{-----} & \vdots & \text{-----} \\ \Gamma & \vdots & I \end{bmatrix}
\begin{bmatrix} I_{A_x}^{'m} \\ \text{----} \\ I_{A_x}^{''m} \end{bmatrix}
=
\begin{bmatrix} C^{\dagger} & \vdots & C^{\dagger}F \\ \text{-----} & \vdots & \text{-----} \\ 0 & \vdots & A^{\dagger} \end{bmatrix}
\begin{bmatrix} I_{B_x}^{'m} \\ \text{----} \\ I_{B_x}^{''m} \end{bmatrix}
$$

$$
\mathbf{A}_{np} = \int_{y_l}^{y_u} I_{B_y}^{''n}(y)^* I_{A_y}^{''p}(y)\, dy
$$

$$
\mathbf{C}_{np} = \int_{y_l}^{y_u} V_{B_y}^{'n}(y)^* V_{A_y}^{'p}(y)\, dy
$$

$$
\mathbf{F}_{np} = \frac{k_z^m \omega \varepsilon_0}{k_{T_m}^2} \int_{y_l}^{y_u} V_{B_y}^{'n}(y)^* V_{B_y}^{''p}(y)\, dy
$$

$$
\Phi_{np} = \frac{\omega \varepsilon_0}{k_z^m} \int_{y_l}^{y_u} V_{A_y}^{'n}(y)^* V_{A_y}^{''p}(y)\, dy
$$

$$
\mathbf{G}_{np} = \frac{k_z^m \omega \mu_0}{k_{T_m}^2} \int_{y_l}^{y_u} I_{B_y}^{''n}(y)^* I_{B_y}^{'p}(y)\, dy
$$

$$
\Gamma_{np} = \frac{\omega \mu_0}{k_z^m} \int_{y_l}^{y_u} I_{A_y}^{''n}(y)^* I_{A_y}^{'p}(y)\, dy
$$

IV.7   TE, TM-TO-Z MODES IN A, TE, TM-TO-X MODES IN B

$$\begin{bmatrix} \mathbf{I} & \vdots & -\mathbf{F} \\ \text{-----} & \vdots & \text{-----} \\ \mathbf{G} & \vdots & \mathbf{I} \end{bmatrix} \begin{bmatrix} V_{B_x}^{'m} \\ \text{----} \\ V_{B_x}^{''m} \end{bmatrix} = \begin{bmatrix} \mathbf{C} & \vdots & \mathbf{0} \\ \text{-----} & \vdots & \text{-----} \\ -\mathbf{A}\Gamma & \vdots & \mathbf{A} \end{bmatrix} \begin{bmatrix} V_{A_x}^{'m} \\ \text{----} \\ V_{A_x}^{''m} \end{bmatrix}$$

$$\begin{bmatrix} \mathbf{I} & \vdots & \Phi \\ \text{-----} & \vdots & \text{-----} \\ \mathbf{0} & \vdots & \mathbf{I} \end{bmatrix} \begin{bmatrix} I_{A_x}^{'m} \\ \text{----} \\ I_{A_x}^{''m} \end{bmatrix} = \begin{bmatrix} \mathbf{C}^\dagger & \vdots & -\mathbf{C}^\dagger\mathbf{F} \\ \text{-----} & \vdots & \text{-----} \\ \mathbf{A}^\dagger\mathbf{G} & \vdots & \mathbf{A}^\dagger \end{bmatrix} \begin{bmatrix} I_{B_x}^{'m} \\ \text{----} \\ I_{B_x}^{''m} \end{bmatrix}$$

$$\mathbf{A}_{np} = \int_{y_l}^{y_u} I_{B_y}^{''n}(y)^* I_{A_y}^{''p}(y)\, dy$$

$$\mathbf{C}_{np} = \int_{y_l}^{y_u} V_{B_y}^{'n}(y)^* V_{A_y}^{'p}(y)\, dy$$

$$\mathbf{F}_{np} = \frac{\omega\varepsilon_0}{k_z^m} \int_{y_l}^{y_u} V_{B_y}^{'n}(y)^* V_{B_y}^{''p}(y)\, dy$$

$$\Phi_{np} = \frac{k_z^m \omega\varepsilon_0}{k_{T_m}^2} \int_{y_l}^{y_u} V_{A_y}^{'n}(y)^* V_{A_y}^{''p}(y)\, dy$$

$$\mathbf{G}_{np} = \frac{\omega\mu_0}{k_z^m} \int_{y_l}^{y_u} I_{B_y}^{''n}(y)^* I_{B_y}^{'p}(y)\, dy$$

$$\Gamma_{np} = \frac{k_z^m \omega\mu_0}{k_{T_m}^2} \int_{y_l}^{y_u} I_{A_y}^{''n}(y)^* I_{A_y}^{'p}(y)\, dy$$

IV.8 TE, TM-TO-Y MODES IN A, TE, TM-TO-Z MODES IN B

$$
\begin{bmatrix} \mathbf{I} & | & \mathbf{0} \\ \hline -\mathbf{G} & | & \mathbf{I} \end{bmatrix}
\begin{bmatrix} V_{B_x}^{'m} \\ \hline V_{B_x}^{''m} \end{bmatrix}
=
\begin{bmatrix} \mathbf{C} & | & -\mathbf{C\Phi} \\ \hline \mathbf{0} & | & \mathbf{A} \end{bmatrix}
\begin{bmatrix} V_{A_x}^{'m} \\ \hline V_{A_x}^{''m} \end{bmatrix}
$$

$$
\begin{bmatrix} \mathbf{I} & | & \mathbf{0} \\ \hline \Gamma & | & \mathbf{I} \end{bmatrix}
\begin{bmatrix} I_{A_x}^{'m} \\ \hline I_{A_x}^{''m} \end{bmatrix}
=
\begin{bmatrix} \mathbf{C}^{\dagger} & | & \mathbf{C}^{\dagger}\mathbf{F} \\ \hline \mathbf{0} & | & \mathbf{A}^{\dagger} \end{bmatrix}
\begin{bmatrix} I_{B_x}^{'m} \\ \hline I_{B_x}^{''m} \end{bmatrix}
$$

$$
\mathbf{A}_{np} = \int_{y_l}^{y_u} \frac{I_{B_y}^{''n}(y)^* \, I_{A_y}^{''p}(y)}{\varepsilon_A(y)} \, dy
$$

$$
\mathbf{C}_{np} = \int_{y_l}^{y_u} V_{B_y}^{'n}(y)^* \, V_{A_y}^{'p}(y) \, dy
$$

$$
\mathbf{F}_{np} = \frac{k_z^m \omega \varepsilon_0}{k_{T_m}^2} \int_{y_l}^{y_u} V_{B_y}^{'n}(y)^* \, V_{B_y}^{''p}(y) \, dy
$$

$$
\Phi_{np} = \frac{k_z^m \omega \varepsilon_0}{k_{u_{p_A}}^{''2}} \int_{y_l}^{y_u} V_{A_y}^{'n}(y)^* \, V_{A_y}^{''p}(y) \, dy
$$

$$
\mathbf{G}_{np} = \frac{k_z^m \omega \mu_0}{k_{T_m}^2} \int_{y_l}^{y_u} I_{B_y}^{''n}(y)^* \, I_{B_y}^{'p}(y) \, dy
$$

$$
\Gamma_{np} = \frac{k_z^m \omega \mu_0}{k_{u_{p_A}}^{'2}} \int_{y_l}^{y_u} \frac{I_{A_y}^{''n}(y)^* \, I_{A_y}^{'p}(y)}{\varepsilon_A(y)} \, dy
$$

IV.9   TE, TM-TO-Z MODES IN A, TE, TM-TO-Y MODES IN B

$$
\begin{bmatrix} \mathbf{I} & -\mathbf{F} \\ \mathbf{0} & \mathbf{I} \end{bmatrix}
\begin{bmatrix} V_{B_x}^{\prime m} \\ V_{B_x}^{\prime\prime m} \end{bmatrix}
=
\begin{bmatrix} \mathbf{C} & \mathbf{0} \\ -\mathbf{A}\boldsymbol{\Gamma} & \mathbf{A} \end{bmatrix}
\begin{bmatrix} V_{A_x}^{\prime m} \\ V_{A_x}^{\prime\prime m} \end{bmatrix}
$$

$$
\begin{bmatrix} \mathbf{I} & \boldsymbol{\Phi} \\ \mathbf{0} & \mathbf{I} \end{bmatrix}
\begin{bmatrix} I_{A_x}^{\prime m} \\ I_{A_x}^{\prime\prime m} \end{bmatrix}
=
\begin{bmatrix} \mathbf{C}^{\dagger} & \mathbf{0} \\ \mathbf{A}^{\dagger}\mathbf{G} & \mathbf{A}^{\dagger} \end{bmatrix}
\begin{bmatrix} I_{B_x}^{\prime m} \\ I_{B_x}^{\prime\prime m} \end{bmatrix}
$$

$$
\mathbf{A}_{np} = \int_{y_l}^{y_u} I_{B_y}^{\prime\prime n}(y)^* I_{A_y}^{\prime\prime p}(y)\, dy
$$

$$
\mathbf{C}_{np} = \int_{y_l}^{y_u} V_{B_y}^{\prime n}(y)^* V_{A_y}^{\prime p}(y)\, dy
$$

$$
\mathbf{F}_{np} = \frac{k_z^m \omega \varepsilon_0}{k_{u_{p_B}}^{\prime\prime 2}} \int_{y_l}^{y_u} V_{B_y}^{\prime n}(y)^* V_{B_y}^{\prime\prime p}(y)\, dy
$$

$$
\boldsymbol{\Phi}_{np} = \frac{k_z^m \omega \mu_0}{k_{T_m}^2} \int_{y_l}^{y_u} V_{A_y}^{\prime n}(y)^* V_{A_y}^{\prime\prime p}(y)\, dy
$$

$$
\mathbf{G}_{np} = \frac{k_z^m \omega \mu_0}{k_{u_{p_B}}^{\prime 2}} \int_{y_l}^{y_u} \frac{I_{B_y}^{\prime\prime n}(y)^* I_{B_y}^{\prime p}(y)}{\varepsilon_B(y)}\, dy
$$

$$
\boldsymbol{\Gamma}_{np} = \frac{k_z^m \omega \mu_0}{k_{T_m}^2} \int_{y_l}^{y_u} I_{A_y}^{\prime\prime n}(y)^* I_{A_y}^{\prime p}(y)\, dy
$$

THIS PAGE INTENTIONALLY BLANK

APPENDIX V ANALYTIC ZERO, POLE LOCATION TECHNIQUE

From the moments S_n derived from Cauchy's Theorem as discussed in Section 2.3.2.7, the position of zeroes and poles of a function within a given contour can be determined analytically in the following cases.

$S_0 = 0$

Can handle no zeroes or poles, or one zero and one pole. If there are no zeroes or poles, then S_1 also equals zero. For one zero and one pole

$$S_1 = z_1 - p_1$$
$$S_2 = z_1^2 - p_1^2 = (z_1 - p_1)(z_1 + p_1) = S_1(z_1 + p_1)$$

So

$$z_1 = \frac{1}{2}\left[S_1 + \frac{S_2}{S_1}\right]$$

$$p_1 = \frac{1}{2}\left[\frac{S_2}{S_1} - S_1\right]$$

$S_0 = 1$

Can handle one zero, or two zeroes and one pole. For one zero, $z_1 = S_1$. For two zeroes and one pole

$$S_1 = z_1 + z_2 - p_1$$
$$S_2 = z_1^2 + z_2^2 - p_1^2$$
$$S_3 = z_1^3 + z_2^3 - p_1^3$$

So

$$z_1 + z_2 = \frac{2}{3}\frac{S_3 - S_1^3}{S_2 - S_1^2} = C$$

and

$$p_1 = C - S_1$$

Hence, z_1 and z_2 may be separated as

$$z_1 = \frac{1}{2}\left[C + \sqrt{C^2 + 2S_1^2 - 4CS_1 + 2S_2}\right]$$

$$z_2 = \frac{1}{2}\left[C - \sqrt{C^2 + 2S_1^2 - 4CS_1 + 2S_2}\right]$$

$S_0 = -1$

Can handle one zero, or two poles and one zero. For one zero, $p_1 = -S_1$. For two zeroes and one pole

$$S_1 = z_1 - p_2 - p_1$$
$$S_2 = z_1^2 - p_1^2 - p_2^2$$
$$S_3 = z_1^3 - p_1^3 - p_2^3$$

So

$$p_1 + p_2 = \frac{2}{3}\frac{S_3 - S_1^3}{S_2 + S_1^2} = C$$

and

$$z_1 = C + S_1$$

Hence p_1 and p_2 may be separated as

$$p_1 = \frac{1}{2}\left[C + \sqrt{C^2 + 2S_1^2 + 4CS_1 - 2S_2}\right]$$
$$p_2 = \frac{1}{2}\left[C - \sqrt{C^2 + 2S_1^2 + 4CS_1 - 2S_2}\right]$$

$S_0 = 2$

Can handle two zeroes

$$S_1 = z_1 + z_2$$
$$S_2 = z_1^2 + z_2^2$$

where z_1 and z_2 are given by

$$z_1 = \frac{1}{2}\left[S_1 - \sqrt{2S_2 - S_1^2}\right]$$
$$z_2 = \frac{1}{2}\left[S_1 + \sqrt{2S_2 - S_1^2}\right]$$

$S_0 = -2$

Can handle two poles

$$S_1 = p_1 + p_2$$
$$S_2 = p_1^2 + p_1^2$$

where p_1 and p_2 are given by

$$p_1 = \frac{1}{2}\left[-S_1 + \sqrt{-2S_2 - S_1^2}\right]$$
$$p_2 = \frac{1}{2}\left[-S_1 - \sqrt{-2S_2 - S_1^2}\right]$$

APPENDIX VI   CROSS SECTION FIELD EXPANSIONS

For evaluating the z-mode fields in each section for output and for calculating the coupling between z-modes in adjacent sections, the z-mode fields are expressed in terms of the x-mode and y-mode equivalent network voltages and currents. These voltages and currents are defined in Section 2.3.1 for y-modes and Section 2.3.2 for x-modes. The derivation of the x-components of **E** and **H** from the y and z-components is described in Section 2.3.2.9. The y and z-components are written directly from the definitions of the y-mode and x-mode field in Sections 2.3.1 and 2.3.2. The power transmitted in the z-direction by the z-modes in each two-dimensional section is derived from the field expansions as discussed in Section 2.3.2.9.

VI.1   TE, TM-TO-Y MODES

$$E_y^m = \sum_n^{N_y^{TM}} V_x''^{mn}(x) \frac{I_y''^n(y)}{\varepsilon_r(y)}$$

$$E_z^m = \sum_n^{N_y^{TE}} V_x'^{mn}(x) V_y'^n(y) - \sum_n^{N_y^{TM}} \frac{k_z^m \omega \varepsilon_0}{k_{u_n}''^2} V_x''^{mn}(x) V_y''^n(y)$$

$$H_y^m = -\sum_n^{N_y^{TE}} I_x'^{mn}(x) V_y'^n(y)$$

$$H_z^m = \sum_n^{N_y^{TE}} \frac{k_z^m \omega \mu_0}{k_{u_n}'^2} I_x'^{mn}(x) I_y'^n(y) + \sum_n^{N_y^{TM}} I_x''^{mn}(x) I_y''^n(y)$$

Therefore

$$E_x^m = \sum_n^{N_y^{TE}} \frac{k_z^m \omega \mu_0}{k_{u_n}'^2} I_x'^{mn}(x) V_y'^n(y) - \sum_n^{N_y^{TM}} I_x''^{mn}(x) V_y''^n(y)$$

and

$$H_x^m = \sum_n^{N_y^{TE}} V_x'^{mn}(x) I_y'^n(y) - \sum_n^{N_y^{TM}} \frac{k_z^m \omega \varepsilon_0}{k_{u_n}''^2} V_x''^{mn}(x) I_y''^n(y)$$

The power flow in the mth z-mode through the two-dimensional section is given by

$$P_z^m = \sum_n^{N_y^{TM}} \sum_p^{N_y^{TE}} \int_{x_l}^{x_u} I_x^{"mn}(x) I_x^{'mp}(x)^* dx \int_{y_l}^{y_u} V_y^{"n}(y) V_y^{'p}(y)^* dy$$

$$- \sum_n^{N_y^{TM}} \sum_p^{N_y^{TE}} \int_{x_l}^{x_u} V_x^{"mn}(x) V_x^{'mp}(x)^* dx \int_{y_l}^{y_u} \frac{I_y^{"n}(y) I_y^{'p}(y)^*}{\varepsilon_r(y)} dy$$

$$+ \sum_n^{N_y^{TE}} \sum_p^{N_y^{TE}} \frac{k_z^m \omega \mu_0}{k_{u_n}^{'2}} \int_{x_l}^{x_u} I_x^{'mn}(x) I_x^{'mp}(x)^* dx \int_{y_l}^{y_u} V_y^{'n}(y) V_y^{'p}(y)^* dy$$

$$+ \sum_n^{N_y^{TM}} \sum_p^{N_y^{TM}} \frac{k_z^{m*} \omega \varepsilon_0}{k_{u_p}^{"2}} \int_{x_l}^{x_u} V_x^{"mn}(x) V_x^{"mp}(x)^* dx \int_{y_l}^{y_u} \frac{I_y^{"n}(y) I_y^{"p}(y)^*}{\varepsilon_r(y)} dy$$

VI.2 TE, TM-TO-X MODES

$$E_y^m = \sum_n^{N_y^{TM}} \frac{\omega \mu_0}{k_z^m} V_x^{'mn}(x) I_y^{'n}(y) + \sum_n^{N_y^{TE}} V_x^{"mn}(x) I_y^{"n}(y)$$

$$E_z^m = \sum_n^{N_y^{TM}} V_x^{'mn}(x) V_y^{'n}(y) - \sum_n^{N_y^{TE}} \frac{\omega \varepsilon_0}{k_z^m} V_x^{"mn}(x) V_y^{"n}(y)$$

$$H_y^m = -\sum_n^{N_y^{TM}} I_x^{'mn}(x) V_y^{'n}(y) + \sum_n^{N_y^{TE}} \frac{\omega \varepsilon_0}{k_z^m} I_x^{"mn}(x) V_y^{"n}(y)$$

$$H_z^m = \sum_n^{N_y^{TM}} \frac{\omega \mu_0}{k_z^m} I_x^{'mn}(x) I_y^{'n}(y) + \sum_n^{N_y^{TE}} I_x^{"mn}(x) I_y^{"n}(y)$$

Therefore

$$E_x^m = -\sum_n^{N_y^{TM}} \frac{\left[k_0^2 \varepsilon_r - k_{x_{mn}}^{'2}\right]}{k_z^m \omega \varepsilon_0 \varepsilon_r} I_x^{'mn}(x) V_y^{'n}(y)$$

and

$$H_x^m = -\sum_n^{N_y^{TE}} \frac{\left[k_0^2 \varepsilon_r - k_{x_{mn}}^{"2}\right]}{k_z^m \omega \mu_0} V_x^{"mn}(x) I_y^{"n}(y)$$

The power flow in the mth z-mode through the two-dimensional section is given by

$$P_z^m = -\sum_n^{N_y^{TM}} \sum_p^{N_y^{TE}} \frac{\left[k_0^2 \varepsilon_r - k_{xmp}^{'2}\right]^*}{k_z^m k_z^{m*} \varepsilon_r} \int_{x_l}^{x_u} I_x^{'mn}(x) I_x^{''mp}(x)^* dx \int_{y_l}^{y_u} V_y^{'n}(y) V_y^{''p}(y)^* dy$$

$$+ \sum_n^{N_y^{TM}} \sum_p^{N_y^{TE}} \frac{\left[k_0^2 \varepsilon_r - k_{xmp}^{''2}\right]}{k_z^m k_z^{m*}} \int_{x_l}^{x_u} V_x^{'mn}(x) V_x^{''mp}(x)^* dx \int_{y_l}^{y_u} I_y^{'n}(y) I_y^{''p}(y)^* dy$$

$$+ \sum_n^{N_y^{TM}} \sum_p^{N_y^{TM}} \frac{\left[k_0^2 \varepsilon_r - k_{xmn}^{'2}\right]}{k_z^m \omega \varepsilon_0 \varepsilon_r} \int_{x_l}^{x_u} I_x^{'mn}(x) I_x^{'mp}(x)^* dx \int_{y_l}^{y_u} V_y^{'n}(y) V_y^{'p}(y)^* dy$$

$$+ \sum_n^{N_y^{TE}} \sum_p^{N_y^{TE}} \frac{\left[k_0^2 \varepsilon_r - k_{xmp}^{''2}\right]^*}{k_z^{m*} \omega \mu_0} \int_{x_l}^{x_u} V_x^{''mn}(x) V_x^{''mp}(x)^* dx \int_{y_l}^{y_u} I_y^{''n}(y) I_y^{''p}(y)^* dy$$

VI.3   TE, TM-TO-Z MODES

$$E_y^m = \sum_n^{N_y^{TE}} V_x^{''mn}(x) I_y^{''n}(y) - \sum_n^{N_y^{TM}} \frac{k_z^m \omega \mu_0}{k_{T_m}^2} V_x^{'mn}(x) I_y^{'n}(y)$$

$$E_z^m = \sum_n^{N_y^{TM}} V_x^{'mn}(x) V_y^{'n}(y)$$

$$H_y^m = -\sum_n^{N_y^{TM}} I_x^{'mn}(x) V_y^{'n}(y) - \sum_n^{N_y^{TE}} \frac{k_z^m \omega \varepsilon_0}{k_{T_m}^2} I_x^{''mn}(x) V_y^{''n}(y)$$

$$H_z^m = \sum_n^{N_y^{TE}} I_x^{''mn}(x) I_y^{''n}(y)$$

Hence

$$E_x^m = -\sum_n^{N_y^{TE}} \frac{k_0^2}{k_{T_m}^2} I_x^{''mn}(x) V_y^{''n}(y) - \sum_n^{N_y^{TM}} \frac{k_z^m}{\omega \varepsilon_0 \varepsilon_r} I_x^{'mn}(x) V_y^{'n}(y)$$

and

$$H_x^m = \sum_n^{N_y^{TM}} \frac{k_0^2 \varepsilon_r}{k_{T_m}^2} V_x^{'mn}(x) I_y^{'n}(y) - \sum_n^{N_y^{TE}} \frac{k_z^m}{\omega \mu_0} V_x^{''mn}(x) I_y^{''n}(y)$$

The power flow in the mth z-mode through the two-dimensional section is given by

$$
\begin{aligned}
P_z^m = &\sum_n^{N_y^{TE}} \sum_p^{N_y^{TM}} \frac{k_0^2}{k_{T_m}^2} \int_{x_l}^{x_u} I_x''^{mn}(x) I_x'^{mp}(x)^* dx \int_{y_l}^{y_u} V_y''^n(y) V_y'^p(y)^* dy \\
&- \sum_n^{N_y^{TE}} \sum_p^{N_y^{TM}} \frac{k_0^2 \varepsilon_r}{k_{T_m}^2}^* \int_{x_l}^{x_u} V_x''^{mn}(x) V_x'^{mp}(x)^* dx \int_{y_l}^{y_u} I_y''^n(y) I_y'^p(y)^* dy \\
&+ \sum_n^{N_y^{TM}} \sum_p^{N_y^{TE}} \frac{k_z^m k_z^{m*}}{k_{T_m}^2} \frac{1}{\varepsilon_r} \int_{x_l}^{x_u} I_x'^{mn}(x) I_x''^{mp}(x)^* dx \int_{y_l}^{y_u} V_y'^n(y) V_y''^p(y)^* dy \\
&- \sum_n^{N_y^{TM}} \sum_p^{N_y^{TE}} \frac{k_z^m k_z^{m*}}{k_{T_m}^2} \int_{x_l}^{x_u} V_x'^{mn}(x) V_x''^{mp}(x)^* dx \int_{y_l}^{y_u} I_y'^n(y) I_y''^p(y)^* dy \\
&+ \sum_n^{N_y^{TM}} \sum_p^{N_y^{TM}} \frac{k_z^m}{\omega \varepsilon_0 \varepsilon_r} \int_{x_l}^{x_u} I_x'^{mn}(x) I_x'^{mp}(x)^* dx \int_{y_l}^{y_u} V_y'^n(y) V_y'^p(y)^* dy \\
&+ \sum_n^{N_y^{TM}} \sum_p^{N_y^{TM}} \frac{k_0^2 k_z^m \omega \mu_0 \varepsilon_r}{k_{T_m}^2 k_{T_m}^{2*}} \int_{x_l}^{x_u} V_x'^{mn}(x) V_x'^{mp}(x)^* dx \int_{y_l}^{y_u} I_y'^n(y) I_y'^p(y)^* dy \\
&+ \sum_n^{N_y^{TE}} \sum_p^{N_y^{TE}} \frac{k_0^2 k_z^{m*} \omega \varepsilon_0}{k_{T_m}^2 k_{T_m}^{2*}} \int_{x_l}^{x_u} I_x''^{mn}(x) I_x''^{mp}(x)^* dx \int_{y_l}^{y_u} V_y''^n(y) V_y''^p(y)^* dy \\
&+ \sum_n^{N_y^{TE}} \sum_p^{N_y^{TE}} \frac{k_z^{m*}}{\omega \mu_0} \int_{x_l}^{x_u} V_x''^{mn}(x) V_x''^{mp}(x)^* dx \int_{y_l}^{y_u} I_y''^n(y) I_y''^p(y)^* dy
\end{aligned}
$$

APPENDIX VII   SECTION COUPLING

To evaluate the coupling between z-modes in adjacent sections A and B, the components of the electric and magnetic fields tangential to the section interface were matched over the interface The technique used for the derivations in this appendix is identical to the approach used in Section 2.3.3.1 for TE and TM-to-y y-modes in both section A and section B.

Calculation of the section z-mode coupling allowed the individual sections to be cascaded together to form the complete element being analysed as discussed in Sections 2.3.3.2 and 2.3.3.3.

VII.1   TE, TM-TO-X COUPLING

VII.1.1 Electric Field Matching

To evaluate the z-mode coupling between adjacent sections A and B, where the y-modes are TE and TM-to-x in both sections, the x and y-components of the electric field tangential to the section interface are matched. This section of Appendix VII describes this process, which closely follows the TE and TM-to-y mode analysis in Section 2.3.3.1.

x-component

$$\sum_m^{N_z^B} V_{B_z}^m \left[\sum_n^{N_B^{TM}} \frac{\left[k_0^2 \varepsilon_B - k_{x_{B_{mn}}}'^2 \right]}{k_{z_B}^m \omega \varepsilon_0 \varepsilon_B} I_{B_x}'^{mn}(x) V_{B_y}'^n(y) \right]$$

$$= \sum_p^{N_z^A} V_{A_z}^p \left[\sum_q^{N_A^{TM}} \frac{\left[k_0^2 \varepsilon_A - k_{x_{A_{pq}}}'^2 \right]}{k_{z_A}^p \omega \varepsilon_0 \varepsilon_A} I_{A_x}'^{pq}(x) V_{A_y}'^q(y) \right] \tag{VII.1}$$

Both sides of Equation VII.1 were multiplied by

$$\sum_s^{N_B^{TM}} I_{B_x}'^{rs}(x)^* V_{B_y}'^s(y)^*$$

Integrating over the aperture in the x and y directions and applying orthonormality of the y-modes yields

$$\mathbf{A} \mathbf{V}_{B_z} = \mathbf{B} \mathbf{V}_{A_z}$$

where

$$A_{mn} = \sum_p^{N_B^{TM}} \frac{[k_0^2 \varepsilon_B - k_{x_{B_{np}}}'^2]}{k_{z_B}^n \omega \varepsilon_0 \varepsilon_B} \int_{x_l}^{x_u} I_{B_x}'^{np}(x) I_{B_x}'^{mp}(x)^* dx$$

$$B_{mn} = \sum_p^{N_B^{TM}} \sum_q^{N_A^{TM}} \frac{[k_0^2 \varepsilon_A - k_{x_{A_{nq}}}'^2]}{k_{z_A}^n \omega \varepsilon_0 \varepsilon_A} \int_{x_l}^{x_u} I_{A_x}'^{nq}(x) I_{B_x}'^{mp}(x)^* dx \int_{y_l}^{y_u} V_{A_y}'^q(y) V_{B_y}'^p(y)^* dy$$

In addition, multiplying both sides of Equation VII.1 by

$$\sum_{s}^{N_B^{TE}} \frac{\omega \varepsilon_0}{k_{z_B}^{r}}^* I_{B_x}^{'rs}(x)^* V_{B_y}^{'s}(y)^*$$

and integrating over the aperture yields

$$SV_{B_z} = TV_{A_z}$$

where

$$S_{mn} = \sum_{p}^{N_B^{TE}} \sum_{q}^{N_B^{TM}} \frac{\left[k_0^2 \varepsilon_B - k_{x_{B_{nq}}}^{'2} \right]}{k_{z_B}^{n} k_{z_B}^{m}^* \varepsilon_B} \int_{x_l}^{x_u} I_{B_x}^{'nq}(x) I_{B_x}^{''mp}(x)^* dx \int_{y_l}^{y_u} V_{B_y}^{'q}(y) V_{B_y}^{''p}(y)^* dy$$

$$T_{mn} = \sum_{p}^{N_B^{TE}} \sum_{q}^{N_A^{TM}} \frac{\left[k_0^2 \varepsilon_A - k_{x_{A_{nq}}}^{'2} \right]}{k_{z_A}^{n} k_{z_B}^{m}^* \varepsilon_A} \int_{x_l}^{x_u} I_{A_x}^{'nq}(x) I_{B_x}^{''mp}(x)^* dx \int_{y_l}^{y_u} V_{A_y}^{'q}(y) V_{B_y}^{''p}(y)^* dy$$

y-component

$$\sum_{m}^{N_z^B} V_{B_z}^{m} \left[\sum_{n}^{N_B^{TE}} V_{B_x}^{''mn}(x) I_{B_y}^{''n}(y) + \frac{\omega \mu_0}{k_{z_B}^{m}} \sum_{p}^{N_B^{TM}} V_{B_x}^{'mp}(x) I_{B_y}^{'p}(y) \right]$$

$$= \sum_{i}^{N_z^A} V_{A_z}^{i} \left[\sum_{j}^{N_A^{TE}} V_{A_x}^{''ij}(x) I_{A_y}^{''j}(y) + \frac{\omega \mu_0}{k_{z_A}^{i}} \sum_{k}^{N_A^{TM}} V_{A_x}^{'ik}(x) I_{A_y}^{'k}(y) \right] \qquad \text{(VII.2)}$$

Both sides of Equation VII.2 were multiplied by

$$\sum_{s}^{N_B^{TE}} \frac{\left[k_0^2 \varepsilon_B - k_{x_{B_{rs}}}^{''2} \right]^*}{k_{z_B}^{r}^* \omega \mu_0} V_{B_x}^{''rs}(x)^* I_{B_y}^{''s}(y)^*$$

Integrating over the aperture in the *x* and *y* directions and using orthonormality of the *y*-modes yields

$$HV_{B_z} = JV_{A_z}$$

where

$$H_{mn} = \sum_p^{N_B^{TE}} \left[\frac{\left[k_0^2 \varepsilon_B - k_{x B_{mp}}^{''2} \right]^*}{k_{z_B}^{m\,*} \omega \mu_0} \int_{x_l}^{x_u} V_{B_x}^{''np}(x) V_{B_x}^{''mp}(x)^* dx + \sum_q^{N_B^{TM}} \frac{\left[k_0^2 \varepsilon_B - k_{x B_{mp}}^{''2} \right]^*}{k_{z_B}^{m\,*} k_{z_B}^{n}} \int_{x_l}^{x_u} V_{B_x}^{'nq}(x) V_{B_x}^{''mp}(x)^* dx \int_{y_l}^{y_u} I_{B_y}^{'q}(y) I_{B_y}^{''p}(y)^* dy \right]$$

$$J_{mn} = \sum_p^{N_B^{TE}} \left[\sum_q^{N_A^{TE}} \frac{\left[k_0^2 \varepsilon_B - k_{x B_{mp}}^{''2} \right]^*}{k_{z_B}^{m\,*} \omega \mu_0} \int_{x_l}^{x_u} V_{A_x}^{''nq}(x) V_{B_x}^{''mp}(x)^* dx \int_{y_l}^{y_u} I_{A_y}^{''q}(y) I_{B_y}^{''p}(y)^* dy + \sum_r^{N_A^{TM}} \frac{\left[k_0^2 \varepsilon_B - k_{x B_{mp}}^{''2} \right]^*}{k_{z_B}^{m\,*} k_{z_A}^{n}} \int_{x_l}^{x_u} V_{A_x}^{'nr}(x) V_{B_x}^{''mp}(x)^* dx \int_{y_l}^{y_u} I_{A_y}^{'r}(y) I_{B_y}^{''p}(y)^* dy \right]$$

VII.1.2 Magnetic Field Matching

To evaluate the z-mode coupling between adjacent sections A and B, where the y-modes are TE and TM-to-x in both sections, the x and y-components of the magnetic field tangential to the section interface are matched. This section of Appendix VII describes this process, which closely follows the TE and TM-to-y mode analysis in Section 2.3.3.1.

x-component

$$\sum_m^{N_z^A} I_{A_z}^m \sum_n^{N_A^{TE}} \frac{\left[k_0^2 \varepsilon_A - k_{x A_{mn}}^{''2} \right]}{k_{z_A}^m \omega \mu_0} V_{A_x}^{''mn}(x) I_{A_y}^{''n}(y)$$

$$= \sum_p^{N_z^B} I_{B_z}^p \sum_q^{N_B^{TE}} \frac{\left[k_0^2 \varepsilon_B - k_{x B_{pq}}^{''2} \right]}{k_{z_B}^m \omega \mu_0} V_{B_x}^{''pq}(x) I_{B_y}^{''q}(y) \tag{VII.3}$$

Both sides of Equation VII.3 were multiplied by

$$\sum_s^{N_A^{TE}} V_{A_x}^{''rs}(x)^* I_{A_y}^{''s}(y)^*$$

Integrating over the aperture in the x and y directions and using orthonormality of the y-modes yields

$$\mathbf{K} \mathbf{I}_{A_z} = \mathbf{L} \mathbf{I}_{B_z}$$

where

$$K_{mn} = \sum_{p}^{N_A^{TE}} \frac{\left[k_0^2 \varepsilon_A - k_{xA_{np}}^{"2}\right]}{k_{zA}^n \omega\mu_0} \int_{x_l}^{x_u} V_{A_x}^{"np}(x) V_{A_x}^{"mp}(x)^* dx$$

$$L_{mn} = \sum_{p}^{N_A^{TE}} \sum_{q}^{N_B^{TE}} \frac{\left[k_0^2 \varepsilon_B - k_{xB_{nq}}^{"2}\right]}{k_{zB}^n \omega\mu_0} \int_{x_l}^{x_u} V_{B_x}^{"nq}(x) V_{A_x}^{"mp}(x)^* dx \int_{y_l}^{y_u} I_{B_y}^{"q}(y) I_{A_y}^{"p}(y)^* dy$$

In addition, multiplying both sides of Equation VII.3 by

$$\sum_{s}^{N_A^{TM}} \frac{\omega\mu_0}{k_{zA}^r} V_{A_x}^{'rs}(x)^* I_{A_y}^{'s}(y)^*$$

and integrating over the aperture yields

$$\mathbf{FI}_{A_z} = \mathbf{GI}_{B_z}$$

where

$$F_{mn} = \sum_{p}^{N_A^{TM}} \sum_{q}^{N_A^{TE}} \frac{\left[k_0^2 \varepsilon_A - k_{xA_{nq}}^{"2}\right]}{k_{zA}^n k_{zA}^m} \int_{x_l}^{x_u} V_{A_x}^{"nq}(x) V_{A_x}^{'mp}(x)^* dx \int_{y_l}^{y_u} I_{A_y}^{"q}(y) I_{A_y}^{'p}(y)^* dy$$

$$G_{mn} = \sum_{p}^{N_A^{TM}} \sum_{q}^{N_B^{TE}} \frac{\left[k_0^2 \varepsilon_B - k_{xB_{nq}}^{"2}\right]}{k_{zB}^n k_{zA}^m} \int_{x_l}^{x_u} V_{B_x}^{"nq}(x) V_{A_x}^{'mp}(x)^* dx \int_{y_l}^{y_u} I_{B_y}^{"q}(y) I_{A_y}^{'p}(y)^* dy$$

y-component

$$\sum_{m}^{N_z^A} I_{A_z}^m \left[\sum_{n}^{N_A^{TM}} I_{A_x}^{'mn}(x) V_{A_y}^{'n}(y) - \sum_{p}^{N_A^{TE}} \frac{\omega\varepsilon_0}{k_{zA}^m} I_{A_x}^{"mp}(x) V_{A_y}^{"p}(y) \right]$$

$$= \sum_{i}^{N_z^B} I_{B_z}^i \left[\sum_{j}^{N_B^{TM}} I_{B_x}^{'ij}(x) V_{B_y}^{'j}(y) - \sum_{k}^{N_B^{TE}} \frac{\omega\varepsilon_0}{k_{zB}^i} I_{A_x}^{"ik}(x) V_{A_y}^{"k}(y) \right] \quad \text{(VII.4)}$$

Both sides of Equation VII.4 were multiplied by

$$\sum_{s}^{N_A^{TM}} \frac{\left[k_0^2 \varepsilon_A - k_{xA_{rs}}^{"2}\right]^*}{k_{zA}^r \omega\varepsilon_0\varepsilon_A} I_{A_x}^{'rs}(x)^* V_{A_y}^{'s}(y)^*$$

Integrating over the aperture in the x and y directions and applying orthonormality of the y-modes yields

$$\mathbf{CI}_{A_z} = \mathbf{DI}_{B_z}$$

where

$$
C_{mn} = \sum_p^{N_A^{TM}} \left[\frac{\left[k_0^2 \varepsilon_A - k_{x_{A_{mp}}}^{'2} \right]^*}{k_{z_A}^{m\,*} \omega \varepsilon_0 \varepsilon_A} \int_{x_l}^{x_u} I_{A_x}^{'np}(x) I_{A_x}^{'mp}(x)^* dx \right.
$$
$$
\left. - \sum_q^{N_A^{TE}} \frac{\left[k_0^2 \varepsilon_A - k_{x_{A_{mp}}}^{'2} \right]^*}{k_{z_A}^{m\,*} k_{z_A}^{n} \varepsilon_A} \int_{x_l}^{x_u} I_{A_x}^{"nq}(x) I_{A_x}^{'mp}(x)^* dx \int_{y_l}^{y_u} V_{A_y}^{"q}(y) V_{A_y}^{'p}(y)^* dy \right]
$$

$$
D_{mn} = \sum_p^{N_A^{TM}} \left[\sum_q^{N_B^{TM}} \frac{\left[k_0^2 \varepsilon_A - k_{x_{A_{mp}}}^{'2} \right]^*}{k_{z_A}^{m\,*} \omega \varepsilon_0 \varepsilon_A} \int_{x_l}^{x_u} I_{B_x}^{'nq}(x) I_{A_x}^{'mp}(x)^* dx \int_{y_l}^{y_u} V_{B_y}^{'q}(y) V_{A_y}^{'p}(y)^* dy \right.
$$
$$
\left. - \sum_r^{N_B^{TE}} \frac{\left[k_0^2 \varepsilon_A - k_{x_{A_{mp}}}^{'2} \right]^*}{k_{z_A}^{m\,*} k_{z_B}^{n} \varepsilon_A} \int_{x_l}^{x_u} I_{B_x}^{"nr}(x) I_{A_x}^{'mp}(x)^* dx \int_{y_l}^{y_u} V_{B_y}^{"r}(y) V_{A_y}^{'p}(y)^* dy \right]
$$

VII.1.3 Complex Power Conservation

As for TE and TM-to-y modes, using the field relations in Section 2.3.2.8, the power flow through any given section is

$$
P_z^{tot} = \sum_m^{N_z^A} \sum_n^{N_z^A} V_{A_z}^m I_{A_z}^{n\,*} + \left[\sum_p^{N_y^{TE}} \sum_q^{N_y^{TM}} \left[\frac{[k_0^2 \varepsilon_r - k_{x_{mp}}^{"2}]^*}{k_z^{m\,*} k_z^n} \int_{x_l}^{x_u} V_x^{'nq}(x) V_x^{"mp}(x)^* dx \int_{y_l}^{y_u} I_y^{'q}(y) I_y^{"p}(y)^* dy \right. \right.
$$
$$
\left. \left. - \frac{[k_0^2 \varepsilon_r - k_{x_{nq}}^{'2}]}{k_z^{m\,*} k_z^n \varepsilon_r} \int_{x_l}^{x_u} I_x^{'nq}(x) I_x^{"mp}(x)^* dx \int_{y_l}^{y_u} V_y^{'q}(y) V_y^{"p}(y)^* dy \right] \right.
$$
$$
+ \sum_p^{N_y^{TM}} \frac{[k_0^2 \varepsilon_r - k_{x_{np}}^{"2}]}{k_z^n \omega \varepsilon_0 \varepsilon_r} \int_{x_l}^{x_u} I_x^{'np}(x) I_x^{'mp}(x)^* dx
$$
$$
+ \sum_p^{N_y^{TM}} \frac{[k_0^2 \varepsilon_r - k_{x_{mp}}^{'2}]^*}{k_z^{m\,*} \omega \mu_0} \int_{x_l}^{x_u} V_x^{"np}(x) V_x^{"mp}(x)^* dx
$$

In terms of the previously derived coupling matrices

$$P_{A_z}^{tot} = \left[I_{A_z}\right]^\dagger \left[C^\dagger + F^\dagger + K^\dagger\right]\left[V_{A_z}\right]$$

$$= \left[I_{B_z}\right]^\dagger \left[D^\dagger + G^\dagger + L^\dagger\right]\left[V_{A_z}\right]$$

and

$$P_{B_z}^{tot} = \left[I_{B_z}\right]^\dagger [A + H - S]\left[V_{B_z}\right]$$

$$= \left[I_{B_z}\right]^\dagger [B + J - T]\left[V_{A_z}\right]$$

So for conservation of complex power, require

$$D^\dagger + N^\dagger - L^\dagger = B + J - Q$$

This is true by inspection. Therefore, to ensure complex power conservation regardless of the number of z-modes used in each section, the following expressions for the current and voltage coupling will be used

$$[C_I] = [C + F + K]^{-1}[D + G + L]$$

$$[C_V] = [A + H - S]^{-1}[B + J - T]$$

$$= [A + H - S]^{-1}\left[D^\dagger + G^\dagger + L^\dagger\right]$$

VII.2   TE, TM-TO-Z COUPLING

VII.2.1 Electric Field Matching

To evaluate the z-mode coupling between adjacent sections A and B, where the y-modes are TE and TM-to-z in both sections, the x and y-components of the electric field tangential to the section interface are matched. This section of Appendix VII describes this process, which closely follows the TE and TM-to-y mode analysis in Section 2.3.3.1.

x-component

$$\sum_m^{N_z^B} V_{B_z}^m \left[\frac{k_{z_B}^m}{\omega \varepsilon_0 \varepsilon_B} \sum_n^{N_B^{TM}} I_{B_x}^{'mn}(x)V_{B_y}^{'n}(y) + \frac{k_0^2}{k_{T_{B_m}}^2} \sum_p^{N_B^{TE}} I_{B_x}^{''mp}(x)V_{B_y}^{''p}(y) \right]$$

$$= \sum_i^{N_z^A} V_{A_z}^i \left[\frac{k_{z_A}^i}{\omega \varepsilon_0 \varepsilon_A} \sum_j^{N_A^{TM}} I_{A_x}^{'ij}(x)V_{A_y}^{'j}(y) + \frac{k_0^2}{k_{T_{A_i}}^2} \sum_k^{N_A^{TE}} I_{A_x}^{''ik}(x)V_{A_y}^{''k}(y) \right] \qquad \text{(VII.5)}$$

Both sides of Equation VII.5 were multiplied by

$$\sum_s^{N_B^{TM}} I_{B_x}^{'rs}(x)^* V_{B_y}^{'s}(y)^*$$

Integrating over the aperture in the x and y directions and applying orthonormality of the y-modes yields

$$\mathbf{AV}_{B_z} = \mathbf{BV}_{A_z}$$

where

$$A_{mn} = \sum_p^{N_B^{TM}} \left[\begin{array}{l} \dfrac{k_{z_B}^n}{\omega \varepsilon_0 \varepsilon_B} \int_{x_l}^{x_u} I_{B_x}^{'np}(x) I_{B_x}^{'mp}(x)^* dx \\[3ex] + \dfrac{k_0^2}{k_{T_{B_n}}^2} \sum_q^{N_B^{TE}} \int_{x_l}^{x_u} I_{B_x}^{"nq}(x) I_{B_x}^{'mp}(x)^* dx \int_{y_l}^{y_u} V_{B_y}^{"q}(y) V_{B_y}^{'p}(y)^* dy \end{array} \right]$$

$$B_{mn} = \sum_p^{N_B^{TM}} \left[\begin{array}{l} \dfrac{k_{z_A}^n}{\omega \varepsilon_0 \varepsilon_A} \sum_q^{N_A^{TM}} \int_{x_l}^{x_u} I_{A_x}^{'nq}(x) I_{B_x}^{'mp}(x)^* dx \int_{y_l}^{y_u} V_{A_y}^{'q}(y) V_{B_y}^{'p}(y)^* dy \\[3ex] + \dfrac{k_0^2}{k_{T_{A_n}}^2} \sum_r^{N_B^{TM}} \int_{x_l}^{x_u} I_{A_x}^{"nr}(x) I_{B_x}^{'mp}(x)^* dx \int_{y_l}^{y_u} V_{A_y}^{"r}(y) V_{B_y}^{'p}(y)^* dy \end{array} \right]$$

In addition, multiplying both sides of Equation VII.5 by

$$\dfrac{k_{z_B}^r{}^*\omega \varepsilon_0}{k_{T_{B_r}}^2{}^*} \sum_s^{N_B^{TE}} I_{B_x}^{"rs}(x)^* V_{B_y}^{"s}(y)^*$$

and integrating over the aperture yields

$$\mathbf{SV}_{B_z} = \mathbf{TV}_{A_z}$$

where

$$S_{mn} = \sum_p^{N_B^{TE}} \left[\begin{array}{l} \dfrac{k_{z_B}^n k_{z_B}^m{}^*}{k_{T_{B_m}}^2{}^* \varepsilon_B} \sum_q^{N_B^{TM}} \int_{x_l}^{x_u} I_{B_x}^{'nq}(x) I_{B_x}^{"mp}(x)^* dx \int_{y_l}^{y_u} V_{B_y}^{'q}(y) V_{B_y}^{"p}(y)^* dy \\[3ex] + \dfrac{k_0^2 k_{z_B}^m{}^* \omega \varepsilon_0}{k_{T_{B_m}}^2{}^* k_{T_{B_n}}^2} \sum_r^{N_B^{TE}} \int_{x_l}^{x_u} I_{B_x}^{"nr}(x) I_{B_x}^{"mp}(x)^* dx \int_{y_l}^{y_u} V_{B_y}^{"r}(y) V_{B_y}^{"p}(y)^* dy \end{array} \right]$$

$$T_{mn} = \sum_p^{N_B^{TE}} \left[\begin{array}{l} \dfrac{k_{z_A}^n k_{z_B}^m{}^*}{k_{T_{B_m}}^2{}^* \varepsilon_A} \sum_q^{N_A^{TM}} \int_{x_l}^{x_u} I_{A_x}^{'nq}(x) I_{B_x}^{"mp}(x)^* dx \int_{y_l}^{y_u} V_{A_y}^{'q}(y) V_{B_y}^{"p}(y)^* dy \\[3ex] + \dfrac{k_0^2 k_{z_B}^m{}^* \omega \varepsilon_0}{k_{T_{B_m}}^2{}^* k_{T_{A_n}}^2} \sum_r^{N_A^{TE}} \int_{x_l}^{x_u} I_{A_x}^{"nr}(x) I_{B_x}^{"mp}(x)^* dx \int_{y_l}^{y_u} V_{A_y}^{"r}(y) V_{B_y}^{"p}(y)^* dy \end{array} \right]$$

y-component

$$\sum_m^{N_z^B} V_{B_z}^m \left[-\frac{k_{z_B}^{m*} \omega \mu_0}{k_{T_{B_m}}^2} \sum_n^{N_B^{TM}} V_{B_x}^{'mn}(x) I_{B_y}^{'n}(y) + \sum_p^{N_B^{TE}} V_{B_x}^{''mp}(x) I_{B_y}^{''p}(y) \right]$$

$$= \sum_i^{N_z^A} V_{A_z}^i \left[-\frac{k_{z_A}^{i*} \omega \mu_0}{k_{T_{A_i}}^2} \sum_j^{N_A^{TM}} V_{A_x}^{'ij}(x) I_{A_y}^{'j}(y) + \sum_k^{N_A^{TE}} V_{A_x}^{''ik}(x) I_{A_y}^{''k}(y) \right]$$ (VII.6)

Both sides of Equation VII.6 were multiplied by

$$\frac{k_{z_B}^{r*}}{\omega \mu_0} \sum_s^{N_B^{TE}} V_{B_x}^{''rs}(x)^* I_{B_y}^{''s}(y)^*$$

Integrating over the aperture in the x and y directions and applying orthonormality of the y-modes yields

$$\mathbf{HV}_{B_z} = \mathbf{JV}_{A_z}$$

where

$$H_{mn} = \sum_p^{N_B^{TE}} \left[\begin{array}{l} \dfrac{k_{z_B}^{m*}}{\omega \mu_0} \displaystyle\int_{x_l}^{x_u} V_{B_x}^{''np}(x) V_{B_x}^{''mp}(x)^* dx \\[2em] -\dfrac{k_{z_B}^{m*} k_{z_B}^n}{k_{T_{B_n}}^2} \displaystyle\sum_q^{N_B^{TM}} \int_{x_l}^{x_u} V_{B_x}^{'nq}(x) V_{B_x}^{''mp}(x)^* dx \int_{y_l}^{y_u} I_{B_y}^{'q}(y) I_{B_y}^{''p}(y)^* dy \end{array} \right]$$

$$J_{mn} = \sum_p^{N_B^{TE}} \left[\begin{array}{l} \dfrac{k_{z_B}^{m*}}{\omega \mu_0} \displaystyle\sum_q^{N_A^{TE}} \int_{x_l}^{x_u} V_{A_x}^{''nq}(x) V_{B_x}^{''mp}(x)^* dx \int_{y_l}^{y_u} I_{A_y}^{''q}(y) I_{B_y}^{''p}(y)^* dy \\[2em] +\dfrac{k_{z_B}^{m*} k_{z_A}^n}{k_{T_{A_n}}^2} \displaystyle\sum_r^{N_A^{TM}} \int_{x_l}^{x_u} V_{A_x}^{'nr}(x) V_{B_x}^{''mp}(x)^* dx \int_{y_l}^{y_u} I_{A_y}^{'r}(y) I_{B_y}^{''p}(y)^* dy \end{array} \right]$$

In addition, multiplying both sides of Equation VII.6 by

$$\frac{k_0^2 \varepsilon_0}{k_{T_{B_r}}^{2*}} \sum_s^{N_B^{TM}} V_{B_x}^{'rs}(x)^* I_{B_y}^{'s}(y)^*$$

and integrating over the aperture yields

$$\mathbf{PV}_{B_z} = \mathbf{QV}_{A_z}$$

where

$$
P_{mn} = \sum_{p}^{N_B^{TM}} \left[\begin{array}{l} \dfrac{k_0^2 \varepsilon_B}{k_{T_{B_m}}^2{}^*} \sum_{q}^{N_B^{TE}} \int_{x_l}^{x_u} V_{B_x}^{''nq}(x) V_{B_x}^{'mp}(x)^* dx \int_{y_l}^{y_u} I_{B_y}^{''q}(y) I_{B_y}^{'p}(y)^* dy \\[3ex] - \dfrac{k_0^2 k_{z_B}^n \omega \varepsilon_0 \varepsilon_B}{k_{T_{B_m}}^2{}^* k_{T_{B_n}}^2} \sum_{r}^{N_B^{TM}} \int_{x_l}^{x_u} V_{B_x}^{'nr}(x) V_{B_x}^{'mp}(x)^* dx \int_{y_l}^{y_u} I_{B_y}^{'r}(y) I_{B_y}^{'p}(y)^* dy \end{array} \right]
$$

$$
Q_{mn} = \sum_{p}^{N_B^{TM}} \left[\begin{array}{l} \dfrac{k_0^2 \varepsilon_B}{k_{T_{B_m}}^2{}^*} \sum_{q}^{N_A^{TE}} \int_{x_l}^{x_u} V_{A_x}^{''nq}(x) V_{B_x}^{'mp}(x)^* dx \int_{y_l}^{y_u} I_{A_y}^{''q}(y) I_{B_y}^{'p}(y)^* dy \\[3ex] - \dfrac{k_0^2 k_{z_A}^n \omega \varepsilon_0 \varepsilon_B}{k_{T_{B_m}}^2{}^* k_{T_{A_n}}^2} \sum_{r}^{N_A^{TM}} \int_{x_l}^{x_u} V_{A_x}^{'nr}(x) V_{B_x}^{'mp}(x)^* dx \int_{y_l}^{y_u} I_{A_y}^{'r}(y) I_{B_y}^{'p}(y)^* dy \end{array} \right]
$$

VII.2.2 Magnetic Field Matching

To evaluate the z-mode coupling between adjacent sections A and B, where the y-modes are TE and TM-to-z in both sections, the x and y-components of the magnetic field tangential to the section interface are matched. This section of Appendix VII describes this process, which closely follows the TE and TM-to-y mode analysis in Section 2.3.3.1.

x-component

$$
\sum_{m}^{N_z^A} I_{A_z}^m \left[\dfrac{k_{z_A}^m}{\omega \mu_0} \sum_{n}^{N_A^{TE}} V_{A_x}^{''mn}(x) I_{A_y}^{''n}(y) - \dfrac{k_0^2 \varepsilon_A}{k_{T_{A_m}}^2} \sum_{p}^{N_A^{TM}} V_{A_x}^{'mp}(x) I_{A_y}^{'p}(y) \right]
$$

$$
= \sum_{i}^{N_z^B} I_{B_z}^i \left[\dfrac{k_{z_B}^i}{\omega \mu_0} \sum_{j}^{N_B^{TE}} V_{B_x}^{''ij}(x) I_{B_y}^{''j}(y) - \dfrac{k_0^2 \varepsilon_B}{k_{T_{B_i}}^2} \sum_{k}^{N_B^{TM}} V_{B_x}^{'ik}(x) I_{B_y}^{'k}(y) \right] \quad \text{(VII.7)}
$$

Both sides of Equation VII.7 were multiplied by

$$
\sum_{s}^{N_A^{TE}} V_{A_x}^{''rs}(x)^* I_{A_y}^{''s}(y)^*
$$

Integrating over the aperture in the x and y directions and applying orthonormality of the y-modes yields

$$
\mathbf{K} \mathbf{I}_{A_z} = \mathbf{L} \mathbf{I}_{B_z}
$$

where

$$K_{mn} = \sum_{p}^{N_A^{TE}} \left[\begin{array}{l} \dfrac{k_{z_A}^n}{\omega\mu_0} \displaystyle\int_{x_l}^{x_u} V_{A_x}^{''np}(x) V_{A_x}^{''mp}(x)^* dx \\[2em] -\dfrac{k_0^2 \varepsilon_A}{k_{T_{A_n}}^2} \sum_{q}^{N_A^{TM}} \displaystyle\int_{x_l}^{x_u} V_{A_x}^{'nq}(x) V_{A_x}^{''mp}(x)^* dx \int_{y_l}^{y_u} I_{A_y}^{'q}(y) I_{A_y}^{''p}(y)^* dy \end{array} \right]$$

$$L_{mn} = \sum_{p}^{N_A^{TE}} \left[\begin{array}{l} \displaystyle\sum_{q}^{N_B^{TE}} \dfrac{k_{z_B}^n}{\omega\mu_0} \int_{x_l}^{x_u} V_{B_x}^{''nq}(x) V_{A_x}^{''mp}(x)^* dx \int_{y_l}^{y_u} I_{B_y}^{''r}(y) I_{A_y}^{''p}(y)^* dy \\[2em] -\dfrac{k_0^2 \varepsilon_B}{k_{T_{B_n}}^2} \displaystyle\sum_{r}^{N_B^{TM}} \int_{x_l}^{x_u} V_{B_x}^{'nr}(x) V_{A_x}^{''mp}(x)^* dx \int_{y_l}^{y_u} I_{B_y}^{'r}(y) I_{A_y}^{''p}(y)^* dy \end{array} \right]$$

In addition, multiplying both sides of Equation VII.7 by

$$\frac{k_{z_A}^r {}^* \omega\mu_0}{k_{T_{A_r}}^2 {}^*} \sum_{s}^{N_A^{TM}} V_{A_x}^{'rs}(x)^* I_{A_y}^{'s}(y)^*$$

and integrating over the aperture yields

$$\mathbf{FI}_{A_z} = \mathbf{GI}_{B_z}$$

where

$$F_{mn} = \sum_{p}^{N_A^{TM}} \left[\begin{array}{l} \dfrac{k_{z_A}^m {}^* k_{z_A}^n}{k_{T_{A_m}}^2 {}^*} \displaystyle\sum_{q}^{N_A^{TE}} \int_{x_l}^{x_u} V_{A_x}^{''nq}(x) V_{A_x}^{'mp}(x)^* dx \int_{y_l}^{y_u} I_{A_y}^{''q}(y) I_{A_y}^{'p}(y)^* dy \\[2em] -\dfrac{k_{z_A}^m {}^* k_0^2 \omega\mu_0 \varepsilon_A}{k_{T_{A_m}}^2 {}^* k_{T_{A_n}}^2} \displaystyle\sum_{r}^{N_A^{TM}} \int_{x_l}^{x_u} V_{A_x}^{'nr}(x) V_{A_x}^{'mp}(x)^* dx \int_{y_l}^{y_u} I_{A_y}^{'r}(y) I_{A_y}^{'p}(y)^* dy \end{array} \right]$$

$$G_{mn} = \sum_{p}^{N_A^{TM}} \left[\begin{array}{l} \dfrac{k_{z_A}^m {}^* k_{z_B}^n}{k_{T_{A_m}}^2 {}^*} \displaystyle\sum_{q}^{N_B^{TE}} \int_{x_l}^{x_u} V_{B_x}^{''nq}(x) V_{A_x}^{'mp}(x)^* dx \int_{y_l}^{y_u} I_{B_y}^{''q}(y) I_{A_y}^{'p}(y)^* dy \\[2em] -\dfrac{k_{z_A}^m {}^* k_0^2 \omega\mu_0 \varepsilon_B}{k_{T_{A_m}}^2 {}^* k_{T_{B_n}}^2} \displaystyle\sum_{r}^{N_B^{TM}} \int_{x_l}^{x_u} V_{B_x}^{'nr}(x) V_{A_x}^{'mp}(x)^* dx \int_{y_l}^{y_u} I_{B_y}^{'r}(y) I_{A_y}^{'p}(y)^* dy \end{array} \right]$$

y-component

$$\sum_{m}^{N_z^A} I_{A_z}^m \left[\sum_{n}^{N_A^{TM}} I_{A_x}^{'mn}(x) V_{A_y}^{'n}(y) + \frac{k_{z_A}^m \omega \varepsilon_0}{k_{T A_m}^2} \sum_{p}^{N_A^{TE}} I_{A_x}^{''mp}(x) V_{A_y}^{''p}(y) \right]$$

$$= \sum_{i}^{N_z^B} I_{B_z}^i \left[\sum_{j}^{N_B^{TM}} I_{B_x}^{'ij}(x) V_{B_y}^{'j}(y) + \frac{k_{z_B}^i \omega \varepsilon_0}{k_{T B_i}^2} \sum_{k}^{N_B^{TE}} I_{A_x}^{''ik}(x) V_{A_y}^{''k}(y) \right] \quad \text{(VII.8)}$$

Both sides of Equation VII.8 were multiplied by

$$\frac{k_{z_A}^r{}^*}{\omega \varepsilon_0 \varepsilon_A} \sum_{s}^{N_A^{TM}} I_{A_x}^{'rs}(x)^* V_{A_y}^{'s}(y)^*$$

Integrating over the aperture in the x and y directions and applying orthonormality of the y-modes yields

$$\mathbf{CI}_{A_z} = \mathbf{DI}_{B_z}$$

where

$$C_{mn} = \sum_{p}^{N_A^{TM}} \left[\begin{array}{l} \dfrac{k_{z_A}^m{}^*}{\omega \varepsilon_0 \varepsilon_A} \displaystyle\int_{x_l}^{x_u} I_{A_x}^{'np}(x) I_{A_x}^{'mp}(x)^* dx \\[2ex] + \dfrac{k_{z_A}^m{}^* k_{z_A}^n}{k_{T A_n}^2 \varepsilon_A} \displaystyle\sum_{q}^{N_A^{TE}} \int_{x_l}^{x_u} I_{A_x}^{''nq}(x) I_{A_x}^{'mp}(x)^* dx \int_{y_l}^{y_u} V_{A_y}^{''q}(y) V_{A_y}^{'p}(y)^* dy \end{array} \right]$$

$$D_{mn} = \sum_{p}^{N_A^{TM}} \left[\begin{array}{l} \dfrac{k_{z_A}^m{}^*}{\omega \varepsilon_0 \varepsilon_A} \displaystyle\sum_{q}^{N_B^{TM}} \int_{x_l}^{x_u} I_{B_x}^{'nq}(x) I_{A_x}^{'mp}(x)^* dx \int_{y_l}^{y_u} V_{B_y}^{'q}(y) V_{A_y}^{'p}(y)^* dy \\[2ex] + \dfrac{k_{z_A}^m{}^* k_{z_B}^n}{k_{T B_n}^2 \varepsilon_A} \displaystyle\sum_{r}^{N_B^{TE}} \int_{x_l}^{x_u} I_{B_x}^{''nr}(x) I_{A_x}^{'mp}(x)^* dx \int_{y_l}^{y_u} V_{B_y}^{''r}(y) V_{A_y}^{'p}(y)^* dy \end{array} \right]$$

In addition, multiplying both sides of Equation VII.8 by

$$\frac{k_0^2}{k_{T A_r}^2{}^*} \sum_{s}^{N_A^{TE}} I_{A_x}^{''rs}(x)^* V_{A_y}^{''s}(y)^*$$

and integrating over the aperture yields

$$\mathbf{MV}_{B_z} = \mathbf{NV}_{A_z}$$

where

$$
M_{mn} = \sum_{p}^{N_A^{TE}} \left[\begin{array}{l} \dfrac{k_0^2}{k_{T_{A_m}}^2{}^*} \sum_{q}^{N_A^{TM}} \int_{x_l}^{x_u} I_{A_x}^{'nq}(x) I_{A_x}^{''mp}(x)^* dx \int_{y_l}^{y_u} V_{A_y}^{'q}(y) V_{A_y}^{''p}(y)^* dy \\[4ex] + \dfrac{k_0^2 k_{z_A}^n \omega \varepsilon_0}{k_{T_{A_m}}^2{}^* k_{T_{A_n}}^2} \sum_{r}^{N_A^{TE}} \int_{x_l}^{x_u} I_{A_x}^{''nr}(x) I_{A_x}^{''mp}(x)^* dx \int_{y_l}^{y_u} V_{A_y}^{''r}(y) V_{A_y}^{''p}(y)^* dy \end{array} \right]
$$

$$
N_{mn} = \sum_{p}^{N_A^{TE}} \left[\begin{array}{l} \dfrac{k_0^2}{k_{T_{A_m}}^2{}^*} \sum_{q}^{N_B^{TM}} \int_{x_l}^{x_u} I_{B_x}^{'nq}(x) I_{A_x}^{''mp}(x)^* dx \int_{y_l}^{y_u} V_{B_y}^{'q}(y) V_{A_y}^{''p}(y)^* dy \\[4ex] + \dfrac{k_0^2 k_{z_B}^n \omega \varepsilon_0}{k_{T_{A_m}}^2{}^* k_{T_{B_n}}^2} \sum_{r}^{N_B^{TE}} \int_{x_l}^{x_u} I_{B_x}^{''nr}(x) I_{A_x}^{''mp}(x)^* dx \int_{y_l}^{y_u} V_{B_y}^{''r}(y) V_{A_y}^{''p}(y)^* dy \end{array} \right]
$$

VII.2.3 Complex Power Conservation

As for TE and TM-to-y modes, using the field relations in Section 2.3.2.8, the power flow through any given section is

$$P_z^{tot} = \sum_m^{N_z^A} \sum_n^{N_z^A} V_{A_z}^m I_{A_z}^{n}{}^{*} \left[\begin{array}{l} \dfrac{k_0^2}{k_{T_n}^2} \sum_p^{N_y^{TM}} \sum_q^{N_y^{TE}} \int_{x_l}^{x_u} I_x^{"nq}(x) I_x^{'mp}(x)^* dx \int_{y_l}^{y_u} V_y^{"q}(y) V_y^{'p}(y)^* dy \\[2ex] -\dfrac{k_0^2 \varepsilon_r}{k_{T_m}^2{}^{*}} \sum_p^{N_y^{TM}} \sum_q^{N_y^{TE}} \int_{x_l}^{x_u} V_x^{"nq}(x) V_x^{'mp}(x)^* dx \int_{y_l}^{y_u} I_y^{"q}(y) I_y^{'p}(y)^* dy \\[2ex] +\dfrac{k_z^n k_z^{m*}}{k_{T_m}^2{}^{*} \varepsilon_r} \sum_p^{N_y^{TE}} \sum_q^{N_y^{TM}} \int_{x_l}^{x_u} I_x^{'nq}(x) I_x^{"mp}(x)^* dx \int_{y_l}^{y_u} V_y^{'q}(y) V_y^{"p}(y)^* dy \\[2ex] -\dfrac{k_z^n k_z^{m*}}{k_{T_n}^2} \sum_p^{N_y^{TE}} \sum_q^{N_y^{TM}} \int_{x_l}^{x_u} V_x^{'nq}(x) V_x^{"mp}(x)^* dx \int_{y_l}^{y_u} I_y^{'q}(y) I_y^{"p}(y)^* dy \\[2ex] +\dfrac{k_z^n}{\omega \varepsilon_0 \varepsilon_r} \sum_p^{N_y^{TM}} \sum_q^{N_y^{TM}} \int_{x_l}^{x_u} I_x^{'nq}(x) I_x^{'mp}(x)^* dx \int_{y_l}^{y_u} V_y^{'q}(y) V_y^{'p}(y)^* dy \\[2ex] +\dfrac{k_0^2 k_z^n \omega \mu_0 \varepsilon_r}{k_{T_n}^2 k_{T_m}^2{}^{*}} \sum_p^{N_y^{TM}} \sum_q^{N_y^{TM}} \int_{x_l}^{x_u} V_x^{'nq}(x) V_x^{'mp}(x)^* dx \int_{y_l}^{y_u} I_y^{'q}(y) I_y^{'p}(y)^* dy \\[2ex] +\dfrac{k_0^2 k_z^{m*} \omega \varepsilon_0}{k_{T_n}^2 k_{T_m}^2{}^{*}} \sum_p^{N_y^{TE}} \sum_q^{N_y^{TE}} \int_{x_l}^{x_u} I_x^{"nq}(x) I_x^{"mp}(x)^* dx \int_{y_l}^{y_u} V_y^{"q}(y) V_y^{"p}(y)^* dy \\[2ex] +\dfrac{k_z^{m*}}{\omega \mu_0} \sum_p^{N_y^{TE}} \sum_q^{N_y^{TE}} \int_{x_l}^{x_u} V_x^{"nq}(x) V_x^{"mp}(x)^* dx \int_{y_l}^{y_u} I_y^{"q}(y) I_y^{"p}(y)^* dy \end{array} \right]$$

In terms of the previously derived coupling matrices

$$P_{A_z}^{tot} = \left[I_{A_z} \right] \left[C^\dagger - F^\dagger + K^\dagger + M^\dagger \right] \left[V_{A_z} \right]$$

$$= \left[I_{B_z} \right]^\dagger \left[D^\dagger - G^\dagger + L^\dagger + N^\dagger \right] \left[V_{A_z} \right]$$

and

$$P_{B_z}^{tot} = \left[I_{B_z} \right] \left[A + H - P + S \right] \left[V_{B_z} \right]$$

$$= \left[I_{B_z} \right]^{\intercal} \left[B + J - Q + T \right] \left[V_{A_z} \right]$$

So for conservation of complex power, require

$$D^\dagger - G^\dagger + L^\dagger + N^\dagger = B + J - Q + T$$

This is true by inspection. Therefore, to ensure complex power conservation regardless of the number of z-modes used in each section, the following expressions for the current and voltage coupling will be used

$$\left[\mathbf{C_I}\right] = \left[\mathbf{C} - \mathbf{F} + \mathbf{K} + \mathbf{M}\right]^{-1} \left[\mathbf{D} - \mathbf{G} + \mathbf{L} + \mathbf{N}\right]$$

$$\left[\mathbf{C_V}\right] = \left[\mathbf{A} + \mathbf{H} - \mathbf{P} + \mathbf{S}\right]^{-1} \left[\mathbf{B} + \mathbf{J} - \mathbf{Q} + \mathbf{T}\right]$$

$$= \left[\mathbf{A} + \mathbf{H} - \mathbf{P} + \mathbf{S}\right]^{-1} \left[\mathbf{D}^{\dagger} - \mathbf{G}^{\dagger} + \mathbf{L}^{\dagger} + \mathbf{N}^{\dagger}\right]$$

APPENDIX VIII   SECTION COUPLING SUMMARY

The coupling between adjacent sections with the same choice of eigenmode (TE, TM-to-x, y, or z) has been determined using a field matching technique in Section 2.3.3.1 for TE and TM-to-y y-modes in both sections in the element, and Appendix VII for TE and TM-to-x or z y-modes in both sections in the element. The coupling expressions are formulated in such a manner as to ensure that the complex power crossing the two-dimensional discontinuity is conserved, regardless of the number of z-modes that are included. The coupling expressions for two sections A and B where the fields are expressed in terms of y-modes with arbitrary reference directions, i.e., TE, TM-to-x, y, or z, are listed in this section. The full derivations were not considered worthy of repetition and follow Section 2.3.3.1 and Appendix VII.

VIII.1   TE, TM-TO-Y MODES IN SECTION A, TE, TM-TO-Y MODES IN SECTION B

$$\left[\mathbf{C_I}\right] = \left[\mathbf{C} - \mathbf{K} + \mathbf{M}\right]^{-1}\left[\mathbf{D} - \mathbf{L} + \mathbf{N}\right]$$

$$\left[\mathbf{C_V}\right] = \left[\mathbf{A} + \mathbf{H} - \mathbf{P}\right]^{-1}\left[\mathbf{D}^\dagger - \mathbf{L}^\dagger + \mathbf{N}^\dagger\right]$$

$$A_{mn} = \sum_{p}^{N_B^{TE}}\left[\begin{array}{l}\dfrac{k_{z_B}^n \omega\mu_0}{k_{u_{p_B}}^{'2}}\displaystyle\int_{x_l}^{x_u} I_{B_x}^{'np}(x)I_{B_x}^{'mp}(x)^* dx \\[2em] + \displaystyle\sum_{q}^{N_B^{TM}}\int_{x_l}^{x_u} I_{B_x}^{''nq}(x)I_{B_x}^{'mp}(x)^* dx \int_{y_l}^{y_u} V_{B_y}^{''q}(y)V_{B_y}^{'p}(y)^* dy\end{array}\right]$$

$$H_{mn} = \sum_{p}^{N_B^{TM}}\dfrac{k_{z_B}^{m}{}^* \omega\varepsilon_0}{k_{u_{p_B}}^{''2}}\int_{x_l}^{x_u} V_{B_x}^{''np}(x)V_{B_x}^{''mp}(x)^* dx$$

$$P_{mn} = \sum_{p}^{N_B^{TE}}\sum_{q}^{N_B^{TM}}\int_{x_l}^{x_u} V_{B_x}^{''nq}(x)V_{B_x}^{'mp}(x)^* dx \int_{y_l}^{y_u}\dfrac{I_{B_y}^{''q}(y)I_{B_y}^{'p}(y)^*}{\varepsilon_B(y)}dy$$

$$D_{mn} = \sum_{p}^{N_A^{TE}}\sum_{q}^{N_B^{TE}}\dfrac{k_{z_A}^{m}{}^* \omega\mu_0}{k_{u_{p_A}}^{'2}}\int_{x_l}^{x_u} I_{B_x}^{'nq}(x)I_{A_x}^{'mp}(x)^* dx \int_{y_l}^{y_u} V_{B_y}^{'q}(y)V_{A_y}^{'p}(y)^* dy$$

$$N_{mn} = \sum_{p}^{N_A^{TM}}\sum_{q}^{N_B^{TE}}\int_{x_l}^{x_u} I_{B_x}^{'nq}(x)I_{B_x}^{''mp}(x)^* dx \int_{y_l}^{y_u} V_{B_y}^{'q}(y)V_{B_y}^{''p}(y)^* dy$$

$$L_{mn} = \sum_{p}^{N_A^{TM}}\left[\begin{array}{l}\displaystyle\sum_{q}^{N_B^{TE}}\int_{x_l}^{x_u} V_{B_x}^{'nq}(x)V_{A_x}^{''mp}(x)^* dx \int_{y_l}^{y_u}\dfrac{I_{B_y}^{'q}(y)I_{A_y}^{''p}(y)^*}{\varepsilon_A(y)}dy \\[2.5em] -\displaystyle\sum_{r}^{N_B^{TM}}\dfrac{k_{z_B}^n \omega\varepsilon_0}{k_{u_{r_B}}^{''2}}\int_{x_l}^{x_u} V_{B_x}^{''nr}(x)V_{A_x}^{''mp}(x)^* dx \int_{y_l}^{y_u}\dfrac{I_{B_y}^{''r}(y)I_{A_y}^{''p}(y)^*}{\varepsilon_A(y)}dy\end{array}\right]$$

$$C_{mn} = \sum_{p}^{N_A^{TE}} \frac{k_{z_A}^{m\,*} \omega\mu_0}{k_{u_{p_A}}^{'2}} \int_{x_l}^{x_u} I_{A_x}^{'np}(x) I_{A_x}^{'mp}(x)^* dx$$

$$K_{mn} = \sum_{p}^{N_A^{TM}} \left[\begin{array}{c} \displaystyle\sum_{q}^{N_A^{TE}} \int_{x_l}^{x_u} V_{A_x}^{'nq}(x) V_{A_x}^{''mp}(x)^* dx \int_{y_l}^{y_u} \frac{I_{A_y}^{'q}(y) I_{A_y}^{''p}(y)^*}{\varepsilon_A(y)} dy \\[4mm] \displaystyle -\frac{k_{z_A}^{n} \omega\varepsilon_0}{k_{u_{p_A}}^{''2}} \int_{x_l}^{x_u} V_{A_x}^{''np}(x) V_{A_x}^{''mp}(x)^* dx \end{array} \right]$$

$$M_{mn} = \sum_{p}^{N_A^{TM}} \sum_{q}^{N_A^{TE}} \int_{x_l}^{x_u} I_{A_x}^{'nq}(x) I_{A_x}^{''mp}(x)^* dx \int_{y_l}^{y_u} V_{A_y}^{'q}(y) V_{A_y}^{''p}(y)^* dx$$

VIII.2 TE, TM-TO-X MODES IN SECTION A, TE, TM-TO-X MODES IN SECTION B

$$[\mathbf{C_I}] = [\mathbf{C} + \mathbf{F} + \mathbf{K}]^{-1} [\mathbf{D} + \mathbf{G} + \mathbf{L}]$$

$$[\mathbf{C_V}] = [\mathbf{A} + \mathbf{H} - \mathbf{S}]^{-1} \left[\mathbf{D}^\dagger + \mathbf{G}^\dagger + \mathbf{L}^\dagger \right]$$

$$A_{mn} = \sum_{p}^{N_B^{TM}} \frac{\left[k_0^2 \varepsilon_B - k_{x_{B_{mp}}}^{'2} \right]}{k_{z_B}^{m} \omega\varepsilon_0 \varepsilon_B} \int_{x_l}^{x_u} I_{B_x}^{'np}(x) I_{B_x}^{'mp}(x)^* dx$$

$$H_{mn} = \sum_{p}^{N_B^{TE}} \left[\begin{array}{c} \dfrac{\left[k_0^2 \varepsilon_B - k_{x_{B_{mp}}}^{''2} \right]^*}{k_{z_B}^{m\,*} \omega\mu_0} \displaystyle\int_{x_l}^{x_u} V_{B_x}^{''np}(x) V_{B_x}^{''mp}(x)^* dx \\[4mm] + \displaystyle\sum_{p}^{N_B^{TM}} \dfrac{\left[k_0^2 \varepsilon_B - k_{x_{B_{mp}}}^{'2} \right]^*}{k_{z_B}^{m\,*} k_{z_B}^{n}} \int_{x_l}^{x_u} V_{B_x}^{'nq}(x) V_{B_x}^{''mp}(x)^* dx \int_{y_l}^{y_u} I_{B_y}^{'q}(y) I_{B_y}^{''p}(y)^* dy \end{array} \right]$$

$$S_{mn} = \sum_{p}^{N_B^{TE}} \sum_{q}^{N_B^{TM}} \frac{\left[k_0^2 \varepsilon_B - k_{x_{B_{nq}}}^{'2} \right]}{k_{z_B}^{n} k_{z_B}^{m\,*} \varepsilon_B} \int_{x_l}^{x_u} I_{B_x}^{'nq}(x) I_{B_x}^{''mp}(x)^* dx \int_{y_l}^{y_u} V_{B_y}^{'q}(y) V_{B_y}^{''p}(y)^* dy$$

$$D_{mn} = \sum_{p}^{N_A^{TM}} \left[\begin{array}{c} \displaystyle\sum_{q}^{N_B^{TM}} \dfrac{\left[k_0^2 \varepsilon_A - k_{x_{A_{mp}}}^{\circledcirc\,*} \right]}{k_{z_A}^{m\,*} \omega\varepsilon_0 \varepsilon_A} \int_{x_l}^{x_u} I_{B_x}^{\circledcirc q}(x) I_{A_x}^{\circledcirc p}(x)^* dx \int_{y_l}^{y_u} V_{B_y}^{\circledcirc}(y) V_{A_y}^{\circledcirc}(y)^* dy \\[4mm] - \displaystyle\sum_{r}^{N_B^{TE}} \dfrac{\left[k_0^2 \varepsilon_A - k_{x_{A_{mp}}}^{\circledcirc} \right]^*}{k_{z_A}^{m\,*} k_{z_B}^{n} \varepsilon_A} \int_{x_l}^{x_u} I_{B_x}^{''nr}(x) I_{A_x}^{\circledcirc p}(x)^* dx \int_{y_l}^{y_u} V_{B_y}^{''r}(y) V_{A_y}^{\circledcirc}(y)^* dy \end{array} \right]$$

$$G_{mn} = \sum_p^{N_A^{TM}} \sum_q^{N_B^{TE}} \frac{\left[k_0^2 \varepsilon_B - k_{x_{B_{nq}}}^{"2} \right]}{k_{z_B}^n k_{z_A}^{m\,*}} \int_{x_l}^{x_u} V_{B_x}^{"nq}(x) V_{A_x}^{'mp}(x)^* dx \int_{y_l}^{y_u} I_{B_y}^{"q}(y) I_{A_y}^{'p}(y)^* dy$$

$$L_{mn} = \sum_p^{N_A^{TE}} \sum_q^{N_B^{TE}} \frac{\left[k_0^2 \varepsilon_B - k_{x_{B_{nq}}}^{"2} \right]}{k_{z_B}^n \omega \mu_0} \int_{x_l}^{x_u} V_{B_x}^{"nq}(x) V_{A_x}^{"mp}(x)^* dx \int_{y_l}^{y_u} I_{B_y}^{"q}(y) I_{A_y}^{"p}(y)^* dy$$

$$C_{mn} = \sum_p^{N_A^{TM}} \left[\begin{array}{c} \dfrac{\left[k_0^2 \varepsilon_A - k_{x_{A_{mp}}}^{'2}{}^* \right]}{k_{z_A}^{m\,*} \omega \varepsilon_0 \varepsilon_A} \displaystyle\int_{x_l}^{x_u} I_{A_x}^{'nq}(x) I_{A_x}^{'mp}(x)^* dx \\[4mm] - \displaystyle\sum_q^{N_A^{TE}} \dfrac{[k_0^2 \varepsilon_A - k_{x_{A_{mp}}}^{'2}]^*}{k_{z_A}^{m\,*} k_{z_A}^n \varepsilon_A} \displaystyle\int_{x_l}^{x_u} I_{A_x}^{"nr}(x) I_{A_x}^{'mp}(x)^* dx \int_{y_l}^{y_u} V_{A_y}^{"q}(y) V_{A_y}^{'p}(y)^* dy \end{array} \right]$$

$$F_{mn} = \sum_p^{N_A^{TM}} \sum_q^{N_A^{TE}} \frac{\left[k_0^2 \varepsilon_A - k_{x_{A_{nq}}}^{"2} \right]}{k_{z_A}^n k_{z_A}^{m\,*}} \int_{x_l}^{x_u} V_{A_x}^{"nq}(x) V_{A_x}^{'mp}(x)^* dx \int_{y_l}^{y_u} I_{A_y}^{"q}(y) I_{A_y}^{'p}(y)^* dy$$

$$K_{mn} = \sum_p^{N_A^{TE}} \frac{\left[k_0^2 \varepsilon_A - k_{x_{A_{np}}}^{"2} \right]}{k_{z_A}^n \omega \mu_0} \int_{x_l}^{x_u} V_{A_x}^{"np}(x) V_{A_x}^{"mp}(x)^* dx$$

VIII.3   TE, TM-TO-Z MODES IN SECTION A, TE, TM-TO-Z MODES IN SECTION B

$$\left[\mathbf{C_I} \right] = \left[\mathbf{C} - \mathbf{F} + \mathbf{K} + \mathbf{M} \right]^{-1} \left[\mathbf{D} - \mathbf{G} + \mathbf{L} + \mathbf{N} \right]$$

$$\left[\mathbf{C_V} \right] = \left[\mathbf{A} + \mathbf{H} - \mathbf{P} + \mathbf{S} \right]^{-1} \left[\mathbf{D}^\dagger - \mathbf{G}^\dagger + \mathbf{L}^\dagger + \mathbf{N}^\dagger \right]$$

$$A_{mn} = \sum_p^{N_B^{TM}} \left[\begin{array}{c} \dfrac{k_{z_B}^n}{\omega \varepsilon_0 \varepsilon_B} \displaystyle\int_{x_l}^{x_u} I_{B_x}^{'np}(x) I_{B_x}^{'mp}(x)^* dx \\[4mm] + \dfrac{k_0^2}{k_{T_{B_n}}^2} \displaystyle\sum_q^{N_B^{TE}} \int_{x_l}^{x_u} I_{B_x}^{"nq}(x) I_{B_x}^{'mp}(x)^* dx \int_{y_l}^{y_u} V_{B_y}^{"q}(y) V_{B_y}^{'p}(y)^* dy \end{array} \right]$$

$$H_{mn} = \sum_p^{N_B^{TE}} \left[\begin{array}{c} \dfrac{k_{z_B}^{m\,*}}{\omega \mu_0} \displaystyle\int_{x_l}^{x_u} V_{B_x}^{"np}(x) V_{B_x}^{"mp}(x)^* dx \\[4mm] - \dfrac{k_{z_B}^{m\,*} k_{z_B}^n}{k_{T_{B_n}}^2} \displaystyle\sum_p^{N_B^{TM}} \int_{x_l}^{x_u} V_{B_x}^{'nq}(x) V_{B_x}^{"mp}(x)^* dx \int_{y_l}^{y_u} I_{B_y}^{'q}(y) I_{B_y}^{"p}(y)^* dy \end{array} \right]$$

$$P_{mn} = \sum_{p}^{N_B^{TM}} \left[\begin{array}{l} \dfrac{k_0^2 \varepsilon_B}{k_{T_{B_m}}^{2*}} \displaystyle\sum_{q}^{N_B^{TE}} \int_{x_l}^{x_u} V_{B_x}^{''nq}(x) V_{B_x}^{'mp}(x)^* dx \int_{y_l}^{y_u} I_{B_y}^{''q}(y) I_{B_y}^{'p}(y)^* dy \\[2em] - \displaystyle\sum_{r}^{N_B^{TM}} \dfrac{k_0^2 k_{z_B}^n \omega \mu_0 \varepsilon_B}{k_{T_{B_m}}^{2*} k_{T_{B_n}}^2} \int_{x_l}^{x_u} V_{B_x}^{'nr}(x) V_{B_x}^{'mp}(x)^* dx \int_{y_l}^{y_u} I_{B_y}^{'r}(y) I_{B_y}^{'p}(y)^* dy \end{array} \right]$$

$$S_{mn} = \sum_{p}^{N_B^{TE}} \left[\begin{array}{l} \dfrac{k_{z_B}^n k_{z_B}^{m*}}{k_{T_{B_m}}^{2*} \varepsilon_B} \displaystyle\sum_{q}^{N_B^{TM}} \int_{x_l}^{x_u} I_{B_x}^{'nq}(x) I_{B_x}^{''mp}(x)^* dx \int_{y_l}^{y_u} V_{B_y}^{'q}(y) V_{B_y}^{''p}(y)^* dy \\[2em] + \dfrac{k_0^2 k_{z_B}^{m*} \omega \varepsilon_0}{k_{T_{B_m}}^{2*} k_{T_{B_n}}^2} \displaystyle\sum_{r}^{N_B^{TE}} \int_{x_l}^{x_u} I_{B_x}^{''nr}(x) I_{B_x}^{''mp}(x)^* dx \int_{y_l}^{y_u} V_{B_y}^{''r}(y) V_{B_y}^{''p}(y)^* dy \end{array} \right]$$

$$D_{mn} = \sum_{p}^{N_A^{TM}} \left[\begin{array}{l} \dfrac{k_{z_A}^{m*}}{\omega \varepsilon_0 \varepsilon_A} \displaystyle\sum_{q}^{N_B^{TM}} \int_{x_l}^{x_u} I_{B_x}^{'nq}(x) I_{A_x}^{'mp}(x)^* dx \int_{y_l}^{y_u} V_{B_y}^{'q}(y) V_{A_y}^{'p}(y)^* dy \\[2em] + \dfrac{k_{z_A}^{m*} k_{z_B}^n}{k_{T_{B_n}}^2 \varepsilon_A} \displaystyle\sum_{r}^{N_B^{TE}} \int_{x_l}^{x_u} I_{B_x}^{''nr}(x) I_{A_x}^{'mp}(x)^* dx \int_{y_l}^{y_u} V_{B_y}^{''r}(y) V_{A_y}^{'p}(y)^* dy \end{array} \right]$$

$$G_{mn} = \sum_{p}^{N_A^{TM}} \left[\begin{array}{l} \dfrac{k_{z_A}^{m*} k_{z_B}^n}{k_{T_{A_m}}^{2*}} \displaystyle\sum_{q}^{N_B^{TE}} \int_{x_l}^{x_u} V_{B_x}^{''nq}(x) V_{A_x}^{'mp}(x)^* dx \int_{y_l}^{y_u} I_{B_y}^{''q}(y) I_{A_y}^{'p}(y)^* dy \\[2em] - \dfrac{k_{z_A}^{m*} k_0^2 \omega \mu_0 \varepsilon_B}{k_{T_{A_m}}^{2*} k_{T_{B_n}}^2} \displaystyle\sum_{r}^{N_B^{TM}} \int_{x_l}^{x_u} V_{B_x}^{'nr}(x) V_{A_x}^{'mp}(x)^* dx \int_{y_l}^{y_u} I_{B_y}^{'r}(y) I_{A_y}^{'p}(y)^* dy \end{array} \right]$$

$$L_{mn} = \sum_{p}^{N_A^{TE}} \left[\begin{array}{l} \dfrac{k_{z_B}^n}{\omega \mu_0} \displaystyle\sum_{q}^{N_B^{TE}} \int_{x_l}^{x_u} V_{B_x}^{''nq}(x) V_{A_x}^{''mp}(x)^* dx \int_{y_l}^{y_u} I_{B_y}^{''q}(y) I_{A_y}^{''p}(y)^* dy \\[2em] - \dfrac{k_0^2 \varepsilon_B}{k_{T_{B_n}}^2} \displaystyle\sum_{r}^{N_B^{TM}} \int_{x_l}^{x_u} V_{B_x}^{'nr}(x) V_{A_x}^{''mp}(x)^* dx \int_{y_l}^{y_u} I_{B_y}^{'r}(y) I_{A_y}^{''p}(y)^* dy \end{array} \right]$$

$$N_{mn} = \sum_{p}^{N_A^{TE}} \left[\begin{array}{l} \dfrac{k_0^2}{k_{T_{A_m}}^{2*}} \displaystyle\sum_{q}^{N_B^{TM}} \int_{x_l}^{x_u} I_{B_x}^{'nq}(x) I_{A_x}^{''mp}(x)^* dx \int_{y_l}^{y_u} V_{B_y}^{'q}(y) V_{A_y}^{''p}(y)^* dy \\[2em] + \dfrac{k_0^2 k_{z_B}^n \omega \varepsilon_0}{k_{T_{A_m}}^{2*} k_{T_{B_n}}^2} \displaystyle\sum_{r}^{N_B^{TE}} \int_{x_l}^{x_u} I_{B_x}^{''nr}(x) I_{A_x}^{''mp}(x)^* dx \int_{y_l}^{y_u} V_{B_y}^{''r}(y) V_{A_y}^{''p}(y)^* dy \end{array} \right]$$

$$C_{mn} = \sum_{p}^{N_A^{TM}} \left[\begin{array}{l} \dfrac{k_{z_A}^{m\,*}}{\omega \varepsilon_0 \varepsilon_A} \int_{x_l}^{x_u} I_{A_x}^{'np}(x) I_{A_x}^{'mp}(x)^* dx \\[2em] + \dfrac{k_{z_A}^{m\,*} k_{z_A}^{n}}{k_{T_{A_n}}^2 \varepsilon_A} \sum_{q}^{N_A^{TE}} \int_{x_l}^{x_u} I_{A_x}^{''nq}(x) I_{A_x}^{'mp}(x)^* dx \int_{y_l}^{y_u} V_{A_y}^{''q}(y) V_{A_y}^{'p}(y)^* dy \end{array} \right]$$

$$F_{mn} = \sum_{p}^{N_A^{TM}} \left[\begin{array}{l} \dfrac{k_{z_A}^{m\,*} k_{z_A}^{n}}{k_{T_{A_m}}^{2\,*}} \sum_{q}^{N_A^{TE}} \int_{x_l}^{x_u} V_{A_x}^{''nq}(x) V_{A_x}^{'mp}(x)^* dx \int_{y_l}^{y_u} I_{A_y}^{''q}(y) I_{A_y}^{'p}(y)^* dy \\[2em] - \dfrac{k_{z_A}^{m\,*} k_0^2 \omega \mu_0 \varepsilon_A}{k_{T_{A_m}}^{2\,*} k_{T_{A_n}}^2} \sum_{r}^{N_A^{TM}} \int_{x_l}^{x_u} V_{A_x}^{'nr}(x) V_{A_x}^{'mp}(x)^* dx \int_{y_l}^{y_u} I_{A_y}^{'r}(y) I_{A_y}^{'p}(y)^* dy \end{array} \right]$$

$$K_{mn} = \sum_{p}^{N_A^{TE}} \left[\begin{array}{l} \dfrac{k_{z_A}^{n}}{\omega \mu_0} \int_{x_l}^{x_u} V_{A_x}^{''np}(x) V_{A_x}^{''mp}(x)^* dx \\[2em] - \dfrac{k_0^2 \varepsilon_A}{k_{T_{A_n}}^2} \sum_{q}^{N_A^{TM}} \int_{x_l}^{x_u} V_{A_x}^{'nq}(x) V_{A_x}^{''mp}(x)^* dx \int_{y_l}^{y_u} I_{A_y}^{'q}(y) I_{A_y}^{''p}(y)^* dy \end{array} \right]$$

$$M_{mn} = \sum_{p}^{N_A^{TE}} \left[\begin{array}{l} \dfrac{k_0^2}{k_{T_{A_m}}^{2\,*}} \sum_{q}^{N_A^{TM}} \int_{x_l}^{x_u} I_{A_x}^{'nq}(x) I_{A_x}^{''mp}(x)^* dx \int_{y_l}^{y_u} V_{A_y}^{'q}(y) V_{A_y}^{''p}(y)^* dy \\[2em] + \dfrac{k_0^2 k_{z_A}^{n} \omega \varepsilon_0}{k_{T_{A_m}}^{2\,*} k_{T_{A_n}}^2} \sum_{r}^{N_A^{TE}} \int_{x_l}^{x_u} I_{A_x}^{''nr}(x) I_{A_x}^{''mp}(x)^* dx \int_{y_l}^{y_u} V_{A_y}^{''r}(y) V_{A_y}^{''p}(y)^* dy \end{array} \right]$$

VIII.4 TE, TM-TO-Y MODES IN SECTION A, TE, TM-TO-X MODES IN SECTION B

$$[C_I] = [C + M - K]^{-1} [D - L + N]$$

$$[C_V] = [A + H - S]^{-1} \left[D^\dagger - L^\dagger + N^\dagger \right]$$

$$A_{mn} = \sum_{p}^{N_B^{TM}} \frac{\left[k_0^2 \varepsilon_B - k_{x_{B_{mp}}}^{'2} \right]}{k_{z_B}^{m} \omega \varepsilon_0 \varepsilon_B} \int_{x_l}^{x_u} I_{B_x}^{'np}(x) I_{B_x}^{'mp}(x)^* dx$$

$$H_{mn} = \sum_p^{N_B^{TE}} \left[\frac{\left[k_0^2 \varepsilon_B - k_{x B_{mp}}^{"2} \right]^*}{k_{z_B}^{m\,*} \omega\mu_0} \int_{x_l}^{x_u} V_{B_x}^{"np}(x) V_{B_x}^{"mp}(x)^* dx \right.$$
$$\left. + \sum_q^{N_B^{TM}} \frac{\left[k_0^2 \varepsilon_B - k_{x B_{mp}}^{'2} \right]^*}{k_{z_B}^{m\,*} k_{z_B}^n} \int_{x_l}^{x_u} V_{B_x}^{'nq}(x) V_{B_x}^{"mp}(x)^* dx \int_{y_l}^{y_u} I_{B_y}^{'q}(y) I_{B_y}^{"p}(y)^* dy \right]$$

$$S_{mn} = \sum_p^{N_B^{TE}} \sum_q^{N_B^{TM}} \frac{\left[k_0^2 \varepsilon_B - k_{x B_{nq}}^{'2} \right]}{k_{z_B}^n k_{z_B}^{m\,*} \varepsilon_B} \int_{x_l}^{x_u} I_{B_x}^{'nq}(x) I_{B_x}^{"mp}(x)^* dx \int_{y_l}^{y_u} V_{B_y}^{'q}(y) V_{B_y}^{"p}(y)^* dy$$

$$D_{mn} = \sum_p^{N_A^{TE}} \left[-\sum_q^{N_B^{TE}} \frac{k_0^2 k_{z_A}^{m\,*}}{k_{z_B}^n k_{u_{p_A}}^{'2}} \int_{x_l}^{x_u} I_{B_x}^{"nq}(x) I_{A_x}^{"mp}(x)^* dx \int_{y_l}^{y_u} V_{B_y}^{"q}(y) V_{A_y}^{'p}(y)^* dy \right.$$
$$\left. + \sum_r^{N_B^{TM}} \frac{k_{z_A}^{m\,*} \omega\mu_0}{k_{u_{p_A}}^{'2}} \int_{x_l}^{x_u} I_{B_x}^{'nr}(x) I_{A_x}^{'mp}(x)^* dx \int_{y_l}^{y_u} V_{B_y}^{'r}(y) V_{A_y}^{'p}(y)^* dy \right]$$

$$L_{mn} = -\sum_p^{N_A^{TM}} \sum_q^{N_B^{TE}} \frac{\left[k_0^2 \varepsilon_B - k_{x B_{nq}}^{"2} \right]}{k_{z_B}^n \omega\mu_0} \int_{x_l}^{x_u} V_{B_x}^{"nq}(x) V_{A_x}^{"mp}(x)^* dx \int_{y_l}^{y_u} \frac{I_{B_y}^{"q}(y) I_{A_y}^{"p}(y)^*}{\varepsilon_A(y)} dy$$

$$N_{mn} = \sum_p^{N_A^{TM}} \left[-\sum_q^{N_B^{TE}} \frac{\omega\varepsilon_0}{k_{z_B}^n} \int_{x_l}^{x_u} I_{B_x}^{"nq}(x) I_{A_x}^{"mp}(x)^* dx \int_{y_l}^{y_u} V_{B_y}^{"q}(y) V_{A_y}^{"p}(y)^* dy \right.$$
$$\left. + \sum_r^{N_B^{TM}} \int_{x_l}^{x_u} I_{B_x}^{'nr}(x) I_{A_x}^{"mp}(x)^* dx \int_{y_l}^{y_u} V_{B_y}^{'r}(y) V_{A_y}^{"p}(y)^* dy \right]$$

$$C_{mn} = \sum_p^{N_A^{TE}} \frac{k_{z_A}^{m\,*} \omega\mu_0}{k_{u_{p_A}}^{'2}} \int_{x_l}^{x_u} I_{A_x}^{'np}(x) I_{A_x}^{'mp}(x)^* dx$$

$$K_{mn} = \sum_p^{N_A^{TM}} \left[\sum_q^{N_A^{TE}} \int_{x_l}^{x_u} V_{A_x}^{'nq}(x) V_{A_x}^{"mp}(x)^* dx \int_{y_l}^{y_u} \frac{I_{A_y}^{'q}(y) I_{A_y}^{"p}(y)^*}{\varepsilon_A(y)} dy \right.$$
$$\left. - \frac{k_{z_A}^{n\,*} \omega\varepsilon_0}{k_{u_{p_A}}^{"2}} \int_{x_l}^{x_u} V_{A_x}^{"np}(x) V_{A_x}^{"mp}(x)^* dx \right]$$

$$M_{mn} = \sum_{p}^{N_A^{TM}} \sum_{q}^{N_A^{TE}} \int_{x_l}^{x_u} I_{A_x}^{'nq}(x) I_{A_x}^{''mp}(x)^* dx \int_{y_l}^{y_u} V_{A_y}^{'q}(y) V_{A_y}^{''p}(y)^* dx$$

VIII.5 TE, TM-TO-X MODES IN SECTION A, TE, TM-TO-Y MODES IN SECTION B

$$[C_I] = [C + F + K]^{-1}[D + G + L]$$

$$[C_V] = [A + H - P]^{-1}[D^{\leq} + G^{\leq} + L^{\leq}]$$

$$A_{mn} = \sum_{p}^{N_B^{TE}} \left[\frac{k_{z_B}^n \omega \mu_0}{k_{u_{p_B}}^{'2}} \int_{x_l}^{x_u} I_{B_x}^{'np}(x) I_{B_x}^{'mp}(x)^* dx \right.$$
$$\left. + \sum_{q}^{N_B^{TM}} \int_{x_l}^{x_u} I_{B_x}^{''nq}(x) I_{B_x}^{'mp}(x)^* dx \int_{y_l}^{y_u} V_{B_y}^{''q}(y) V_{B_y}^{'p}(y)^* dy \right]$$

$$H_{mn} = \sum_{p}^{N_B^{TM}} \frac{k_{z_B}^{m}{}^* \omega \varepsilon_0}{k_{u_{p_B}}^{''2}} \int_{x_l}^{x_u} V_{B_x}^{''np}(x) V_{B_x}^{''mp}(x)^* dx$$

$$P_{mn} = \sum_{p}^{N_B^{TE}} \sum_{q}^{N_B^{TM}} \int_{x_l}^{x_u} V_{B_x}^{''nq}(x) V_{B_x}^{'mp}(x)^* dx \int_{y_l}^{y_u} \frac{I_{B_y}^{''q}(y) I_{B_y}^{'p}(y)^*}{\varepsilon_B(y)} dy$$

$$D_{mn} = \sum_{p}^{N_A^{TM}} \sum_{q}^{N_B^{TE}} \frac{\left[k_0^2 \varepsilon_A - k_{x_{A_{mp}}}^{'2}{}^* \right]}{k_{z_A}^{m}{}^* \omega \varepsilon_0 \varepsilon_A} \int_{x_l}^{x_u} I_{B_x}^{'nq}(x) I_{A_x}^{'mp}(x)^* dx \int_{y_l}^{y_u} V_{B_y}^{'q}(y) V_{A_y}^{'p}(y)^* dy$$

$$G_{mn} = \sum_{p}^{N_A^{TM}} \left[- \sum_{q}^{N_B^{TE}} \frac{\omega \mu_0}{k_{z_A}^{m}{}^*} \int_{x_l}^{x_u} V_{B_x}^{'nq}(x) V_{A_x}^{'mp}(x)^* dx \int_{y_l}^{y_u} I_{B_y}^{'q}(y) I_{A_y}^{'p}(y)^* dy \right.$$
$$\left. + \sum_{r}^{N_B^{TM}} \frac{k_0^2 k_{z_B}^n}{k_{u_{r_B}}^{''2} k_{z_A}^{m}{}^*} \int_{x_l}^{x_u} V_{B_x}^{''nr}(x) V_{A_x}^{'mp}(x)^* dx \int_{y_l}^{y_u} I_{B_y}^{''r}(y) I_{A_y}^{'p}(y)^* dy \right]$$

$$L_{mn} = \sum_{p}^{N_A^{TE}} \left[- \sum_{q}^{N_B^{TE}} \int_{x_l}^{x_u} V_{B_x}^{'nq}(x) V_{A_x}^{''mp}(x)^* dx \int_{y_l}^{y_u} I_{B_y}^{'q}(y) I_{A_y}^{''p}(y)^* dy \right.$$
$$\left. + \sum_{r}^{N_B^{TM}} \frac{k_{z_B}^n \omega \varepsilon_0}{k_{u_{r_B}}^{''2}} \int_{x_l}^{x_u} V_{B_x}^{''nr}(x) V_{A_x}^{''mp}(x)^* dx \int_{y_l}^{y_u} I_{B_y}^{''r}(y) I_{A_y}^{''p}(y)^* dy \right]$$

$$C_{mn} = \sum_{p}^{N_A^{TM}} \left[\frac{\left[k_0^2 \varepsilon_A - k_{x_{A_{mp}}}^{'2} \right]^*}{k_{z_A}^{m^*} \omega \varepsilon_0 \varepsilon_A} \int_{x_l}^{x_u} I_{A_x}^{'np}(x) I_{A_x}^{'mp}(x)^* dx \right.$$
$$\left. - \sum_{q}^{N_A^{TE}} \frac{\left[k_0^2 \varepsilon_A - k_{x_{A_{mp}}}^{'2} \right]^*}{k_{z_A}^{m^*} k_{z_A}^{n} \varepsilon_A} \int_{x_l}^{x_u} I_{A_x}^{''nq}(x) I_{A_x}^{'mp}(x)^* dx \int_{y_l}^{y_u} V_{A_y}^{''q}(y) V_{A_y}^{'p}(y)^* dy \right]$$

$$F_{mn} = \sum_{p}^{N_A^{TM}} \sum_{q}^{N_A^{TE}} \frac{\left[k_0^2 \varepsilon_A - k_{x_{A_{nq}}}^{''2} \right]}{k_{z_A}^{n} k_{z_A}^{m^*}} \int_{x_l}^{x_u} V_{A_x}^{''nq}(x) V_{A_x}^{'mp}(x)^* dx \int_{y_l}^{y_u} I_{A_y}^{''q}(y) I_{A_y}^{'p}(y)^* dy$$

$$K_{mn} = \sum_{p}^{N_A^{TE}} \frac{\left[k_0^2 \varepsilon_A - k_{x_{A_{np}}}^{''2} \right]}{k_{z_A}^{n} \omega \mu_0} \int_{x_l}^{x_u} V_{A_x}^{''np}(x) V_{A_x}^{''mp}(x)^* dx$$

VIII.6   TE, TM-TO-X MODES IN SECTION A, TE, TM-TO-Z MODES IN SECTION B

$$[C_I] = [C + F + K]^{-1}[D + G + L]$$

$$[C_V] = [A + H - P + S]^{-1} \left[D^\dagger + G^\dagger + L^\dagger \right]$$

$$A_{mn} = \sum_{p}^{N_B^{TM}} \left[\frac{k_{z_B}^{n}}{\omega \varepsilon_0 \varepsilon_B} \int_{x_l}^{x_u} I_{B_x}^{'np}(x) I_{B_x}^{'mp}(x)^* dx \right.$$
$$\left. + \frac{k_0^2}{k_{T_{B_n}}^2} \sum_{q}^{N_B^{TE}} \int_{x_l}^{x_u} I_{B_x}^{''nq}(x) I_{B_x}^{'mp}(x)^* dx \int_{y_l}^{y_u} V_{B_y}^{''q}(y) V_{B_y}^{'p}(y)^* dy \right]$$

$$H_{mn} = \sum_{p}^{N_B^{TE}} \left[\frac{k_{z_B}^{m^*}}{\omega \mu_0} \int_{x_l}^{x_u} V_{B_x}^{''np}(x) V_{B_x}^{''mp}(x)^* dx \right.$$
$$\left. - \frac{k_{z_B}^{m^*} k_{z_B}^{n}}{k_{T_{B_n}}^2} \sum_{p}^{N_B^{TM}} \int_{x_l}^{x_u} V_{B_x}^{'nq}(x) V_{B_x}^{''mp}(x)^* dx \int_{y_l}^{y_u} I_{B_y}^{'q}(y) I_{B_y}^{''p}(y)^* dy \right]$$

$$P_{mn} = \sum_{p}^{N_B^{TM}} \left[\frac{k_0^2 \varepsilon_B}{k_{T_{B_m}}^{2^*}} \sum_{q}^{N_B^{TE}} \int_{x_l}^{x_u} V_{B_x}^{''nq}(x) V_{B_x}^{'mp}(x)^* dx \int_{y_l}^{y_u} I_{B_y}^{''q}(y) I_{B_y}^{'p}(y)^* dy \right.$$
$$\left. - \sum_{r}^{N_B^{TM}} \frac{k_0^2 k_{z_B}^{n} \omega \mu_0 \varepsilon_B}{k_{T_{B_m}}^{2^*} k_{T_{B_n}}^{2}} \int_{x_l}^{x_u} V_{B_x}^{'nr}(x) V_{B_x}^{'mp}(x)^* dx \int_{y_l}^{y_u} I_{B_y}^{'r}(y) I_{B_y}^{'p}(y)^* dy \right]$$

$$S_{mn} = \sum_{p}^{N_B^{TE}} \left[\begin{array}{l} \dfrac{k_{z_B}^n k_{z_B}^{m\,*}}{k_{T_{B_m}}^{2\,*} \varepsilon_B} \sum_{q}^{N_B^{TM}} \int_{x_l}^{x_u} I_{B_x}^{'nq}(x) I_{B_x}^{''mp}(x)^* dx \int_{y_l}^{y_u} V_{B_y}^{'q}(y) V_{B_y}^{''p}(y)^* dy \\[2em] + \dfrac{k_0^2 k_{z_B}^{m\,*} \omega \varepsilon_0}{k_{T_{B_m}}^{2\,*} k_{T_{B_n}}^{2}} \sum_{r}^{N_B^{TE}} \int_{x_l}^{x_u} I_{B_x}^{''nr}(x) I_{B_x}^{''mp}(x)^* dx \int_{y_l}^{y_u} V_{B_y}^{''r}(y) V_{B_y}^{''p}(y)^* dy \end{array} \right]$$

$$D_{mn} = \sum_{p}^{N_A^{TM}} \left[\begin{array}{l} \sum_{q}^{N_B^{TM}} \dfrac{k_0^2 \varepsilon_A - k_{x_{A_{mp}}}^{'2\,*}}{k_{z_A}^{m\,*} \omega \varepsilon_0 \varepsilon_A} \int_{x_l}^{x_u} I_{B_x}^{'nq}(x) I_{A_x}^{'mp}(x)^* dx \int_{y_l}^{y_u} V_{B_y}^{'q}(y) V_{A_y}^{'p}(y)^* dy \\[2em] + \sum_{r}^{N_B^{TE}} \dfrac{\left[k_0^2 \varepsilon_A - k_{x_{A_{mp}}}^{''2\,*} \right] k_{z_B}^n}{k_{z_A}^{m\,*} k_{T_{B_n}}^2 \varepsilon_A} \int_{x_l}^{x_u} I_{B_x}^{''nr}(x) I_{A_x}^{'mp}(x)^* dx \int_{y_l}^{y_u} V_{B_y}^{''r}(y) V_{A_y}^{'p}(y)^* dy \end{array} \right]$$

$$G_{mn} = \sum_{p}^{N_A^{TM}} \left[\begin{array}{l} - \sum_{q}^{N_B^{TM}} \dfrac{k_0^2 \varepsilon_B \omega \mu_0}{k_{T_{B_n}}^2 k_{z_A}^{m\,*}} \int_{x_l}^{x_u} V_{B_x}^{'nq}(x) V_{A_x}^{'mp}(x)^* dx \int_{y_l}^{y_u} I_{B_y}^{'q}(y) I_{A_y}^{'p}(y)^* dy \\[2em] + \sum_{r}^{N_B^{TE}} \dfrac{k_{z_B}^n}{k_{z_A}^{m\,*}} \int_{x_l}^{x_u} V_{B_x}^{''nr}(x) V_{A_x}^{'mp}(x)^* dx \int_{y_l}^{y_u} I_{B_y}^{''r}(y) I_{A_y}^{'p}(y)^* dy \end{array} \right]$$

$$L_{mn} = \sum_{p}^{N_A^{TE}} \left[\begin{array}{l} - \sum_{q}^{N_B^{TM}} \dfrac{k_0^2 \varepsilon_B}{k_{T_{B_n}}^2} \int_{x_l}^{x_u} V_{B_x}^{'nq}(x) V_{A_x}^{''mp}(x)^* dx \int_{y_l}^{y_u} I_{B_y}^{'q}(y) I_{A_y}^{''p}(y)^* dy \\[2em] + \sum_{r}^{N_B^{TE}} \dfrac{k_{z_B}^n}{\omega \mu_0} \int_{x_l}^{x_u} V_{B_x}^{''nr}(x) V_{A_x}^{''mp}(x)^* dx \int_{y_l}^{y_u} I_{B_y}^{''r}(y) I_{A_y}^{''p}(y)^* dy \end{array} \right]$$

$$C_{mn} = \sum_{p}^{N_A^{TM}} \left[\begin{array}{l} \dfrac{\left[k_0^2 \varepsilon_A - k_{x_{A_{mp}}}^{'2\,*} \right]}{k_{z_A}^{m\,*} \omega \varepsilon_0 \varepsilon_A} \int_{x_l}^{x_u} I_{A_x}^{'np}(x) I_{A_x}^{'mp}(x)^* dx \\[2em] - \sum_{q}^{N_A^{TE}} \dfrac{\left[k_0^2 \varepsilon_A - k_{x_{A_{mp}}}^{'2\,*} \right]}{k_{z_A}^{m\,*} k_{z_A}^n \varepsilon_A} \int_{x_l}^{x_u} I_{A_x}^{''nq}(x) I_{A_x}^{'mp}(x)^* dx \int_{y_l}^{y_u} V_{A_y}^{''q}(y) V_{A_y}^{'p}(y)^* dy \end{array} \right]$$

$$F_{mn} = \sum_{p}^{N_A^{TM}} \sum_{q}^{N_A^{TE}} \dfrac{\left[k_0^2 \varepsilon_A - k_{x_{A_{nq}}}^{''2} \right]}{k_{z_A}^n k_{z_A}^{m\,*}} \int_{x_l}^{x_u} V_{A_x}^{''nq}(x) V_{A_x}^{'mp}(x)^* dx \int_{y_l}^{y_u} I_{A_y}^{''q}(y) I_{A_y}^{'p}(y)^* dy$$

$$K_{mn} = \sum_p^{N_A^{TE}} \frac{\left[k_0^2 \varepsilon_A - k_{x_{A_{np}}}^{"2}\right]}{k_{z_A}^n \omega \mu_0} \int_{x_l}^{x_u} V_{A_x}^{"np}(x) V_{A_x}^{"mp}(x)^* dx$$

VIII.7   TE, TM-TO-Z MODES IN SECTION A, TE, TM-TO-X MODES IN SECTION B

$$[\mathbf{C_I}] = [\mathbf{C} - \mathbf{F} + \mathbf{K} + \mathbf{M}]^{-1}[\mathbf{D} - \mathbf{G} + \mathbf{L} + \mathbf{N}]$$

$$[\mathbf{C_V}] = [\mathbf{A} + \mathbf{H} - \mathbf{S}]^{-1}\left[\mathbf{D}^\dagger - \mathbf{G}^\dagger + \mathbf{L}^\dagger + \mathbf{N}^\dagger\right]$$

$$A_{mn} = \sum_p^{N_B^{TM}} \frac{\left[k_0^2 \varepsilon_B - k_{x_{B_{mp}}}^{'2}\right]}{k_{z_B}^m \omega \varepsilon_0 \varepsilon_B} \int_{x_l}^{x_u} I_{B_x}^{'np}(x) I_{B_x}^{'mp}(x)^* dx$$

$$H_{mn} = \sum_p^{N_B^{TE}} \left[\frac{\left[k_0^2 \varepsilon_B - k_{x_{B_{mp}}}^{"2}\right]^*}{k_{z_B}^{m*} \omega \mu_0} \int_{x_l}^{x_u} V_{B_x}^{"np}(x) V_{B_x}^{"mp}(x)^* dx \right.$$
$$\left. + \sum_p^{N_B^{TM}} \frac{\left[k_0^2 \varepsilon_B - k_{x_{B_{mp}}}^{'2}\right]^*}{k_{z_B}^{m*} k_{z_B}^n} \int_{x_l}^{x_u} V_{B_x}^{'nq}(x) V_{B_x}^{"mp}(x)^* dx \int_{y_l}^{y_u} I_{B_y}^{'q}(y) I_{B_y}^{"p}(y)^* dy \right]$$

$$S_{mn} = \sum_p^{N_B^{TE}} \sum_q^{N_B^{TM}} \frac{\left[k_0^2 \varepsilon_B - k_{x_{B_{nq}}}^{'2}\right]}{k_{z_B}^n k_{z_B}^{m*} \varepsilon_B} \int_{x_l}^{x_u} I_{B_x}^{'nq}(x) I_{B_x}^{"mp}(x)^* dx \int_{y_l}^{y_u} V_{B_y}^{'q}(y) V_{B_y}^{"p}(y)^* dy$$

$$D_{mn} = \sum_p^{N_A^{TM}} \left[\sum_q^{N_B^{TM}} \frac{k_{z_A}^{m*}}{\omega \varepsilon_0 \varepsilon_A} \int_{x_l}^{x_u} I_{B_x}^{'nq}(x) I_{A_x}^{'mp}(x)^* dx \int_{y_l}^{y_u} V_{B_y}^{'q}(y) V_{A_y}^{'p}(y)^* dy \right.$$
$$\left. - \sum_r^{N_B^{TE}} \frac{k_{z_A}^{m*}}{k_{z_B}^n \varepsilon_A} \int_{x_l}^{x_u} I_{B_x}^{"nr}(x) I_{A_x}^{'mp}(x)^* dx \int_{y_l}^{y_u} V_{B_y}^{"r}(y) V_{A_y}^{'p}(y)^* dy \right]$$

$$G_{mn} = \sum_p^{N_A^{TM}} \sum_q^{N_B^{TE}} \frac{\left[k_0^2 \varepsilon_B - k_{x_{B_{nq}}}^2\right] k_{z_A}^{m*}}{k_{z_B}^n k_{T_{A_m}}^{2*}} \int_{x_l}^{x_u} V_{B_x}^{"nq}(x) V_{A_x}^{'mp}(x)^* dx \int_{y_l}^{y_u} I_{B_y}^{"q}(y) I_{A_y}^{'p}(y)^* dy$$

$$L_{mn} = \sum_p^{N_A^{TE}} \sum_q^{N_B^{TE}} \frac{\left[k_0^2 \varepsilon_B - k_{x_{B_{nq}}}^2\right]}{k_{z_B}^n \omega \mu_0} \int_{x_l}^{x_u} V_{B_x}^{"nq}(x) V_{A_x}^{"mp}(x)^* dx \int_{y_l}^{y_u} I_{B_y}^{"q}(y) I_{A_y}^{"p}(y)^* dy$$

$$N_{mn} = \sum_{p}^{N_A^{TE}} \left[\begin{array}{l} \sum_{q}^{N_B^{TM}} \frac{k_0^2}{k_{T_{A_m}}^{2*}} \int_{x_l}^{x_u} I_{B_x}^{'nq}(x) I_{A_x}^{''mp}(x)^* dx \int_{y_l}^{y_u} V_{B_y}^{'q}(y) V_{A_y}^{''p}(y)^* dy \\[4mm] - \sum_{r}^{N_B^{TE}} \frac{k_0^2 \omega \varepsilon_0}{k_{z_B}^n k_{T_{A_m}}^{2*}} \int_{x_l}^{x_u} I_{B_x}^{''nr}(x) I_{A_x}^{''mp}(x)^* dx \int_{y_l}^{y_u} V_{B_y}^{''r}(y) V_{A_y}^{''p}(y)^* dy \end{array} \right]$$

$$C_{mn} = \sum_{p}^{N_A^{TM}} \left[\begin{array}{l} \frac{k_{z_A}^{m*}}{\omega \varepsilon_0 \varepsilon_A} \int_{x_l}^{x_u} I_{A_x}^{'np}(x) I_{A_x}^{'mp}(x)^* dx \\[4mm] + \frac{k_{z_A}^{m*} k_{z_A}^n}{k_{T_{A_n}}^2 \varepsilon_A} \sum_{q}^{N_A^{TE}} \int_{x_l}^{x_u} I_{A_x}^{''nq}(x) I_{A_x}^{'mp}(x)^* dx \int_{y_l}^{y_u} V_{A_y}^{''q}(y) V_{A_y}^{'p}(y)^* dy \end{array} \right]$$

$$F_{mn} = \sum_{p}^{N_A^{TM}} \left[\begin{array}{l} \frac{k_{z_A}^{m*} k_{z_A}^n}{k_{T_{A_m}}^{2*}} \sum_{q}^{N_A^{TE}} \int_{x_l}^{x_u} V_{A_x}^{''nq}(x) V_{A_x}^{'mp}(x)^* dx \int_{y_l}^{y_u} I_{A_y}^{''q}(y) I_{A_y}^{'p}(y)^* dy \\[4mm] - \frac{k_{z_A}^{m*} k_0^2 \omega \mu_0 \varepsilon_A}{k_{T_{A_m}}^{2*} k_{T_{A_n}}^2} \sum_{r}^{N_A^{TM}} \int_{x_l}^{x_u} V_{A_x}^{'nr}(x) V_{A_x}^{'mp}(x)^* dx \int_{y_l}^{y_u} I_{A_y}^{'r}(y) I_{A_y}^{'p}(y)^* dy \end{array} \right]$$

$$K_{mn} = \sum_{p}^{N_A^{TE}} \left[\begin{array}{l} \frac{k_{z_A}^n}{\omega \mu_0} \int_{x_l}^{x_u} V_{A_x}^{''np}(x) V_{A_x}^{''mp}(x)^* dx \\[4mm] - \frac{k_0^2 \varepsilon_A}{k_{T_{A_n}}^2} \sum_{q}^{N_A^{TM}} \int_{x_l}^{x_u} V_{A_x}^{'nq}(x) V_{A_x}^{''mp}(x)^* dx \int_{y_l}^{y_u} I_{A_y}^{'q}(y) I_{A_y}^{''p}(y)^* dy \end{array} \right]$$

$$M_{mn} = \sum_{p}^{N_A^{TE}} \left[\begin{array}{l} \frac{k_0^2}{k_{T_{A_m}}^{2*}} \sum_{q}^{N_A^{TM}} \int_{x_l}^{x_u} I_{A_x}^{'nq}(x) I_{A_x}^{''mp}(x)^* dx \int_{y_l}^{y_u} V_{A_y}^{'q}(y) V_{A_y}^{''p}(y)^* dy \\[4mm] + \frac{k_0^2 k_{z_A}^n \omega \varepsilon_0}{k_{T_{A_m}}^{2*} k_{T_{A_n}}^2} \sum_{r}^{N_A^{TE}} \int_{x_l}^{x_u} I_{A_x}^{''nr}(x) I_{A_x}^{''mp}(x)^* dx \int_{y_l}^{y_u} V_{A_y}^{''r}(y) V_{A_y}^{''p}(y)^* dy \end{array} \right]$$

VIII.8 TE, TM-TO-Y MODES IN SECTION A, TE, TM-TO-Z MODES IN SECTION B

$$[C_I] = [C - K + M]^{-1} [D - L + N]$$

$$[C_V] = [A + H - P + S]^{-1} [D^\dagger - L^\dagger + N^\dagger]$$

$$A_{mn} = \sum_{p}^{N_B^{TM}} \left[\begin{array}{l} \dfrac{k_{z_B}^n}{\omega \varepsilon_0 \varepsilon_B} \int_{x_l}^{x_u} I_{B_x}^{'np}(x) I_{B_x}^{'mp}(x)^* dx \\[3ex] + \dfrac{k_0^2}{k_{T_{B_n}}^2} \sum_{q}^{N_B^{TE}} \int_{x_l}^{x_u} I_{B_x}^{''nq}(x) I_{B_x}^{'mp}(x)^* dx \int_{y_l}^{y_u} V_{B_y}^{''q}(y) V_{B_y}^{'p}(y)^* dy \end{array} \right]$$

$$H_{mn} = \sum_{p}^{N_B^{TE}} \left[\begin{array}{l} \dfrac{k_{z_B}^{m\,*}}{\omega \mu_0} \int_{x_l}^{x_u} V_{B_x}^{''np}(x) V_{B_x}^{''mp}(x)^* dx \\[3ex] - \dfrac{k_{z_B}^{m\,*} k_{z_B}^n}{k_{T_{B_n}}^2} \sum_{p}^{N_B^{TM}} \int_{x_l}^{x_u} V_{B_x}^{'nq}(x) V_{B_x}^{''mp}(x)^* dx \int_{y_l}^{y_u} I_{B_y}^{'q}(y) I_{B_y}^{''p}(y)^* dy \end{array} \right]$$

$$P_{mn} = \sum_{p}^{N_B^{TM}} \left[\begin{array}{l} \dfrac{k_0^2 \varepsilon_B}{k_{T_{B_m}}^{2\,*}} \sum_{q}^{N_B^{TE}} \int_{x_l}^{x_u} V_{B_x}^{''nq}(x) V_{B_x}^{'mp}(x)^* dx \int_{y_l}^{y_u} I_{B_y}^{'q}(y) I_{B_y}^{'p}(y)^* dy \\[3ex] - \sum_{r}^{N_B^{TM}} \dfrac{k_0^2 k_{z_B}^n \omega \mu_0 \varepsilon_B}{k_{T_{B_m}}^{2\,*} k_{T_{B_n}}^2} \int_{x_l}^{x_u} V_{B_x}^{'nr}(x) V_{B_x}^{'mp}(x)^* dx \int_{y_l}^{y_u} I_{B_y}^{'r}(y) I_{B_y}^{'p}(y)^* dy \end{array} \right]$$

$$S_{mn} = \sum_{p}^{N_B^{TE}} \left[\begin{array}{l} \dfrac{k_{z_B}^n k_{z_B}^{m\,*}}{k_{T_{B_m}}^{2\,*} \varepsilon_B} \sum_{q}^{N_B^{TM}} \int_{x_l}^{x_u} I_{B_x}^{'nq}(x) I_{B_x}^{''mp}(x)^* dx \int_{y_l}^{y_u} V_{B_y}^{'q}(y) V_{B_y}^{''p}(y)^* dy \\[3ex] + \dfrac{k_0^2 k_{z_B}^{m\,*} \omega \varepsilon_0}{k_{T_{B_m}}^{2\,*} k_{T_{B_n}}^2} \sum_{r}^{N_B^{TE}} \int_{x_l}^{x_u} I_{B_x}^{''nr}(x) I_{B_x}^{''mp}(x)^* dx \int_{y_l}^{y_u} V_{B_y}^{''r}(y) V_{B_y}^{''p}(y)^* dy \end{array} \right]$$

$$D_{mn} = \sum_{p}^{N_A^{TE}} \left[\begin{array}{l} \sum_{q}^{N_B^{TE}} \dfrac{k_{z_A}^{m\,*} k_{z_B}^n k_0^2}{k_{T_{B_n}}^2 k_{u_{p_A}}^{'2}} \int_{x_l}^{x_u} I_{B_x}^{''nq}(x) I_{A_x}^{'mp}(x)^* dx \int_{y_l}^{y_u} V_{B_y}^{''q}(y) V_{A_y}^{'p}(y)^* dy \\[3ex] + \sum_{r}^{N_B^{TM}} \dfrac{k_{z_A}^{m\,*} \omega \mu_0}{k_{u_{p_A}}^{'2}} \int_{x_l}^{x_u} I_{B_x}^{'nr}(x) I_{A_x}^{'mp}(x)^* dx \int_{y_l}^{y_u} V_{B_y}^{'r}(y) V_{A_y}^{'p}(y)^* dy \end{array} \right]$$

$$L_{mn} = \sum_{p}^{N_A^{TM}} \left[\begin{array}{l} -\sum_{q}^{N_B^{TE}} \dfrac{k_{z_B}^n}{\omega \mu_0} \int_{x_l}^{x_u} V_{B_x}^{''nq}(x) V_{A_x}^{''mp}(x)^* dx \int_{y_l}^{y_u} \dfrac{I_{B_y}^{''q}(y) I_{A_y}^{''p}(y)^*}{\varepsilon_A(y)} dy \\[3ex] + \sum_{r}^{N_B^{TM}} \dfrac{k_0^2 \varepsilon_B}{k_{T_{B_n}}^2} \int_{x_l}^{x_u} V_{B_x}^{'nr}(x) V_{A_x}^{''mp}(x)^* dx \int_{y_l}^{y_u} \dfrac{I_{B_y}^{'r}(y) I_{A_y}^{''p}(y)^*}{\varepsilon_A(y)} dy \end{array} \right]$$

$$N_{mn} = \sum_{p}^{N_A^{TM}} \begin{bmatrix} \sum_{q}^{N_B^{TE}} \frac{k_{z_B}^n \omega \varepsilon_0}{k_T^2 {}_{B_n}} \int_{x_l}^{x_u} I_{B_x}^{'nq}(x) I_{A_x}^{''mp}(x)^* dx \int_{y_l}^{y_u} V_{B_y}^{''q}(y) V_{A_y}^{''p}(y)^* dy \\ + \sum_{r}^{N_B^{TM}} \int_{x_l}^{x_u} I_{B_x}^{'nr}(x) I_{A_x}^{''mp}(x)^* dx \int_{y_l}^{y_u} V_{B_y}^{'r}(y) V_{A_y}^{''p}(y)^* dy \end{bmatrix}$$

$$C_{mn} = \sum_{p}^{N_A^{TE}} \frac{k_{z_A}^m {}^* \omega \mu_0}{k_{u_{p_A}}^{'2}} \int_{x_l}^{x_u} I_{A_x}^{'np}(x) I_{A_x}^{'mp}(x)^* dx$$

$$K_{mn} = \sum_{p}^{N_A^{TM}} \begin{bmatrix} \sum_{q}^{N_A^{TE}} \int_{x_l}^{x_u} V_{A_x}^{'nq}(x) V_{A_x}^{''mp}(x)^* dx \int_{y_l}^{y_u} \frac{I_{A_y}^{'q}(y) I_{A_y}^{''p}(y)^*}{\varepsilon_A(y)} dy \\ - \frac{k_{z_A}^n {}^* \omega \varepsilon_0}{k_{u_{p_A}}^{''2}} \int_{x_l}^{x_u} V_{A_x}^{''np}(x) V_{A_x}^{''mp}(x)^* dx \end{bmatrix}$$

$$M_{mn} = \sum_{p}^{N_A^{TM}} \sum_{q}^{N_A^{TE}} \int_{x_l}^{x_u} I_{A_x}^{'nq}(x) I_{A_x}^{''mp}(x)^* dx \int_{y_l}^{y_u} V_{A_y}^{'q}(y) V_{A_y}^{''p}(y)^* dx$$

VIII.9 TE, TM-TO-Z MODES IN SECTION A, TE, TM-TO-YMODES IN SECTION B

$$[C_I] = [C - F + K + M]^{-1}[D - G + L + N]$$

$$[C_V] = [A + H - P]^{-1}[D^\dagger - G^\dagger + L^\dagger + N^\dagger]$$

$$A_{mn} = \sum_{p}^{N_B^{TE}} \begin{bmatrix} \frac{k_{z_B}^n \omega \mu_0}{k_{u_{p_B}}^{'2}} \int_{x_l}^{x_u} I_{B_x}^{'np}(x) I_{B_x}^{'mp}(x)^* dx \\ + \sum_{q}^{N_B^{TM}} \int_{x_l}^{x_u} I_{B_x}^{''nq}(x) I_{B_x}^{'mp}(x)^* dx \int_{y_l}^{y_u} V_{B_y}^{''q}(y) V_{B_y}^{'p}(y)^* dy \end{bmatrix}$$

$$H_{mn} = \sum_{p}^{N_B^{TM}} \frac{k_{z_B}^m {}^* \omega \varepsilon_0}{k_{u_{p_B}}^{''2}} \int_{x_l}^{x_u} V_{B_x}^{''np}(x) V_{B_x}^{''mp}(x)^* dx$$

$$P_{mn} = \sum_{p}^{N_B^{TE}} \sum_{q}^{N_B^{TM}} \int_{x_l}^{x_u} V_{B_x}^{''nq}(x) V_{B_x}^{'mp}(x)^* dx \int_{y_l}^{y_u} \frac{I_{B_y}^{''q}(y) I_{B_y}^{'p}(y)^*}{\varepsilon_B(y)} dy$$

$$D_{mn} = \sum_p^{N_A^{TM}} \sum_q^{N_B^{TE}} \frac{k_{z_A}^{m*}}{\omega \varepsilon_0 \varepsilon_A} \int_{x_l}^{x_u} I_{B_x}^{'nq}(x) I_{A_x}^{'mp}(x)^* dx \int_{y_l}^{y_u} V_{B_y}^{'q}(y) V_{A_y}^{'p}(y)^* dy$$

$$G_{mn} = \sum_p^{N_A^{TM}} \left[\begin{array}{l} \displaystyle\sum_q^{N_B^{TM}} \frac{k_{z_A}^{m*} k_{z_B}^n k_0^2}{k_{T_{A_m}}^{2*} k_{u_{q_B}}^{''2}} \int_{x_l}^{x_u} V_{B_x}^{''nq}(x) V_{A_x}^{'mp}(x)^* dx \int_{y_l}^{y_u} I_{B_y}^{''q}(y) I_{A_y}^{'p}(y)^* dy \\[2em] \displaystyle -\sum_r^{N_B^{TE}} \frac{k_{z_A}^{m*} \omega \mu_0}{k_{T_{A_m}}^{2*}} \int_{x_l}^{x_u} V_{B_x}^{'nr}(x) V_{A_x}^{'mp}(x)^* dx \int_{y_l}^{y_u} I_{B_y}^{'r}(y) I_{A_y}^{'p}(y)^* dy \end{array} \right]$$

$$L_{mn} = \sum_p^{N_A^{TE}} \left[\begin{array}{l} \displaystyle\sum_q^{N_B^{TM}} \frac{k_{z_B}^n \omega \varepsilon_0}{k_{u_{q_B}}^{''2}} \int_{x_l}^{x_u} V_{B_x}^{''nq}(x) V_{A_x}^{''mp}(x)^* dx \int_{y_l}^{y_u} I_{B_y}^{''q}(y) I_{A_y}^{''p}(y)^* dy \\[2em] \displaystyle -\sum_r^{N_B^{TE}} \int_{x_l}^{x_u} V_{B_x}^{'nr}(x) V_{A_x}^{''mp}(x)^* dx \int_{y_l}^{y_u} I_{B_y}^{'r}(y) I_{A_y}^{''p}(y)^* dy \end{array} \right]$$

$$N_{mn} = \sum_p^{N_A^{TE}} \sum_q^{N_B^{TE}} \frac{k_0^2}{k_{T_{A_m}}^{2*}} \int_{x_l}^{x_u} I_{B_x}^{'nq}(x) I_{A_x}^{''mp}(x)^* dx \int_{y_l}^{y_u} V_{B_y}^{'q}(y) V_{A_y}^{''p}(y)^* dy$$

$$C_{mn} = \sum_p^{N_A^{TM}} \left[\begin{array}{l} \displaystyle\frac{k_{z_A}^{m*}}{\omega \varepsilon_0 \varepsilon_A} \int_{x_l}^{x_u} I_{A_x}^{'np}(x) I_{A_x}^{'mp}(x)^* dx \\[2em] \displaystyle +\frac{k_{z_A}^{m*} k_{z_A}^n}{k_{T_{A_n}}^2 \varepsilon_A} \sum_q^{N_A^{TE}} \int_{x_l}^{x_u} I_{A_x}^{''nq}(x) I_{A_x}^{'mp}(x)^* dx \int_{y_l}^{y_u} V_{A_y}^{''q}(y) V_{A_y}^{'p}(y)^* dy \end{array} \right]$$

$$F_{mn} = \sum_p^{N_A^{TM}} \left[\begin{array}{l} \displaystyle\frac{k_{z_A}^{m*} k_{z_A}^n}{k_{T_{A_m}}^{2*}} \sum_q^{N_A^{TE}} \int_{x_l}^{x_u} V_{A_x}^{''nq}(x) V_{A_x}^{'mp}(x)^* dx \int_{y_l}^{y_u} I_{A_y}^{''q}(y) I_{A_y}^{'p}(y)^* dy \\[2em] \displaystyle -\frac{k_{z_A}^{m*} k_0^2 \omega \mu_0 \varepsilon_A}{k_{T_{A_m}}^{2*} k_{T_{A_n}}^2} \sum_r^{N_A^{TM}} \int_{x_l}^{x_u} V_{A_x}^{'nr}(x) V_{A_x}^{'mp}(x)^* dx \int_{y_l}^{y_u} I_{A_y}^{'r}(y) I_{A_y}^{'p}(y)^* dy \end{array} \right]$$

$$K_{mn} = \sum_p^{N_A^{TE}} \left[\begin{array}{l} \displaystyle\frac{k_{z_A}^n}{\omega \mu_0} \int_{x_l}^{x_u} V_{A_x}^{''np}(x) V_{A_x}^{''mp}(x)^* dx \\[2em] \displaystyle -\frac{k_0^2 \varepsilon_A}{k_{T_{A_n}}^2} \sum_q^{N_A^{TM}} \int_{x_l}^{x_u} V_{A_x}^{'nq}(x) V_{A_x}^{''mp}(x)^* dx \int_{y_l}^{y_u} I_{A_y}^{'q}(y) I_{A_y}^{''p}(y)^* dy \end{array} \right]$$

$$M_{mn} = \sum_p^{N_A^{TE}} \left[\begin{array}{l} \dfrac{k_0^2}{k_{T_{A_m}}^2} \sum_q^{N_A^{TM}} \int_{x_l}^{x_u} I_{A_x}^{'nq}(x) I_{A_x}^{''mp}(x)^* dx \int_{y_l}^{y_u} V_{A_y}^{'q}(y) V_{A_y}^{''p}(y)^* dy \\[3mm] + \dfrac{k_0^2 k_{z_A}^n \omega \varepsilon_0}{k_{T_{A_m}}^2 k_{T_{A_n}}^2} \sum_r^{N_A^{TE}} \int_{x_l}^{x_u} I_{A_x}^{''nr}(x) I_{A_x}^{''mp}(x)^* dx \int_{y_l}^{y_u} V_{A_y}^{''r}(y) V_{A_y}^{''p}(y)^* dy \end{array} \right]$$

THIS PAGE INTENTIONALLY BLANK

Transverse Resonance Analysis Technique for
Microwave and Millimetre-Wave Circuits

Bevan D. Bates and Geoffrey W. Staines

(DSTO-RR-0027)

DISTRIBUTION LIST

Number of Copies

DEPARTMENT OF DEFENCE

Defence Science and Technology Organisation

Chief Defence Scientist and members of the	) 1 shared copy
DSTO Central Office Executive	) for circulation
Counsellor Defence Science, London	Doc Control Data Sheet Only
Counsellor Defence Science, Washington	Doc Control Data Sheet Only
Scientific Adviser POLCOM	1
Senior Defence Scientific Adviser	1
Assistant Secretary Scientific Analysis	1
Director, Aeronautical and Maritime Research Laboratory	1

Electronics and Surveillance Research Laboratory

Director, Electronic and Surveillance Research Laboratory	1
Chief, Electronic Warfare Division	1
Research Leader, Signal and Information Processing	1
Research Leader, Electronic Countermeasures	1
Head, Advanced Concepts Group	1
Dr Bevan D. Bates, Advanced Concepts Group	1
Dr Geoffrey W. Staines, Advanced Concepts Group	1
Dr Anthony Lindsay, Advanced Concepts Group	1
Mr Ken Harvey, Advanced Concepts Group	1

Navy Office

Navy Scientific Adviser	1

Army Office

Scientific Adviser - Army	1

Air Office

Air Force Scientific Adviser	1

Libraries and Information Services

Defence Central Library, Technical Reports Centre	1
Manager, Document Exchange Centre (for retention)	1
National Technical Information Services, United States	2
Defence Research Information Centre, United Kingdom	2
Director, Scientific Information Services, Canada	1

Ministry of Defence, New Zealand	1
National Library of Australia	1
Defence Science and Technology Organisation Salisbury, Research Library	2
Library Defence Signals Directorate, Canberra	1
AGPS	1
British Library, Document Supply Centre	1
Parliamentary Library of South Australia	1
The State Library of South Australia	1
Spares, DSTOS, Research Library	6

Department of Defence

DOCUMENT CONTROL DATA SHEET

3a. AR Number	3b. Establishment Number	3c. Type of Report	4. Task Number
AR-009-211	DSTO-RR-0027	RESEARCH REPORT	DST 93/334

5. Document Date	6. Cost Code	7. Security Classification	8. No. of Pages	142
FEBRUARY 1994	230	U | U | U	9. No. of Refs.	55

10. Title	
TRANSVERSE RESONANCE ANALYSIS TECHNIQUE FOR MICROWAVE AND MILLIMETRE-WAVE CIRCUITS	Document Title Abstract S (Secret C (Confi) R (Rest) U (Unclass) * For UNCLASSIFIED docs with a secondary distribution LIMITATION, use (L) in document box.

11. Author(s)	12. Downgrading/ Delimiting Instructions
Bevan D. Bates Geoffrey W. Staines	

13a. Corporate Author and Address	14. Officer/Position responsible for
Electronics and Surveillance Research Laboratory PO Box 1500 SALISBURY SA 5108	Security SOESRL Downgrading CEWD
13b. Task Sponsor DSTO	Approval for release CEWD

15. Secondary Release of this Document

APPROVED FOR PUBLIC RELEASE.

Any enquiries outside stated limitations should be referred through DSTIC, Defence Information Services, Department of Defence, Anzac Park West, Canberra, ACT 2600.

16a. Deliberate Announcement

No limitation.

16b. Casual Announcement (for citation in other documents)

√	No Limitation			Ref. by Author & Doc No only

17. DEFTEST Descriptors		18. DISCAT Subject Codes
Antennas	Waveguides	0049A
Impedance Matching	Electronic Warfare	0049B

19. Abstract

A transverse resonance mode matching technique has been developed to analyse passive microwave and millimeter-wave waveguides and components. This technique possesses superior computational efficiency when compared to more general approaches such as the finite element method. This advantage is particularly useful for analysing broadband components used in electronic warfare systems. In this report, the theory behind this transverse resonance analysis is presented in detail. Theoretical results for several waveguiding structures are presented and compared with experimental or published data to verify the analysis.